5-21-2015 12:00 AM

# Exploring the Chemistry of η5-Cyclopentadienyl-Cobalt-η4-Cyclobutadiene Containing Polymers; Synthesis, Properties, and Self-Assembly

Mahboubeh Hadadpour, *The University of Western Ontario*

Supervisor: Prof. Paul J. Ragogna, *The University of Western Ontario*

A thesis submitted in partial fulfillment of the requirements for the Doctor of Philosophy degree in Chemistry

# EXPLORING THE CHEMISTRY OF $\eta^5$-CYCLOPENTADIENYL-COBALT-$\eta^4$-CYCLOBUTADIENE CONTAINING POLYMERS; SYNTHESIS, PROPERTIES, AND SELF-ASSEMBLY

Thesis Format: Integrated Article

by

Mahboubeh Hadadpour

Graduate program in Chemistry
A thesis submitted in partial fulfillment
of the requirements for the degree of
Doctor of Philosophy

The School of Graduate and Postdoctoral Studies
The University of Western Ontario
London, Ontario, Canada

# Abstract

Metal containing polymers (metallopolymers) bring together the synthetic efficiency and versatility of conventional organic polymers with unique redox, responsive, and catalytic properties of inorganic metals. Over the last decade, metallopolymers have gained increased attention because of their unique physical and chemical properties that arise from the incorporation of metal centers into a polymer. Since the first report on a metallocene-based metallopolymer in 1955, there has been growing interest in this class of material. Ferrocene-based metallopolymers represent the vast majority of metallocene containing polymers in the literature. In 1992, the Manners Group established a major milestone in the field of metallopolymers by reporting the ring opening polymerization (ROP) of the strained [1]silaferrocenophane to synthesize polyferrocenylsilane (PFS). The novelty of PFS has attracted attention to incorporate other metallocenes into polymer chains. In comparison to well-studied ferrocene containing polymers, cobaltocene have received far less attention due to the difficulties in preparing its derivatives. In fact, only a few key contributions on this subject have been reported. Cobaltocene with 19 electrons is not stable and is readily oxidized to a cationic 18 electron cobaltocenium. The Tang Group has developed a synthetic methodology to synthesize highly pure cobaltocenium derivatives and incorporated them into well-defined polymers.

Alternatively, the Ragogna Group reported the first neutral side-chain $\eta^5$-cyclopentadienyl-cobalt-$\eta^4$-cyclobutadiene (CpCoCb) functionalized metallopolymer. This mixed sandwich metallocene is an 18 electron complex, electronically neutral and isoelectronic to ferrocene and cobaltocenium. In this dissertation, the synthesis of well-defined side-chain functionalized CpCoCb containing homo- and block metallopolymers *via* reversible addition fragmentation transfer (RAFT) polymerization is detailed. Development of a controlled polymerization method to obtain well-defined high molecular weight CpCoCb containing metallopolymers is discussed. Several block copolymers were prepared *via* sequential RAFT polymerization. Synthesis, characterization, solution and solid-state self-assembly of the metal containing block copolymers is discussed in detail. These materials are used as ink in soft lithography to transfer patterns using a polydimethylsiloxane (PDMS) stamp. Synthesis of a series of

CpCoCb monomers where the Cb ring is decorated with different substituents such as ferrocene and thiophene is reported. These highly metalized monomers are used to make metal rich materials with tunable metal content.

## Keywords

Metallopolymer. $\eta^5$-cyclopentadienyl-cobalt-$\eta^4$-cyclobutadiene (CpCoCb). Reversible addition fragmentation transfer (RAFT) polymerization. Controlled polymerization. Block copolymer. Solution-state self-assembly. Solid-state self-assembly. Pyrolysis. Polyelectrolyte. Soft lithography. Magnetic ceramic.

## Co-Authorship Statement

The research discussed in chapters 2, 3, 4, and 5 of this dissertation are the results of major contributions from the author, Mahboubeh Hadadpour, under the supervision of Prof. Paul J. Ragogna. Coworkers from the University of Western Ontario and the University of Bristol contributed to the work, and their detailed contribution are described here.

**Chapter 2** describes work published in *macromolecules,* **2014**, *47*, 6207-6217. coauthored by Mahboubeh Hadadpour, Dr. Yuqing Q. Liu, Dr. Preeti Chadha, Prof. Paul J. Ragogna.

Dr. Chadha instructed the author on the synthesis of $\eta^5$-cyclopentadienyl-cobalt-$\eta^4$-cyclobutadiene (CpCoCb) compounds. Dr. Li instructed the author on reversible addition fragmentation transfer (RAFT) polymerization technique throughout the project. All synthesis, characterizations, and analysis were done by the author under the supervision of Prof. Ragogna. The manuscript was drafted by the author and Prof. Ragogna provided great assistance with editing it.

**Chapter 3** describes work that is submitted to *Chemistry of Materials* coauthored by Mahboubeh Hadadpour, Dr. Jessica Gwyther, Prof. Ian Manners, and Prof. Paul J. Ragogna.

The project was proposed by the author who performed all synthetic and characterization work under the supervision of Prof. Ragogna. Dr. Gwyther from the University of Bristol instructed the author on the bulk solid-state self-assembly of block copolymers. Some characterization were performed at the University of Bristol in the Prof. Manners laboratory by the author. The manuscript was drafted by the author and Prof. Ragogna and Prof. Manners provided great assistance with editing it.

**Chapter 4** describes work proposed by the author. All the synthetic and characterization work was performed by the author under the supervision of Prof. Ragogna. The manuscript was drafted by the author and Prof. Ragogna provided great assistance with editing.

**Chapter 5** describes work initiated by Dr. Preeti Chadha. Charlene Moulin and Scott Middlemiss each synthesized one of the monomers and attempted its polymerization

under the author's supervision. The author reproduced the materials and completed compound characterization and expanded the project under the supervision of Prof. Ragogna. The author drafted the manuscript that was edited by Prof. Ragogna.

# Acknowledgments

To my amazing supervisor, Prof. Paul Ragogna,

to the love of my life, Dr. Ali Nazemi,

and to my lovely mom and dad;

No words can describe how much I appreciate everything you have done for me.

Thank you from the bottom of my heart.

# Table of Contents

# List of Tables

# List of Figures

## Chapter 1

# List of Schemes

# List of Abbreviations

| | |
|---|---|
| AIBN | 2,2'-azobisisobutyronitrile |
| *aq.* | aqueous |
| ATRP | atom transfer radical polymerization |
| AuNP | gold nanoparticle |
| b | broad |
| *ca.* | *approximately* |
| Cb | cyclobutadiene |
| Cp | cyclopentadienyl |
| CpCoCb | $\eta^5$-cyclopentadienyl-cobalt-$\eta^4$-cyclobutadiene |
| d | doublet |
| DCM | dichloromethane |
| dd | doublet of doublets |
| DLS | dynamic light scattering |
| DMF | *N*,*N*-dimethylformamide |
| DP | degree of polymerization |
| DSC | differential scanning calorimetry |
| *e.g.* | *exempli gratia* (for example) |
| EBL | electron beam lithography |
| *et al.* | *et alii* (and others) |
| Fc | ferrocene |
| g | gram |
| GPC | gel permeation chromatography |
| HRMS | high-resolution mass spectrometry |
| IR | infrared |
| *i.e.* | *id est* (that is) |
| *in vacuo* | in a vacuum |
| *J* | coupling constant |

| | |
|---|---|
| kDa | kilo dalton |
| m | multiple |
| MA | methyl acrylate |
| min | minute |
| mL | millilitre |
| $M_n$ | number average molecular weight |
| $M_w$ | weight average molecular weight |
| $NEt_3$ | *N,N,N*-triethylamine |
| NMR | nuclear magnetic resonance |
| PDI | polydispersity index |
| PFS | polyferrocenylsilane |
| Ph | phenyl |
| PMA | poly(methylacrylate) |
| PS | polystyrene |
| *p*t | pseudo triplet |
| RAFT | reversible addition fragmentation transfer polymerization |
| RI | refractive index |
| ROMP | ring opening metathesis polymerization |
| ROP | ring opening polymerization |
| SEM | scanning electron microscopy |
| SSL | strong segregation limit |
| $T_d$ | decomposition temperature |
| TEM | transmission electron microscopy |
| $T_g$ | glass transition temperature |
| TGA | thermal gravimetric analysis |
| Th | Thiophene |
| THF | tetrahydrofuran |
| *via* | by way of |
| *vs* | versus |
| WSL | weak segregation limit |
| $\{^1H\}$ | proton decoupled |

| | |
|---|---|
| °C | degree Celcius |
| δ | chemical shift |
| Δδ | change in chemical shift |
| μCP | microcontact patterning |
| μL | microlitre |
| Φ | volume fraction |
| χ | Flory-Huggins parameter |

# Chapter 1

# Introduction

### 1.1. General Introduction on Polymers

Polymers are large molecules composed of repeat units called monomers. Words monomer and polymer come from Greek roots; *mono* meaning one, *poly* meaning many, and *mer* meaning part. Therefore, monomer means one part and polymer means many parts.[1] According to the International Union of Pure and Applied Chemistry (IUPAC), a polymer molecule is considered a macromolecule and it is defined as;

"*A molecule of high relative molecular mass, the structure of which essentially comprises the multiple repetition of units derived, actually or conceptually, from molecules of low relative molecular mass*."

Compared to small molecules with definite molar masses, polymers generally display molar mass distributions.[1] Molecular weight distributions are reported as a polydispersity index (PDI). PDI is calculated by $M_w/M_n$ where $M_w$ is the weight average molecular weight and $M_n$ is the number average molecular weight. $M_w$ and $M_n$ are two of the most commonly used average molecular weight values defined based on the statistical method that is applied to calculate the average molar mass. Mathematical description for $M_w$ and $M_n$ are shown below:

$$M_w = \frac{\sum M_i^2 N_i}{\sum M_i N_i} \qquad M_n = \frac{\sum M_i N_i}{\sum N_i} \qquad \text{(Eq. 1.1)}$$

In these equations, $N_i$ is the number of moles of a given polymer molecule ($i$) and $M_i$ is its molar mass. Colligative properties of polymer solutions, such as boiling point elevation, freezing point depression, and osmotic pressure depend on the number of molecules present, and not on the size of particles present in the mixture. For such

properties, number average molecular weight ($M_n$) is relevant. Some polymer properties, such as light scattering, depend on the number of polymer molecules and also on the size or weight of each polymer molecule. Such properties are described by the weight average molecular weight ($M_w$).

Most synthetic polymers have PDI values of equal or greater than one (PDI $\geq$ 1). However, as the polymer chains approach uniform distribution, the PDI approaches unity. Polymers with narrow polydispersity index can be achieved *via* controlled polymerization methods (1.1 $\geq$ PDI > 1). Controlled polymerization is explained later in this chapter.

Gel permeation chromatography (GPC) is one of the most commonly used methods to determine the molecular weight of polymers. In this technique a sample is passed through columns filled with a porous gel. Smaller polymers get trapped in the pores and elute slower, while larger polymers do not, and thus elute faster. GPC instruments are usually coupled with one or multiple detectors to retrieve relative or absolute molecular weight of polymers, respectively. Refractive index (RI) detector is one of the most common detectors used to analyze a polymers molecular weight, relative to a set of polymer standards.

### 1.2. General Introduction on Block Copolymers

Block copolymers are consist of two or more chemically distinct sections bound together at a junction point *via* a covalent or non-covalent bond.[2] In block copolymers, two or more polymeric blocks with different physical and chemical properties are combined and held together in one material. Many different classes of block copolymers exist and are categorized based on number of polymeric blocks involved in the structure (di-, tri-, tetra-, *etc*.), and also based on their relative architecture (linear, grafted, star).[2] Figure 1.1 shows general structure of common copolymers.

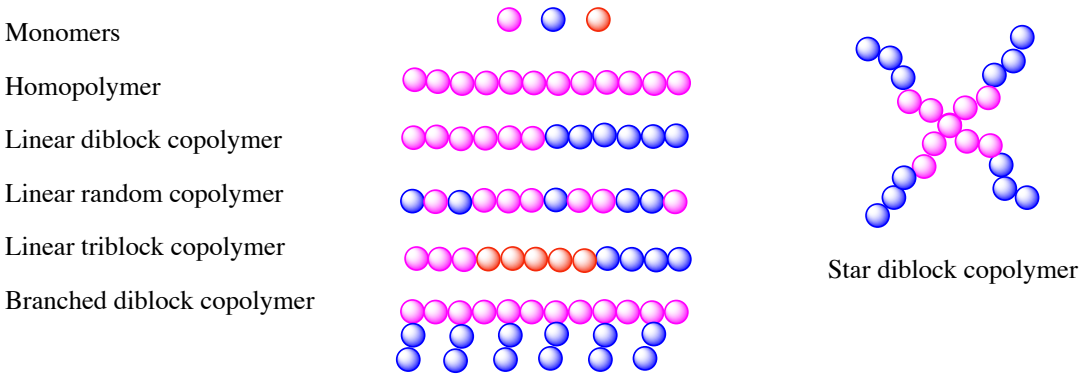


**Figure 1.1.** General structure of common block polymers.

Block copolymers exhibit properties not observed in typical homopolymers. For example, they can self-assemble in solution and solid-state to produce long-ranged nanometer features (see section 1.5).

### 1.3. General Introduction on Polymer Synthesis

A general understanding of the polymerization methods is essential as polymer synthesis is a complicated process that can take place by a variety of methods such as step growth polymerization and chain growth polymerization.[2]

In a step growth method, the polymerization progresses stepwise. A bifunctional monomer is required in this method where two monomers react together to form a dimer. Then dimers react with one another to produce a tetramer. This process continues until all monomers are incorporated into oligomers. The polymer molecular weight increases slowly at the beginning. Near the end, at high monomer conversion, oligomers react together to produce high molecular weight polymers.[3]

Chain growth polymerization refers to a general method of polymerization in which monomers are added one after another to the active propagating site of a growing polymer chain. During polymerization, even at low monomer conversion, high molecular weight polymers along with unreacted monomers are present. In this method, the polymer molecular weight increases gradually and constantly over reaction time.

Free radical polymerization is one of the common chain growth (addition) polymerization methods (Figure 1.2). Initiation is the first step in a free radical polymerization. An initiator is a molecule that begins the polymerization process through its decomposition

products. For free radical polymerization, the degradation products consist of radicals that react with double bond of the monomer, producing a new radical active center. In the propagation step, the active site attacks another monomer and this process is repeated. During this process, growth of the polymer chain may halt because of termination or chain transfer reactions (Figure 1.2).[4]

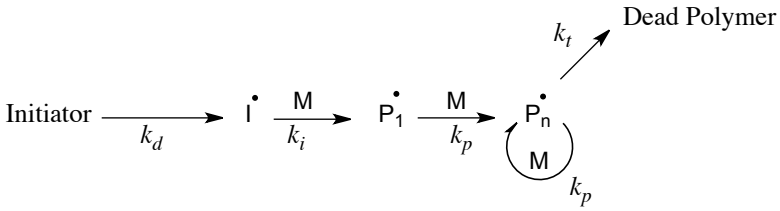


**Figure 1.2.** General mechanism of a free radical polymerization.

In a typical "living" polymerization very few termination or chain transfer reactions occur even after all monomers are consumed.[5] There are number of "living" polymerization methods such as anionic and cationic polymerization, however no radical polymerization can be considered as true "living" polymerization.[6] This is because highly active radical species are prone to react with each other, terminating the chain growth processes. There are number of "controlled" radical polymerization methods in which the concentration of propagating radicals during the polymerization at a given time is minimized, thus reducing the radical collision and minimizing termination of the chain growth process. Atom transfer radical polymerization (ATRP), nitroxide mediated radical polymerization (NMP), and reversible addition fragmentation transfer (RAFT) polymerization are examples of the most common controlled radical polymerization methods. RAFT polymerization is the focus of this dissertation.

### 1.4. Reversible Addition Fragmentation Transfer (RAFT) Polymerization

Reversible addition fragmentation transfer (RAFT) polymerization is one of the few controlled radical polymerization techniques. It is a powerful tool commonly used to make polymers with targeted molecular weight and narrow PDI. RAFT polymerization is perhaps the most useful method among controlled radical polymerization methods that can be used to polymerize variety of monomers. RAFT polymerization can be conducted in a wide variety of reaction media such as in organic or aqueous solutions,[7,8] and in

dispersed phases.[9] Overall, RAFT polymerization requires minimal process development, and in practice it is as simple as a conventional free radical polymerization, just performed in presence of a RAFT agent. RAFT agents are thiocarbonylthio-containing molecule with R and Z group (Figure 1.3).[10] Simplified RAFT polymerization process can be summarized as the insertion of monomers between the S-R bond of the RAFT agent (Figure 1.3). R and Z groups play a very important role on the performance and activity of the RAFT agent (see section 1.4.2).[7,10]

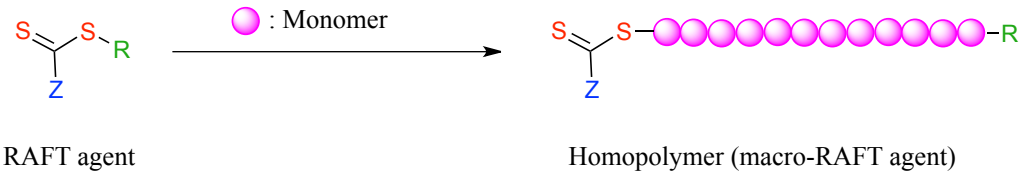


**Figure 1.3.** General structure of a RAFT agent and a simplified RAFT polymerization reaction.

In a RAFT polymerization, termination or irreversible chain transfer is not prevented but dramatically suppressed resulting in good control over molecular weight and polydispersity of the polymers. This is done by rapid equilibration of growing chains with respect to the propagation rate resulting in all chains having an equal opportunity to grow. The propagating polymer radical rapidly alternates between active and dormant species minimizing the concentration of propagating radical species, thus significantly reducing termination and formation of dead polymers (Figure 1.4).[7]

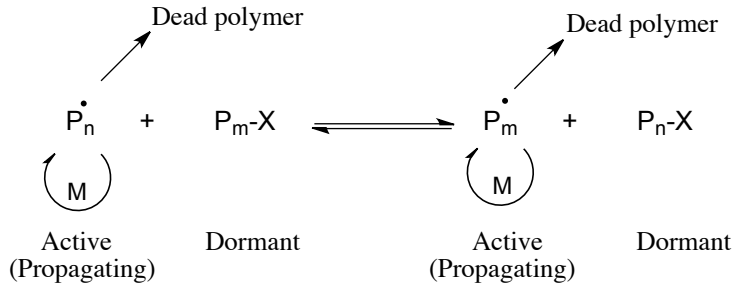


**Figure 1.4**. Propagating radical species rapidly alternates between "active" and "dormant" species *via* undergoing reversible activation/deactivation equilibrium.

### 1.4.1. Mechanism of RAFT Polymerization

Scheme 1.1 provides detailed mechanism of a typical RAFT polymerization. In RAFT polymerization, use of an initiator as radical source is required. Azo compounds such as 2,2'-azobisisobutyronitrile (AIBN) are common radical sources. The first step in RAFT polymerization is initiation to form radical source ($I^{\bullet}$). $I^{\bullet}$ attacks a monomer to make a polymeric radical species with one monomeric unit ($P_1^{\bullet}$). $P_1^{\bullet}$ propagates and reacts with n-1 monomers to produce $P_n^{\bullet}$ polymeric radical species with "n" repeat units. Initiation is followed by pre-equilibrium step, where the RAFT agent rapidly traps the $P_n^{\bullet}$ radical species to make intermediate **1.1**. This intermediate fragments to produce $R^{\bullet}$ and a new RAFT agent in which the original R group is replaced with $P_n$ (**1.2**). This type of RAFT agent is typically called a "macro-RAFT agent" because the original R group is replaced with a polymeric (macro) group. $P_n$ is dormant at this stage confined in the macro-RAFT agent.

$R^{\bullet}$ acts as a radical source and following the same trend as $I^{\bullet}$, it initiates a new polymeric chain with "m" number of repeat units ($P_m^{\bullet}$) in a so-called "reinitiation" step. At this point polymerization enters the main equilibrium stage. Macro-RAFT agent (**1.2**) traps the $P_m^{\bullet}$ propagating species producing intermediate **1.3** with $P_m$ and $P_n$ on each end. Polymerization enters an equilibrium stage at which all polymer chains ($P_m$ and $P_n$) have similar possibility to grow by being trapped and released by intermediate **1.3** at a constant rate.

Initiation:

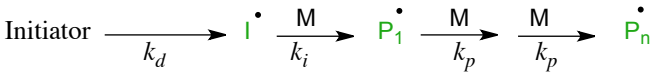


Initiation/ pre-equilibrium:

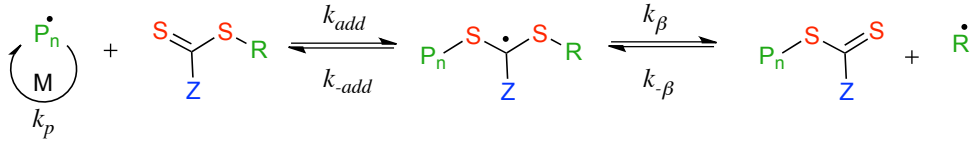


**1.1** **1.2**

Reinitiation:

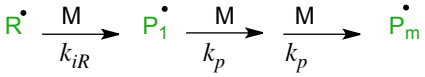


Main equilibrium:

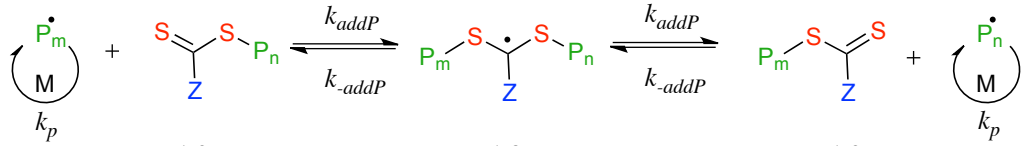


**1.2** **1.3** **1.2**

Termination:

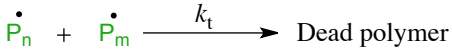


**Scheme 1.1.** Mechanism of a typical RAFT polymerization.

### 1.4.2. Effect of R and Z Group on RAFT Agent's Performance

Selecting an effective RAFT agent with proper R and Z group functionalities is crucial to obtain low PDI polymers with good control over the polymer molecular weight.[7,10] R and Z groups alter the reactivity of the RAFT agent, and their selection depends on the monomer that is being polymerized. The R group must be a good homolytic leaving group ($k_\beta > k_{-add}$) to be able to rapidly produce R$^\bullet$ and quickly start the reinitiation step (Scheme 1.1). Otherwise (if $k_{-add} > k_\beta$) $P_n^\bullet$ will be released instead of R$^\bullet$, resulting in retardation of polymerization. The $k_{-add}$ depends on the structure of $P_n$ that is originated

from the monomer being polymerized. This affinity can be explained in terms of partition coefficient (Φ):

$$\Phi = \frac{k_\beta}{k_{-add} + k_\beta} \qquad \text{(Eq. 1.2)}$$

To polymerize a specific monomer, selecting a RAFT agent that $\Phi \geq 0.5$ is essential. Fast start and rapid completion of reinitiation step is crucial to produce well-controlled polymers with narrow PDI. The general guideline for selecting an R group for a series of monomers is provided in Figure 1.5.

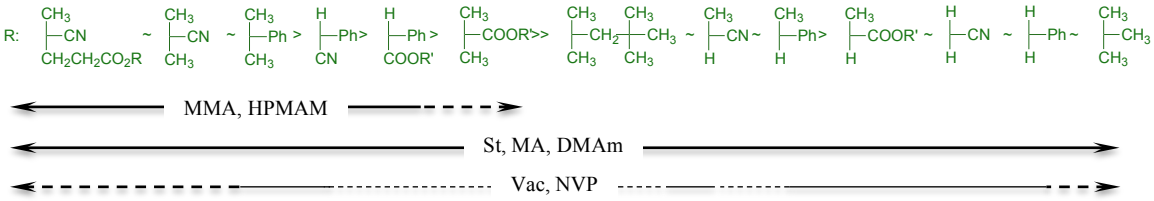


**Figure 1.5.** General guideline for selecting R group of a RAFT agent. Dashed lines mean limited control is provided.

The Z group functionality has an important role in altering reactivity and affinity of the RAFT agent toward trapping radicals. This directly affects the reinitiation step. The Z group affects reactivity of the RAFT agent, stability of the radical, and thus rate of fragmentation of the produced radical intermediate. Z groups with carbon or sulphur adjacent to the thiocarbonyl (C=S) are very active whereas those with nitrogen or oxygen are less reactive. Activity of a RAFT agent directly depends on its ability to do chain transfer. An active RAFT agent provides high number (~100) of chain transfer per propagation cycle. General trend of RAFT agent's activity based on Z group functionality for polymerization of various monomers is provided in Figure 1.6.

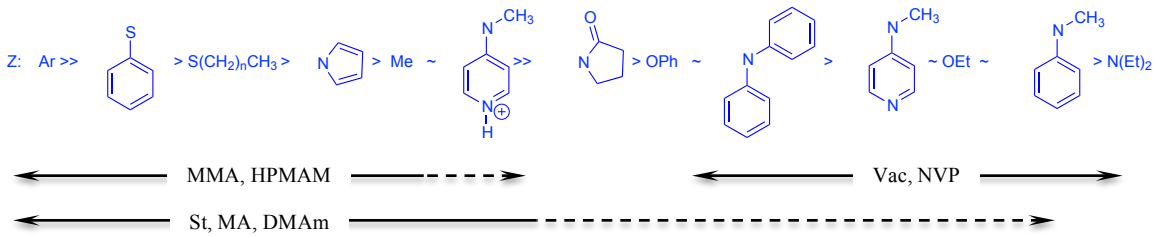


**Figure 1.6.** Activity trend of RAFT agent based on Z functionality for polymerizing variety of monomers. Dashed lines indicate limited control is provided.

### 1.4.3. Synthesis of Block Copolymers *via* RAFT Polymerization

The vast majority of homopolymer chains prepared *via* RAFT polymerization contain the RAFT agent as an end group. Such a homopolymer can be considered a macro-RAFT agent, where the original R group is replaced with a polymeric unit. In principle, a macro-RAFT agent can be used similar to a RAFT agent to synthesize block copolymers *via* subsequent polymerization of another monomer (Figure 1.7).

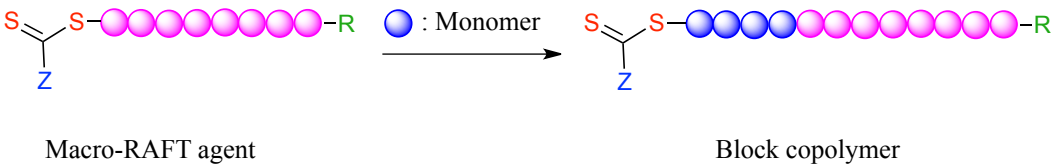


**Figure 1.7.** Block copolymer synthesis *via* RAFT polymerization.

Sequential RAFT polymerization, with purification after each polymerization step, can be utilized to make di-, tri-, and tetra- block copolymers. There are two key factors for preparing well-defined block copolymers *via* sequential RAFT polymerization. First, a RAFT agent with proper Z group functionality for all monomers being polymerized is crucial. The selected RAFT agent should have a high chain transfer coefficient (Φ) for all steps throughout the polymerization. If the Z is not suitable for either of the monomers, the quality of the final product will be affected. Order of polymerization is another important factor, because the first polymeric block functions as the R group of the macro-RAFT agent for the polymerization of the second monomer. Thus all requirements for the RAFT agent R group discussed earlier, apply to the R group of the macro-RAFT agent. It should be a good homolytic leaving group and also a good initiator at the reinitiation step

of the second RAFT polymerization. Thus, monomers that make tertiary radicals should be polymerized prior to those that make secondary radicals.

### 1.5. Self-Assembly of Block Copolymers

Block copolymers are made of two or more chemically distinct polymeric blocks connected together through a covalent or non-covalent bond. Because of different physical and chemical properties of its building blocks, block copolymers can self-assemble (or phase-separate) into a variety of architectures in solution or solid-state.[11,12] Phase-separation of tri- and tetra- block copolymers results in exotic complicated structures that are beyond the scope of this thesis and will not be discussed.[13-17] Figure 1.8 provides some of the common morphologies produced by solution and solid-state self-assembly of diblock copolymers.[18] Solution and solid-state self-assembly of diblock copolymers will be discussed in details.

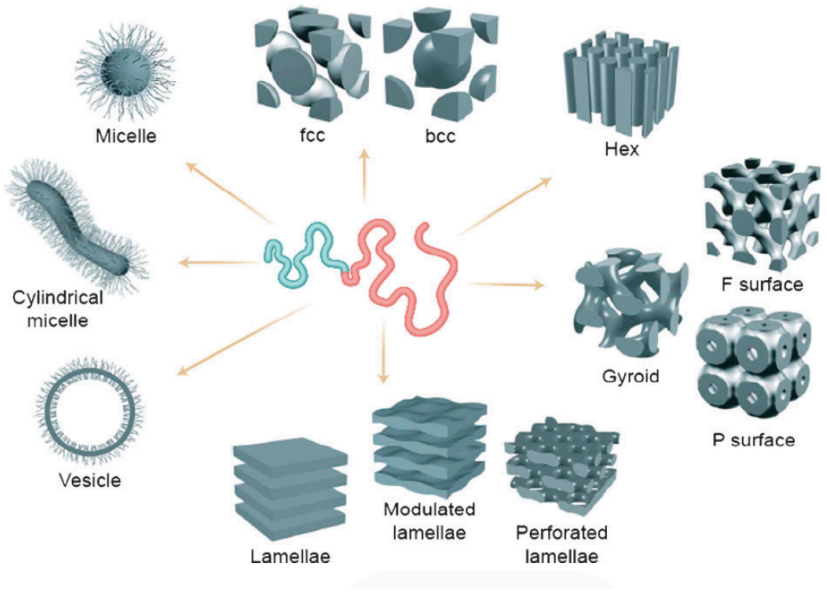


**Figure 1.8.** Possible self-assembled morphologies made of diblock copolymers (Adopted with permission from reference 18).[18]

#### 1.5.1. Solid-State Self-Assembly of Block Copolymers

After this point, "diblock" copolymers are referred to as "block" copolymers. One of the interesting properties of block copolymers is their ability to phase-separate in solid form. Block copolymers, because of inherent immiscibility of its building blocks, can form

well-defined self-assembled structure with predictable size and morphology.[18,19] In order to reduce the total interfacial energy of the two immiscible blocks of a block copolymer ($\Delta G_{mix}$), it self-assembles into a morphology with minimal interfacial area. Formation of different morphologies depends on two competing factors: interfacial energy between the two blocks (enthalpic contribution ($\Delta H_{mix}$)) and chain stretching (entropic contribution ($\Delta S_{mix}$)).[12,20] The correlation between enthalpic and entropic factors is explained by Gibbs free energy of mixing equation as was originally formulated by Flory and Huggins:

$$\frac{\Delta G_{mix}}{RT} = \underbrace{\frac{\Phi_1}{N_1} Ln\Phi_1 + \frac{\Phi_2}{N_2} Ln\Phi_2}_{\text{entropy factor}} + \underbrace{\chi_{12}\Phi_1\Phi_2}_{\text{enthalpy factor}} \qquad \text{(Eq. 1.3)}$$

In this formula, R is the Boltzmann gas constant, $\Phi_1$ is the volume fraction of polymer 1, $N_1$ is the number of repeat units of polymer 1 (also referred to as its degree of polymerization; DP), and $\chi_{12}$ is the Flory-Hoggins parameter for the two blocks which indicates their level of incompatibility. The degree of stretching of a polymeric block directly depends on its volume fraction ($\Phi$). Figure 1.9 illustrates possible block arrangements to minimize the interface of the two blocks, depending on their relative volume fractions.[21]

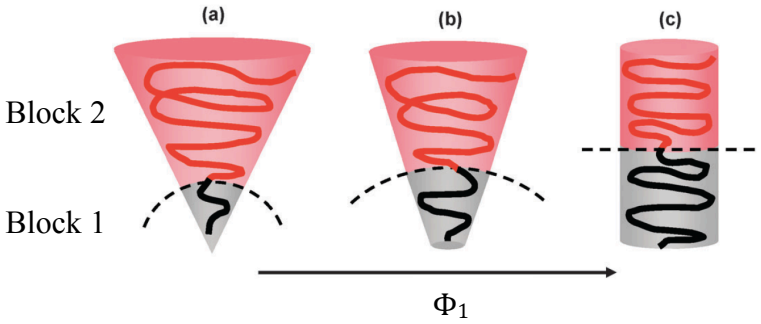


**Figure 1.9.** Possible arrangement to minimize the interface energy of two blocks based on their relative volume fractions ($\boldsymbol{\Phi}$) (Adopted with permission from reference 21).[21]

When the volume fraction of a block is very small, it aggregates into spherical domains while the other block surrounds it (a; Figure 1.9). As the volume fraction increases, to minimize stretching required to reduce the interface, less curved interfaces are adopted

leading to cylinder and lamellae morphologies (b and c; Figure 1.9).[21] Thus, as a function of composition, the two immiscible blocks phase-separate into morphologies including spheres, cylinders, bicontinuous gyroids, and lamellae shown in Figure 1.10. The phase diagram can be used to explain these observed morphologies (Figure 1.10). There are three important factors to be noted in the phase diagram: total degree of polymerization (N, where $N = N_1 + N_2$), relative volume fractions (($\Phi_1$ and $\Phi_2$), ($\Phi_1 + \Phi_2 = 1$)), and the Flory-Huggins parameter ($\chi_{12}$). Block copolymers with $\chi_{12}N < 10$ are considered to have weak segregation limit (WSL) and regardless of the volume fraction of the blocks, produce disordered morphologies. To form ordered morphologies, $\chi_{12}N$ must be more than 10.5, *i.e.* have strong segregation limit (SSL). By manipulating relative volume fraction of the two blocks with a specific $\chi_{12}N$ (where $\chi_{12}N > 10.5$), order-to-order transitions between morphologies occur (Figure 1.10).[11,12,22]

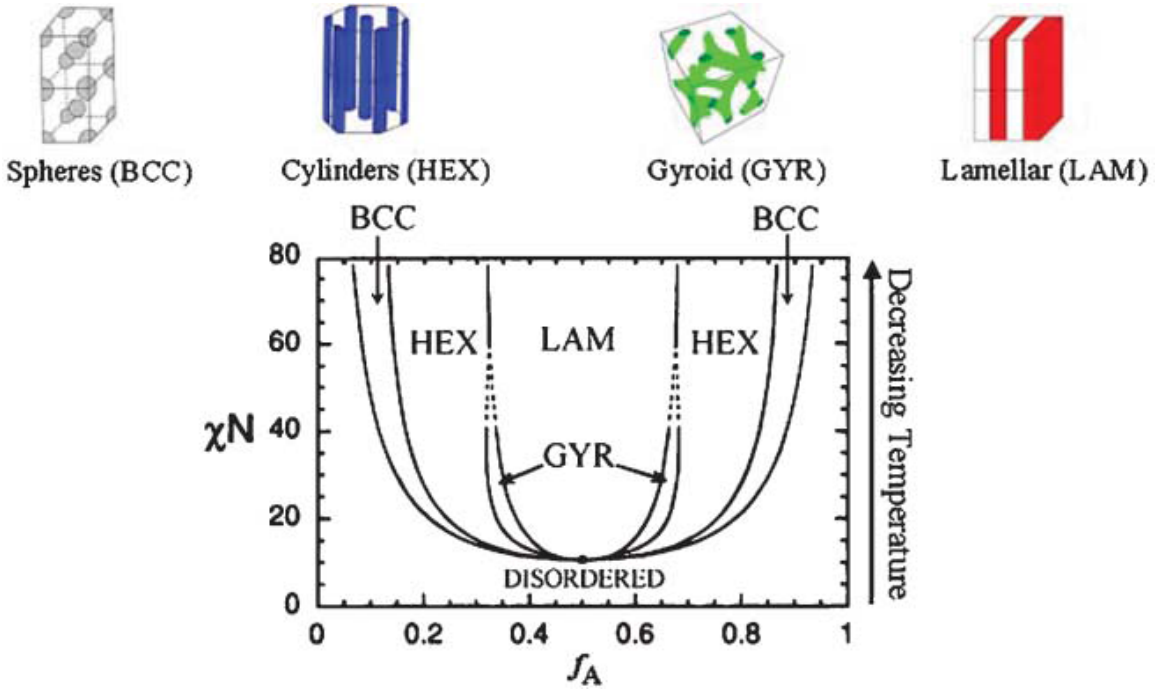


**Figure 1.10.** Top: Solid-sate block copolymers morphologies. Bottom: Phase diagram explaining the correlation of segregation limit ($\chi N$) and volume fraction ($\Phi$ ($f_A$)) with produced morphologies (Adopted with permission from reference 23).[23]

Phase-separated block copolymers can be used as templates to pattern bulk materials *via* top-down approach.[19] A novel potential application of self-assembled block copolymers

is their use as membranes with nanometer pore sizes.[24-27] These materials are excellent structure directing agents for metal salts and preparation of nanoparticles.[28,29] Solid-state self-assembled block copolymer materials have potential applications in photonic crystals,[30] solar cells,[31,32] holography,[33,34] and thin-film nanolithography.[35,36] Polymers containing inorganic elements, such as silicon and transition metals, are great ceramic precursors.[37] Self-assembly of block copolymers with at least one inorganic block produces nanometer inorganic domains. Pyrolysis of these materials form ceramics with good control over the fine structure of the final product.[19]

### 1.5.2. Solution-State Self-Assembly of Block Copolymer

A popular method to obtain solution self-assembly involves two solvents; a common solvent that dissolves both blocks and a selective solvent that only dissolves one of the blocks and is considered an anti-solvent (non-solvent) for the other block. Compared to solid-state self-assembly, introducing solvents increases the level of complexity. In solution-state self-assembly, new terms such as $\chi_{1S}, \chi_{2S}, \chi_{1N,}, \chi_{2N}$, and $\chi_{SN}$ are involved where S stands for the good solvent, N stands for the selective solvent (non-solvent), and 1 and 2 refer to the two individual blocks of the block copolymer.[11] Self-assembly behavior of block copolymers performed in aqueous media represents the majority of the current phase behavior studies, although the same principal may be applied to organic media. Block copolymers where 20-42 % of the overall volume fraction is composed of hydrophilic block ($0.42 > \Phi_{hydrophilic} > 0.2$) are expected to form vesicles (polymersomes). Those with $0.5 > \Phi_{hydrophilic} > 0.42$ form rod micelles, whereas block copolymers with $\Phi_{hydrophilic} > 0.5$ form spherical micelles (Figure 1.11).[38]

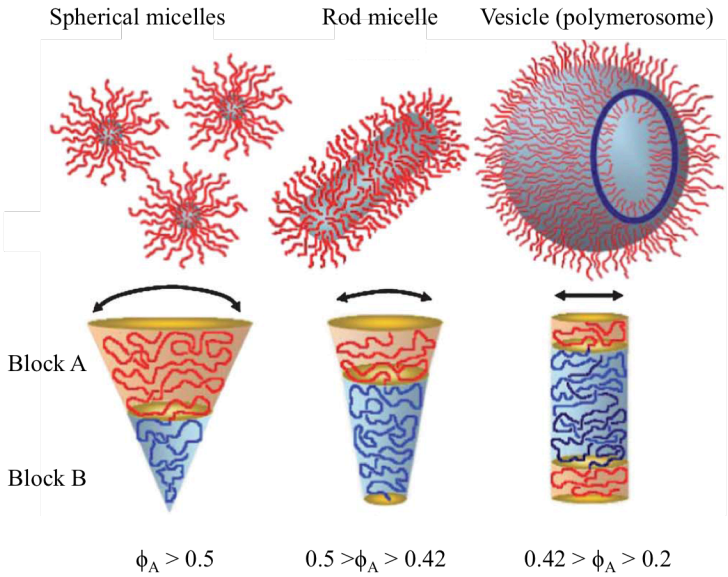


**Figure 1.11.** Solution self-assembled morphologies in aqueous media based on volume fraction of the hydrophilic block (Block A; $\Phi_A$) (Adopted with permission from reference 38).[38]

Solution-state self-assembled structures have potential applications in targeted drug delivery systems, in nanoreactors, as template to make nanoparticles, and as stimuli responsive material.[11,39]

## 1.6. Metallopolymers

### 1.6.1. General Introduction on Metallopolymers

Metal containing polymers (metallopolymers) refer to a large class of macromolecules that contain metal centers. Metallopolymers bring together the synthetic efficiency and versatility of conventional organic polymers with the unique redox, responsive, and catalytic properties of inorganic metals.[40] Coordination polymers are a large class of metallopolymers in which the polymer backbone contains Lewis base sites that coordinate to metals.[41-43] The main focus of this dissertation is on synthetic metallopolymers where the metal center is confined to metallocenes.

Over the last decade, metallopolymers have gained increased attention because of their unique physical and chemical properties that arise from the incorporation of metal centers into a polymer.[40,44-47] Based on the position of the metal center within the macromolecule, this class of material can be divided into main-chain and side-chain functionalized metallopolymers. Main-chain functionalized metallopolymers incorporate

metal atoms within the polymer backbone. Whereas in side-chain functionalized metallopolymers, metal atoms are pendent to an organic polymeric backbone. Figure 1.12 shows a schematic illustration of this two class of metallopolymers.

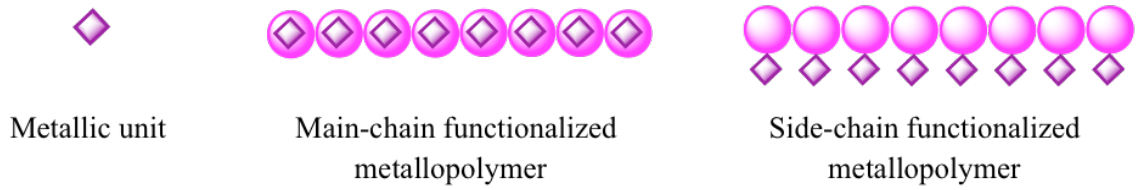


**Figure 1.12.** Schematic representation of a main-chain and a side-chain functionalized metallopolymer.

When the metal segment is incorporated within monomer structure, polymerization results in pre-functionalized metallopolymer.[48] In a post-functionalized metallopolymer, the organic polymer chain is synthesized and then metal segments are incorporated after polymerization. A disadvantage of post functionalizing lies in incomplete incorporation of the metal segment over the entire polymer chain.

Since the first report on metallocene-based metallopolymers in 1955,[49] there has been substantial interest in this class of material because of their unique electrical, optical, biological, thermal, magnetic, and catalytic properties. In 1950s, there was an intense interest in metallopolymers that was identified as a new class of polymeric material with applications in coatings and colorants.[50]

### 1.6.2. Metallocene Containing Metallopolymers

Metallocene refers to compounds consist of two cyclopentadienyl rings coordinated to a metal center where cyclopentadienyl is a $\eta^5$ ligand. Because of their high thermal stability, reversible redox chemistry, and many other fascinating properties that arise from this unique organometallic sandwich-like structure, metallocene containing polymers attract significant attention in material sciences with applications in catalysis, redox sensors, magnetic materials, ceramic materials, nanolithography, and biomedical systems.[40,47]

There are two major types of metallocene containing metallopolymers: main-chain polymers with metallocene being an integral part of the polymer backbone and side-chain

in which the metallocene is a pendant group.[40] Ferrocene-based metallopolymers, either in the side-chain or in the main-chain, are the most studied metallocene-based materials. There are many reports on different metallocene-based metallopolymers where a variety of metal atoms such as Fe, Co, Ni, Cr, and V are incorporated into the polymer chain. This report will highlight some of the recent achievements where ferrocene or cobaltocene is incorporated into the polymer. A broader discussion about other metals contained in a metallopolymer is beyond the scope of this report.

### 1.6.3. Ferrocene-Based Metallopolymers

Iron is the second most abundant metal and the fourth most abundant element. Discovery of ferrocene in 1951 had an intense influence on transition metal chemistry. Ferrocene-based polymers (either side-chain or main-chain) represent the vast majority of metallocene containing polymers in the literature.[51-56] The first reported metallocene containing metallopolymer, poly(vinylferrocene) (**1.5**), was made using free radical polymerization of vinyl ferrocene (**1.4**) (Figure 1.13).[49] Initial attempts were focused on polymerization of vinylferrocene *via* free radical, cationic, and anionic polymerization to produce well-defined high molecular weight poly(vinylferrocene) metallopolymer. Lack of control over polydispersity and molecular weight limited research progress.

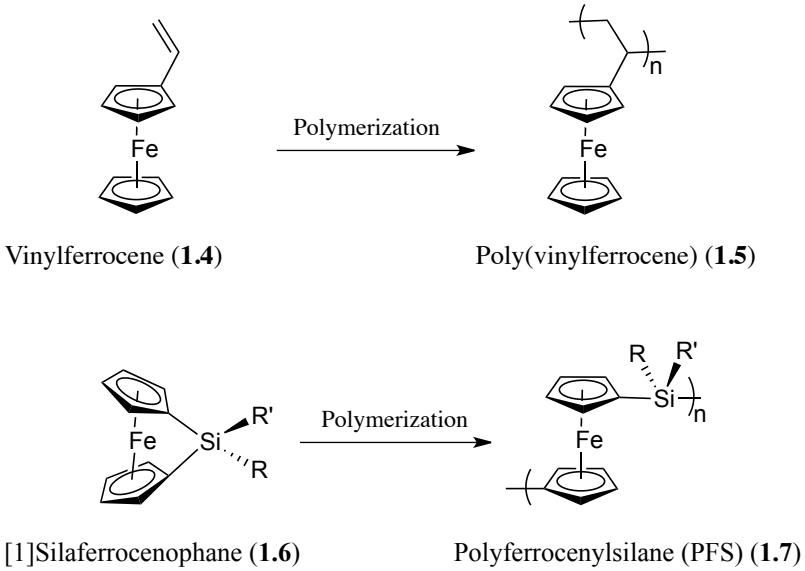


**Figure 1.13.** Polymerization of vinylferrocene (**1.4**) resulted in poly(vinylferrocene) (**1.5**). ROP of strained [1]silaferrocenophanes (**1.6**) resulted in polyferrocenylsilane (PFS) (**1.7**).

In 1992, the Manners Group established a major milestone in the field of metallopolymers by reporting ring opening polymerization (ROP) of the highly strained [1]silaferrocenophane (**1.6**) to synthesize polyferrocenylsilane (PFS; **1.7**) (Figure 1.13).[57] Today, with the advancement of synthetic methodologies and new methods in polymer characterization, well-defined metallopolymer can be prepared in scalable yields.

The Manners Group, a pioneer in this area, utilized thermal and anionic ROP of strained [1]silaferrocenophanes to prepare well-controlled homo- and block copolymers containing polyferrocenylsilane (PFS) blocks.[54-56] After this breakthrough report, the field has expanded dramatically and various PFS containing block copolymers have been developed with applications in material sciences such as magnetic shaped ceramics, plasma etch resist materials, and nanolithography.[56]

#### 1.6.3.1. Self-Assembly of PFS Containing Block Copolymers

Sequential ROP allows the preparation of PFS containing block copolymers.[58-61] Changing the substituents at the silicon center can tune the physical properties of PFS. Symmetrical substituents on silicon (R = R′) result on crystalline PFS, whereas asymmetric substituents (R ≠ R′) result in amorphous PFS (Figure 1.13).[62,63] For solid-state self-assembly purposes, amorphous PFS is preferred to prevent crystal breakout upon thermal annealing. As an example, solid-state phase-separation behavior of PS-*b*-PFS (amorphous PFS with ethyl/methyl substituent) is provided. By changing volume ratio of the constructing blocks, four different morphologies *e.g.* sphere, hexagonally packed cylinder, double gyroid, and lamella were obtained (Figure 1.14).[64-66]

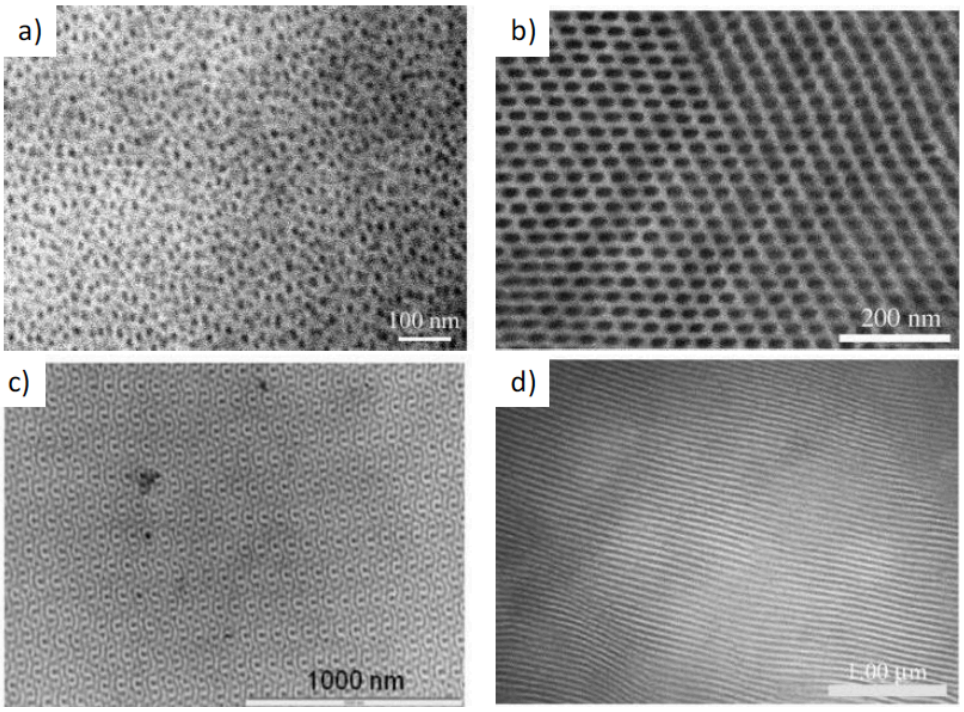


**Figure 1.14.** Solid-state self-assembly behavior of PS-*b*-PFS producing sphere (a),[65] hexagonally packed cylinder (b),[65] double gyroid (c),[66] and lamella (d)[65] obtained by manipulating relative volume fraction of two constructing blocks (Adopted with permission from reference 65 and 66).

PFS was used as a resist material in electron beam lithography (EBL) producing fine patterns (Figure 1.15).[67,68] PFS containing phase-separated structures have found applications in bottom-up lithography.[19] Etching away the non-PFS regions of self-assembled morphologies allows pattern transfer of the self-assembled features onto an underlying substrate.[69] In this method, self-assembly is used to create patterns, followed by selectively etching the non-PFS block and transferring the pattern to the substrate. At the last step PSF is removed leaving behind the patterned substrate.

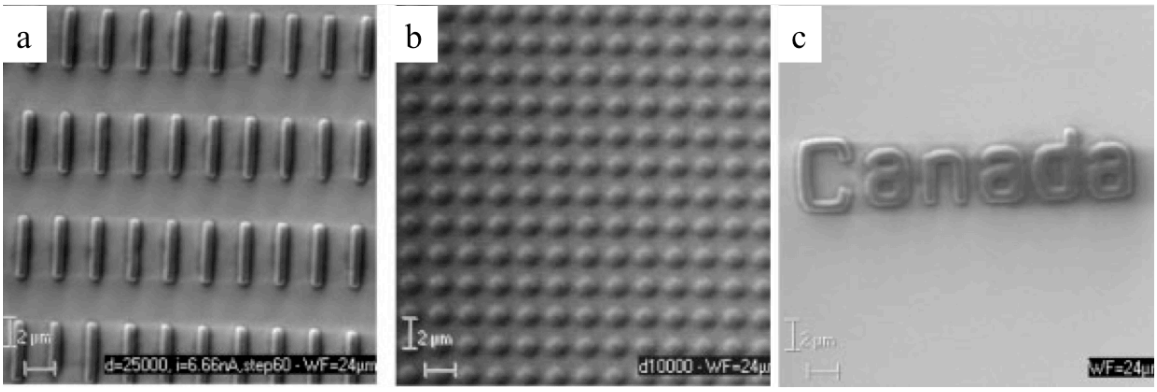


**Figure 1.15.** Patterns created by EBL using PFS as resist material (Adopted with permission from reference 67).[67]

PFS with high char yield has been used in networks or in self-assembled morphologies to make shaped and patterned magnetic ceramics with interesting properties.

Crystalline PFS (R = R´) is commonly used for solution self-assembly studies. Taking advantage of crystalline nature of PFS, exotic structures have been achieved by crystallization driven self-assembly of PFS containing block copolymers.[70-74] Figure 1.16 shows two examples of many interesting structures produced by self-assembly of PFS containing block copolymers.

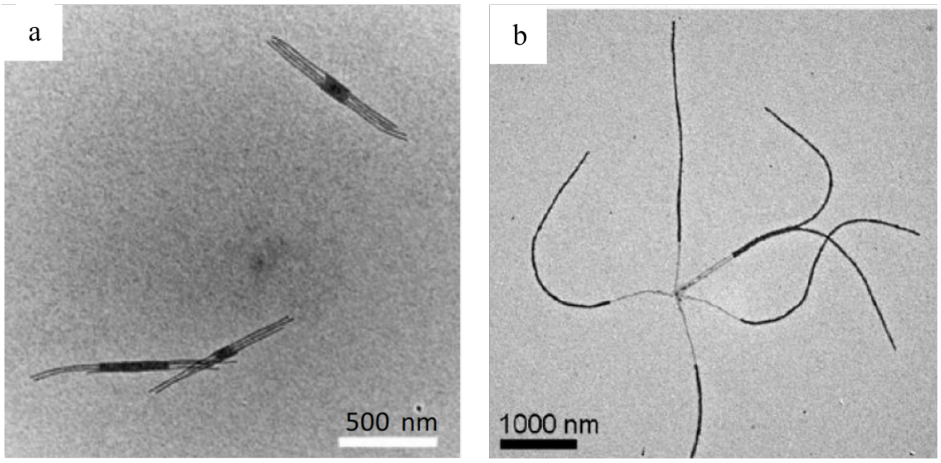


**Figure 1.16.** Two examples of solution self-assembly structures produced by PFS containing block copolymers (a: scarf shape platelets,[74] b: star shape structures[73]) (Adopted with permission from reference 73 and 74).

### 1.6.4. Cobaltocenium Containing Metallopolymers

The novelty of PFS has attracted attention to incorporate other metallocenes into the polymer chain. In comparison to well-studied ferrocene containing metallopolymers, cobaltocene have received far less attention due to the difficulties in preparing its derivatives.[47,75] Cobaltocene (Co(II)) with 19 electrons is not stable and is readily oxidized to a cationic 18 electron cobaltocenium (Co(III)), which is isoelectronic with ferrocene. The synthetic challenges have limited the expansion of cobaltocene and cobaltocenium containing metallopolymer studies.

The Manners Group reported sequential ROP of strained [1]silaferrocenophanes and dicarba [2]cobaltococenophane followed by an oxidation step resulting in PFS-*b*-poly(cobaltoceniumethylene) (PFS-*b*-PCE$^+$; **1.8**) block copolymer (Figure 1.17). This is the only main-chain functionalized cobaltocenium containing metallopolymer to date.[59]

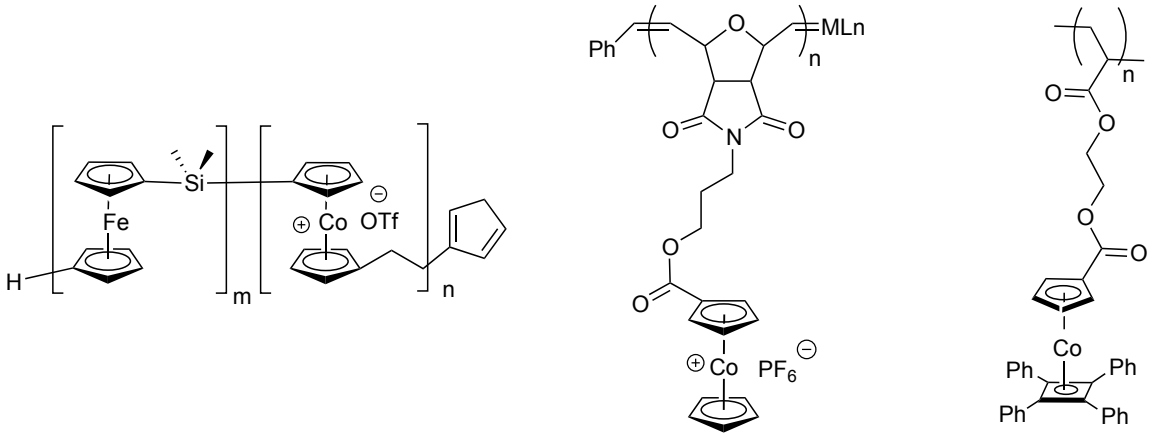


**1.8** **1.9** **1.10**

**Figure 1.17.** Structure of PFS-*b*-(PCE$^+$) block copolymer (**1.8**), side-chain functionalized cobaltocenium containing metallopolymer (**1.9**), and CpCoCb side-chain functionalized metallopolymer (**1.10**).

Because of high affinity of cobaltocene to oxidation and the inertness nature of cobaltocenium salts, is very challenging to functionalize these molecules. The Tang Group has successfully developed a synthetic methodology to functionalize cobaltocenium and made highly pure cobaltocenium monocarboxylic acid as monomeric precursor. This group reported the first example of side-chain functionalized cobaltocenium metallopolymers *via* post functionalization of homo- and block

copolymers, converting 60-80% of available active sites.[76] Although quantitative substitution was not obtained, interesting solvent dependent solution-state self-assembly behavior was observed. Free radical polymerization of cobaltocenium containing monomer resulted in metallopolymers with counter anion dependent tunable solubility properties.[77] To have control over molecular weight and PDI, controlled polymerization methods were explored. RAFT polymerization of methacrylate cobaltocenium containing monomer resulted in first example of well-defined, high molecular weigh side-chain functionalized cobaltocenium metallopolymer.[78] Applying sequential RAFT polymerization, heterobimetallic metallopolymer with cobaltocenium and ferrocene containing blocks was prepared.[79] In 2012, the same group utilized ring opening metathesis polymerization (ROMP) of norbornene-based cobaltocenium containing monomers to prepare high molecular weigh homo- and block copolymers with variable counter anions (**1.9**).[80,81] Interesting counter anion exchange effects were observed for this systems. In a novel study various *β*-lactam antibiotics, including penicillin, ampicillin, amoxicillin, and cefazolin, were incorporated as counter anion and their biological activities were studied.[82]

In all examples mentioned so far, the cobalt center is a cationic cobaltocenium (Co(III)). Alternatively, the Ragogna Group reported the first neutral side-chain $\eta^5$-cyclopentadienyl-cobalt-$\eta^4$-cyclobutadiene (CpCoCb) functionalized metallopolymer (**1.10**). This mixed sandwich metallocene is an 18 electron complex, electronically neutral and isoelectronic to ferrocene and cobaltocenium.[83] The cyclobutadiene (Cb) ring was functionalized with either four methyl, or four phenyl substituents and free radical polymerization was used to prepare metallopolymers. However, polymerization reaction time was lengthy (days) and despite up to 90% monomer conversion, only low molecular weight polymers were produced.[83] Based on the fact that high molecular weight metallopolymers with narrow PDI were not obtained, investigating other methods and techniques to overcome this issue was our interest.

### 1.7. Thesis Scope

The main focus of this thesis is on the synthesis of well-defined side-chain functionalized $\eta^5$-cyclopentadienyl-cobalt-$\eta^4$-cyclobutadiene (CpCoCb) containing homo- and block copolymers *via* reversible addition fragmentation transfer (RAFT) polymerization. The

first goal of this thesis was to develop a controlled polymerization method to obtain well-defined high molecular weight CpCoCb containing metallopolymers. The studies involved establishing protocols are discussed in chapter 2. Once controlled polymerization of CpCoCb monomer was accomplished, several block copolymers were prepared *via* sequential RAFT polymerization. Chapter 3 details preparation of a block copolymer in which one block is a CpCoCb containing metallopolymer and the other block is phosphonium salt functionalized polystyrene. Synthesis, characterization, solution and solid-state self-assembly of this block copolymer is discussed in detail. Chapter 4 reports the synthesis of a block copolymer consists of a polydimethylsiloxane (PDMS) block and CpCoCb containing metallopolymer block. This material is used as ink in soft lithography using PDMS stamps. Solution and solid-state self-assembly of the block copolymer is detailed. Chapter 5 introduces the synthesis of a series of CpCoCb monomers where the Cb ring is decorated with different functionalities such as ferrocene, and thiophene. These highly metalized monomers are used to make metal rich materials. Chapter 6 summarizes the key results discussed throughout previous chapters and provides an outline on the future directions for this research.

**1.8. References**

(1) Elias, H. G., *Macromolecules*,Vol. 2, Wiley-VCH: Weinheim, Germany, 2009.

(2) Odian, G. G., *Principles of polymerization*,Wiley-Interscience: Hoboken, N.J, 2004.

(3) Stille, J. K. *J. Chem. Educ.* **1981**, *58*, 862-866.

(4) Moad, G.; Solomon, D. H., *The chemistry of free radical polymerization*,Pergamon: Tarrytown, N.Y. U.S.A; Oxford, OX, U.K, 1995.

(5) Webster, O. W. *Science* **1991**, *251*, 887-893.

(6) Moad, G.; Rizzardo, E.; Thang, S. H. *Acc. Chem. Res.* **2008**, *41*, 1133-1142.

(7) Keddie, D. J. *Chem. Soc. Rev.* **2014**, *43*, 496-505.

(8) Lowe, A. B.; McCormick, C. L. *Prog. Poly. Sci.* **2007**, *32*, 283-351.

(9) Zetterlund, P. B.; Kagawa, Y.; Okubo, M. *Chem. Rev.* **2008**, *108*, 3747-3794.

(10) Keddie, D. J.; Moad, G.; Rizzardo, E.; Thang, S. H. *Macromolecules* **2012**, *45*, 5321-5342.

(11) Mai, Y.; Eisenberg, A. *Chem. Soc. Rev.* **2012**, *41*, 5969-5985.

(12) Bates, F. S. *Science* **1991**, *251*, 898-905.

(13) Hayashida, K.; Kawashima, W.; Takano, A.; Shinohara, Y.; Amemiya, Y.; Nozue, Y.; Matsushita, Y. *Macromolecules* **2006**, *39*, 4869-4872.

(14) Aissou, K.; Choi, H. K.; Nunns, A.; Manners, I.; Ross, C. A. *Nano Lett.* **2013**, *13*, 835-839.

(15) Aissou, K.; Nunns, A.; Manners, I.; Ross, C. A. *Small* **2013**, *9*, 4077-4084.

(16) Choi, H. K.; Nunns, A.; Sun, X. Y.; Manners, I.; Ross, C. A. *Adv. Mater.* **2014**, *26*, 2474-2479.

(17) Nunns, A.; Ross, C. A.; Manners, I. *Macromolecules* **2013**, *46*, 2628-2635.

(18) Bucknall, D. G.; Anderson, H. L. *Science* **2003**, *302*, 1904-1905.

(19) Nunns, A.; Gwyther, J.; Manners, I. *Polymer* **2013**, *54*, 1269-1284.

(20) Matsen, M. W.; Schick, M. *Phys. Rev. Lett.* **1994**, *72*, 2660-2663.

(21) Discher, D. E.; Ahmed, F. *Annu. Rev. Biomed. Eng.* **2006**, *8*, 323-341.

(22) Palma, C. A.; Cecchini, M.; Samorì, P. *Chem. Soc. Rev.* **2012**, *41*, 3713-3730.

(23) Huck, W. T. S. *Chem. Commun.* **2005**, 4143-4148.

(24) Fu, G. D.; Kang, E. T.; Neoh, K. G. *Langmuir* **2005**, *21*, 3619-3624.

(25) Nunes, S. P.; Car, A. *Ind. Eng. Chem. Res.* **2013**, *52*, 993-1003.

(26) Rao, J.; De, S.; Khan, A. *Chem. Commun.* **2012**, *48*, 3427-3429.

(27) Taubert, A.; Napoli, A.; Meier, W. *Curr. Opin. Chem. Biol.* **2004**, *8*, 598-603.

(28) Lisiecki, I.; Pileni, M. P. *J. Am. Chem. Soc.* **1993**, *115*, 3887-3896.

(29) Yin, D.; Horiuchi, S.; Morita, M.; Takahara, A. *Langmuir* **2005**, *21*, 9352-9358.

(30) Edrington, A. C.; Urbas, A. M.; Derege, P.; Chen, C. X.; Swager, T. M.; Hadjichristidis, N.; Xenidou, M.; Fetters, L. J.; Joannopoulos, J. D.; Fink, Y.; Thomas, E. L. *Adv. Mater.* **2001**, *13*, 421-425.

(31) Botiz, I.; Darling, S. B. *Mater. Today* **2010**, *13*, 42-51.

(32) Orilall, M. C.; Wiesner, U. *Chem. Soc. Rev.* **2011**, *40*, 520-535.

(33) Frenz, C.; Fuchs, A.; Schmidt, H. W.; Theissen, U.; Haarer, D. *Macromol. Chem. Phys.* **2004**, *205*, 1246-1258.

(34) Schumers, J. M.; Fustin, C. A.; Gohy, J. F. *Macromol. Rapid Commun.* **2010**, *31*, 1588-1607.

(35) Kim, H. C.; Park, S. M.; Hinsberg, W. D.; Division, I. R. *Chem. Rev.* **2010**, *110*, 146-177.

(36) Galatsis, K.; Wang, K. L.; Ozkan, M.; Ozkan, C. S.; Huang, Y.; Chang, J. P.; Monbouquette, H. G.; Chen, Y.; Nealey, P.; Botros, Y. *Adv. Mater.* **2010**, *22*, 769-778.

(37) Colombo, P.; Mera, G.; Riedel, R.; Sorarù, G. D. *J. Am. Ceram. Soc.* **2010**, *93*, 1805-1837.

(38) Blanazs, A.; Armes, S. P.; Ryan, A. J. *Macromol. Rapid Commun.* **2009**, *30*, 267-277.

(39) Hu, H.; Gopinadhan, M.; Osuji, C. O. *Soft Matter* **2014**, *10*, 3867-3889.

(40) Hardy, C. G.; Zhang, J.; Yan, Y.; Ren, L.; Tang, C. *Prog. Polym. Sci.* **2014**, *39*, 1742-1796.

(41) Zhang, K.; Zha, Y.; Peng, B.; Chen, Y.; Tew, G. N. *J. Am. Chem. Soc.* **2013**, *135*, 15994-15997.

(42) Shunmugam, R.; Gabriel, G. J.; Aamer, K. A.; Tew, G. N. *Macromol. Rapid Commun.* **2010**, *31*, 784-793.

(43) Shunmugam, R.; Tew, G. N. *Macromol. Rapid Commun.* **2008**, *29*, 1355-1362.

(44) Whittell, G. R.; Hager, M. D.; Schubert, U. S.; Manners, I. *Nat. Mater.* **2011**, *10*, 176-188.

(45) Williams, K. A.; Boydston, A. J.; Bielawski, C. W. *Chem. Soc. Rev.* **2007**, *36*, 729-744.

(46) Whittell, G. R.; Manners, I. *Adv. Mater.* **2007**, *19*, 3439-3468.

(47) Hardy, C. G.; Ren, L.; Zhang, J.; Tang, C. *Isr. J. Chem.* **2012**, *52*, 230-245.

(48) Manners, I. *Angew. Chem., Int. Ed.* **1996**, *35*, 1602-1621.

(49) Arimoto, F. S.; Haven, A. C. *J. Am. Chem. Soc.* **1955**, *77*, 6295-6297.

(50) Eloi, J.-C.; Chabanne, L.; Whittel, G. R.; Manners, I. *Mater. Today* **2008**, *11*, 28-34.

(51) Kumar, M.; Pannell, K. H. *J. Inorg. Organomet. Polym. Mater.* **2007**, *17*, 105-110.

(52) Matsuura, Y.; Matsukawa, K. *Chem. Phys. Lett.* **2007**, *436*, 224-227.

(53) Hardy, C. G.; Ren, L.; Tamboue, T. C.; Tang, C. *J. Polym. Sci., Part A: Polym. Chem.* **2011**, *49*, 1409-1420.

(54) Wang, X.; Liu, K.; Arsenault, A. C.; Rider, D. A.; Ozin, G. A.; Winnik, M. A.; Manners, I. *J. Am. Chem. Soc.* **2007**, *129*, 5630-5639.

(55) Smith, G. S.; Patra, S. K.; Vanderark, L.; Saithong, S.; Charmant, J. P. H.; Manners, I. *Macromol. Chem. Phys.* **2010**, *211*, 303-312.

(56) Schacher, F. H.; Rupar, P. A.; Manners, I. *Angew. Chem., Int. Ed.* **2012**, *51*, 7898-7921.

(57) Foucher, D. A.; Tang, B.; Manners, I. *J. Am. Chem. Soc.* **1992**, *114*, 6246-6248.

(58) Cao, L.; Manners, I.; Winnik, M. A. *Macromolecules* **2001**, *34*, 3353-3360.

(59) Gilroy, J. B.; Patra, S. K.; Mitchels, J. M.; Winnik, M. A.; Manners, I. *Angew. Chem., Int. Ed.* **2011**, *50*, 5851-5855.

(60) Ni, Y.; Rulkens, R.; Manners, I. *J. Am. Chem. Soc.* **1996**, *118*, 4102-4114.

(61) Rulkens, R.; Ni, Y.; Manners, I. *J. Am. Chem. Soc.* **1994**, *116*, 12121-12122.

(62) Rider, D. A.; Cavicchi, K. A.; Power-Billard, N.; Russell, T. P.; Manners, I. *Macromolecules* **2005**, *38*, 6931-6938.

(63) Hsiao, M. S.; Yusoff, S. F. M.; Winnik, M. A.; Manners, I. *Macromolecules* **2014**, *47*, 2361-2372.

(64) Eloi, J. C.; Rider, D. A.; Wang, J. Y.; Russell, T. P.; Manners, I. *Macromolecules* **2008**, *41*, 9474-9479.

(65) Rider, D. A.; Cavicchi, K. A.; Power-Billard, K. N.; Russell, T. P.; Manners, I. *Macromolecules* **2005**, *38*, 6931-6938.

(66) Gwyther, J.; Lotze, G.; Hamley, I.; Manners, I. *Macromol. Chem. Phys.* **2011**, *212*, 198-201.

(67) Clendenning, S. B.; Aouba, S.; Rayat, M. S.; Grozea, D.; Sorge, J. B.; Brodersen, P. M.; Sodhi, R. N. S.; Lu, Z. H.; Yip, C. M.; Freeman, M. R.; Ruda, H. E.; Manners, I. *Adv. Mater.* **2004**, *16*, 215-219.

(68) Wing, Y. C.; Clendenning, S. B.; Berenbaum, A.; Lough, A. J.; Aouba, S.; Ruda, H. E.; Manners, I. *J. Am. Chem. Soc.* **2005**, *127*, 1765-1772.

(69) Gokan, H.; Esho, S.; Ohnishi, Y. *J. Electrochem. Soc.* **1983**, *130*, 143-146.

(70) Gädt, T.; Ieong, N. S.; Cambridge, G.; Winnik, M. A.; Manners, I. *Nat. Mater.* **2009**, *8*, 144-150.

(71) Rupar, P. A.; Chabanne, L.; Winnik, M. A.; Manners, I. *Science* **2012**, *337*, 559-562.

(72) Qiu, H.; Russo, G.; Rupar, P. A.; Chabanne, L.; Winnik, M. A.; Manners, I. *Angew. Chem., Int. Ed.* **2012**, *51*, 11882-11885.

(73) Qiu, H.; Cambridge, G.; Winnik, M. A.; Manners, I. *J. Am. Chem. Soc.* **2013**, *135*, 12180-12183.

(74) Gadt, T.; Ieong, N. S.; Cambridge, G.; Winnik, M. A.; Manners, I. *Nat. Mater.* **2009**, *8*, 144-150.

(75) Issa, I. M.; Aly, M. M. *J. Inorg. Nucl. Chem.* **1973**, *35*, 295-297.

(76) Ren, L.; Hardy, C. G.; Tang, C. *J. Am. Chem. Soc.* **2010**, *132*, 8874-8875.

(77) Ren, L.; Hardy, C. G.; Tang, S.; Doxie, D. B.; Hamidi, N.; Tang, C. *Macromolecules* **2010**, *43*, 9304-9310.

(78) Zhang, J.; Ren, L.; Hardy, C. G.; Tang, C. *Macromolecules* **2012**, *45*, 6857-6863.

(79) Zhang, J.; Yan, Y.; Chen, J.; Chance, W. M.; Hayat, J.; Gai, Z.; Tang, C. *Chem. Mater.* **2014**, *26*, 3185-3190.

(80) Ren, L.; Zhang, J.; Bai, X.; Hardy, C. G.; Shimizu, K. D.; Tang, C. *Chem. Sci.* **2012**, *3*, 580-583.

(81) Ren, L.; Zhang, J.; Hardy, C. G.; Ma, S.; Tang, C. *Macromol. Rapid Commun.* **2012**, *33*, 510-516.

(82) Zhang, J.; Chen, Y. P.; Miller, K. P.; Ganewatta, M. S.; Bam, M.; Yan, Y.; Nagarkatti, M.; Decho, A. W.; Tang, C. *J. Am. Chem. Soc.* **2014**, *136*, 4873-4876.

(83) Chadha, P.; Ragogna, P. J. *Chem. Commun.* **2011**, *47*, 5301-5303.

# Chapter 2

# Overcoming a Tight Coil to Give a Random "Co" Polymer Derived from a Mixed Sandwich Cobaltocene

## 2.1. Introduction

Over the last decade metallopolymers have garnered substantial attention because of the unique physical and chemical properties that arise from incorporating inorganic elements into macromolecular.[1-7] These materials have distinct properties such as high thermal stability,[8] reversible redox switchability,[9] interesting magnetic properties,[10-12] and as a result have found applications in electrocatalysis,[13-15] sensing,[13,16,17] responsive surfaces,[18] electrode modification,[19] and photonic crystals.[20] The synthesis of block copolymers in which at least one block is a metallopolymer is especially interesting as they can self-assemble into a variety of different architectures with nanosized domains.[13,21-24] These constructs are excellent precursors for the production of inorganic nanomaterials through pyrolysis,[8,21] ozonolysis,[25] or etching.[22,26]

Metal ions can be incorporated into the main-chain as an integral component of the polymer backbone (a main-chain functionalized metallopolymer), or as a pendant group, (a side-chain functionalized metallopolymer). There are a vast variety of methods to incorporate metals into polymers, for example in the assembly of coordination polymers or simply having a pendant ligand to the polymer chain that can bind to a metal center.[27-45] Of the many different metallopolymers, those containing metallocenes have demonstrated the greatest potential for application.[43,46-48]

Ferrocene is the ubiquitous sandwich complex and it has been widely incorporated in the main-chain or side-chain of metallopolymers.[47,49-51] The Manners Group have utilized ring opening polymerization (ROP) of strained sila[1]ferrocenophanes as a novel route to prepare high molecular weight, well-controlled homo- and block copolymers.[21,52-57] Block copolymers containing polyferrocenylsilane (PFS) have been utilized as redox-active components of photonic crystal displays,[58] precursors for magnetic ceramics,[59-61]

and catalytically active nanoparticles.[49-51] These discoveries have motivated others to attempt the incorporation of other metallocenes into the polymer chain.[46,62] In comparison to the widely studied ferrocene containing systems, other metallocenes (*e.g.* cobaltocene), have received far less attention because of the difficulties associated with a non 18 electron system. Cobaltocene is a 19 electron species, highly sensitive to the ambient atmosphere and readily gets oxidized to the more stable cationic cobaltocenium ion, which is isoelectronic with ferrocene. Although the cobaltocenium fragment is stable, its incorporation into macromolecular systems can introduce solubility issues due to the cation/anion pair that makes onwards derivatization more difficult.[63] Despite the high level of interest in utilizing cobaltocenium to construct cobalt containing metallopolymers, its incorporation into polymeric materials has not been widely explored. In fact, only few key contributions on this subject have been reported.[8,13,25,64-68] The only example that details the incorporation of cobaltocenium ions in the main-chain of metallopolymers is reported by the Manners Group, where ROP of sila[1]ferrocenophanes is followed by ROP of dicarba[2]cobaltococenophane, resulting in a heterobimetallic block copolymer with ferrocene and cobaltocenium repeat units (**1.8**; Figure 2.1).[13] This block copolymer has interesting redox properties and is able to self-assemble into heterobimetallic micelles. The first example of a side-chain functionalized cobaltocenium containing block copolymer was prepared by the Tang Group *via* post functionalization of one of the blocks using cobaltocenium acyl chloride. However this did not result in the complete incorporation of the cobaltocenium on the desired block.[66] Later, the same group utilized ring opening metathesis polymerization (ROMP) resulting in high molecular weight metallopolymers with narrow polydispersity index (PDI) (**1.9**; Figure 2.1).[25,67] The material developed by the Tang Group has excellent utility in aqueous (polar) solvents especially as antimicrobials, which is directly related to the positively charged cobaltocenium unit.[69] Nevertheless, developing a cobalt containing polymer with solubility in common organic solvents (less polar) is desirable from a processability standpoint and in terms of opening opportunities for onwards chemistry.

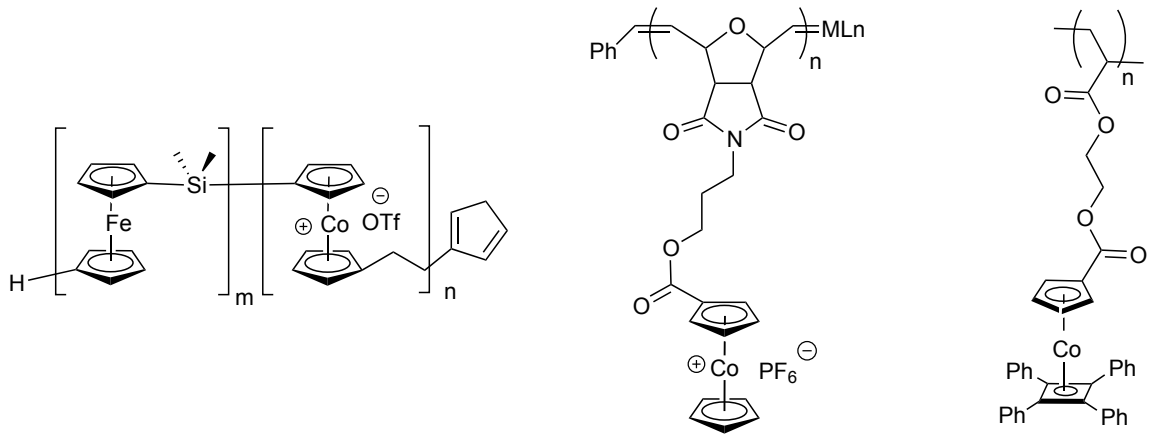


**1.8** **1.9** **1.10**

**Figure 2.1.** Main-chain functionalized metallopolymer with ferrocene and cobaltocenium repeat units (**1.8**). Side-chain functionalized cobaltocenium containing metallopolymer (**1.9**). Side-chain functionalized CpCoCb containing metallopolymer (**1.10**).

Mixed sandwich cobaltocene featuring $\eta^5$-cyclopentadienyl-cobalt-$\eta^4$-cyclobutadiene (CpCoCb) is a neutral, 18 electron species, isoelectronic with ferrocene and cobaltocenium with physical and chemical properties more closely aligned with ferrocene, such as excellent solubility in a wide range of common organic solvents.[70,71] CpCoCb also has the important advantage of the facile preparation of a wide variety of derivatives using well-established cyclodimerization chemistry from substituted alkynes, to install a functionalized cyclobutadiene (Cb) ring, which opens doors for novel, onwards chemistry, or in imposing additional chemical functionality to the sandwich complex.[72,73] The Ragogna Group has previously reported the first metallopolymer derived from polymerization of such a mixed sandwich CpCoCb containing monomer (**1.10**; Figure 2.1). In this study, the polymerization reaction time was lengthy (days) and despite up to 90% monomer conversion, only low molecular weight polymers were produced.[74] These results have motivated us to optimize the polymerization conditions by utilizing controlled radical polymerization methods for the synthesis of well-defined homo- and block copolymers. The ultimate goal was to take advantage of the neutral, organic soluble materials to access self-assembled architectures and cobalt containing nanomaterials. In this context, we have utilized reversible addition fragmentation transfer (RAFT) polymerization to prepare a new class of homo- and block copolymers, containing CpCoCb repeat unit. Through extensive studies on various RAFT conditions

for the controlled polymerization of the CpCoCb containing monomer (**2.3** (CpCoCb); Scheme 2.1), we observed that all of the employed experimental conditions produced low molecular weight polymers (*ca*. 10 kDa) (**2.5** (PolyCpCoCb); Scheme 2.1). As this was an unfortunate roadblock, through extensive studies of our system we established that the steric hindrance of the CpCoCb containing monomer (**2.3**) hampers chain growth and instead, promotes termination and chain transfer reactions, thus precluding the production of high molecular weight polymer. To overcome this steric problem, methyl acrylate (MA) with a low steric demand was utilized as a co-monomer and was copolymerized with **2.3** resulting in well-controlled, high molecular weight random copolymer (**2.8** (PolyCpCoCb-*r*-PMA); Figure 2.6). These results represent the first example of utilizing such a RAFT strategy to generate metal containing polymers using bulky monomeric starting material. This method provided the opportunity to prepare neutral, high molecular weight, organic soluble, cobalt containing polymers with a narrow PDI, which were previously inaccessible. The random copolymer **2.8** was then utilized as a macro-RAFT agent to synthesize block copolymers by polymerizing styrene (**2.9** ((PolyCpCoCb-*r*-PMA)-*b*-PS); Scheme 2.2), also with excellent control over molecular weight and PDI. The block copolymer underwent solid-state self-assembly to produce nanosized architectures, thus exhibiting a proof of principle that these materials can act as viable organic soluble precursors for inorganic nanomaterials. The details on our extensive synthetic work on producing the monomer (**2.3**), and polymers **2.8** and **2.9**, and their characterization is presented as is the preliminary results on their solid-state self-assembly.

## 2.2. Results and Discussion

### 2.2.1. Monomer Synthesis

To synthesize the monomer of interest (**2.3**), an established synthetic protocol was utilized (Scheme 2.1). By refluxing compound **2.1**[75] with 2.2 stoichiometric equivalents of diphenylacetylene in *p*-xylene for 2 days, compound **2.2** was produced and confirmed by multinuclear NMR spectroscopy and X-ray crystallography (Figure A2.1). Compound **2.2** was purified by precipitation in *n*-hexane and subsequently was reacted with acryloyl chloride and triethylamine in dichloromethane (DCM) to obtain monomer **2.3** (Scheme

2.1). Compound **2.3** was purified by column chromatography and its synthesis was verified spectroscopically, by combustion analysis, and by single crystal X-ray diffraction.

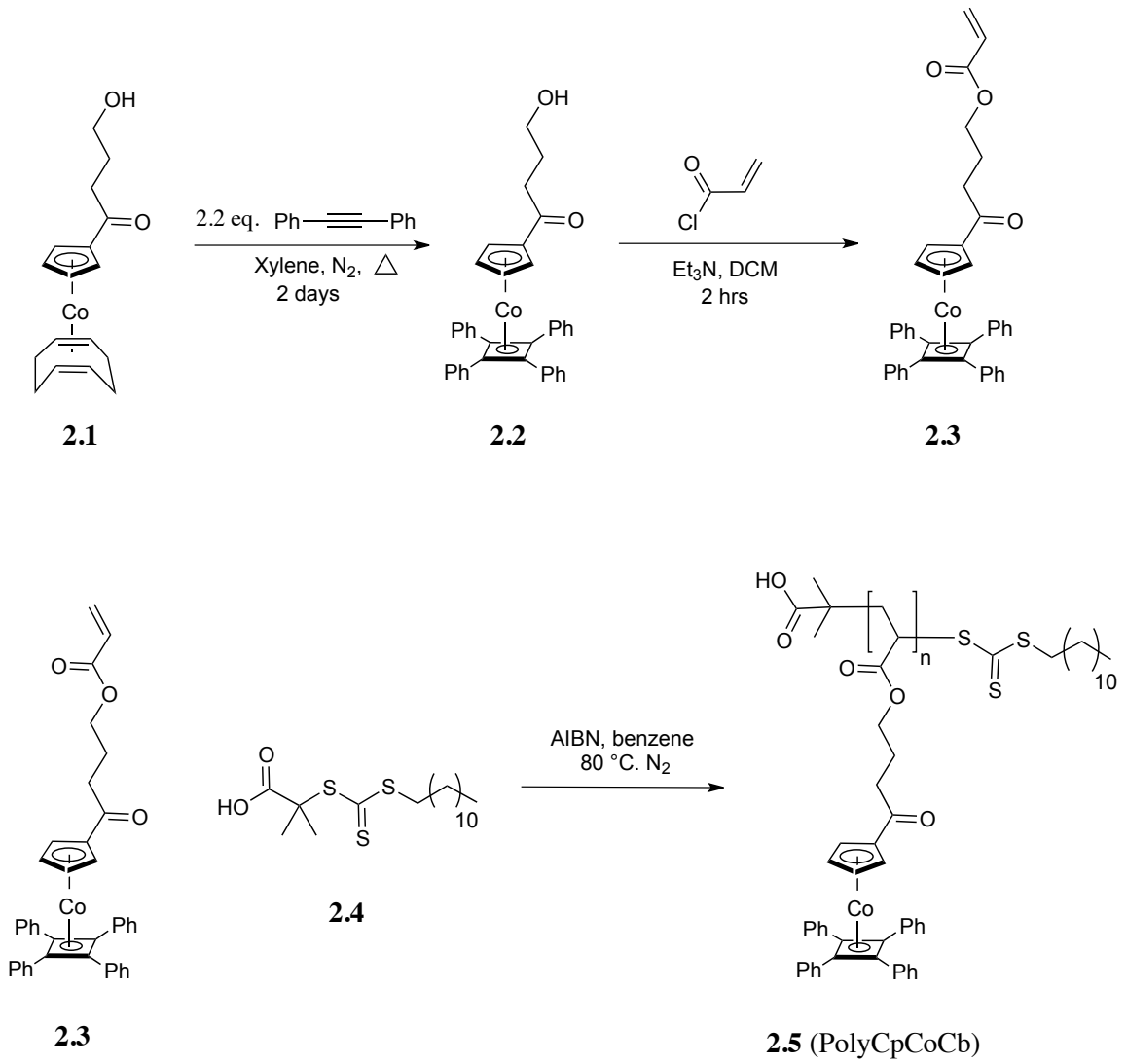


**2.1** **2.2** **2.3**

**2.4**

**2.3** **2.5** (PolyCpCoCb)

**Scheme 2.1.** Synthesis of monomer **2.3** (CpCoCb) and homopolymer **2.5** (PolyCpCoCb).

### 2.2.2. Optimizing RAFT Polymerization Condition

Polymerization of the monomer **2.3** was studied following a RAFT polymerization protocol by the use of 2-(dodecylthiocarbonothioylthio)-2-methylpropionic acid (**2.4**) as the RAFT agent and 2,2´-azobisisobutyronitrile (AIBN) as the initiator in benzene at 80 °C, and a degree of polymerization (DP) of 20 was targeted (Scheme 2.1). After 3

hours, the polymerization was halted by rapidly cooling the reaction flask. The volatiles were removed *in vacuo*, and the residue was analyzed by $^{1}$H NMR spectroscopy. Signal broadening was indicative of polymerization along with the decrease in the relative integration values of the vinyl protons. Since the signals for the end groups were overlapped by other resonances precluding their accurate integration for end group analysis, monomer conversion was used as a guide for the degree of polymerization. By comparing the integration values of unreacted monomer (vinyl protons) to the signals of the polymer, the monomer conversion was calculated to be 70%. Under an ideal set of controlled polymerization conditions, this would result in polymers with 14 repeat units (target DP = 20), and $M_n \approx$ 8 kDa. The GPC analysis of the purified polymer showed a refractive index (RI) trace corresponding to only 2 kDa (relative to PS standards) with PDI of 1.2, far smaller than the predicted value (trace **A**; Figure 2.2). Although the RI traces were analyzed relative to PS standards and the obtained molecular weight values were not absolute, the *drastic* difference between the two values was unexpected and a cause for concern.

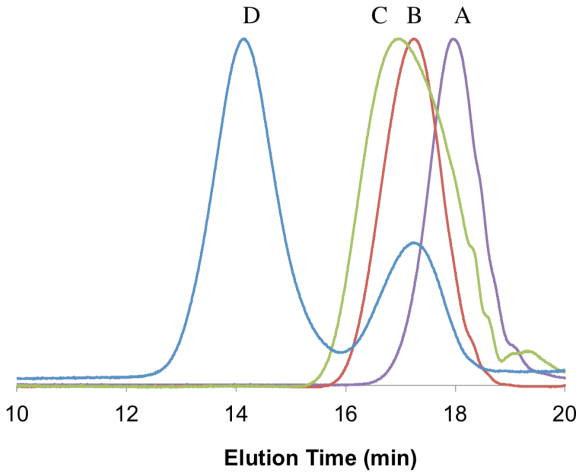


**Figure 2.2.** RI traces of purified **2.5** (target DP; A = 20, B = 60, and C = 120). Trace D is the RI trace of a block copolymer made by using **2.5** (trace B) as a macro-RAFT agent.

An important feature of any controlled polymerization reaction is the constant rate of the monomer consumption leading to the constant increase in polymer molecular weight with narrow PDI. The Ln ($[M_0]/[M_t]$) *vs* reaction time for the polymerization of **2.3** (target DP

of 20) was plotted and a pseudo first order plot was obtained (Figure 2.3). However, these data are not adequate indicators of a controlled polymerization if not supported by GPC data confirming an increase in the molecular weight of the produced polymer over time. Since the molecular weight of the produced polymers did not exceed 2 kDa, we clearly did not have a controlled polymerization condition, which prompted a more thorough examination of the chemistry.

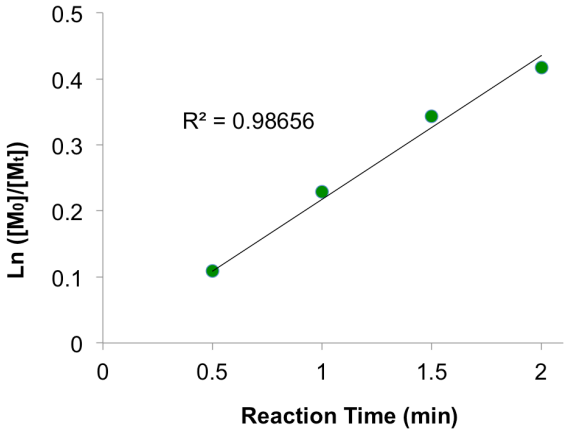


**Figure 2.3.** Ln ($[M_0]/[M_t]$) *vs* reaction time for polymerization of monomer **2.3** (Target DP = 20).

In the first instance, identical RAFT polymerization conditions were employed to target higher molecular weight polymers (*e.g.* DP of 60 and 120). $^1$H NMR spectroscopy for both targeted molecular weights showed high monomer conversion, pointing to the production of high molecular weight polymers. Again this was not substantiated by the GPC data, as there was no appreciable increase in the molecular weight of the produced polymers (Table 2.1, entry 1-3). Figure 2.2 shows the RI traces for the target DP of 60 and 120 corresponding to 3.4 kDa and 3.6 kDa, respectively, which are much smaller than the expected 20 kDa and 37 kDa molecular weights. The presence of shoulders on the RI trace of the produced polymers, specifically trace **C**, and broadening of the molecular weight distributions (PDI = 1.3 and 1.4, respectively) were clear signs of chain transfer and termination reactions competing and dominating the chemistry rather than well-controlled polymer growth. This was further supported by utilizing the homopolymer **2.5** (trace **B**; Figure 2.2) as a macro-RAFT agent for the polymerization of

styrene. In the GPC result collected on the resulting material, a clear bimodal pattern was observed, where one corresponded to the homopolymer **2.5**, and the other indicative of the produced block copolymer (trace **D**; Figure 2.2). The large component of **2.5** in the mixture resulted from radical termination and chain transfer reactions, which rendered the "dead" chain ends. In an attempt to diminish the termination and chain transfer reactions, an *exhaustive* variation of the reaction conditions were employed, such as using different solvents, temperature, RAFT agents, concentration, and [monomer]: [RAFT agent]: [initiator] ratio (Table 2.1).

The influence of the reaction solvent was studied, where benzene, THF, fluorobenzene, chlorobenzene, and acetonitrile/benzene were utilized. The monomer **2.3** was insoluble in acetonitrile, and had limited solubility in THF at high concentrations (*i.e.* at >100 mg/mL). It was observed that using different solvents did not improve the end polymer. Chlorobenzene appeared to be a better solvent, as it resulted in slightly better PDI value when compared to the others (A; Figure 2.4). However the predicted molecular weights were not achieved (Table 2.1, entry 4-7).

Concentration effects can also play a role in chain growth, therefore four different concentrations of monomer were studied; 100, 200, 300, and 400 mg/mL (Table 2.1, entry 8-10). Our hypothesis was that by increasing the concentration we would reduce the chance of chain transfer to the solvent leading to an increase in molecular weight. Under these conditions, we observed that the 400 mg/mL sample was too viscous and the 300 mg/mL gave marginally better result, but still not nearly reaching the targeted molecular weights (B; Figure 2.4).

In order to ascertain the effect of different RAFT agents, which inherently have different chain transfer rates, the RAFT agents **2.4**, **2.6**, and **2.7** (Figure 2.5) were used in the polymerization of monomer **2.3**. RAFT agents **2.6** and **2.7** did not improve the polymerization, however the RAFT agent **2.4** gave a somewhat better result but the targeted polymer was not achieved (C; Figure 2.4 and Table 2.1 entry 9, 11-12).

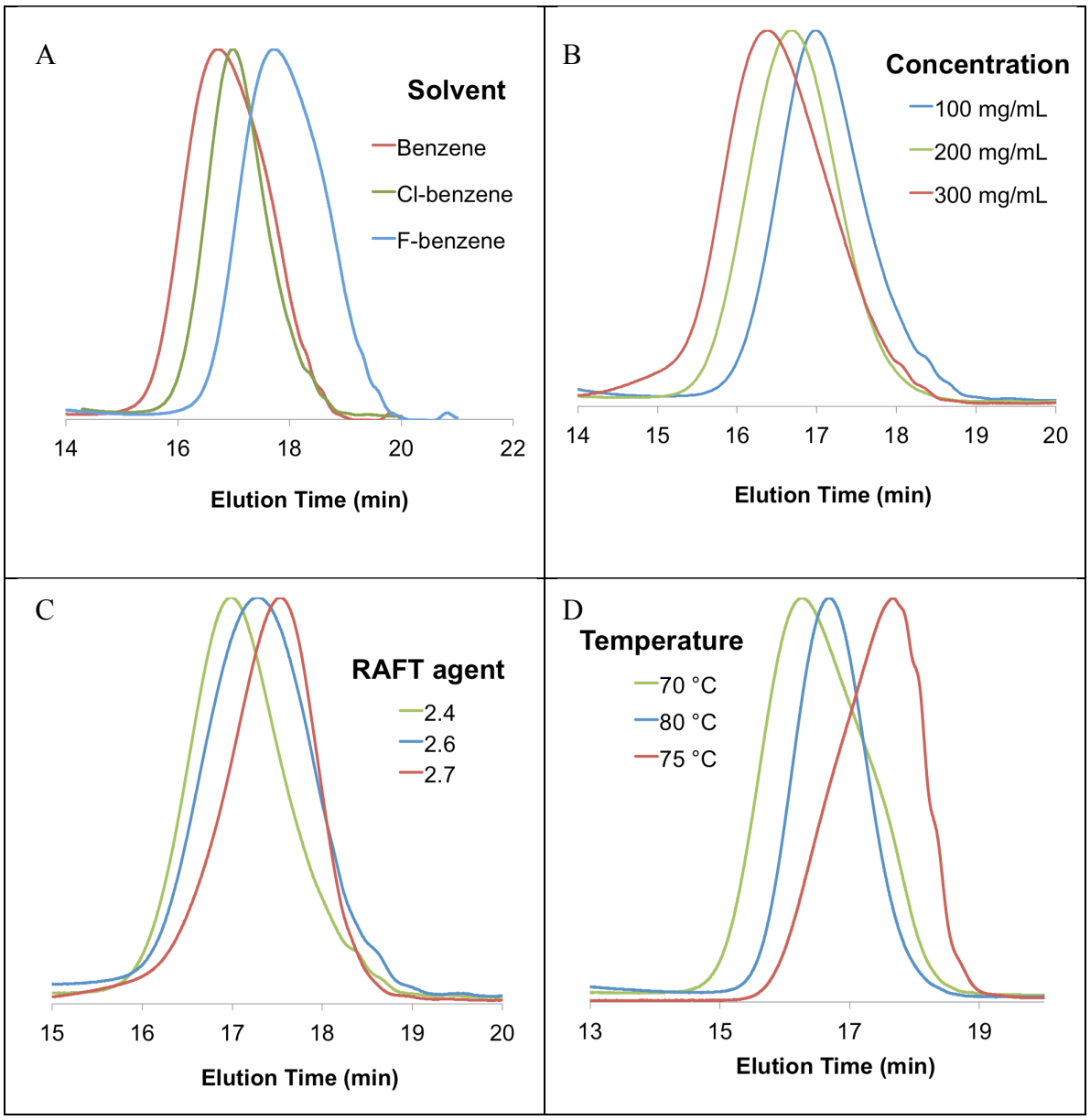


**Figure 2.4.** RI traces of polymer **2.5** produced under different reaction conditions; A: different reaction solvent, B: different monomer concentration, C: different RAFT agents, and D: different reaction temperature.

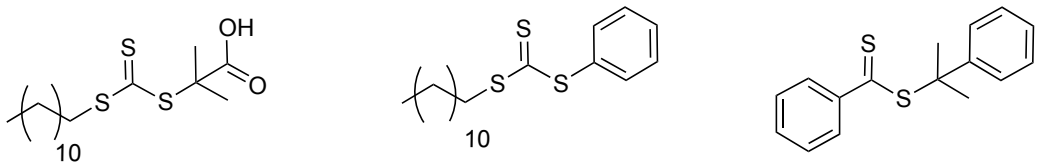


**2.4** **2.6** **2.7**

**Figure 2.5.** Structure of three different RAFT agents used in RAFT polymerization of monomer **2.3**.

Finally, the decomposition rate of AIBN and the initiation step was studied at three different temperatures: 70, 75, and 80 °C. When the reaction temperature was below 80 °C, an increase in the PDI was noted. This was likely a result of the slow decomposition of the initiator therefore leading to a slower than necessary initiation step (D; Figure 2.4 and Table 2.1, entry 13-15). Changing the molar ratio of AIBN relative to the RAFT agent **2.4** did not result in any noticeable improvement in the molecular weight or the PDI of the produced polymer. Based on all these data, summarized in Table 2.1 and Figure 2.4, the optimized condition for the RAFT polymerization of **2.3** was determined to be using **2.4** as the RAFT agent, in a nitrogen-saturated chlorobenzene solution (300 mg/mL) at 80 °C where [AIBN] / [**2.4**] = 0.2. (Table 2.1, entry 15).

Polymerization of **2.3** under the optimized conditions resulted in polymer **2.5** with 90% monomer conversion (see Appendix 2, Figure A2.2 for $^{1}$H NMR spectrum) with an estimated molecular weight of 35 kDa (Figure 2.6). The GPC analysis of the sample revealed a 10.8 kDa polymer, which is drastically smaller than the anticipated molecular weight (*ca.* 35 kDa). Furthermore, the PDI of the produced polymer was 1.3 and not as narrow as expected for a well-controlled polymerization reaction (~1.1) (Figure 2.6). These observations clearly indicate that chain transfer and termination reactions still occur in competition with the controlled growth of the polymer chain, resulting in short polymers with broad PDIs.

**Table 2.1.** Optimizing polymerization conditions of monomer **2.3**.

| | Target DP | Solvent | Concentration (mg/mL) | RAFT agent | Temp. (°C) | Conversion[a] | $M_n$[b] (kDa) | $M_n$[c] (kDa) | PDI[c] |
|---|---|---|---|---|---|---|---|---|---|
| 1 | 20 | Benzene | 100 | **2.4** | 80 | 70 | 8 | 1.9 | 1.2 |
| 2 | 60 | Benzene | 100 | **2.4** | 80 | 55 | 20 | 3.4 | 1.3 |
| 3 | 120 | Benzene | 100 | **2.4** | 80 | 60 | 45 | 3.6 | 1.4 |
| 4 | 60 | F-benzene | 100 | **2.4** | 80 | 40 | 15 | 3.5 | 1.2 |
| 5 | 60 | Cl-benzene | 100 | **2.4** | 80 | 60 | 22 | 4.9 | 1.2 |
| 6 | 60 | THF | 100 | **2.4** | 80 | - | - | - | - |
| 7 | 60 | Acetonitrile/ Benzene | 100 | **2.4** | 80 | - | - | - | - |
| 8 | 60 | Cl-benzene | 200 | **2.4** | 80 | 80 | 30 | 6.5 | 1.2 |
| 9 | 60 | Cl-Benzene | 300 | **2.4** | 80 | 80 | 30 | 9.8 | 1.4 |
| 10 | 60 | Cl-benzene | 400 | **2.4** | 80 | 45 | 17 | 9.9 | 1.5 |
| 11 | 60 | Cl-benzene | 300 | **2.6** | 80 | 30 | 11 | 3.9 | 1.2 |
| 12 | 60 | Cl-benzene | 300 | **2.7** | 80 | 50 | 18 | 5.4 | 1.3 |
| 13 | 60 | Cl-benzene | 300 | **2.4** | 70 | 40 | 15 | 8.5 | 1.4 |
| 14 | 60 | Cl-benzene | 300 | **2.4** | 75 | 15 | 5.6 | 3.9 | 1.3 |
| **15**[d] | 60 | Cl-benzene | 300 | **2.4** | 80 | 95 | 35 | 10.7 | 1.3 |
| **16**[e] | 60 | Cl-benzene | 300 | **2.4** | 80 | 70 | 26 | 24 | 1.1 |

a. Calculated from $^1$H NMR spectroscopy of the crude product, b. Calculated based on monomer conversion, c. Determined by GPC analysis of the purified polymer (relative to PS standard), d. The best polymerization condition among all other conditions (entries 1-14), e. exact same polymerization condition as entry 15 in presence of three stoichiometric equivalents of methyl acrylate relative to **2.3**.

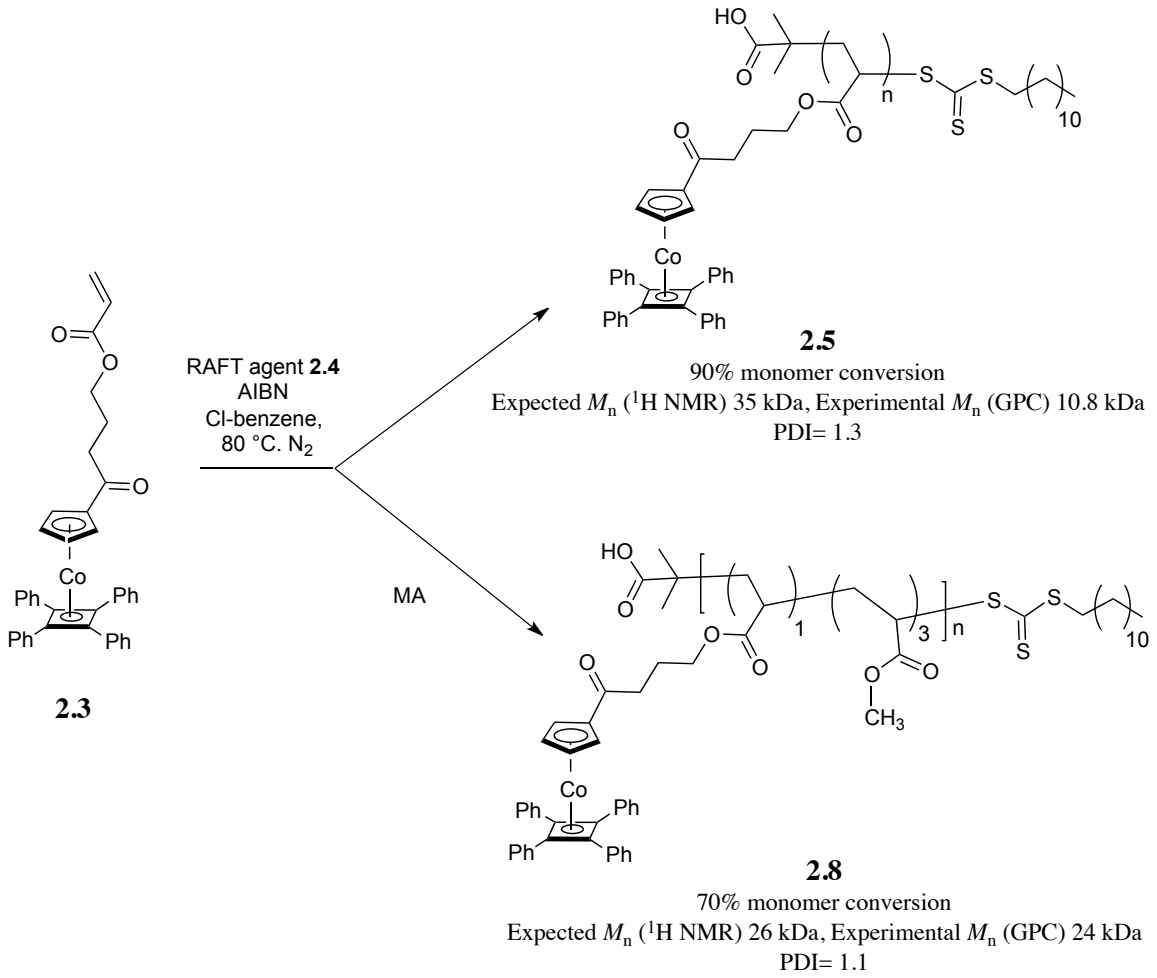


**Figure 2.6.** Polymerization of **2.3** under optimized condition resulting in polymer **2.5** (Table 2.1, entry 15) and the exact same polymerization in presence of 3 *eq.* MA (relative to **2.3**) resulting in random copolymer **2.8** (Table 2.1, entry 16).

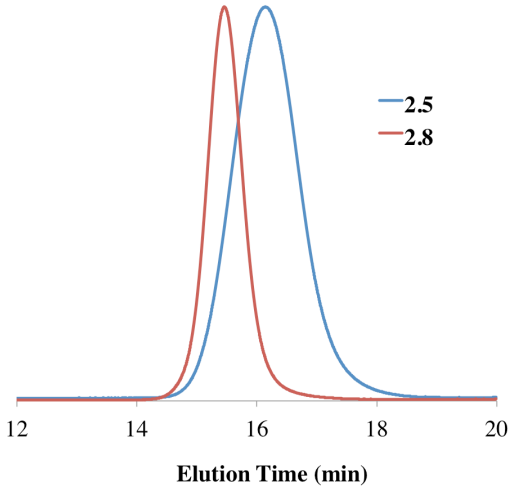


**Figure 2.7.** RI traces of PolyCpCoCb homopolymer (**2.5**) and PolyCpCoCb-*r*-PMA random copolymer (**2.8**).

### 2.2.3. Overcoming Hindrance Problem to Have Controlled Polymerization

Given that all of the key variables of a typical RAFT polymerization under a variety of different conditions were examined and yet the polymerization did not improve, it became clear that the sterically bulky nature of the monomer **2.3** was likely a factor. Solid-state structure of monomer **2.3** is provided in Figure 2.8 showing the bulkiness of this monomeric unit.

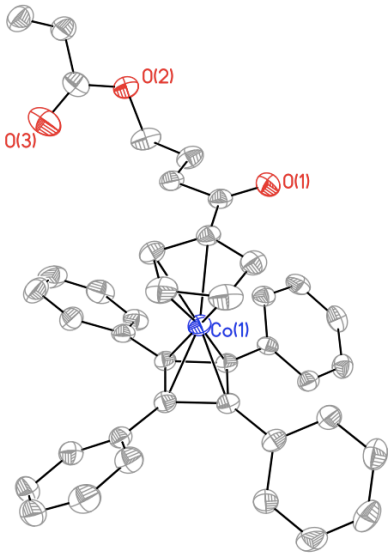


**Figure 2.8.** Solid-state structure of **2.3**.

We believed that as the polymer chain grew, monomer addition became increasingly more difficult due to steric considerations. Consequently, even at the early stages of polymerization in the presence of high monomer concentration, radical propagation was inefficient leading to chain transfer and termination. Although the monomer was constantly consumed over the course of reaction time, the retardation in chain growth leads to polydisperse, low molecular weight polymer. This hypothesis is supported by our experimental observations, as under all of the different reaction conditions described previously, low molecular weight polymers (< 10 kDa) with broad PDIs were produced.

To test this hypothesis, a small monomer, methyl acrylate (MA), was added to the reaction mixture (Figure 2.6). It was hoped that when the polymerization of the bulky monomer **2.3** became sluggish, the addition of the small MA could still occur, thus relieving steric encumbrance at the growing chain end. This would result in a short segment of poly(methylacrylate) (PMA) providing much needed relief for further addition of **2.3**. The optimized RAFT polymerization conditions were followed in the presence of three stoichiometric equivalents of MA relative to **2.3**. The copolymerization of **2.3** and MA resulted in the estimated molecular weight polymer as we had targeted, yet in an even shorter reaction time (Figure 2.6). For example, after 60 minutes of the random copolymerization reaction, 70% of the initial monomer was consumed with an expected molecular weight of 26 kDa (see Figure A2.3 for $^{1}$H NMR spectrum). The GPC data denoted a molecular weight of 24 kDa, which was in very good agreement with the expected molecular weight. The PDI of the produced polymer was 1.1, which is consistent for a controlled polymerization to produce the random copolymer PolyCpCoCb-*r*-PMA (**2.8**) (Figure 2.6).

To study the polymerization process, a stock solution of RAFT agent **2.4** and AIBN with 1: 0.2 mole ratios was prepared. The solution was then charged with monomer **2.3** (60 *eq*. relative to RAFT agent **2.4**) and MA (3 *eq*. relative to monomer **2.3**). The stock solution was divided between small reaction flasks and heated at 80 °C. Polymerization was stopped by removal of reaction flasks from the oil bath at 15 minute time intervals followed by rapid cooling. Monomer conversion as determined by integration of the corresponding $^{1}$H NMR spectra were used to plot $\ln[M_0]/[M_t]$ *vs* reaction time (Figure 2.9) resulting in a pseudo first order plot, characteristic of a controlled polymerization

and indicated the constant consumption of monomer **2.3** over the course of the reaction time. It is worthy to mention that this plot includes data points up to 100 minutes reaction time corresponded to high monomer conversion (*ca.* 90%).

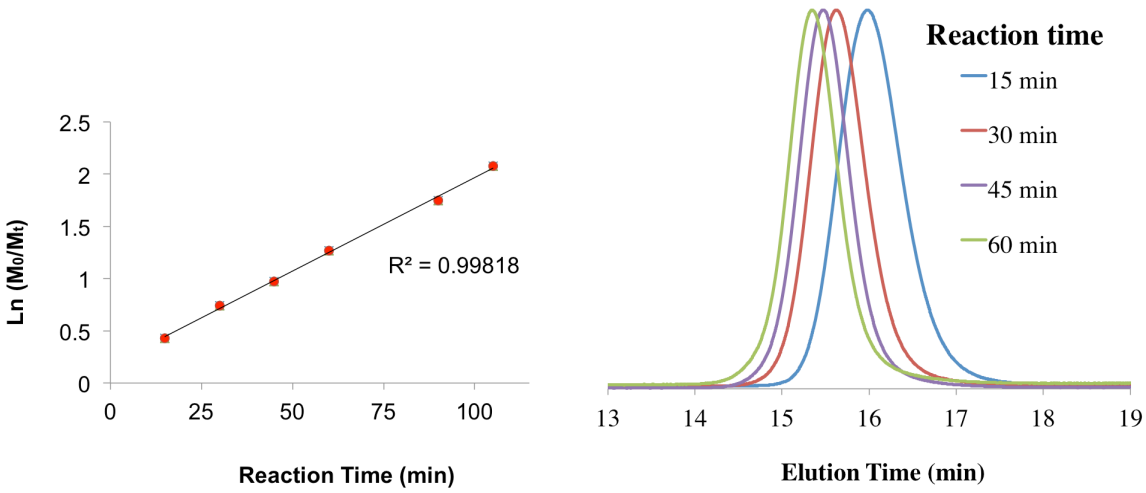


**Figure 2.9.** Left: Ln[$M_0$]/[$M_t$] *vs* reaction time for preparation of polymer **2.8** when targeting DP of 60 (note: M refers to **2.3)**. Right: RI traces of polymer **2.8** at different reaction times.

The increase in the molecular weight of produced polymers at different reaction times was confirmed by GPC analysis as indicated by the gradual decrease in their elution times (Figure 2.9). Molecular weights of the samples ($M_n$ and $M_w$) at different reaction times are provided in Figure 2.10. Polymers up to 30 kDa were prepared with a PDI of ~1.1 indicative of a well-controlled polymerization. The molecular weights obtained by GPC analysis were in good agreement with the estimated molecular weights and they followed the same trend of those calculated from $^1$H NMR spectroscopy (Figure 2.10).

The ratio of the PMA content and the PolyCpCoCb content in the random copolymer **2.8** was analyzed by their relative integration values in the $^1$H NMR spectra of purified samples, resulting in approximately 3 PMA: 1 PolyCpCoCb, similar to their monomer feed ratio.

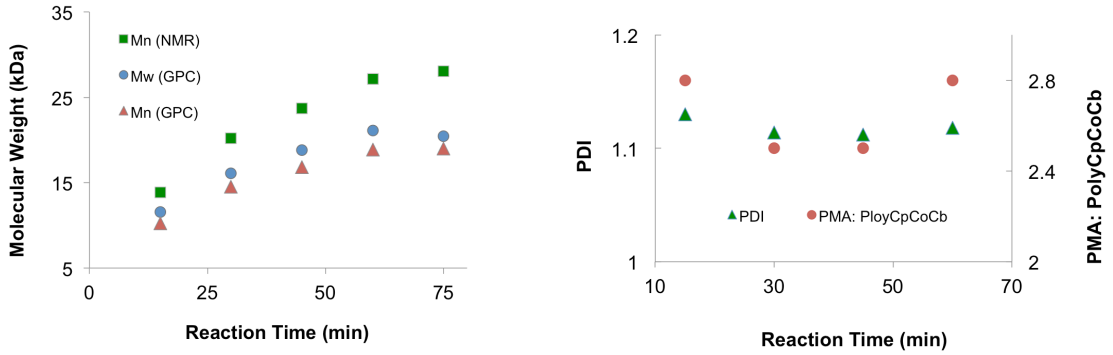


**Figure 2.10.** Left: Molecular weight ($M_n$) of **2.8** calculated by $^1$H NMR spectroscopy compared to $M_n$ and $M_w$ achieved by GPC analysis at different reaction times (Target DP = 60). Right: PDI and block ratios (PMA: PolyCpCoCb) of polymer **2.8** at different reaction times (Target DP = 60).

To verify that the applied RAFT polymerization conditions were valid for the preparation of different molecular weights, DP of 30 and 120 were targeted. For each experiment, the plot of Ln $[M_0]/[M_t]$ *vs* the reaction time up to high monomer conversion (*ca.* 90%) showed a linear correlation (Figure 2.11). Both series of reactions (DP of 30 and 120) showed narrow PDIs (1.1- 1.2) for all samples at different reaction times (Figure A2.5).

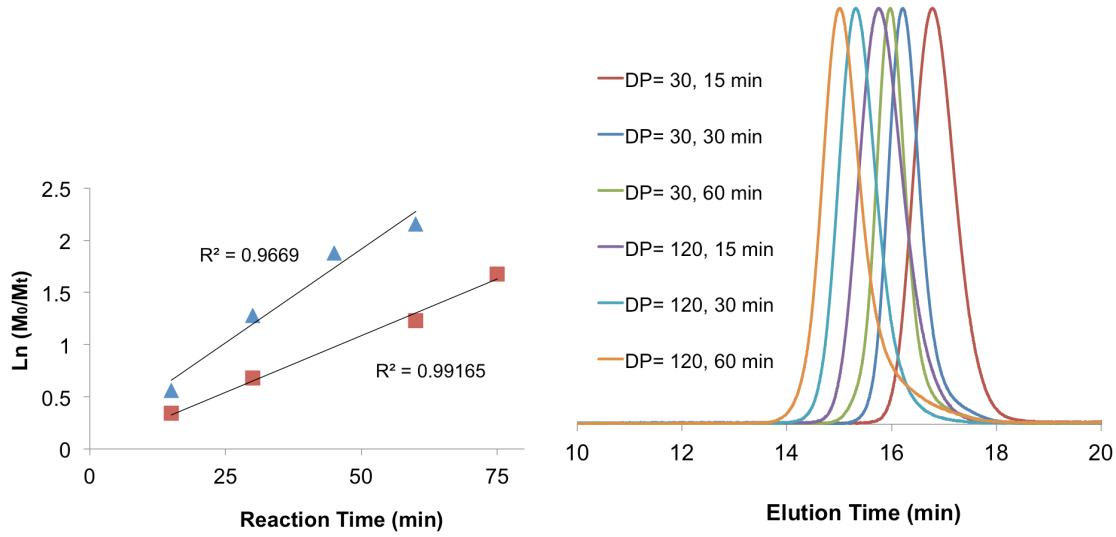


**Figure 2.11.** Left: Ln$[M_0]/[M]$ *vs* time for preparation of **2.8** when target DP of 30 (triangle) and 120 (square). Right: RI traces of **2.8** at different time intervals for target DP of 30 and 120.

The polymer **2.8** was analyzed by differential scanning calorimetry (DSC), where only one $T_g$ value was observed ($T_g$ = 85 °C) (Figure 2.12). Typically PMA homopolymer has

a low $T_g$ around 20 °C.[76] The observed single high $T_g$ (85 °C) signifies that the material was a homogeneous unit made of **2.3** and MA in a random, but consistent fashion over the length of the polymer and therefore was comprised of a regular distribution of the two components.

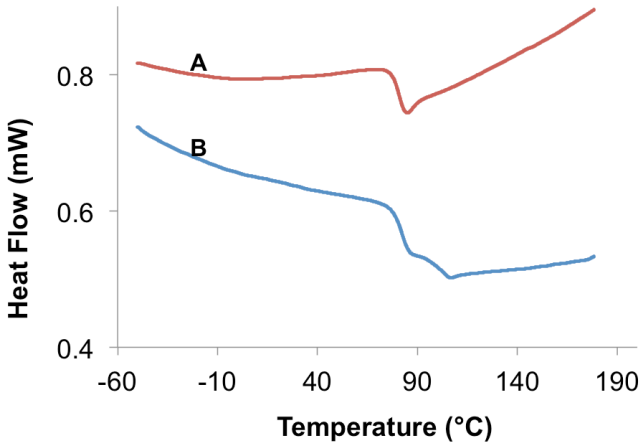


**Figure 2.12.** DSC analysis of **2.8** (curve A; $T_g$ = 85 °C) and **2.9** (curve B; $T_g$ = 85 °C and 104 °C).

Moreover, it is noteworthy that both the UV trace and the RI trace from the GPC analysis of polymer **2.8** were identical. This is in agreement with the description of the material as being a consistent distribution of the two consisting blocks (Figure 2.13).

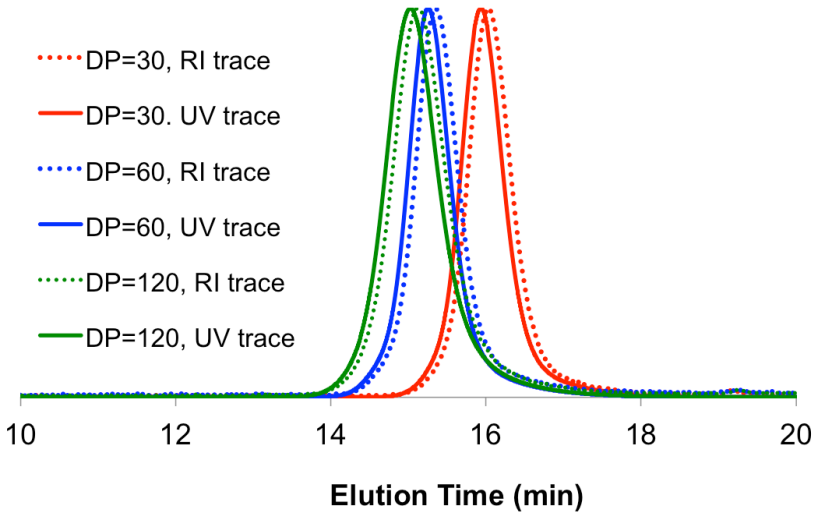


**Figure 2.13.** RI trace and UV trace of **2.8** for three different targeted DP. Note: The UV trace has a slightly shorter elution time compared to the RI trace because the two detectors are set up in series, leading to a short delay between the two signals.

The random copolymerization of **2.3** with less than three stoichiometric equivalents of MA did not lead to controlled polymerization as the necessary steric relief was not achieved and chain transfer/termination reactions occurred resulting in broadened PDIs (Figure A2.6). Even though three stoichiometric equivalents of MA relative to **2.3** was incorporated in polymer **2.8**, the relative mass contribution of MA was less than 30 percent of the entire random copolymer, making PolyCpCoCb the dominant component and contributing to over 70% of the material. To prove this, a typical polymerization reaction in absence of monomer **2.3** was carried out (*i.e.* using MA only) resulting in a drastically shorter polymer chain (Figure A2.6). Therefore the majority component of polymer **2.8** relies on PolyCpCoCb.

### 2.2.4. Block Copolymer Synthesis

To prepare block copolymers, PolyCpCoCb-*r*-PMA (**2.8**) was used as a macro-RAFT agent and reacted with freshly purified, nitrogen-saturated styrene in a 1:10 weight ratio, where styrene was used as the monomer, and the reaction solvent (Scheme 2.2). The reaction vessel was sealed and heated to 120 °C to conduct auto-initiated RAFT polymerization of styrene.[77] The polymerization samples were stopped at 15 minutes time intervals. After purification, the $^{1}$H NMR spectra revealed the presence of new broad peaks at 6.6 and 7.10 ppm (Figure A2.7), indicative of the PS block being incorporated into the polymer sample (**2.9**; (PolyCpCoCb-*r*-PMA)-*b*-PS) (Scheme 2.2).

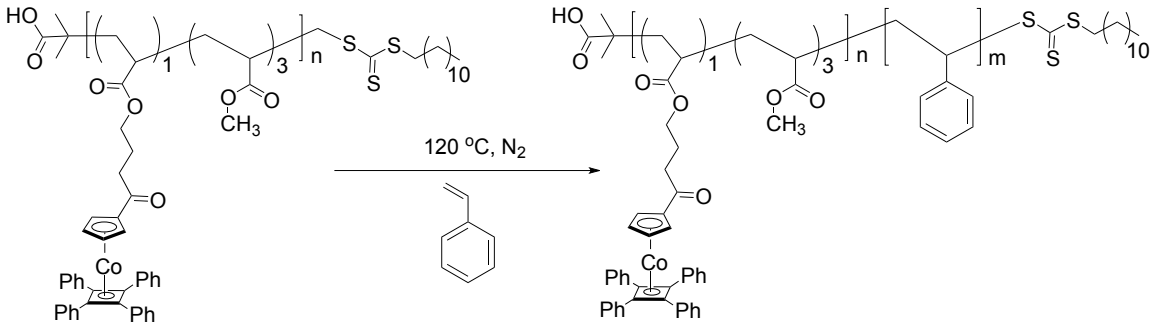


**2.8** **2.9**

**Scheme 2.2.** Utilizing **2.8** as macro-RAFT agent for preparation of **2.9**; (PolyCpCoCb-*r*-PMA)-*b*-PS.

By integrating the broad peaks of the PS block and comparing those to the integration of the random copolymer block, the number of repeat units of the PS block was calculated (Figure A2.7). This value was used to plot the Ln [1/1-C] *vs* reaction time (Figure 2.14), where C is consumed styrene.

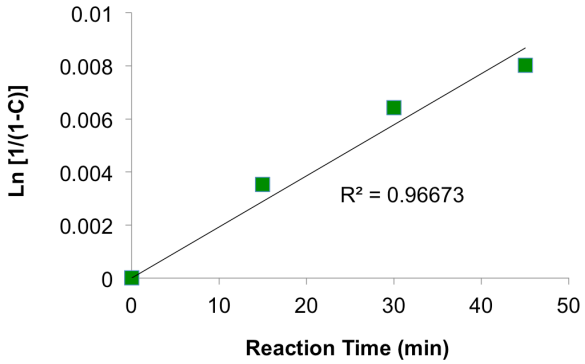


**Figure 2.14.** Ln[1/(1-C)] *vs* reaction time for block copolymer **2.9**.

GPC analysis of the purified block copolymer **2.9** confirmed the increase in the molecular weight of the block copolymer over time (Figure 2.15). The RI traces of the block copolymer **2.9** are monomodal and indicated the preparation of the macro-RAFT agent **2.8** (*i.e.* no "dead" chain ends were present). These data also pointed to a controlled polymerization, where the steric problem associated with controlled polymerization of **2.3** was remedied.

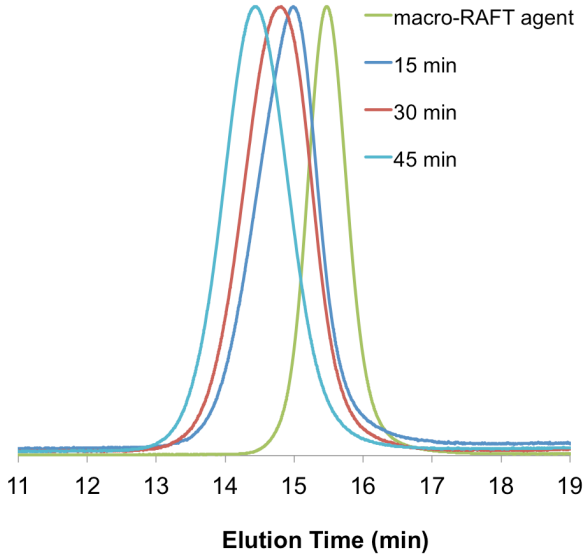


**Figure 2.15.** RI trace of **2.8** (macro-RAFT agent) and **2.9** at different reaction times.

Thermal gravimetric analysis (TGA) of the random copolymer **2.8** and block copolymer **2.9** revealed a char yield of 30% and 20%, respectively (Figure 2.16). Upon measuring the $T_g$ of **2.9** by DSC, two distinct glass transitions were observed; $T_g$ of 85 °C for the PolyCpCoCb-*r*-MA block and 104 °C for the PS block. This was a promising signpost for potential onwards solid-state phase-separation studies as it indicated the two blocks (the PolyCpCoCb-*r*-PMA block and the PS block) have distinct physical properties.

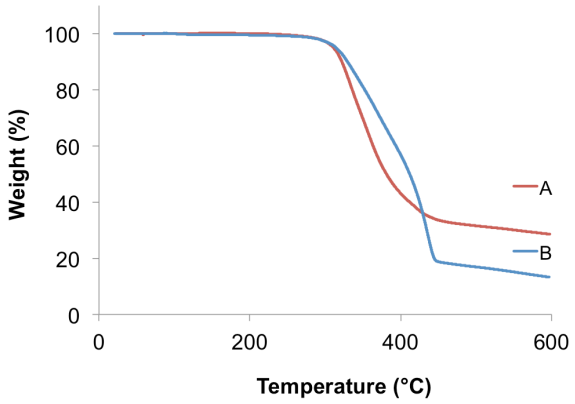


**Figure 2.16.** TGA analysis of **2.8** (A) and **2.9** (B).

### 2.2.5. Solid-State Self-Assembly of Block Copolymer

As a preliminary study of the solid-state self-assembly behavior of block copolymer **2.9**, a thin layer of material was deposited on a glass slide, followed by solvent annealing in presence of dichloromethane vapour and then thermal annealing at 140 °C under reduced pressure. Samples for TEM analysis were prepared by mounting the thin films on two-part epoxy block, and cutting 50 nm thick specimens using an ultramicrotom. The presence of darker (PolyCpCoCb-*r*-PMA block) and lighter (PS block) domains in the TEM images were indicative of the phase-separation of the two blocks and represent proof of principle for these materials to be promising entries into inorganic nanomaterials (Figure 2.17).

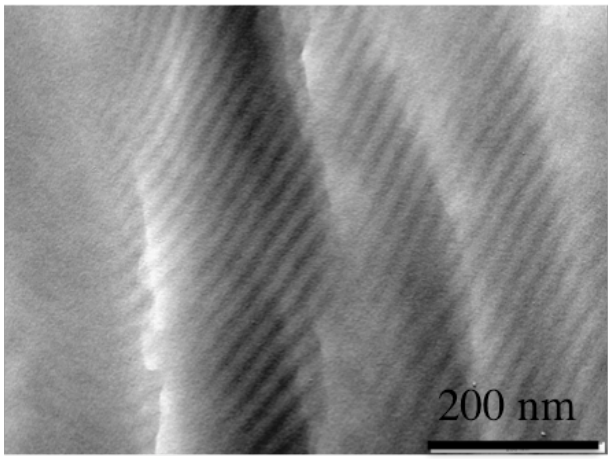


**Figure 2.17.** TEM image of the solid-state self-assembled block copolymer **2.9**.

## 2.3. Conclusion

A cobalt containing monomer featuring $\eta^5$-cyclopentadienyl-cobalt-$\eta^4$-cyclobutadiene (**2.3**; CpCoCb) was prepared and its controlled polymerization *via* RAFT technique was studied. Under a variety of applied RAFT polymerization conditions, the monomer **2.3** resulted in only short oligomers (**2.5**) because of the steric demand associated with the monomer. To overcome this problem, **2.3** was copolymerized along with a smaller monomer (MA) to act as a spacer unit, providing the necessary relief for the addition of the bulky monomer **2.3.** This resulted in a dramatic improvement in the molecular weight and the PDI of the produced random copolymer (**2.8**) and termination and chain transfer

reactions were successfully prevented. This method opens up a new avenue for well-controlled polymerization of wide range of bulky monomers to prepare well-defined and high molecular weight polymers. The random copolymer **2.8** was used as a macro-RAFT agent to prepare high molecular weight block copolymers (**2.9**), which their solid-state self-assembly was studied. These materials self-assembled and underwent phase-separation in the solid-state.

### 2.4. Experimental

All reactions are set up under $N_2$ atmosphere using standard Schlenk line or glovebox techniques unless stated otherwise. Reagents were obtained from either Sigma-Aldrich or Alfa Aesar. RAFT agent **2.7** was purchased from Sigma Aldrich and used as received. Solvents were obtained from Caledon Laboratories. Solvents were dried using an MBraun Solvent purification system (SPS) that utilizes dual molecular sieve columns to dry solvents. Chlorobenzene and fluorobenzene were obtained from Sigma Aldrich and freeze-pump-thawed three cycles then stored over 4 Å molecular sieves. Chloroform-d (99.8 atom % D) for NMR spectroscopy were purchased from Cambridge Isotope Laboratories (CIL). All NMR spectra were recorded on a Varian INOVA 400 MHz spectrometer ($^1$H = 399.76 MHz, $^{13}$C = 100.52 MHz). $^1$H and $^{13}$C{$^1$H} NMR spectra were referenced to residual solvent in the deuterated solvent relative to $SiMe_4$ ($CDCl_3$; $^1$H: $\delta$ = 7.26 ppm, $^{13}$C{$^1$H}: $\delta$ = 77.2 ppm). Fourier transform infrared (FT-IR) spectroscopy was conducted on samples as KBr disk or as a thin film using a Bruker Tensor 27 spectrometer, with a resolution of 4 $cm^{-1}$. Melting points were recorded using a Gallenkamp Variable Heater. Suitable single crystals for X-ray diffraction studies were individually selected under Paratone-N oil, mounted on nylon loops and placed in a cold stream of $N_2$ (150 K). Data was collected on a Bruker Nonius Kappa CCD X-ray diffractometer or Bruker Apex II CCD X-ray diffractometer using graphite monochromated Mo-$K_\alpha$ radiation ($\lambda$ = 0.71073 Å). The solution and subsequent refinement of the data were performed using the SHELXTL suite of programs. All X-ray data were collected and solved by Dr. Jackie Price and Dr. Jonathan Dube. Elemental analysis was performed at Université de Montréal, Montreal, Canada. Doug Hairsine performed high-resolution mass spectroscopy using electron ionization Finnigan MAT 8200 mass spectrometer at Western University. Differential scanning calorimetric (DSC)

was performed on a DSC 822e Mettler Toledo instrument or Q20 DSC TA instrument at a heating rate of 10 °C/min from -100 up to 20 degrees below the $T_d$ of the compound. Glass transition temperatures ($T_g$) were obtained from the second heating cycle of DSC analysis. All thermal analysis experiments were conducted under nitrogen atmosphere. The decomposition temperatures ($T_d$) were determined using a TGA/SDTA 851e Mettler Toledo instrument or Q600 SDT TA Instrument by heating samples at a rate of 10 °C/min over a temperature range of 30-600 °C.

Gel permeation chromatography (GPC) experiments were conducted in chromatography grade THF at concentrations of 3-5 mg/mL using a Viscotek GPCmax VE 2001 GPC instrument equipped with an Agilent PolyPore guard column (PL1113-1500) and two sequential Agilent PolyPore GPC columns packed with porous poly(styrene-*co*-divinylbenzene) particles ($M_W$ range 200 - 2000000 g/mol; PL1113-6500) regulated at a temperature of 30°C. Signal response was measured using a Viscotek VE 3580 RI detector, and molecular weights were determined by comparison of the maximum RI response with a calibration curve (10 points, 1500 - 786000 g/mol) established using monodisperse polystyrene standards supplied by Viscotek.

**Compound 2.2:**

A 250 mL flame dried Schlenk flask was charged with compound **2.1** (2.00 g, 6.28 mmol, 1 *eq.*), diphenylacetylene (2.46 g, 13.8 mmol, 2.2 *eq.*), dry *p*-xylene (100 mL), and a stir bar. A flame dried condenser was mounted and the solution was refluxed under $N_2$ atmosphere for 2 days. After which the reaction mixture was cooled down to room temperature and was added to *n*-hexane (400 mL) to precipitate out the crude product. Orange precipitate was collected by gravity filtration, dissolved in DCM and filtered to remove any black solid. Then the solvent volume was reduced to *ca.* 10 mL followed by addition of *n*-hexane to precipitate out the product in 70% yield. No further purification was performed. $^1$H NMR ($CDCl_3$; δ (ppm)): 7.44-7.42 (m, 8H), 7.30-7.23 (m, 12H), 5.25 (m, 2H), 4.81 (m, 2H), 3.42 (m, 2H), 2.14 (t, $^3J$ = 4.0 Hz, 2H), 1.99 (t, $^3J$ = 4.0 Hz, 1H), 1.50 (p, $^3J$ = 4.0 Hz, 2H). $^{13}$C{$^1$H} NMR ($CDCl_3$; δ (ppm)): 199.4, 169.7, 135.0, 128.7, 128.2, 127.0, 87.7, 83.0, 62.5, 36.7, 26.4. FT-IR ($cm^{-1}$) (ranked intensity): 382 (9), 404 (10), 463 (4), 914 (7), 1097 (13), 1156 (6), 1178 (5), 1312 (11), 1536 (3), 1573 (8), 1890 (1), 1953 (2), 2341 (12), 3027 (15), 3081 (14). HRMS (found/calculated):

566.16538/566.165603. Elemental analysis (EA) (found/calculated): C (78.44/78.21), H (5.51/5.43). Melting point: 195-197 ºC.

**Compound 2.3:**

A 250 mL flame dried round bottom flask was charged with compound **2.2** (5.00 g, 8.80 mmol, 1 *eq.*), dry DCM (150 mL) and triethylamine (1.85 mL, 13.0 mmol, 1.5 *eq.*) followed by the addition of acryloyl chloride (1.07 mL, 13.0 mmol, 1.5 *eq.*). The reaction mixture was stirred under $N_2$ atmosphere for 2 hours after which it was quenched with water (150 mL). Mixture was transferred to a separatory funnel and the DCM layer was collected and washed with brine (3×50 mL). Organic layers was dried over $MgSO_4$, filtered, and concentrated under reduced pressure. The red/orange solid was purified using column chromatography (neutral alumina, hexane: ethyl acetate (12: 1)) to collect compound **2.3** in 90% yield. $^1$H NMR ($CDCl_3$; δ(ppm)): 7.44-7.41 (m, 8H), 7.29-7.22 (m, 12H), 6.39 (dd, $^3J$ = 16.2, $^2J$ = 4.0 Hz, 1H), 6.09 (dd, $^3J$ = 16.2, $^3J$ = 8.0 Hz, 1H), 5.82 (dd, $^3J$ = 8.0, $^2J$ = 4.0 Hz, 1H), 5.25 (m, 2H), 4.80 (m, 2H), 3.93 (t, $^3J$ = 4.0 Hz , 2H), 2.05 (t, $^3J$ = 4.0 Hz, 2H), 1.59 (p, $^3J$ = 4.0 Hz, 2H). $^{13}$C{$^1$H} NMR ($CDCl_3$; δ(ppm)): 197.2, 166.1, 135.8, 130.6, 128.5, 127.6, 126.0, 93.7, 87.2, 63.6, 71.2, 64.0, 35.7, 22.6. FT-IR ($cm^{-1}$) (ranked intensity): 563(6), 588 (13), 696(3), 744(10), 781(12), 1192(5), 1055(11), 1273(8), 1372(15), 1406(9), 1456(7), 1498(4), 1597(14), 1668(2), 1722(1). HRMS (found/calculated): 620.17399/620.17617. Elemental analysis (found/calculated): C (77.15/77.41), H (5.40/5.36). Melting point: 113-114 ºC.

**RAFT agents 2.4**[78] and **2.6**[79] were synthesized following literature procedure.

**Homopolymer 2.5 (PolyCpCoCb)**:

A 5 mL round bottom flask was charged with compound **2.3** (100 mg, 0.160 mmol, 60 *eq.*), **2.4** (0.980 mg, 0.270 µmol, 1 *eq.*), AIBN (260 µg, 0.530 µmol, 0.2 *eq.*) and chlorobenzene (300 µL) under nitrogen. The reaction flask was sealed with rubber septa and submerged into an 80 ºC oil bath. Reaction was stopped by removing the vessel from hot bath and cooling down in iced water bath. The solvent was removed under reduced pressure and the crude $^1$H NMR spectrum was analyzed for calculating monomer conversion. For purification, the crude polymer was dissolved in minimum DCM and added to *n*-hexane. The yellow precipitate was collected and precipitated two more times to remove any unreacted monomer. $^1$H NMR ($CDCl_3$; δ(ppm)): 7.42-7.33 (b), 7.26-7.1

(b), 4.50-4.71 (b), 3.61-3.25 (b), 3.90-3.01(b), 2.03-1.95 (b), 1.60-1.50 (b). $^{13}C\{^{1}H\}$ NMR ($CDCl_3$; δ(ppm)): 135.3, 128.9, 128.4, 127.1, 93.7, 87.5, 83.2, 76.8, 42.1, 36.0, 29.1, 22.7, 22.5, 29.3, 22.9, 22.6,14.3.

**Random copolymer 2.8 (PolyCpCoCb-*r*-PMA)**:

A 5 mL round bottom flask was charged with methyl acrylate (44.0 µL, 0.480 mmol, 120 *eq.*), compound **2.3** (100 mg, 0.160 mmol, 60 *eq.*), **2.4** (0.980 mg, 0.270 µmol, 1 *eq.*), AIBN (260 µg, 0.530 µmol, 0.2 *eq.*) and chlorobenzene (300 µL) under nitrogen. The reaction flask was sealed with a rubber and submerged into 80 ºC oil bath. After desired reaction time the reaction vessel was removed from hot bath and cooled down in ice bath. The volatiles were removed under reduced pressure and the crude $^{1}H$ NMR spectrum was analyzed for calculating monomer conversion. The crude polymer was dissolved in minimal DCM and added to *n*-hexane. The yellow precipitate was collected and precipitated two more times to remove any unreacted monomer. $^{1}H$ NMR ($CDCl_3$; δ(ppm)): 7.39 (b), 7.21(b), 5.22 (b), 4.73 (b), 3.73 (b), 3.58 (b), 2.26 (b), 1.96 (b), 1.61 (b), 1.46 (b), 1.25 (b). $^{13}C\{^{1}H\}$ NMR ($CDCl_3$; δ(ppm)): 198.2, 175.5, 135.6, 128.9, 128.4, 127.1, 94.6, 87.4, 83.5, 76.7, 64.9, 52.3, 41.7, 36.9, 22.4.

**Block copolymer 2.9 (PolyCpCoCb-*r*-PMA)-*b*-PS**:

A 5 mL round bottom flask was charged with **2.8** (100 mg) and styrene (1.00 g), sealed with rubber septa and heated to 120 °C. The reaction was stopped by cooling down in ice bath. The crude product was dissolved in minimum DCM and precipitated in *n*-hexane. The yellow precipitate was collected by centrifuge, dissolved in DCM and precipitated in *n*-hexane four more times. $^{1}H$ NMR ($CDCl_3$; δ(ppm)): 7.39 (b), 7.21 (b), 7.04-7.11 (b), 6.48-6.58 (b), 5.22 (b), 4.73 (b), 3.73 (b), 3.58 (b), 2.26 (b), 1.96 (b), 1.61 (b), 1.46 (b), 1.25 (b). $^{13}C\{^{1}H\}$ NMR ($CDCl_3$; δ(ppm)): 175.6, 145.3, 136.7, 129.1, 128.6, 128.3, 126.5, 125.9, 93.3, 87.1, 83.5, 76.7, 52.3, 41.9, 40.0, 36.4, 22.7.

**Solid-state self-assembly**:

100 mg of **2.9** sample was dissolved in 500 µL DCM and drop casted on a glass slide. Sample was annealed by DCM vapor for 24 hours after which solvent was removed followed by thermal annealing at 140 °C for three days. Samples for TEM analysis were prepared by mounting the produced thin films on epoxy plastic, cutting them into 50 nm thick specimen using ultramicrotom and diamond knife.

**2.5. References**

(1) Eloi, J. C.; Chabanne, L.; Whittell, G. R.; Manners, I. *Mater. Today* **2008**, *11*, 28-36.

(2) Rider, D. A.; Manners, I. *Polym. Rev.* **2007**, *47*, 165-195.

(3) Whittell, G. R.; Manners, I. *Adv. Mater.* **2007**, *19*, 3439-3468.

(4) Stanley, J. M.; Holliday, B. J. *Coord. Chem. Rev.* **2012**, *256*, 1520-1530.

(5) Burnworth, M.; Knapton, D.; Rowan, S. J.; Weder, C. *J. Inorg. Organomet. Polym.* **2007**, *17*, 91-103.

(6) Weder, C. *J. Inorg. and Organomet. Polym. Mater.* **2006**, *16*, 101-113.

(7) Mortimer, R. J.; Dyer, A. L.; Reynolds, J. R. *Displays* **2006**, *27*, 2-18.

(8) Ren, L.; Hardy, C. G.; Tang, S.; Doxie, D. B.; Hamidi, N.; Tang, C. *Macromolecules* **2010**, *43*, 9304-9310.

(9) Lammertink, R. G. H.; Hempenius, M. A.; van den Enk, J. E.; Chan, V. Z. H.; Thomas, E. L.; Vancso, G. J. *Adv. Mater.* **2000**, *12*, 98-103.

(10) MacLachlan, M. J.; Ginzburg, M.; Coombs, N.; Coyle, T. W.; Raju, N. P.; Greedan, J. E.; Ozin, G. A.; Manners, I. *Science* **2000**, *287*, 1460-1463.

(11) Thomas, K. R.; Ionescu, A.; Gwyther, J.; Manners, I.; Barnes, C. H. W.; Steiner, U.; Sivaniah, E. *J. Appl. Phys.* **2012**, *109*, 073904.

(12) Lastella, S.; Mallick, G.; Woo, R.; Karna, S. P.; Rider, D. A.; Manners, I.; Jung, Y. J.; Ryu, C. Y.; Ajayan, P. M. *J. Appl. Phys.* **2006**, *99*, 024302.

(13) Gilroy, J. B.; Patra, S. K.; Mitchels, J. M.; Winnik, M. A.; Manners, I. *Angew. Chem., Int. Ed.* **2011**, *50*, 5851-5855.

(14) Caruana, D. J.; Heller, A. *J. Am. Chem. Soc.* **1999**, *121*, 769-774.

(15) Gajovic, N.; Binyamin, G.; Warsinke, A.; Scheller, F. W.; Heller, A. *Anal. Chem.* **2000**, *72*, 2963-2968.

(16) Djeda, R.; Rapakousiou, A.; Liang, L.; Guidolin, N.; Ruiz, J.; Astruc, D. *Angew. Chem., Int. Ed.* **2010**, *49*, 8152-8156.

(17) Daniel, M. C.; Ruiz, J.; Astruc, D. *J. Am. Chem. Soc.* **2003**, *125*, 1150-1151.

(18) Péter, M.; Lammertink, R. G. H.; Hempenius, M. A.; Vancso, G. J. *Langmuir* **2005**, *21*, 5115-5123.

(19) Valerio, C.; Fillaut, J. L.; Ruiz, J.; Guittard, J.; Blais, J. C.; Astruc, D. *J. Am. Chem. Soc.* **1997**, *119*, 2588-2589.

(20) Arsenault, A. C.; Puzzo, D. P.; Manners, I.; Ozin, G. A. *Nat. Photonics* **2007**, *1*, 468-472.

(21) Chabanne, L.; Matas, I.; Patra, S. K.; Manners, I. *Polym. Chem.* **2011**, *2*, 2651-2660.

(22) Schacher, F. H.; Rupar, P. A.; Manners, I. *Angew. Chem., Int. Ed.* **2012**, *51*, 7898-7921.

(23) Rider, D. A.; Liu, K.; Eloi, J.-C.; Vanderark, L.; Yang, L.; Wang, J.-Y.; Grozea, D.; Lu, Z.-H.; Russell, T. P.; Manners, I. *ACS Nano* **2008**, *2*, 263-270.

(24) Ross, C. A.; Jung, Y. S.; Chuang, V. P.; Ilievski, F.; Yang, J. K. W.; Bita, I.; Thomas, E. L.; Smith, H. I.; Berggren, K. K.; Vancso, G. J.; Cheng, J. Y. *J. Vac. Sci. Technol. B* **2008**, *26*, 2489-2494.

(25) Ren, L.; Zhang, J.; Hardy, C. G.; Ma, S.; Tang, C. *Macromol. Rapid Commun.* **2012**, *33*, 510-516.

(26) Cheng, J. Y.; Ross, C. A.; Chan, V. Z. H.; Thomas, E. L.; Lammertink, R. G. H.; Vancso, G. J. *Adv. Mater.* **2001**, *13*, 1174-1178.

(27) Wild, A.; Teichler, A.; Von Der Ehe, C.; Winter, A.; Hager, M. D.; Yao, B.; Zhang, B.; Xie, Z.; Wong, W. Y.; Schubert, U. S. *Macromol. Chem. Phys.* **2013**, *214*, 1072-1080.

(28) Friebe, C.; Görls, H.; Jäger, M.; Schubert, U. S. *Eur. J. Inorg. Chem.* **2013**, 4191-4202.

(29) Mansfeld, U.; Winter, A.; Hager, M. D.; Günther, W.; Altuntaş, E.; Schubert, U. S. *J. Polym. Sci., Part A: Polym. Chem.* **2013**, *51*, 2006-2015.

(30) Whittell, G. R.; Hager, M. D.; Schubert, U. S.; Manners, I. *Nat. Mater.* **2011**, *10*, 176-188.

(31) Wild, A.; Winter, A.; Hager, M. D.; Schubert, U. S. *Chem. Commun.* **2012**, *48*, 964-966.

(32) Wild, A.; Winter, A.; Hager, M. D.; Schubert, U. S. *Analyst* **2012**, *137*, 2333-2337.

(33) Kupfer, S.; Zedler, L.; Guthmuller, J.; Bode, S.; Hager, M. D.; Schubert, U. S.; Popp, J.; Gräfe, S.; Dietzek, B. *Phys. Chem. Chem. Phys.* **2014**, *16*, 12422-12432.

(34) Friebe, C.; Wild, A.; Perelaer, J.; Schubert, U. S. *Macromol. Rapid Commun.* **2012**, *33*, 503-509.

(35) Wild, A.; Winter, A.; Hager, M. D.; Görls, H.; Schubert, U. S. *Macromol. Rapid Commun.* **2012**, *33*, 517-521.

(36) Zhang, K.; Zha, Y.; Peng, B.; Chen, Y.; Tew, G. N. *J. Am. Chem. Soc.* **2013**, *135*, 15994-15997.

(37) Shunmugam, R.; Gabriel, G. J.; Aamer, K. A.; Tew, G. N. *Macromol. Rapid Commun.* **2010**, *31*, 784-793.

(38) Shunmugam, R.; Tew, G. N. *Macromol. Rapid Commun.* **2008**, *29*, 1355-1362.

(39) Shunmugam, R.; Tew, G. N. *Polym. Adv. Technol.* **2008**, *19*, 596-601.

(40) Aamer, K. A.; Tew, G. N. *Macromolecules* **2007**, *40*, 2737-2744.

(41) Zha, Y.; Thaker, H. D.; Maddikeri, R. R.; Gido, S. P.; Tuominen, M. T.; Tew, G. N. *J. Am. Chem. Soc.* **2012**, *134*, 14534-14541.

(42) Zha, Y.; Maddikeri, R. R.; Gido, S. P.; Tew, G. N. *J. Inorg. Organomet. Polym.* **2013**, *23*, 89-94.

(43) Al-Badri, Z. M.; Maddikeri, R. R.; Zha, Y.; Thaker, H. D.; Dobriyal, P.; Shunmugam, R.; Russell, T. P.; Tew, G. N. *Nat. Commun.* **2011**, *2*, 482.

(44) Mîinea, L. A.; Sessions, L. B.; Ericson, K. D.; Glueck, D. S.; Grubbs, R. B. *Macromolecules* **2004**, *37*, 8967-8972.

(45) Bode, S.; Bose, R. K.; Matthes, S.; Ehrhardt, M.; Seifert, A.; Schacher, F. H.; Paulus, R. M.; Stumpf, S.; Sandmann, B.; Vitz, J.; Winter, A.; Hoeppener, S.; Garcia, S. J.; Spange, S.; Van Der Zwaag, S.; Hager, M. D.; Schubert, U. S. *Polym. Chem.* **2013**, *4*, 4966-4973.

(46) Matsuura, Y.; Matsukawa, K. *Chem. Phys. Lett.* **2007**, *447*, 101-104.

(47) Manners, I. *J. Organomet. Chem.* **2011**, *696*, 1146-1149.

(48) Matsuura, Y.; Matsukawa, K. *Chem. Phys. Lett.* **2007**, *436*, 224-227.

(49) Lastella, S.; Jung, Y. J.; Yang, H.; Vajtai, R.; Ajayan, P. M.; Ryu, C. Y.; Rider, D. A.; Manners, I. *J. Mater. Chem.* **2004**, *14*, 1791-1794.

(50) Smith, G. S.; Patra, S. K.; Vanderark, L.; Saithong, S.; Charmant, J. P. H.; Manners, I. *Macromol. Chem. Phys.* **2010**, *211*, 303-312.

(51) Wang, X.; Liu, K.; Arsenault, A. C.; Rider, D. A.; Ozin, G. A.; Winnik, M. A.; Manners, I. *J. Am. Chem. Soc.* **2007**, *129*, 5630-5639.

(52) Bartole-Scott, A.; Resendes, R.; Jäkle, F.; Lough, A. J.; Manners, I. *Organometallics* **2004**, *23*, 6116-6126.

(53) Baumgartner, T.; Jäkle, F.; Rulkens, R.; Zech, G.; Lough, A. J.; Manners, I. *J. Am. Chem. Soc.* **2002**, *124*, 10062-10070.

(54) Berenbaum, A.; Braunschweig, H.; Dirk, R.; Englert, U.; Green, J. C.; Jakle, F.; Lough, A. J.; Manners, I. *J. Am. Chem. Soc.* **2000**, *122*, 5765-5774.

(55) Bourke, S. C.; MacLachlan, M. J.; Lough, A. J.; Manners, I. *Chem. Eur. J.* **2005**, *11*, 1989-2000.

(56) Chan, W. Y.; Clendenning, S. B.; Berenbaum, A.; Lough, A. J.; Aouba, S.; Ruda, H. E.; Manners, I. *J. Am. Chem. Soc.* **2005**, *127*, 3796-3808.

(57) Chan, W. Y.; Lough, A. J.; Manners, I. *Angew. Chem., Int. Ed.* **2007**, *46*, 9069-9072.

(58) Arsenault, A. C.; Clark, T. J.; Freymann, G. V.; Cademartiri, L.; Sapienza, R.; Bertolotti, J.; Vekris, E.; Wong, S.; Kitaev, V.; Manners, I.; Z., W. R.; John, S.; Wiersma, D.; Ozin, G. A. *Nat. Mater.* **2006**, *5*, 179-184.

(59) Clendenning, S. B.; Manners, I. *J. Vac. Sci. Technol. B* **2004**, *22*, 3493-3496.

(60) Kulbaba, K.; Cheng, A.; Bartole, A.; Greenberg, S.; Resendes, R.; Coombs, N.; Safa-Sefat, A.; Greedan, J. E.; Stöver, H. D. H.; Ozin, G. A.; Manners, I. *J. Am. Chem. Soc.* **2002**, *124*, 12522-12534.

(61) Kulbaba, K.; Resendes, R.; Cheng, A.; Bartole, A.; Safa-Sefat, A.; Coombs, N.; Greedan, J. E.; Ozin, G. A.; Manners, I. *Adv. Mater.* **2001**, *13*, 732-736.

(62) Li, M.-X.; Xu, S.-S.; Song, H.-B.; Liu, B.-Y.; Wang, B.-Q. *Polyhedron* **2011**, *30*, 1313-1317.

(63) Issa, I. M.; Aly, M. M. *J. Inorg. Nucl. Chem.* **1973**, *35*, 295-297.

(64) Cuadrado, I.; Casado, C. M.; Lobete, F.; Alonso, B.; González, B.; Losada, J.; Amador, U. *Organometallics* **1991**, *18*, 4960-4969.

(65) Mayer, U. F. J.; Gilroy, J. B.; O'Hare, D.; Manners, I. *J. Am. Chem. Soc.* **2009**, *131*, 10382-10383.

(66) Ren, L.; Hardy, C. G.; Tang, C. *J. Am. Chem. Soc.* **2010**, *132*, 8874-8875.

(67) Ren, L.; Zhang, J.; Bai, X.; Hardy, C. G.; Shimizu, K. D.; Tang, C. *Chem. Sci.* **2012**, *3*, 580-583.

(68) Qiu, H.; Gilroy, J. B.; Manners, I. *Chem. Commun.* **2013**, *49*, 42-44.

(69) Zhang, J.; Chen, Y. P.; Miller, K. P.; Ganewatta, M. S.; Bam, M.; Yan, Y.; Nagarkatti, M.; Decho, A. W.; Tang, C. *J. Am. Chem. Soc.* **2014**, *136*, 4873-4876.

(70) Rosenblum, M.; North, B. *J. Am. Chem. Soc.* **1968**, *90*, 1060-1061.

(71) Rosenblum, M.; North, B.; Wells, D.; Giering, W. P. *J. Am. Chem. Soc.* **1972**, *94*, 1239-1246.

(72) Taylor, J. E.; Mahon, M. F.; Fossey, J. S. *Angew. Chem., Int. Ed.* **2007**, *46*, 2266-2268.

(73) Rausch, M. D.; Genetti, R. A. *J. Org. Chem.* **1970**, *35*, 3888-3897.

(74) Chadha, P.; Ragogna, P. J. *Chem. Commun.* **2011**, *47*, 5301-5303.

(75) Gleiter, R.; Pflaesterer, G. *Organometallics* **1993**, *12*, 1886-1889.

(76) Gömez Ribelles, J. L.; Monleön Pradas, M.; Gallego Ferrer, G.; Peidro Torres, N.; Ferez Giménez, V.; Pissis, P.; Kyritsis, A. *J. Polym. Sci., Part B: Polym. Phys.* **1999**, *37*, 1587-1599.

(77) Arita, T.; Buback, M.; Vana, P. *Macromolecules* **2005**, *38*, 7935-7943.

(78) Lai, J. T.; Filla, D.; Shea, R. *Macromolecules* **2002**, *35*, 6754-6756.

(79) Sugawara, A.; Shirahata, M.; Sato, S.; Sato, R. *Bull. Chem. Soc. Jpn.* **1984**, *57*, 3353-3354.

# Chapter 3

# A Multifunctional Block Copolymer – Where Polymetallic and Polyelectrolyte Blocks Meet

## 3.1. Introduction

Over the last decade, research to incorporate transition metals into polymers has continually expanded.[1-6] Metallopolymers have shown properties distinct from their organic (conventional polymer) and inorganic (transition metal) components and have found potential applications in catalysis,[7,8] sensors,[9-13] lithography,[14-17] magnetic materials,[18-20] electrochromic materials,[21-25] and as ceramic precursors.[14,17,26,27] Well-defined metallopolymers with controlled molecular weights and narrow polydispersity indices (PDIs)[28-30] have allowed for the development of solution and solid-state self-assembly to fabricate complex and unique nanostructures with metallic domains.[31-34] Metal containing nanostructures such as micelles, vesicles, platelets, and rods in solution, and lamella, cylinders, spheres, and gyroids in the solid-state,[34-37] are promising precursors for the synthesis of well-defined metal nanoparticles *via* thermal decomposition,[27,38,39] radiation treatment,[40] or reduction of metal salts.[41-43]

Running in parallel to the flourishing metallopolymer developments, is a special focus in metal containing polyelectrolytes as a novel class of multifunctional materials. There are different methods available to incorporate metallic units and ionic functionality into one polymeric building block. The Tang Group has synthesized metal containing polyelectrolytes by applying a number of controlled polymerization methods to polymerize cobaltocenium containing monomers.[28,44-48] These metallopolymers carrying a charged cobaltocenium side group paired with different counter anions, have shown interesting applications such as in antimicrobial and electroactive materials with tunable magnetic properties (**3.1**; Figure 3.1).[49-51]

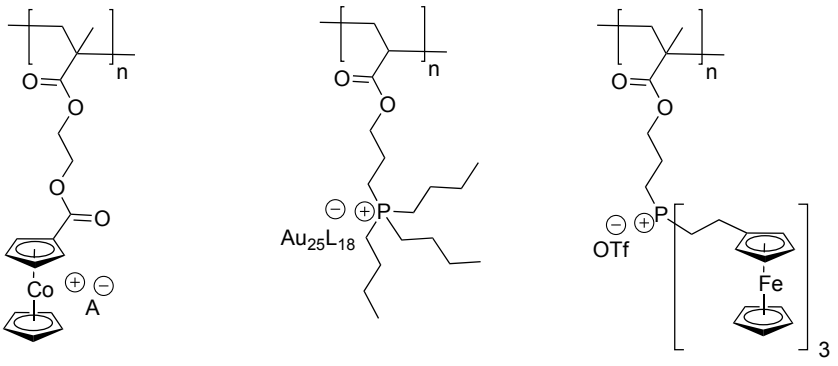


**3.1** **3.2** **3.3**

**Figure 3.1.** Side-chain functionalized cobaltocenium containing polyelectrolyte (**3.1**). Cross-linked network of photo-polymerized phosphonium-acrylate, functionalized with gold cluster anion (**3.2**). Highly metallized phosphonium-based polyelectrolyte with three ferrocenes per repeat unit (**3.3**).

Among the large class of polyelectrolytes, phosphonium-based polyelectrolytes have attracted increasing interest due to their unique properties such as high thermal stability,[52] flame retardancy,[53] and biocompatibility,[54] leading to potential applications in molecular recognition,[55,56] humidity sensors,[57-62] and biocides[63]. Coexistence of phosphorus centers and metallic centers in the polymeric backbone,[64-71] or utilizing coordination chemistry in binding the lone pair of electrons on the phosphorus to coordinate metal ions has been known for decades.[56,72-74] The Ragogna Group has utilized photo-polymerization methods as a strategy to generate charged, mechanically robust, highly cross-linked phosphonium containing networks with a high degree of surface tunability (**3.2**; Figure 3.1).[75] By utilizing salt metathesis chemistry of polyelectrolytes, anionic gold cluster [$(Au_{25}L_{18})^-$] was incorporated onto the phosphonium-based network.

Utilizing phosphonium-based polyelectrolytes to develop charged metallopolymers is a novel approach that has not been explored. To the best of our knowledge, the only example of metal containing phosphonium-based polyelectrolytes is reported by the Gilroy Group *via* free radical polymerization of phosphonium acrylate monomer bearing three ferrocenes per repeat unit (**3.3**; Figure 3.1).[39] This highly metalized phosphonium-based polyelectrolyte has shown to be redox-active and a promising precursor for the formation of iron-rich nanoparticles *via* pyrolysis.[39]

In this context, we introduce the first example of block copolymers consisting of a phosphonium-based polyelectrolyte block and a cobalt containing metallopolymer block

*via* sequential reversible addition fragmentation transfer (RAFT) polymerization (Scheme 3.3). This material is composed of a mixed sandwich cobaltocene repeat units featuring $\eta^5$-cyclopentadienyl-cobalt-$\eta^4$-cyclobutadiene (CpCoCb) and a phosphonium salt functionalized styrene. The synthesis and characterization of this novel class of materials has been detailed and the solution and solid-state self-assembly of metalized polyelectrolyte block copolymer was studied. By means of salt metathesis of the polyelectrolyte block, gold anions could be easily incorporated into the system, resulting in a heterobimetallic block copolymer with gold and cobalt containing blocks. Subjecting these heterobimetallic micelles to reducing conditions resulted in the production of gold nanoparticles (AuNPs) stabilized by a cobalt containing polymer. Phase-separation behavior of this unique metalized polyelectrolyte block copolymer was also examined. The first example of utilizing a $HAuCl_4$ solution to selectively stain phosphonium containing domains in phase-separated block copolymers *via* a simple and quick salt metathesis reaction is reported. Pyrolysis of the bulk self-assembled block copolymers was studied resulting in cobalt-phosphate nanoparticles with 17% char yield. The pyrolyzed materials were attracted to permanent magnet, indicating the presence of magnetic particles.

## 3.2. Results and Discussion

### 3.2.1. Optimizing the Polymerization Conditions

The synthesis and full characterization of $\eta^5$-cyclopentadienyl-cobalt-$\eta^4$-cyclobutadiene monomer (CpCoCb) (**2.3**; Figure 3.2) is discussed in details in chapter 2.[76] We have previously shown that polymerization of CpCoCb monomer (**2.3**) under variety of applied reversible addition fragmentation transfer (RAFT) polymerization conditions was not controlled, unless carried out in the presence of a small co-monomer, *e.g.* methyl acrylate (MA), to act as a spacer. The copolymerization of CpCoCb (**2.3**) and MA resulted in PolyCpCoCb-*r*-PMA random copolymer (**2.8**) with excellent control over molecular weight and polydispersity (PDI) (Figure 3.2).[76] As an advantage of using RAFT polymerization, the PolyCpCoCb-*r*-PMA random copolymer (**2.8**) can be used as a macro-RAFT agent to prepare block copolymers. To obtain a metallopolymer-*b*-

polyelectrolyte copolymer, **2.8** was utilized as macro-RAFT agent to polymerize a phosphonium salt functionalized styrene monomer (**3.5**; Figure 3.2).

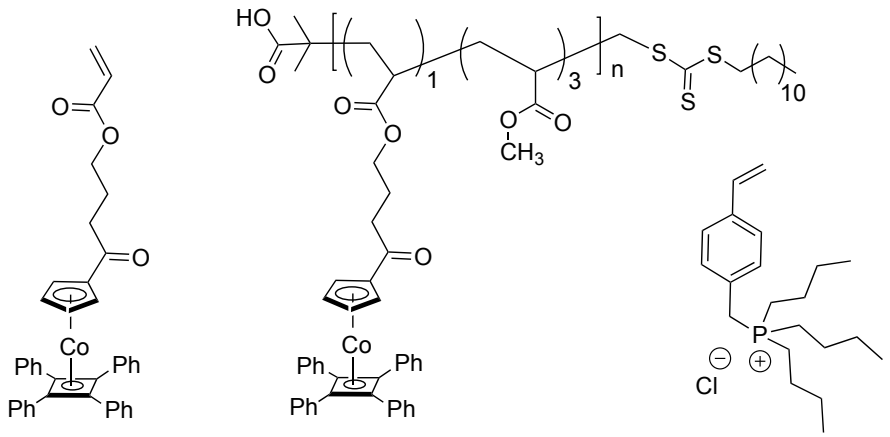


**2.3** **2.8** **3.5**

**Figure 3.2.** Chemical structure of $\eta^5$-cyclopentadienyl-cobalt-$\eta^4$-cyclobutadiene monomer (CpCoCb (**2.3**)), PolyCpCoCb-*r*-PMA random copolymer (**2.8**), and phosphonium salt functionalized styrene monomer with chloride counter anion (**3.5**).

Molecular weight distribution analysis of homo- and block copolymers containing a polyelectrolyte block by commonly used techniques, such as gel permeation chromatography (GPC), is challenging because of the strong interaction of polyelectrolytes with GPC columns.[77-81] There are some recent advanced methodologies to reduce these interactions, making GPC analysis of polyelectrolytes achievable.[82,83] Nevertheless utilizing other outlets such as $^1$H NMR spectroscopy for end group analysis provides a reliable estimate of the polymer molecular weight ($M_n$). The $^1$H NMR spectrum of a polyelectrolyte consisting of **3.5** as repeat units (*i.e.* phosphonium salt functionalized polystyrene with chloride counter anion; (**PS(P$^+$Cl$^-$)**)) revealed that signals of this polyelectrolyte are either drastically broadened or overlap with the signals of macro-RAFT agent **2.8** (Figure A3.1). Consequently, end group analysis of a block copolymers made from **2.8** and **PS(P$^+$Cl$^-$)** by $^1$H NMR spectroscopy was not accurate. Therefore, we utilized a tagging strategy, where fluorine atoms were installed on the phosphonium containing monomer (**3.6**; Figure 3.3) and on a RAFT agent (**3.7**; Scheme 3.1) enabling the use of $^{19}$F{$^1$H} NMR spectroscopy for end group analysis.

### 3.2.2. Fluorine Tagged Phosphonium Monomer

The phosphonium monomer was simply fluorine tagged *via* salt metathesis reaction replacing chloride anion with trifluoromethanesulfonate (triflate; $OTf^-$) anion. Monomer **3.5** was stirred with lithium triflate in dichloromethane (DCM) for 8 hours (Figure 3.3). Lithium chloride was removed by filtration, and organic layer was washed with distilled water to remove any residues of the inorganic salt byproduct (*e.g.* LiCl) and excess lithium triflate. Silver nitrate tests were performed on the aqueous washings to confirm there was no chloride anion trace present. Removing volatiles from the organic fraction *in vacuo* afforded the phosphonium monomer paired with the triflate anion (**3.6**; Figure 3.3). Negative and positive ion mass spectroscopy of purified **3.6** confirmed the absence of chloride in the sample (Figure A3.2). Purified monomer **3.6** was comprehensively characterized by multinuclear NMR spectroscopy ($\delta_P$ = 31.7; $\delta_F$ = -78.3) (Figure 3.3).

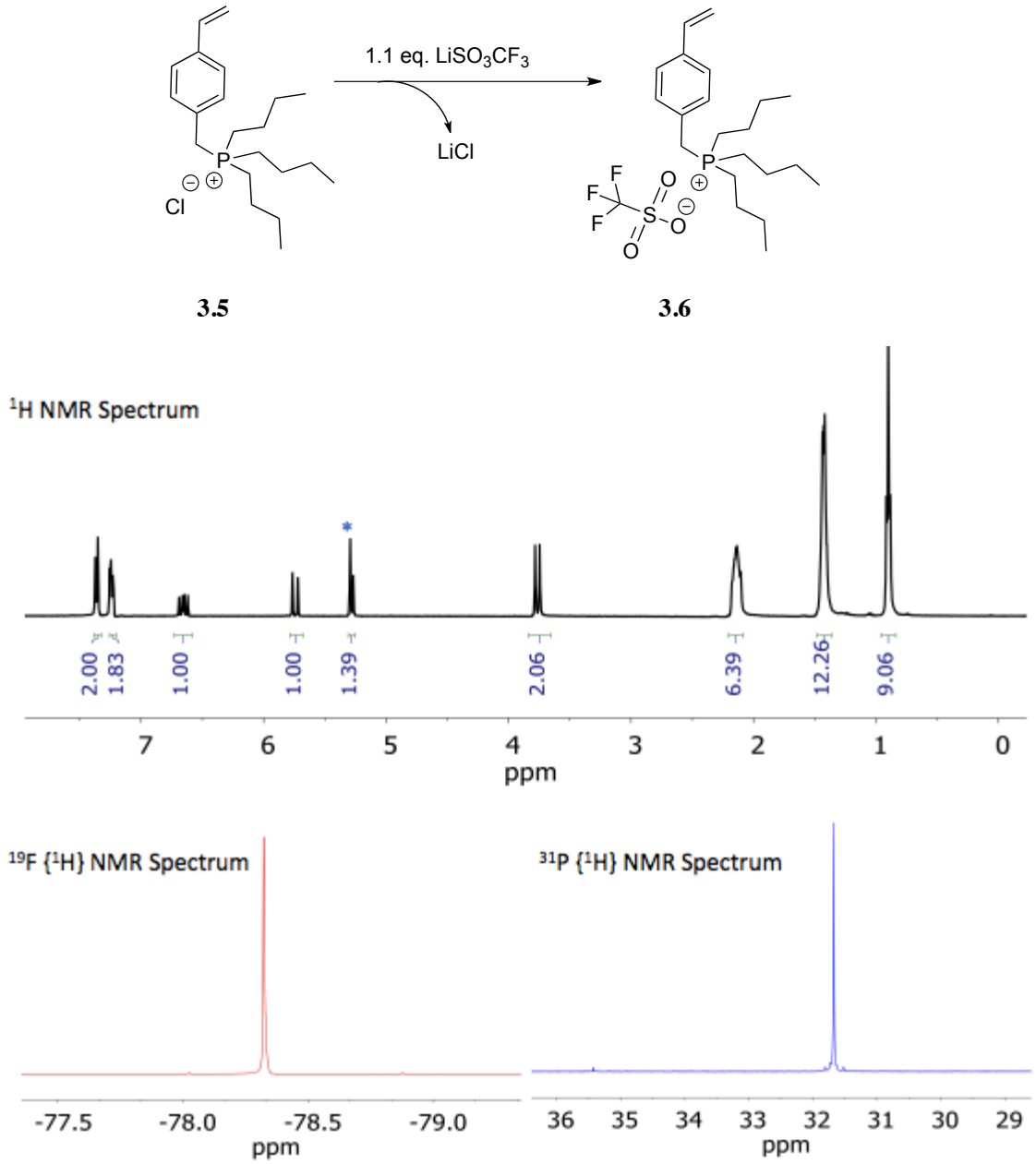


**Figure 3.3.** Salt metathesis reaction of **3.5** and lithium triflate to prepare fluorine tagged phosphonium monomer **3.6**. $^{1}H$, $^{19}F\{^{1}H\}$, and $^{31}P\{^{1}H\}$ NMR spectra of purified **3.6** in deutrated chloroform. (*trace of DCM).

### 3.2.3. Fluorine Tagged RAFT Agent

Following a well-established trithiocarbonate synthesis, a fluorine end-capped RAFT agent was synthesized (Scheme 3.1). 1-dodecanethiol was dissolved in nitrogen-saturated toluene and chilled to 0 °C. Aqueous sodium hydroxide and Aliquat 336 (phase transfer

agent) was added to the reaction mixture. After 30 minutes, carbon disulfide was added followed by addition of 4-(trifluoromethyl)benzyl bromide. The organic layer was washed with water, then brine, and dried over magnesium sulfate. The volatiles were removed *in vacuo* to yield the crude product as yellow liquid. After purification by column chromatography, the pure fluorine end-capped RAFT agent (**3.7**; Scheme 3.1) was isolated as a yellow solid. Purified **3.7** was characterized by multinuclear NMR spectroscopy (see Figure A3.3 for $^{1}H$ NMR spectrum). The $^{19}F\{^{1}H\}$ NMR spectrum of the RAFT agent **3.7** showed a singlet resonance at -62.6 ppm (Figure 3.5). This key $^{19}F$ resonance will subsequently be used as an internal reference for the end group analysis of the fluorine tagged polyelectrolyte synthesized *via* RAFT polymerization of monomer **3.6**.

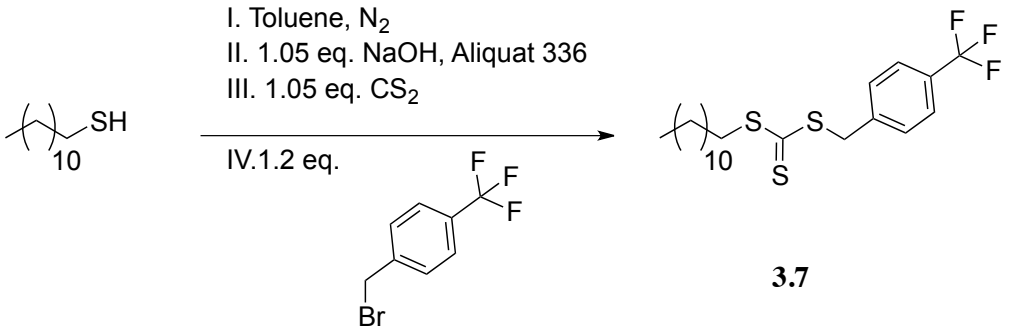


**Scheme 3.1.** Synthesis of fluorine tagged RAFT agent (**3.7**).

### 3.2.4. Fluorine Tagged Metallopolymer macro-RAFT Agent

Following our established RAFT polymerization protocols of CpCoCb monomer (**2.3**),[76] the fluorine tagged RAFT agent **3.7** was dissolved in nitrogen-saturated chlorobenzene and charged with 2,2′-azobisisobutyronitrile (AIBN) (0.2 *eq.*), monomer **2.3** (60 *eq.*), and MA (180 *eq.*) (Scheme 3.2). The reaction mixture was heated at 80 °C and sample aliquots were collected at 20 minute time intervals.

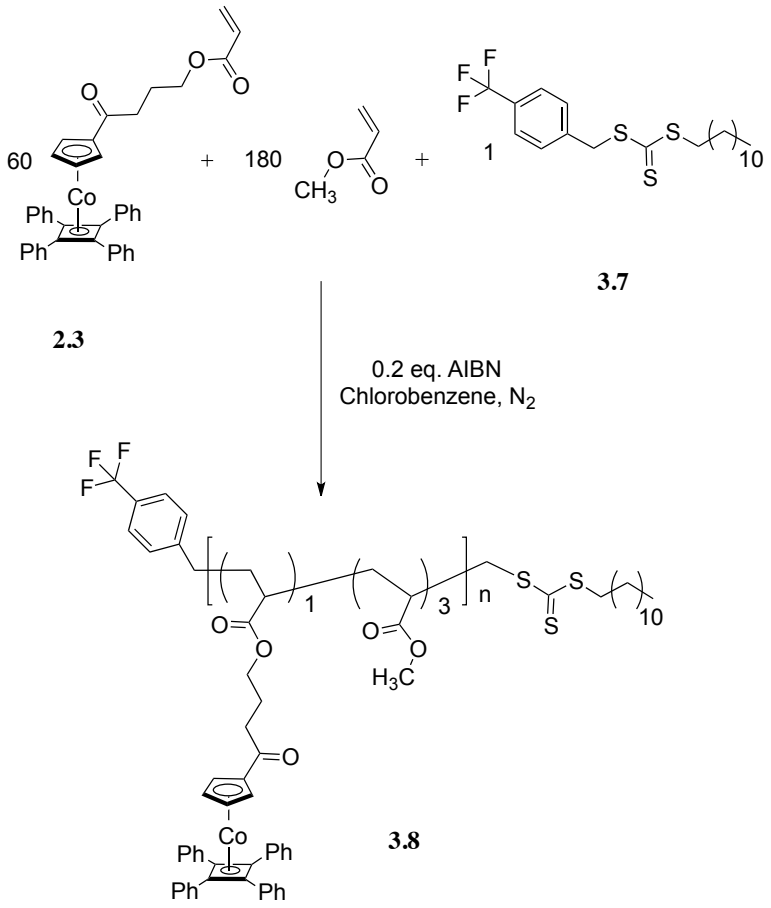


**Scheme 3.2.** Synthesis of fluorine tagged metallopolymer **3.8** to be used as macro-RAFT agent.

Signal broadening in the $^1$H NMR spectra of the crude polymer samples was indicative of polymerization along with the decrease in the relative integration values of the vinyl protons (Figure A3.4-6). $^1$H NMR spectra of the crude polymer samples were used to calculate the concentration of monomer **2.3** at a given time ($[M_t]$) to plot $\ln[M_0]/[M_t]$ *vs* reaction time (Figure 3.4). The resultant pseudo first order plot was characteristic of a controlled polymerization, indicating the constant consumption of **2.3** over the course of the polymerization reaction.

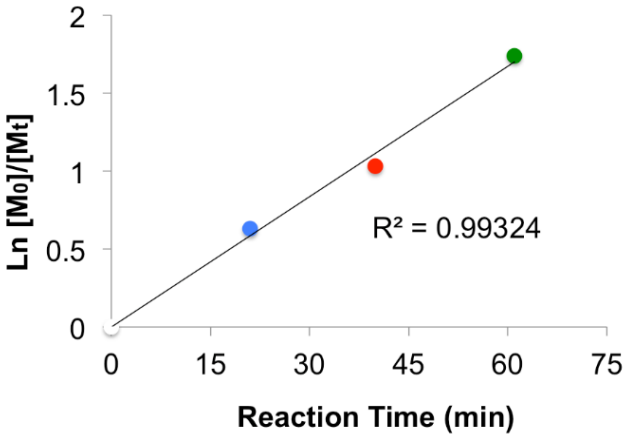


**Figure 3.4.** ln[$M_0$]/[$M_t$] *vs* reaction time during random copolymerization reaction. (note; M refers to monomer **2.3**).

Polymer samples were purified by precipitation in hexane to remove any unreacted monomer. The purified polymer **3.8** was analyzed by $^{1}H$ and $^{19}F\{^{1}H\}$ NMR spectroscopy (Figure A3.7 and Figure 3.5). It is noteworthy to note that in the $^{19}F\{^{1}H\}$ NMR spectrum of the polymer sample, there was a slight downfield shift ($\Delta\delta$ = 0.3 ppm) and the resonance broadened as expected for polymers (Figure 3.5). This resonance sets up an internal standard for end group analysis of the fluorine tagged polyelectrolyte block (**PS($P^{+}OTf^{-}$)**) in the subsequent step.

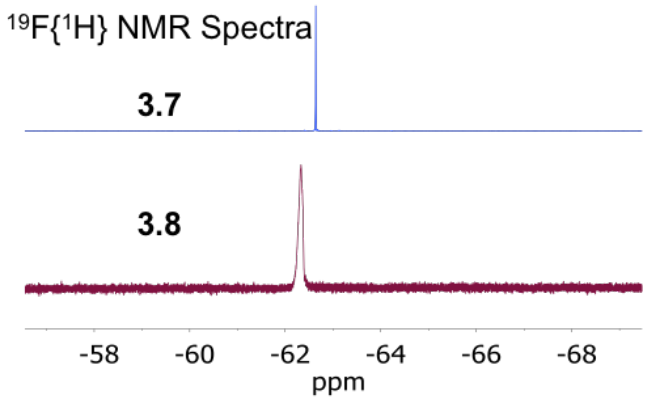


**Figure 3.5.** $^{19}F\{^{1}H\}$ NMR spectrum of fluorine end-capped RAFT agent **3.7** and purified fluorine end-capped macro-RAFT agent (**3.8**).

Chain growth of PolyCpCoCb-*r*-PMA (**3.8**) during the polymerization reaction was confirmed by the gradual decrease in relative integration values of the vinyl signals (Figure A3.4-6) and further supported by a shift to shorter elution times for the corresponding GPC analyses (Figure 3.6). Refractive index (RI) traces were analyzed relative to polystyrene (PS) standards to obtain molecular weight and polydispersity index (PDI) of the produced metallopolymer. In a typical reaction, 60 repeat units of CpCoCb monomer (**2.3**) were targeted resulting in *ca*. 20 kDa polymers with degree of polymerization (DP) of 50 at 82% monomer conversion (Figure A3.6). PDI of all samples were 1.1, indicative of narrow molecular weight distribution and characteristic of a controlled polymerization (Figure 3.6).

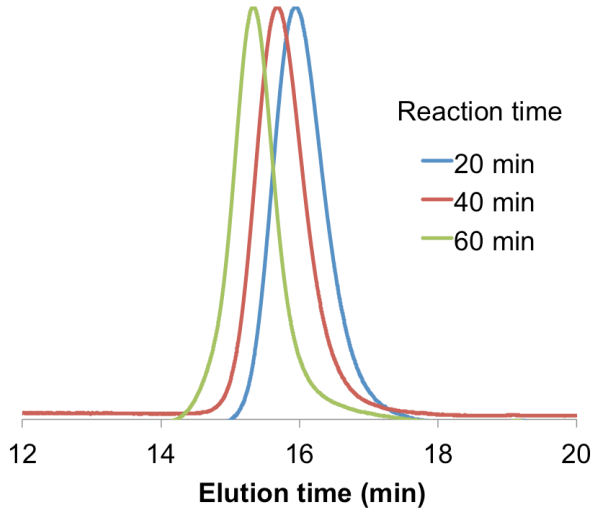


| Reaction Time | DP[a] | $M_n$ (kDa)[b] | PDI |
|---|---|---|---|
| 20 min | 28 | 11 | 1.1 |
| 40 min | 46 | 14.5 | 1.1 |
| 60 min | 50 | 19.6 | 1.1 |

**Figure 3.6.** RI Trace, DP, $M_n$, and PDI of random copolymer **3.8** at 20 minutes time intervals. (a: based on monomer **2.3** conversion. b: relative to PS Standards).

### 3.2.5. Synthesis of Metallopolymer-*b*-Polyelectrolyte

The well-defined metallopolymer **3.8** with 50 repeat units of CpCoCb was used as a macro-RAFT agent to polymerize the fluorine tagged phosphonium salt functionalized

styrene monomer (**3.6**). The relative integration ratio of PolyCpCoCb and PMA was *ca.* 3, which was similar to the monomers feed ratio and in line with our previous study. The macro-RAFT agent **3.8** (1 *eq.*) and monomer **3.6** (60 *eq.*) were dissolved in nitrogen-saturated chlorobenzene, charged with AIBN (0.2 *eq.*), and heated at 80 °C (Scheme 3.3). Aliquots of the reaction mixture were taken at time intervals of 15 minutes. $^{31}P\{^{1}H\}$ NMR spectra of the crude polymer samples showed a sharp phosphorus signal for unreacted monomer **3.6** and a broad signal further upfield for the polyelectrolyte block. The polyelectrolyte consist of **3.6** repeat units is a phosphonium salt functionalized polystyrene with triflate counter anion and will be so-called "**PS($P^+$OTf)**". Unreacted monomer **3.6** was removed by precipitating the reaction mixture into diethyl ether. The absence of a sharp phosphorus signals indicated unreacted monomer is removed (Figure A3.8). Purified (PolyCpCoCb$_{50}$-*r*-PMA$_{150}$)-*b*-(PS($P^+OTf^-$)) block copolymer (**3.9**; Scheme 3.3) was analyzed by multinuclear NMR spectroscopy (Figure A3.8-13).

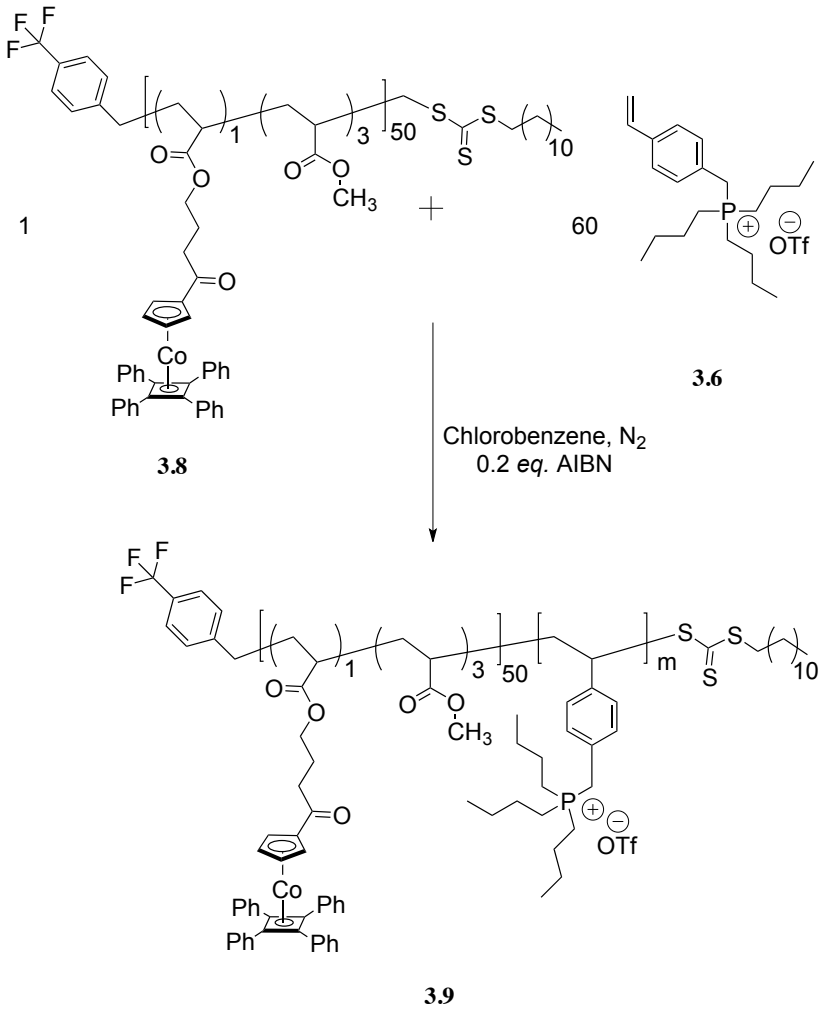


**Scheme 3.3.** Synthesis of **3.9**; (PolyCpCoCb$_{50}$-*r*-PMA$_{150}$)-*b*-(PS(P$^{+}$OTf$^{-}$)$_{m}$).

$^{19}F\{^{1}H\}$ NMR spectroscopy of purified aliquots were used for block copolymers end group analysis. The relative integration value of the fluorine signals of the **PS(P$^{+}$OTf$^{-}$)** block to the fluorine signals of the RAFT agent increased as the polyelectrolyte block grew over time (Figure 3.7 and Figure A3.9-12).

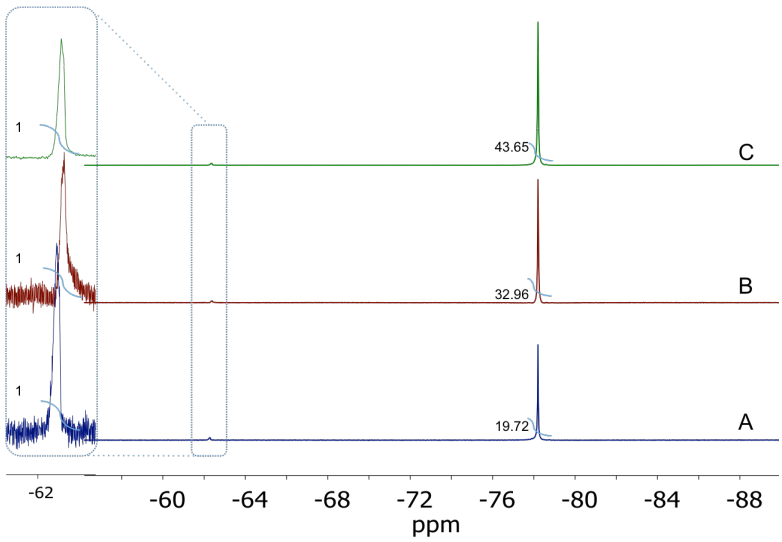


**Figure 3.7.** Stack plot of $^{19}F\{^{1}H\}$ NMR spectra of purified block copolymer **3.9** at 15 minutes time intervals.

These values were used to calculate DP and molecular weight ($M_n$) of the **PS($P^+OTf^-$)** segment. Plotting changes in monomer concentration over polymerization reaction time showed a pseudo first order plot, indicative of constant monomer **3.6** consumption and characteristic for a controlled polymerization (Figure 3.8).

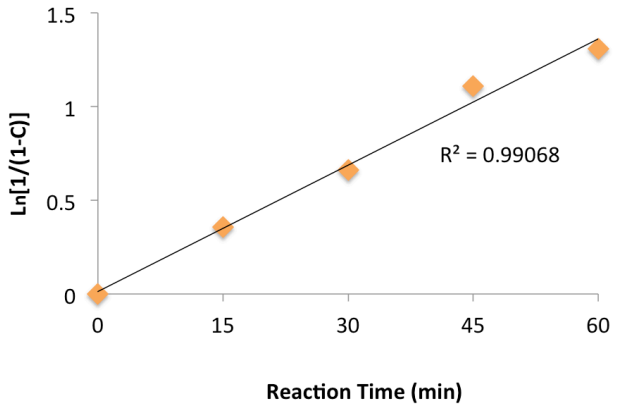


**Figure 3.8.** Ln[1/(1-C)] *vs* reaction time during block copolymer **3.9** synthesis.

By manipulating monomer feed ratio and reaction time, block copolymers with two different polyelectrolyte block lengths; [(PolyCpCoCb$_{50}$-*r*-PMA$_{150}$)-*b*-(PS($P^+OTf^-$)$_{30}$) and (PolyCpCoCb$_{50}$-*r*-PMA$_{150}$)-*b*-(PS($P^+OTf^-$)$_{100}$)], were prepared (Figure A3. 14-15).

Samples were analyzed by thermal gravimetric analysis (TGA) and differential scanning calorimetry (DSC) to obtain the decomposition temperature ($T_d$), char yield, and glass transition temperature ($T_g$). Block copolymer **3.9** had a $T_d$ of 300 °C, and showed 17% char yield regardless of the length of **PS($P^+OTf^-$)** (Figure 3.9). Two $T_g$ were observed in the DSC analysis of the block copolymers and each correspond to one of the individual constructing blocks; one for PolyCpCoCb-*r*-PMA block at 80 °C and one for PS($P^+OTf^-$) at 140 °C (Figure 3.9).

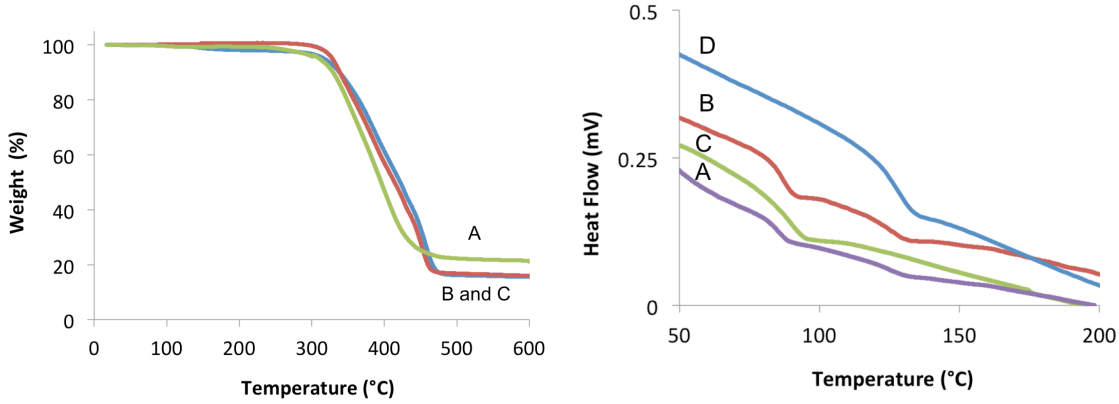


**Figure 3.9.** Left: TGA analysis of **3.8** (A) and **3.9** (B; m = 30, C; m = 100). Right: DSC analysis of homopolymer **3.8** (C), homopolymer **PS($P^+OTf^-$)** (D) and block copolymer **3.9** (A; m = 30, B; m =100).

### 3.2.6. Solution-State Self-Assembly

To examine the solution-state self-assembly behavior, block copolymer samples were dissolved in tetrahydrofuran (THF), a good solvent for both blocks and injected into methanol, which is a selective solvent for the polyelectrolyte block (**PS($P^+OTf^-$)**). This resulted in micelle formation with a metallopolymer core and polyelectrolyte corona. The presence of spherical micelles was confirmed by TEM imaging (Figure 3.10). The copolymer (PolyCpCoCb$_{50}$-*r*-PMA$_{150}$)-*b*-(PS($P^+OTf^-$)$_{30}$) resulted in 25±5 nm diameter spherical micelles.

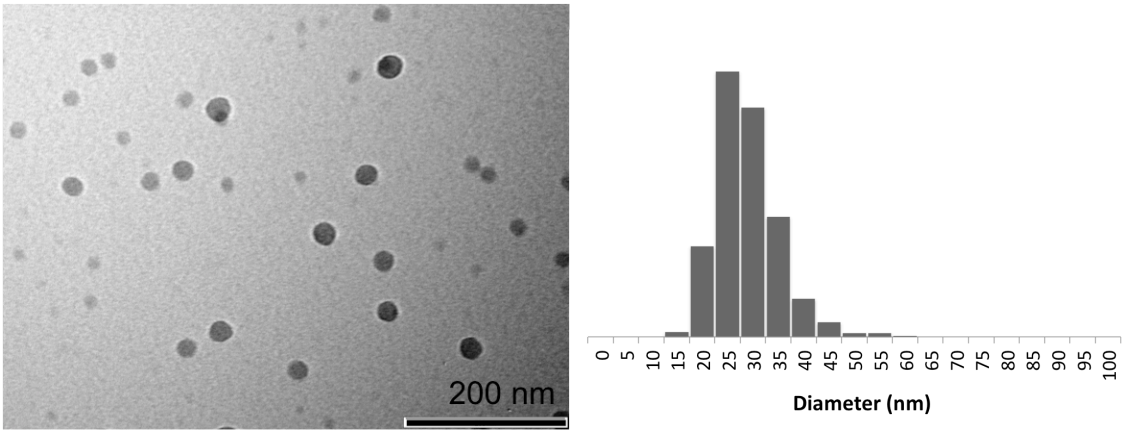


**Figure 3.10.** TEM image and size distribution of micelles made of block copolymer **3.9**.

Size distribution was also probed using dynamic light scattering (DLS), which indicated uniformly dispersed micelles with average hydrodynamic radius of 50 nm (Figure 3.11).

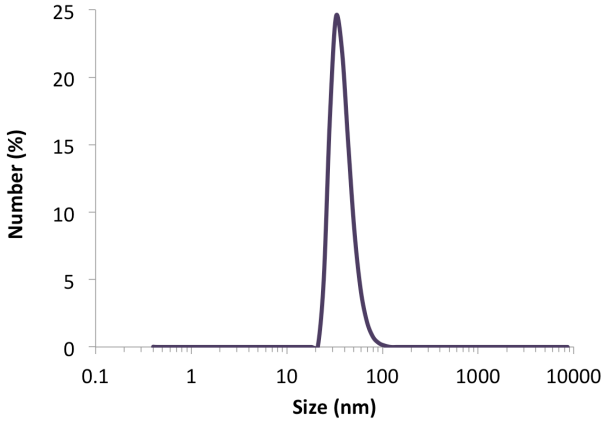


**Figure 3.11.** DLS of micelles made of block copolymer **3.9**.

Elemental composition of the micelles were examined by energy dispersive X-ray (EDX) and confirmed the presence of cobalt, phosphorus, and fluorine within the assemblies (Figure 3.12).

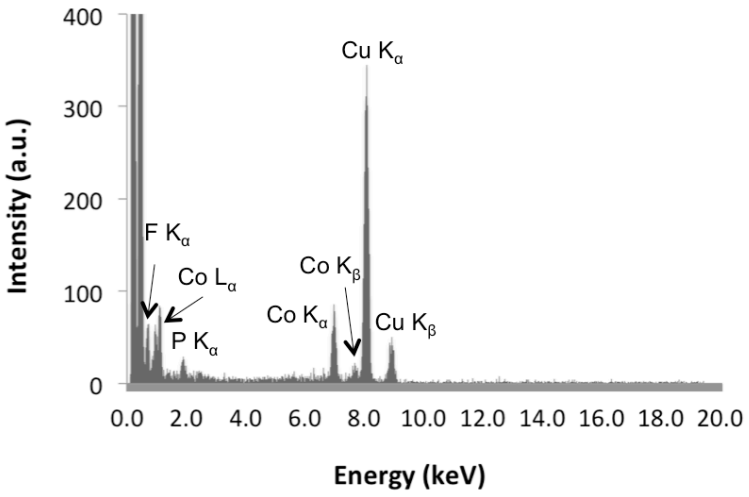


**Figure 3.12.** EDX of micelles made of block copolymer **3.9**. (note: Copper signal is from copper grid).

TEM analysis of the micelles made from the block copolymer **3.9** with longer polyelectrolyte block, (PolyCpCoCb$_{50}$-*r*-PMA$_{150}$)-*b*-(PS(P$^{+}$OTf$^{-}$)$_{100}$), revealed spherical micelles with 55±10 nm in diameter (Figure A3.16). DLS Analysis indicated a uniform micelle distribution with a hydrodynamic radius of 130 nm (Figure A3.17).

### 3.2.7. Incorporation of Gold Anion *via* Salt Metathesis

Polyelectrolytes posses interesting properties and functionalities and a simple demonstration of this point are salt metathesis reaction, which offers the opportunity to introduce extended functionality into a system. In this context, a salt metathesis reaction was carried out to exchange the triflate anion of the polyelectrolyte block with a gold anion ($AuCl_4^-$). Following a typical salt metathesis reaction, (PolyCpCoCb$_{50}$-*r*-PMA$_{150}$)-*b*-(PS(P$^{+}$OTf$^{-}$)$_m$) block copolymer (m = 30 and 100) was dissolved in DCM and stirred with aqueous solution of chloroauric acid ($HAuCl_4$) (Scheme 3.4). As the gold salt was consumed, the color of aqueous phase has changed from yellow to colorless. The organic layer was isolated and washed with water to remove any unreacted $HAuCl_4$. The resulted gold functionalized block copolymer (**3.10**; (PolyCpCoCb$_{50}$-*r*-PMA$_{150}$)-*b*-(PS(AuCl$_4$)$_m$)) was used for solution self-assembly studies with the goal of creating heterobimetallic nano structures.

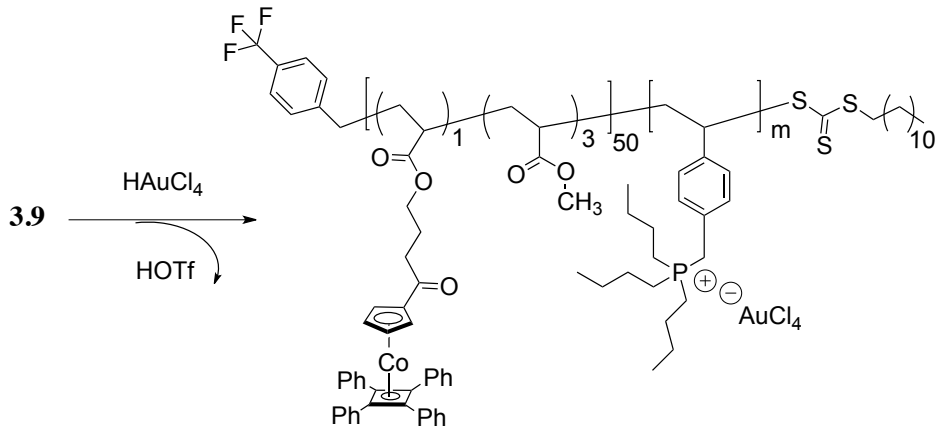


**3.10**

**Scheme 3.4.** Salt metathesis reaction of block copolymer **3.9** and $HAuCl_4$ to replace triflate anion with gold anion resulting in **3.10**; (PolyCpCoCb$_{50}$-*r*-PMA$_{150}$)-*b*-(PS($P^+AuCl_4^-$)$_m$).

Replacement of the triflate anion with $AuCl_4^-$ resulted in distinctive changes in the physical properties of the block copolymer, most notably solubility properties. Before salt metathesis reaction, the block copolymer **3.9** (with OTf anion) was soluble in benzene and no self-assembly was observed in this solvent. After salt metathesis reaction, **3.10** (with $AuCl_4^-$ anion) was not anymore soluble in benzene. This anion-induced property was used as a means to self-assemble micelles with a gold containing core and cobalt containing corona. Injection of a DCM solution of **3.10** into benzene resulted in the production of spherical micelles, confirmed by TEM imaging (Figure 3.13). Different sizes of spherical heterobimetallic micelles were obtained by using block copolymers with different PS($P^+AuCl_4^-$) block length. Based on the TEM data, (PolyCpCoCb$_{50}$-*r*-PMA$_{150}$)-*b*-(PS($P^+AuCl_4^-$)$_{30}$) resulted in spherical micelles with 40±5 nm diameter (Figure 3.13), whereas (PolyCpCoCb$_{50}$-*r*-PMA$_{150}$)-*b*-(PS($P^+AuCl_4^-$)$_{100}$) resulted in 50±7 nm structures (Figure A3.18).

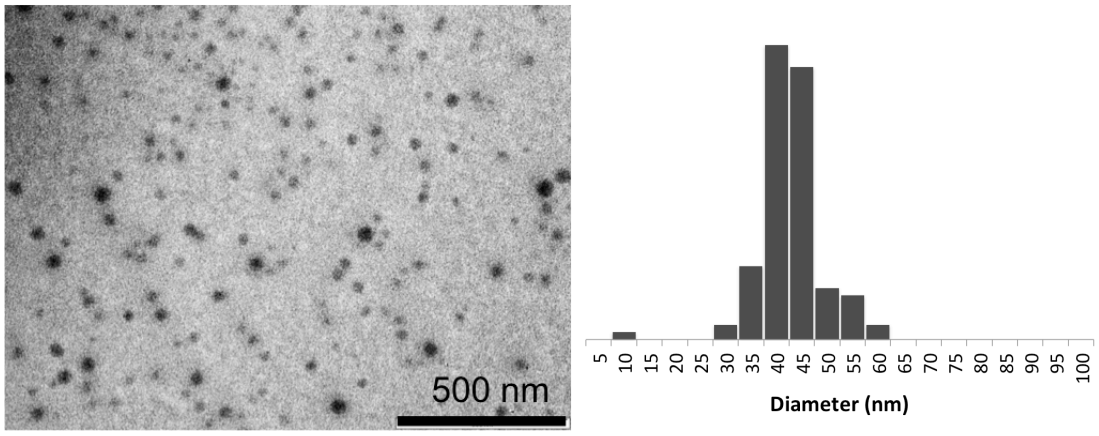


**Figure 3.13.** TEM image and size distribution of spherical micelles with gold containing core and cobalt containing corona.

DLS Analysis confirmed presence of uniform distribution of spherical micelles with hydrodynamic radii of 50 nm for m = 30 (Figure 3.14) and 65 nm for m = 100 (Figure A3.19). The presence of cobalt, gold, and phosphorus was identified using EDX analysis (Figure 3.14).

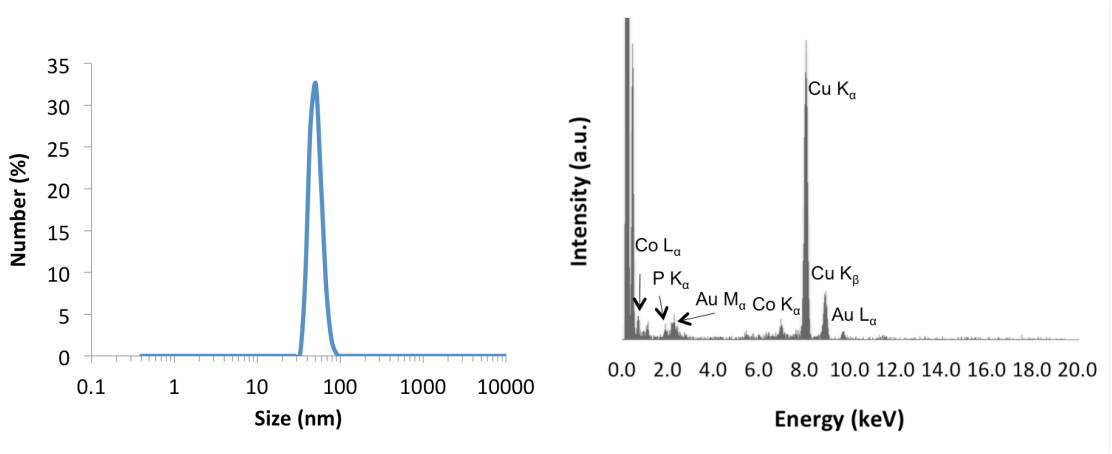


**Figure 3.14.** DLS and EDX analysis of spherical micelles with gold containing core and cobalt containing corona.

### 3.2.8. Synthesis of AuNPs

Incorporation of gold anions into self-assembled morphologies provided a convenient opportunity to produce AuNPs *via* reduction. Micelle samples were stirred over freshly prepared sodium borohydride solution for 8 hours. During this time the solution color changed from yellow to red, indicative of the presence of AuNPs (Figure A3.20). This

hypothesis was confirmed by measuring the UV-vis spectrum of the reduced samples, which showed a plasmon band at 525 nm that is characteristic of AuNPs larger than *ca.* 3 nm in diameter (Figure 3.15).

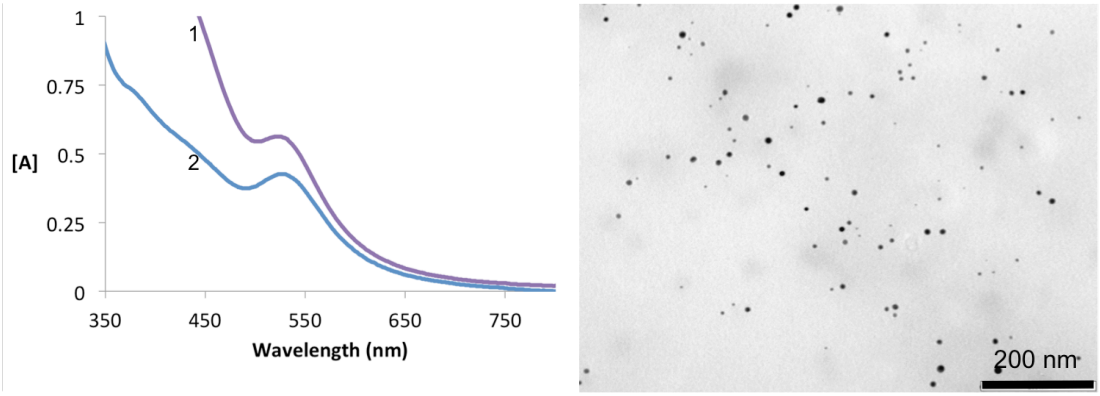


**Figure 3.15.** UV-vis (Left) and TEM images (right) of AuNP made by reduction of spherical micelles made of **3.10** (1: m =30, 2: m =100).

Size distribution and morphology of the AuNPs examined by TEM imaging and revealed the production of 10±5 nm AuNPs, regardless of the PS($P^+AuCl_4^-$) block length (Figure 3.15 Figure A3.21). Upon comparing the size of AuNPs to their originating micelles, there was a significant size decrease. Moreover, the produced AuNPs have similar size distribution, despite being made from micelles with different sizes. This observation is postulated to be because of the formation of a rigid core in the AuNPs, compared to the soft solvent expanded core of the original micelles. The close packed crystalline core of the AuNPs resulted in similar sizes, regardless of the core making block length. The elemental composition of AuNPs was studied by EDX analysis indicating the presence of gold and cobalt in the nano structures (Figure A3.22).

### 3.2.9. Solid-State Self-Assembly Behavior

Bulk solid-state self-assembly of block copolymer **3.9** (m = 30 and 100) was examined. Samples were prepared by drop-casting polymer **3.9** (50 mg/mL in DCM) onto a glass slide followed by thermal annealing under reduced pressure at 180 °C for four days. Annealing process was quenched with liquid $N_2$ and samples were microtomed to 50 nm thin slices using a diamond knife. No features were observed by TEM imaging the microtomed slides. This was possibly because of the similar contrast of the two blocks

under TEM. To reveal the morphology, samples were stained with $RuO_4$, which is a selective stain for components that have unsaturated bonds. Both blocks of the block copolymer **3.9** contain unsaturated bonds, however the metallopolymer block with four phenyl rings has more sites to react with the $RuO_4$ and therefore is more prone to staining. TEM analysis of $RuO_4$ stained microtomed slides indicated the presence of dark regions of hexagonally packed cylinders in a comparatively less dark background. The dark hexagonally packed cylinders were assigned as the metallopolymer block in the sea of lighter polyelectrolyte region (Figure 3.16 and Figure A3.23). EDX analysis of stained microtomed sections confirmed the presence of cobalt and ruthenium in the sample (Figure A3.24).

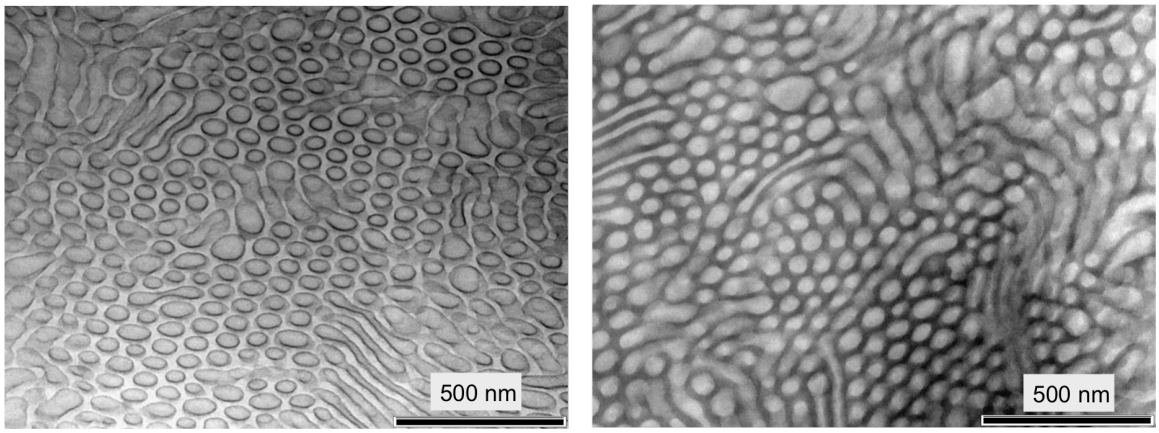


**Figure 3.16.** TEM image of microtomed section of phase-separated **3.9** stained with $RuO_4$ (left) and stained with $HAuCl_4$ (right).

### 3.2.10. Salt Metathesis; a Novel Staining Method

To clarify the discrimination and assignment of phase-separated domains, a selective staining method that exclusively stains only one of the blocks would be most informative. Taking advantage of the salt metathesis ability of the polyelectrolyte block, we were interested to use this reactivity handle as a means to selectively stain the PS($P^+OTf^-$) regions with gold anions. There is only one report on utilizing metal salts such as silver nitrate and chloroauric acid as a staining reagent, however that method has multiple steps and requires a time intensive photoreduction.[84] To our knowledge, there has not been any

report detailing the utilization of salt metathesis to selectively stain polyelectrolyte domains within a solid-state self-assembled block copolymer.

For this purpose it is essential to use a TEM grid that is not prone to redox activity during the salt metathesis reaction. In this context, the commonly used copper grid reacts with $HAuCl_4$ solution giving a Galvanic deposition of Au so use of gold TEM grids were necessary. A gold TEM grid was loaded with microtomed block copolymer **3.9** sections and then covered with a droplet of 0.01M $HAuCl_4$. After 30 seconds, the gold salt solution was gently removed and the grid was dipped into distilled water to rinse away any unreacted salt. The dried grid visualized by TEM imaging revealed the presence of bright spherical regions in a hexagonal arrangement. That was assigned to the PolyCpCoCb-*r*-PMA region left intact during the staining process. The polyelectrolyte domains undergo anion exchange and appeared as dark background region (Figure 3.16 and Figure A3.23). The patterns obtained by $RuO_4$ and $HAuCl_4$ staining methods are complementary, indicative that $RuO_4$ mostly stained metallopolymer region and $HAuCl_4$ selectively stained polyelectrolyte region.

Staining *via* salt metathesis is a quick, simple, and selective method can be used to stain polyelectrolyte containing phase-separated block copolymers with variety of metal salts (*e.g.* Ag, Au) opening new avenue for surface patterning and surface functionalization.

Thermal annealed block copolymers **3.9** were pyrolyzed at 800 °C under $N_2$ atmosphere to obtain cobalt-phosphide nanoparticles. In this preliminary study, the size, morphology, and composition of produced nanoparticles were studied by TEM and EDX analysis indicating presence of cobalt-phosphide containing nanomaterials (Figure A3.25). The pyrolyzed materials were attracted to permanent magnets indicating the presence of magnetic material in the sample (Figure A3.26). More in depth studies on magnetic properties of this material is in progress.

### 3.3. Conclusion

Reversible addition fragmentation transfer (RAFT) polymerization of cobalt containing monomer featuring $\eta^5$-cyclopentadienyl-cobalt-$\eta^4$-cyclobutadiene (**2.3**) and methyl acrylate (MA) by using a fluorine tagged RAFT agent (**3.7**) result in a fluorine end-capped cobalt containing macro-RAFT agent (**3.8**; $PolyCpCoCb_{50}$-*r*-$PMA_{150}$). The macro-RAFT agent (**3.8**) was used to polymerize fluorine tagged phosphonium-

functionalized styrene (**3.6**) to prepare the first example of block copolymer consist of polyelectrolytes and metallopolymers (**3.9**; (PolyCpCoCb$_{50}$-*r*-PMA$_{150}$)-*b*-(PS(P$^+$OTf$^-$)$_m$)). $^{19}$F NMR spectroscopy was used for end group analysis of the produced block copolymer and a reliable estimate on molecular weight ($M_n$) of polyelectrolyte block was calculated. Salt metathesis reaction of polyelectrolyte block with gold salt ($HAuCl_4$) result in heterobimetallic block copolymer with gold decorated polyelectrolyte block and cobalt containing metallic block (**3.10**; (PolyCpCoCb$_{50}$-*r*-PMA$_{150}$)-*b*-(PS(P$^+$AuCl$_4^-$)$_m$). Solution self-assembly of heterobimetallic block copolymer results in spherical micelles with phosphonium-based polyelectrolyte core with pendant gold anions and cobalt containing metallopolymer corona. Reduction of this heterobimetallic micelles results in gold nanoparticles (AuNPs) stabilized with metallopolymers. Phase-separation behavior of block copolymer **3.9** showed hexagonally packed cylinders of metallopolymer in the sea of polyelectrolyte. To clarify the discrimination and assignment of phase-separated domains, salt metathesis with gold anion in solid-state was used to selectively stain the polyelectrolyte block. This is the first example of using salt metathesis reaction to stain phosphonium-based polyelectrolyte domains in a phase-separated block copolymer. To further confirm domain assignments, cobalt containing metallopolymer domain was stained with $RuO_4$ resulting in complementary pattern. Pyrolysis of metallized polyelectrolytes results in 17% char yield cobalt-phosphide materials that get attracted to permanent magnets, indicative of magnetic materials being present. Further studies on magnetic property of this material are in process.

### 3.4. Experimental

All reactions are set up under $N_2$ atmosphere using standard Schlenk line or glovebox techniques unless stated otherwise. Reagents were obtained from either Sigma-Aldrich or Alfa Aesar and used as received without further purification. Ruthenium tetroxide (0.5% stabilized aqueous solution), formvar carbon coated copper grid (400 mesh), copper gilder grids (400 mesh), and gold gilder grids (400 mesh) were obtained from the Electron Microscopy Science (EMS). All solvents were obtained from Caledon Laboratories except chlorobenzene that was obtained from Sigma-Aldrich, and freeze-pump-thawed three cycles, and stored over 4 Å molecular sieves. Chloroform-d, 99.8 atom % D was purchased from Cambridge Isotope Laboratories (CIL).

Nuclear magnetic resonance (NMR) spectroscopy was conducted on a Varian INOVA 400 MHz spectrometer ($^{1}$H: 399.76 MHz, $^{13}$C{$^{1}$H}: 100.52 MHz, $^{31}$P{$^{1}$H}: 161.82 MHz, $^{19}$F{$^{1}$H}: 376.15 MHz). All $^{1}$H and $^{13}$C{$^{1}$H} spectra were referenced relative to chloroform residue using chloroform-d, 99.8 atom % D ($^{1}$H: $\delta$H = 7.26 ppm, $^{13}$C: $\delta$C 77 ppm). The chemical shifts for $^{31}$P{$^{1}$H} and $^{19}$F{$^{1}$H} NMR spectroscopy were referenced using external standards; phosphoric acid ($H_3PO_4$) ($\delta$P = 0 ppm) and trifluoro acetic acid ($CF_3COOH$) ($\delta$F = -76.55 ppm), respectively.

Fourier transform infrared (FT-IR) spectroscopy was conducted as a thin film using a Bruker Tensor 27 spectrometer, with a resolution of 4 $cm^{-1}$. Elemental analysis was performed at Université de Montréal, Montreal, Canada. Doug Hairsine performed high-resolution mass spectroscopy using electron ionization Finnigan MAT 8200 mass spectrometer at Western University.

The decomposition temperatures ($T_d$) were determined using a TGA/SDTA 851e Mettler Toledo instrument or Q600 SDT TA Instrument by heating samples at a rate of 10 °C/min over a temperature range of 30-600 °C.

Differential scanning calorimetric (DSC) was performed on a DSC 822e Mettler Toledo instrument or Q20 DSC TA instrument at a heating rate of 10 °C/min from -60 up to 20 degrees below the $T_d$ of the compound. Glass transition temperatures ($T_g$) were obtained from the second heating cycle of DSC analysis.

Gel permeation chromatography (GPC) experiments were conducted in chromatography grade THF at concentrations of 3-5 mg/mL using a Viscotek GPCmax VE 2001 GPC instrument equipped with an Agilent PolyPore guard column (PL1113-1500) and two sequential Agilent PolyPore GPC columns packed with porous poly(styrene-*co*-divinylbenzene) particles ($M_W$ range 200 - 2000000 g/mol; PL1113-6500) regulated at a temperature of 30°C. Signal response was measured using a Viscotek VE 3580 RI detector, and molecular weights were determined by comparison of the maximum RI response with a calibration curve (10 points, 1500 - 786000 g/mol) established using monodisperse polystyrene standards supplied by Viscotek.

Transmission electron microscopy (TEM) imaging was done using a Jeol 1200EX Mk2 microscope, operating with a tungsten filament at 120 kV. Dynamic light scattering (DLS) was performed on Malvern Zetasizer Nano Series equipped with a laser with a

wavelength of 633 nm and a detector oriented at 173° to the incident radiation. Size Distributions were determined by CONTIN and cumulant analysis of DLS data using the software provided by the manufacturer.

**Synthesis:**

**Fluorine tagged RAFT agent (3.7):**

A 250 mL Schlenk flask was charged with dodecanethiol (2.00 g, 9.88 mmol, 1 *eq*.), aliquat 336 (200 mg, 0.494 mmol, 0.05 *eq*.), and toluene (100 mL) and purged with nitrogen for 15 minutes. After which the reaction was cooled to 0 °C in an ice bath, and NaOH (410 mg, 10.4 mmol, 1.05 *eq*.) was added. After 20 minutes, $CS_2$ (630 µL, 10.4 mmol, 1.05 *eq*.) was injected followed by addition of 4-(trifluoromethyl) benzyl bromide (2.83 g, 11.8 mmol, 1.20 *eq*.). The mixture was stirred for 8 hours under nitrogen. The organic layer was washed with water (3×50 mL) and brine (1×50 mL), dried over magnesium sulfate, filtered, and removed *in vacuo* to yield crude product as yellow oil. Crude product was purified by column chromatography using hexane as eluent to yield pure product as yellow solid in 85% yield. $^{1}$H NMR ($CDCl_3$; δ (ppm)): 7.65 (dd, $^{3}J$ = 8.4 Hz, $^{4}J$ = 2.0 Hz, 2H), 7.48 (dd, $^{3}J$ = 8.4 Hz, $^{4}J$ = 2.0 Hz, 2H), 4.66 (s, 2H), 3.39 (m, 2H), 1.71 (m, 2H), 1.41 (m, 2H), 1.28 (m, 16H), 0.90 (*t*, $^{3}J$ = 6.8 Hz, 3H). $^{13}$C{$^{1}$H} NMR (CDCl3; δ (ppm)): 233.0, 139.9, 129.6, 125, 7, 122.8, 120.1, 40.4, 37.4, 32.0, 28.0, 29.0, 29.2, 29.5, 29.7, 29.8, 22.8, 14.2. $^{19}$F{$^{1}$H} NMR: -62.64 ppm (s, 3F). FT-IR ($cm^{-1}$) (ranked intensity): 626 (14), 718 (9), 755 (15), 823 (5), 878 (12), 1018 (10), 1067 (3), 1135 (4), 1170 (11), 1328 (1), 1415 (7), 1470 (6), 1617 (13), 2851 (8), 2921 (2). HRMS (found/ calculated): 436.15403/ 436.15400. Elemental analysis (found/calculated): C (57.81/57.76), H (7.30/7.16), S (22.10/22.03). Melting point: 31 °C.

**Fluorine end-capped PolyCpCoCb$_{50}$-*r*-PMA$_{150}$ (3.8):**

A 5 mL round bottom flask was charged with RAFT agent **3.7** (0.972 mg, 2.66 µmol, 1 *eq*.), monomer (100 mg, 0.160 mmol, 60 *eq*.), methyl acrylate (MA) (44.0 µL, 0.483 mmol, 180 *eq*.), AIBN (260 µg, 0.530 µmol, 0.2 *eq*.), and chlorobenzene (300 µL) under nitrogen. The reaction flask was sealed with rubber septa and submerged into an 80 ºC oil bath. Reaction was stopped by removing the vessel from hot bath and cooling down in an ice bath. Volatiles were removed *in vacuo.* The crude $^{1}$H NMR spectrum was analyzed for calculating monomer conversion. Polymer was purified by its repetitive dissolution in

minimal dichloromethane and precipitation into stirring *n*-hexane. Purified homopolymer was analyzed by GPC (relative to PS standards) without any further purification (no size exclusion chromatography (SEC) column was done to further purify the polymer). $^{1}$H NMR ($CDCl_3$; δ(ppm)): 7.42-7.33 (b), 7.26-7.1 (b), 4.50-4.71 (b), 3.90-3.01(b), 3.61-3.25 (b), 2.03-1.95 (b), 1.60-1.50 (b). $^{13}C\{^{1}H\}$ NMR ($CDCl_3$; δ(ppm)): 135.3, 128.9, 128.4, 127.1, 93.7, 87.5, 83.2, 76.8, 42.1, 36.0, 29.1, 22.7, 22.5, 29.3, 22.9, 22.6, 14.3. $^{19}F\{^{1}H\}$ NMR: -62.33 ppm. FT-IR ($cm^{-1}$) (ranked intensity): 696 (3), 743 (8), 781 (14), 825 (13),1026 (9),1055 (15),1164 (2),1259 (11), 1371 (12),1451 (5), 1499 (4),1597 (10),1670 (6),1736 (1), 2950 (7).

**Compound 3.6:**

A 50 mL reaction flask was charged with **3.5** (5.00 g, 14.1 mmol, 1 *eq.*), lithium triflate (2.42 g, 15.4 mmol, 1.1 *eq.*), and DCM (25 mL) and stirred for 8 hours. After which the mixture was filtered and the filtrate was washed with water (10×25 mL). Silver nitrate test was performed on the aqueous layer to confirm all chloride anion is removed. Organic solvent was removed *in vacuo* resulting in **3.6** as a white liquid in 98% yield. $^{1}$H NMR ($CDCl_3$; δ (ppm)): 7.36 ($^{3}J$ = 8.4, $^{4}J$ = 2.0 Hz, 2H), 7.23 (dd, $^{3}J$ = 8.4, $^{4}J$ = 2.0 Hz, 2H), 6.65 (dd, $^{3}J$ = 17.6, 9.6 Hz, 1H), 5.74 (d, $^{3}J$ = 17.6 Hz, 1H), 5.26 (d, $^{3}J$ = 9.6 Hz, 1H), 3.75 (d, $J_{H\text{-}P}$ = 18 Hz), 2.14 (m, 6H), 1.42 (m, 12H), 0.90 (*t*, $^{3}J$ = 6.8 Hz, 9H). $^{13}C\{^{1}H\}$ NMR ($CDCl_3$; δ (ppm)): 137.7 ($J_{C\text{-}P}$ = 15.6 Hz), 135.7 ($J_{C\text{-}P}$ = 12.0 Hz), 130.1 ($J_{C\text{-}P}$ = 20.8 Hz), 127.5 ($J_{C\text{-}P}$ = 35.6 Hz), 127.1 ($J_{C\text{-}P}$ = 13.2 Hz), 122.4, 119.2, 114.9, 26.3 ($J_{C\text{-}P}$ = 178.4 Hz), 23.8 ($J_{C\text{-}P}$ = 61.2 Hz), 23.3 ($J_{C\text{-}P}$ = 19.2 Hz), 18.2 ($J_{C\text{-}P}$ = 186.5 Hz), 13.2. $^{19}F\{^{1}H\}$ NMR: -78.32 ppm (s, 3F). $^{31}P\{^{1}H\}$ NMR: 31.67 ppm (s, 1P). FT-IR ($cm^{-1}$) (ranked intensity): 635 (2), 721 (14), 756 (15), 853 (6), 903 (7), 1028 (1), 1097 (10), 1161 (5), 1224 (13), 1278 (4), 1410 (11), 1466 (8), 1514 (9), 2875 (12), 2962 (3). Elemental analysis (found/calculated): C (55.49/ 56.39), H (7.82/7.74), S (6.96/6.84).

**Block copolymer 3.9:**

A 5 mL round bottom flask was charged with **3.8** (100 mg, 2.81 μmol, 1 *eq.*) **3.6** (80.0 mg, 0.168 mmol, 60 *eq.*), AIBN (92.3 μg, 0.562 μmol, 0.2 *eq.*), and chlorobenzene (500 μL) under nitrogen. The reaction flask was sealed with rubber septa and submerged into an 80 ºC oil bath. Reaction was stopped by removing the vessel from hot bath and cooling down in ice bath. The reaction mixture was added to stirring *n*-hexane. The bright

yellow precipitate was collected, and dissolved in minimal dichloromethane, and precipitated into ether to remove any unreacted monomer. This process was repeated five times to remove any unreacted monomer. $^{1}$H NMR ($CDCl_3$; δ (ppm)): 7.44 (b), 7.25 (b), 5.27 (b), 4.78 (b), 3.64 (b), 2.31 (b), 2.02 (b), 1.67 (b), 1.49 (b), 0.94 (b). $^{13}C\{^{1}H\}$ NMR ($CDCl_3$; δ(ppm)): 197.6, 174.9, 174.4, 135.2, 128.8, 128.3, 126.9, 93.6, 87.5, 83.0, 76.6, 64.1, 51.8, 41.5, 35.8, 35.0, 24.1, 23.4, 22.5, 18.5, 13.4. $^{19}F\{^{1}H\}$ NMR: -78.2, -62.28 ppm. $^{31}P\{^{1}H\}$ NMR: 31.53 ppm; FT-IR ($cm^{-1}$) (ranked intensity): 636 (2), 695 (6), 742 (12), 824 (11), 910 (13), 1029 (4), 1152 (8), 1259 (1), 1456 (7), 1499 (10), 1597 (14), 1669 (9), 1738 (3), 2875 (15), 2961 (5).

**Solution-state self-assembly:**

A 10 mg/mL stock solution of **3.9** in THF was prepared. Solution-state self-assembly samples were prepared by injecting 100 μL of the stock solution into 900 μL methanol (a selective solvent for polyelectrolyte block). The self-assembly structures was characterized by TEM and DLS. TEM samples were prepared by putting a droplet on carbon coated copper TEM grid.

**Solid-state self-assembly:**

Bulk films of **3.9** were prepared by drop-casting a 50 mg/mL DCM solution of the sample onto a glass slide until an approximately 2 mm film of was obtained. The films were left to air dry over night followed by thermal annealing under reduced pressure at 180 °C for 72 hours. The films were cut into ~50 nm thick slices using a microtome equipped with a diamond knife. Microtomed sections were stained by exposing them to $RuO_4$ vapor in a sealed chamber, for 8 hours to improve contrast. Stained microtomed sections visualized analyzed by TEM. For Staining with $HAuCl_4$, microtomed sections were transferred to gold grid and a droplet one 0.01 M $HAuCl_4$ was put on the grid for 30 second. After which the droplet was removed by a touch of paper towel and the grid was rinsed with distilled water to remove any unreacted gold salt. TEM grid was imaged after being dried over night.

**Synthesis of heterobimetallic micelles**:

5 mg of **3.9** was dissolved in 5 mL dichloromethane. 5 mL freshly prepared 0.01 M $HAuCl_4$ was added and the mixture was stirred for 1 hour. Aqueous layer was removed and the organic layer was washed with distilled water 3×5 mL. 100 μL of the solution

was injected into 1 mL benzene solution and left for 3 hours before TEM samples being prepared.

**Synthesis of AuNPs**:

To the freshly prepared heterobimetallic micelles (1 mL) was added 0.01 M freshly prepared aqueous sodium borohydride solution. The mixture was stirred over night. Aqueous layer was removed and the organic layer was washed with distilled water 3×5 mL. TEM samples were prepared by putting a droplet of the sample on TEM grid. TEM grid was left to dry before being imaged.

### 3.5. References

(1) Abd-El-Aziz, A. S.; Shipman, P. O.; Boden, B. N.; McNeil, W. S. *Prog. Polym. Sci.* **2010**, *35*, 714-836.

(2) de Hatten, X.; Bell, N.; Yufa, N.; Christmann, G.; Nitschke, J. R. *J. Am. Chem. Soc.* **2011**, *133*, 3158-3164.

(3) Manners, I., *Synthetic Metal Containing Polymers*, Wiley-VCH: Weinheim ; Cambridge, 2004.

(4) Manners, I. *J. Organomet. Chem.* **2011**, *696*, 1146-1149.

(5) Whittell, G. R.; Manners, I. *Adv. Mater.* **2007**, *19*, 3439-3468.

(6) Williams, K. A.; Boydston, A. J.; Bielawski, C. W. *Chem. Soc. Rev.* **2007**, *36*, 729-744.

(7) Hanafy, A. I.; Lykourinou-Tibbs, V.; Bisht, K. S.; Ming, L. J. *Inorg. Chim. Acta* **2005**, *358*, 1247-1252.

(8) Pomogailo, A. D. *Kinet. Catal.* **2004**, *45*, 61-103.

(9) Corrêa, C. C.; Jannuzzi, S. A. V.; Santhiago, M.; Timm, R. A.; Formiga, A. L. B.; Kubota, L. T. *Electrochim. Acta* **2013**, *113*, 332-339.

(10) Fegley, M. E. A.; Pinnock, S. S.; Malele, C. N.; Jones Jr, W. E. *Inorg. Chim. Acta* **2012**, *381*, 78-84.

(11) Singh, S.; Yadav, B. C.; Tandon, P.; Singh, M.; Shukla, A.; Dzhardimalieva, G. I.; Pomogailo, S. I.; Golubeva, N. D.; Pomogailo, A. D. *Sensor Actuat. B-Chem.* **2012**, *166-167*, 281-291.

(12) Wild, A.; Winter, A.; Hager, M. D.; Schubert, U. S. *Analyst* **2012**, *137*, 2333-2337.

(13) Whittell, G. R.; Hager, M. D.; Schubert, U. S.; Manners, I. *Nat. Mater.* **2011**, *10*, 176-188.

(14) Clendenning, S. B.; Aouba, S.; Rayat, M. S.; Grozea, D.; Sorge, J. B.; Brodersen, P. M.; Sodhi, R. N. S.; Lu, Z. H.; Yip, C. M.; Freeman, M. R.; Ruda, H. E.; Manners, I. *Adv. Mater.* **2004**, *16*, 215-219.

(15) Dong, Q.; Li, G.; Ho, C. L.; Leung, C. W.; Pong, P. W. T.; Manners, I.; Wong, W. Y. *Adv. Funct. Mater.* **2014**, *24*, 857-862.

(16) Fritea, L.; Haddache, F.; Reuillard, B.; Le Goff, A.; Gorgy, K.; Gondran, C.; Holzinger, M.; Săndulescu, R.; Cosnier, S. *Electrochem. Commun.* **2014**, *46*, 75-78.

(17) Liu, K.; Fournier-Bidoz, S.; Ozin, G. A.; Manners, I. *Chem. Mater.* **2009**, *21*, 1781-1783.

(18) Djukic, B.; Seda, T.; Gorelsky, S. I.; Lough, A. J.; Lemaire, M. T. *Inorg. Chem.* **2011**, *50*, 7334-7343.

(19) Hamam, Y. A.; Ghanem, H. M. E.; Arafa, I. M.; Said, M. R.; Aljarayish, I. A. *Polym. Int.* **2007**, *56*, 376-380.

(20) Özkale, B.; Pellicer, E.; Zeeshan, M. A.; López-Barberá, J. F.; Nogués, J.; Sort, J.; Nelson, B. J.; Pané, S. *Nanoscale* **2014**, *6*, 4683-4690.

(21) Bao, X.; Zhao, Q.; Wang, H.; Liu, K.; Qiu, D. *Inorg. Chem. Commun.* **2013**, *38*, 88-91.

(22) Et Taouil, A.; Husson, J.; Guyard, L. *J. Electroanal. Chem.* **2014**, *728*, 81-85.

(23) Mortimer, R. J.; Dyer, A. L.; Reynolds, J. R. *Displays* **2006**, *27*, 2-18.

(24) Ren, X.; Mandal, S. K.; Pickup, P. G. *J. Electroanal. Chem.* **1995**, *389*, 115-121.

(25) Zeng, Q.; McNally, A.; Keyes, T. E.; Forster, R. J. *Electrochim. Acta* **2008**, *53*, 7033-7038.

(26) Clendenning, S. B.; Han, S.; Coombs, N.; Paquet, C.; Rayat, M. S.; Grozea, D.; Brodersen, P. M.; Sodhi, R. N. S.; Yip, C. M.; Lu, Z. H.; Manners, I. *Adv. Mater.* **2004**, *16*, 291-296.

(27) Kong, J.; Kong, M.; Zhang, X.; Chen, L.; An, L. *ACS Appl. Mater. Interfaces* **2013**, *5*, 10367-10375.

(28) Hardy, C. G.; Zhang, J.; Yan, Y.; Ren, L.; Tang, C. *Prog. Polym. Sci.* **2014**, *39*, 1742-1796.

(29) Braunschweig, H.; Friedrich, M.; Kupfer, T.; Radacki, K. *Chem. Commun.* **2011**, *47*, 3998-4000.

(30) Baljak, S.; Russell, A. D.; Binding, S. C.; Haddow, M. F.; O'Hare, D.; Manners, I. *J. Am. Chem. Soc.* **2014**, *136*, 5864-5867.

(31) Choi, H. K.; Nunns, A.; Sun, X. Y.; Manners, I.; Ross, C. A. *Adv. Mater.* **2014**, *26*, 2474-2479.

(32) Finnegan, J. R.; Lunn, D. J.; Gould, O. E. C.; Hudson, Z. M.; Whittell, G. R.; Winnik, M. A.; Manners, I. *J. Am. Chem. Soc.* **2014**, *136*, 13835-13844.

(33) Hsiao, M. S.; Yusoff, S. F. M.; Winnik, M. A.; Manners, I. *Macromolecules* **2014**, *47*, 2361-2372.

(34) Zhou, J.; Whittell, G. R.; Manners, I. *Macromolecules* **2014**, *47*, 3529-3543.

(35) Burnworth, M.; Knapton, D.; Rowan, S. J.; Weder, C. *J. Inorg. Organomet. Polym.* **2007**, *17*, 91-103.

(36) Grubbs, R. B. *J. Polym. Sci., Part A: Polym. Chem.* **2005**, *43*, 4323-4336.

(37) Schacher, F. H.; Rupar, P. A.; Manners, I. *Angew. Chem., Int. Ed.* **2012**, *51*, 7898-7921.

(38) Ławecka, M.; Kopcewicz, M.; Ślawska-Waniewska, A.; Leonowicz, M.; Kozubowski, J.; Dzhardimalieva, G. I.; Rozenberg, A. S.; Pomogailo, A. D. *J. Nanopart. Res.* **2003**, *5*, 373-381.

(39) Rabiee Kenaree, A.; Berven, B. M.; Ragogna, P. J.; Gilroy, J. B. *Chem. Commun.* **2014**, *50*, 10714-10717.

(40) Yashtulov, N. A.; Bol'Shakova, A. N.; Revina, A. A.; Flida, V. R. *Russ. Chem. Bull.* **2011**, *60*, 1581-1585.

(41) Devadoss, A.; Spehar-Délèze, A. M.; Tanner, D. A.; Bertoncello, P.; Marthi, R.; Keyes, T. E.; Forster, R. J. *Langmuir* **2010**, *26*, 2130-2135.

(42) Lu, X.; Yavuz, M. S.; Tuan, H. Y.; Korgel, B. A.; Xia, Y. *J. Am. Chem. Soc.* **2008**, *130*, 8900-8901.

(43) Zou, W.; Wang, Y.; Wang, Z.; Zhou, A.; Li, J.; Chang, A.; Wang, Q.; Komura, M.; Ito, K.; Iyoda, T. *Nanotechnology* **2011**, *22*, 335301.

(44) Hardy, C. G.; Ren, L.; Zhang, J.; Tang, C. *Isr. J. Chem.* **2012**, *52*, 230-245.

(45) Ren, L.; Zhang, J.; Hardy, C. G.; Doxie, D.; Fleming, B.; Tang, C. *Macromolecules* **2012**, *45*, 2267-2275.

(46) Ren, L.; Zhang, J.; Hardy, C. G.; Ma, S.; Tang, C. *Macromol. Rapid Commun.* **2012**, *33*, 510-516.

(47) Yan, Y.; Zhang, J.; Qiao, Y.; Tang, C. *Macromol. Rapid Commun.* **2014**, *35*, 254-259.

(48) Zhang, J.; Ren, L.; Hardy, C. G.; Tang, C. *Macromolecules* **2012**, *45*, 6857-6863.

(49) Zhang, J.; Chen, Y. P.; Miller, K. P.; Ganewatta, M. S.; Bam, M.; Yan, Y.; Nagarkatti, M.; Decho, A. W.; Tang, C. *J. Am. Chem. Soc.* **2014**, *136*, 4873-4876.

(50) Wei, J.; Ren, L.; Tang, C.; Su, Z. *Polym. Chem.* **2014**, *5*, 6480-6488.

(51) Zhang, J.; Yan, Y.; Chen, J.; Chance, W. M.; Hayat, J.; Gai, Z.; Tang, C. *Chem. Mater.* **2014**, *26*, 3185-3190.

(52) Xie, W.; Xie, R.; Pan, W. P.; Hunter, D.; Koene, B.; Tan, L. S.; Vaia, R. *Chem. Mater.* **2002**, *14*, 4837-4845.

(53) Ren, H.; Sun, J.; Wu, B.; Zhou, Q. *Polym. Degrad. Stab.* **2007**, *92*, 956-961.

(54) Monge, S.; Canniccioni, B.; Graillot, A.; Robin, J. J. *Biomacromolecules* **2011**, *12*, 1973-1982.

(55) Mather, B. D.; Baker, M. B.; Beyer, F. L.; Green, M. D.; Berg, M. A. G.; Long, T. E. *Macromolecules* **2007**, *40*, 4396-4398.

(56) Sebastian, M.; Hissler, M.; Fave, C.; Rault-Berthelot, J.; Odin, C.; Réau, R. *Angew. Chem., Int. Ed.* **2006**, *45*, 6152-6155.

(57) Gong, M. S.; Park, J. S.; Lee, M. H.; Rhee, H. W. *Sensor Actuat. B-Chem.* **2002**, *86*, 160-167.

(58) Lee, C. W.; Gong, M. S. *Macromol. Res.* **2003**, *11*, 322-327.

(59) Lee, C. W.; Rhee, H. W.; Gong, M. S. *Synth. Met.* **1999**, *106*, 177-182.

(60) Lee, C. W.; Kim, J. G.; Gong, M. S. *Macromol. Res.* **2005**, *13*, 265-272.

(61) Lee, C. W.; Kim, O.; Gong, M. S. *J. Appl. Polym. Sci.* **2003**, *89*, 1062-1070.

(62) Lee, C. W.; Park, H. S.; Kim, J. G.; Choi, B. K.; Joo, S. W.; Gong, M. S. *Sensor Actuat. B-Chem.* **2005**, *109*, 315-322.

(63) Kenawy, E. R.; Worley, S. D.; Broughton, R. *Biomacromolecules* **2007**, *8*, 1359-1384.

(64) Humphrey, S. M.; Allan, P. K.; Oungoulian, S. E.; Ironside, M. S.; Wise, E. R. *Dalton Trans.* **2009**, 2298-2305.

(65) Ainscough, E. W.; Allcock, H. R.; Brodie, A. M.; Gordon, K. C.; Hindenlang, M. D.; Horvath, R.; Otter, C. A. *Eur. J. Inorg. Chem.* **2011**, 3691-3704.

(66) Wang, X.; Cao, K.; Liu, Y.; Tsang, B.; Liew, S. *J. Am. Chem. Soc.* **2013**, *135*, 3399-3402.

(67) Cao, K.; Tsang, B.; Liu, Y.; Chelladural, D.; Power, W. P.; Wang, X. *Organometallics* **2014**, *33*, 531-539.

(68) Mizuta, T.; Imamura, Y.; Miyoshi, K. *J. Am. Chem. Soc.* **2003**, *125*, 2068-2069.

(69) Peckham, T. J.; Massey, J. A.; Honeyman, C. H.; Manners, I. *Macromolecules* **1999**, *32*, 2830-2837.

(70) Allcock, H. R.; Dodge, J. A.; Manners, I.; Riding, G. H. *J. Am. Chem. Soc.* **1991**, *113*, 9596-9603.

(71) Honeyman, C. H.; Foucher, D. A.; Dahmen, F. Y.; Rulkens, R.; Lough, A. J.; Manners, I. *Organometallics* **1995**, *14*, 5503-5512.

(72) Carriedo, G. A.; López, S.; Suárez-Suárez, S.; Presa-Soto, D.; Presa-Soto, A. *Eur. J. Inorg. Chem.* **2011**, 1442-1447.

(73) Noonan, K. J. T.; Gillon, B. H.; Cappello, V.; Gates, D. P. *J. Am. Chem. Soc.* **2008**, *130*, 12876-12877.

(74) Diaz, C.; Valenzuela, M. L. *Macromolecules* **2006**, *39*, 103-111.

(75) Guterman, R.; Hesari, M.; Ragogna, P. J.; Workentin, M. S. *Langmuir* **2013**, *29*, 6460-6466.

(76) Hadadpour, M.; Liu, Y. Q.; Chadha, P.; Ragogna, P. J. *Macromolecules* **2014**, *47*, 6207-6217.

(77) Kristufek, S. L.; Maltais, T. R.; Tennyson, E. G.; Osti, N. C.; Perahia, D.; Tennyson, A. G.; Smith, R. C. *Polym. Chem.* **2013**, *4*, 5387-5394.

(78) Tennyson, A. G.; Kamplain, J. W.; Bielawski, C. W. *Chem. Commun.* **2009**, 2124-2126.

(79) Vijayakrishna, K.; Jewrajka, S. K.; Ruiz, A.; Marcilla, R.; Pomposo, J. A.; Mecerreyes, D.; Taton, D.; Gnanou, Y. *Macromolecules* **2008**, *41*, 6299-6308.

(80) Cheng, S. J.; Beyer, F. L.; Mather, B. D.; Moore, R. B.; Long, T. E. *Macromolecules* **2011**, *44*, 6509-6517.

(81) Coupillaud, P.; Fèvre, M.; Wirotius, A. L.; Aissou, K.; Fleury, G.; Debuigne, A.; Detrembleur, C.; Mecerreyes, D.; Vignolle, J.; Taton, D. *Macromol. Rapid Commun.* **2014**, *35*, 422-430.

(82) Hemp, S. T.; Zhang, M.; Allen Jr, M. H.; Cheng, S.; Moore, R. B.; Long, T. E. *Macromol. Chem. Phys.* **2013**, *214*, 2099-2107.

(83) He, H.; Zhong, M.; Adzima, B.; Luebke, D.; Nulwala, H.; Matyjaszewski, K. *J. Am. Chem. Soc.* **2013**, *135*, 4227-4230.

(84) Li, J. Z.; Wang, Y.; Hong Wang, Z.; Mei, D.; Zou, W.; Min Chang, A.; Wang, Q.; Komura, M.; Ito, K.; Iyoda, T. *Ultramicroscopy* **2010**, *110*, 1338-1342.

# Chapter 4

# Nano- and Micropatterning of Cobalt Containing Block Copolymer *via* Phase-separation and Lithographic Techniques

## 4.1. Introduction

Facile and reproducible patterning of long-ranged micro- and nanoscale morphologies have attracted significant interest over the past several decades because of their potential applications in memory devices,[1] semiconductors,[2,3] and solar cells.[4,5] Phase-separation of copolymers and lithography methods are the two promising pathways to make well-defined, long-ranged patterns with micro- and nanometer scale domains.[6-12]

Copolymers made of two or more distinct polymeric segments can self-assemble into nanosized domains in solution and solid-state to produce complex and unique structures with morphologies such as micelles, vesicles, platelets, and rods in solution, and lamella, cylinders, spheres, and gyroids in the solid-state.[13-16] By incorporating transition metals into copolymers, new properties can be united with unique optical,[17] electrochemical,[18-22] and magnetic[23-26] properties of inorganic metals. Phase-separation of metal containing block copolymers results in localized nanoscale metallic domains. These nanostructures are excellent precursors for the synthesis of well-defined metal nanoparticles *via* thermal decomposition,[27-29] radiation treatment,[30] and reduction.[31-33] Among a wide variety of metallopolymers, iron, nickel, or cobalt containing metallopolymers enable the use of block copolymer self-assemblies to form well-defined magnetic nanoparticles.[34-38] These materials are important because of their potential applications ranging from microelectronics to medicine.[13,39-41] As a result, many researchers have been focused on metallopolymer synthesis and studying the size dependency of their magnetic behavior. The Manners Group is one the pioneers in studying self-assembly behavior and properties of metallopolymers especially those containing polyferrocenylsilane (PFS). PFS can readily be used to produce bulk shaped magnetic ceramics,[24] magnetic thin films,[42] and nanopatterned ceramics.[37,43] The incorporation of other metallic elements such as cobalt

and nickel is attracting growing interest.[36] For example the Tang Group has achieved unique results by incorporating cobaltocenium in metallopolymers and studying their self-assembly behavior as well as their magnetic and biological properties.[44-48,49]

Lithography methods are an alternative pathway to produce monodisperse, long-ranged well-defined nano- and micrometer features.[50-57] Metallopolymers with high metal content have found applications in electron beam lithography (EBL)[43,58-61] and block copolymer lithography[2,8,35,51,62] to pattern high-resolution nanometer domains. However these methods are lengthy and costly. Soft lithography or microcontact patterning (μCP) is a quick, facile, and low cost method commonly used to make reproducible patterns.

We have recently reported the reversible addition fragmentation transfer (RAFT) polymerization of $\eta^5$-cyclopentadienyl-cobalt-$\eta^4$-cyclobutadiene (CpCoCb) containing monomer (**2.3**; Scheme 4.1).[63] The monomer **2.3** is an 18 electron, neutral, mixed sandwich cobaltocene that was polymerized to produce well-defined homo- and block copolymers. To overcome the steric demand of the bulky CpCoCb monomer, its random copolymerization with methyl acrylate (MA), to act as a spacer was essential.[63]

In this study, RAFT agent functionalized polydimethylsiloxane (PDMS-RAFT) (**4.1**; Scheme 4.1) was utilized as a macro-RAFT agent to polymerize CpCoCb monomer (**2.3**). This RAFT polymerization resulted in a novel block copolymer consisting of a PDMS block and a cobalt containing metallopolymer block (**4.2**; Scheme 4.1). Solution and solid-state self-assembly of the PDMS-*b*-(PolyCpCoCb-*r*-PMA) block copolymer was studied. By means of pyrolysis, magnetic silicon-cobalt nanocomposite was obtained. The block copolymer was used as ink material to print different micrometer patterns *via* microcontact printing (μCP).

## 4.2. Results and Discussion

### 4.2.1. PDMS Macro-RAFT Agent

The reversible addition fragmentation transfer (RAFT) agent functionalized polydimethylsiloxane (PDMS-RAFT) (**4.1**; Scheme 4.1) was prepared following previously reported esterification reaction of commercially available hydroxyl terminated polydimethylsiloxane (PDMS-OH) with a carboxylic acid functionalized RAFT agent.[64] PDMS-$RAFT_{5k}$ and PDMS-$RAFT_{10k}$ with respectively 67 and 134 repeat units were

prepared.[64] These two samples were then utilized as macro-RAFT agents to polymerize $\eta^5$-cyclopentadienyl-cobalt-$\eta^4$-cyclobutadiene (CpCoCb) containing monomer (**2.3**; Scheme 4.1).

### 4.2.2. Block Copolymer Synthesis and Characterization

Applying previously optimized RAFT polymerization conditions of **2.3**, PDMS-RAFT$_{5k}$ (**4.1**), CpCoCb monomer (**2.3**), methyl acrylate (MA), and AIBN in a 1: 30: 90: 0.2 stoichiometric equivalent were dissolved in nitrogen-saturated chlorobenzene (Scheme 4.1).

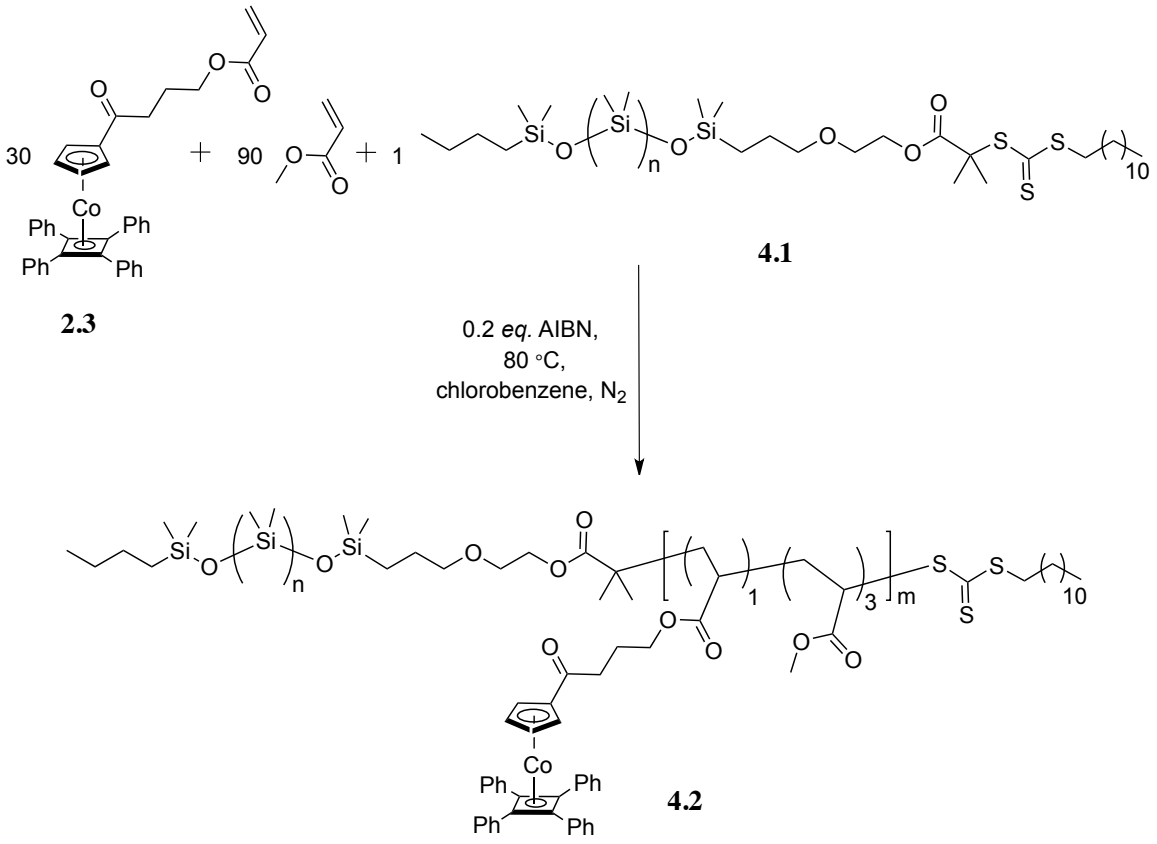


**Scheme 4.1.** Synthesis of block copolymer **4.2**; PDMS-*b*-(PolyCpCoCb-*r*-PMA) (n = 76 for PDMS-RAFT$_{5k}$, and n =134 for PDMS-RAFT$_{10k}$).

Polymerization was conducted at 80 °C and after the desired reaction time, it was quenched by submerging the reaction vessel into ice water, resulting in a viscous orange material. The volatiles were removed *in vacuo* and the $^1$H NMR spectrum of the crude material was obtained. As expected, the relative integration value of the vinyl signals

decreased and broad signals representative of polymers were observed (Figure 4.1; spectra 1 and 2). By comparing the relative integration values of unreacted monomer to the polymer, conversion was calculated to be 64%, corresponding to 18 repeat units (Figure 4.1; spectrum 2). By repeated dissolution in a minimum of dichloromethane followed by precipitation into stirring methanol, unreacted monomer was removed. The purified polymer was collected in 60% yield and analyzed by $^{1}$H NMR spectroscopy (Figure 4.1; spectrum 3). The produced block copolymer is consists of a PDMS block and a metallopolymer block (**4.2**; Scheme 4.1). By using end group analysis and comparing the relative integration values of the terminal methyl groups at either end of the polymer relative to the cyclopentadiene (Cp) ring protons, the degree of polymerization (DP) for monomer **2.3** could be calculated. Relative values confirmed that 18 repeat units were incorporated giving a *ca.* 18 kDa PolyCpCoCb-*r*-PMA block. The relative integration ratio of PolyCpCoCb and PMA was *ca.* 3.5, which was similar to the monomer feed ratio and in line with our previous study on this random copolymer.[63]

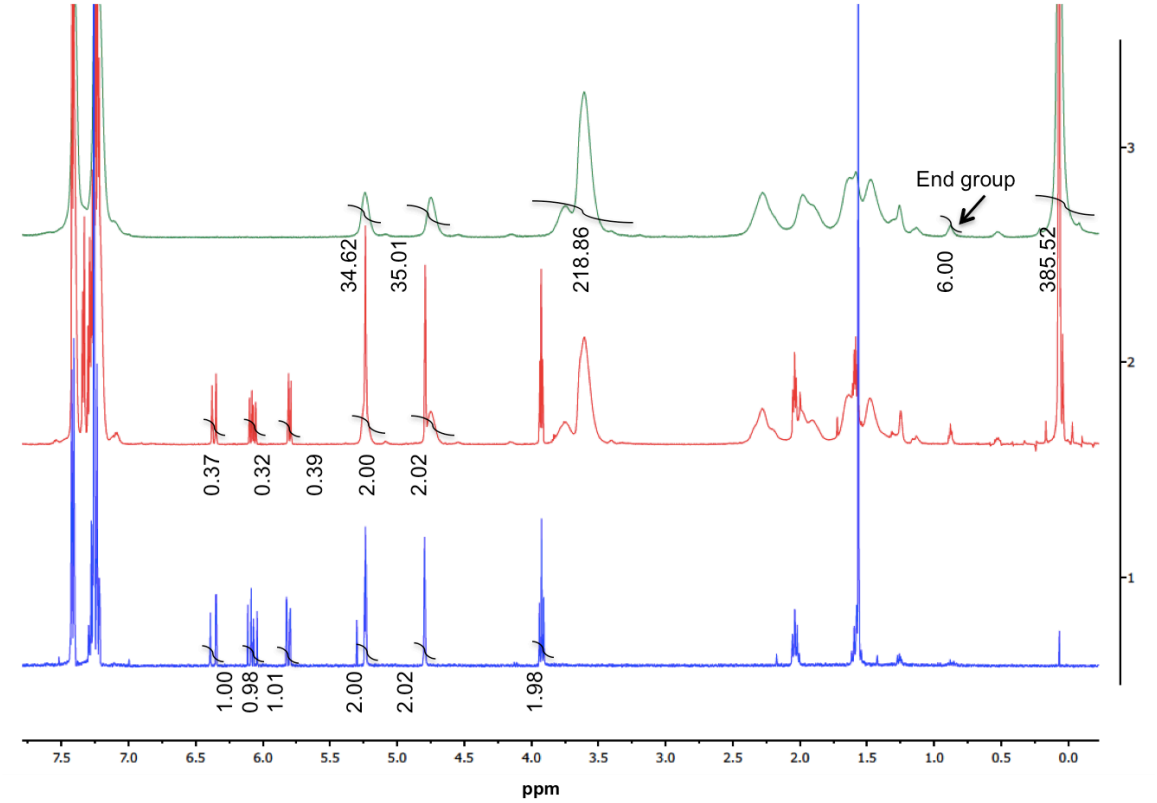


**Figure 4.1.** $^{1}$H NMR spectra of monomer **2.3** (1), crude polymer **4.2** showing 64% monomer conversion (2), and purified polymer **4.2** (3). (see Figure A4.1 and 2 for detailed spectra).

Changes in monomer **2.3** concentration over the polymerization reaction period were monitored by $^{1}$H NMR spectroscopy at different time intervals. Plotting Ln $[M_0]/[M_t]$ *vs* polymerization reaction time resulted in a pseudo first order plot indicating constant consumption of the CpCoCb monomer during the reaction, a characteristic feature of a controlled polymerization reaction (Figure 4.2).

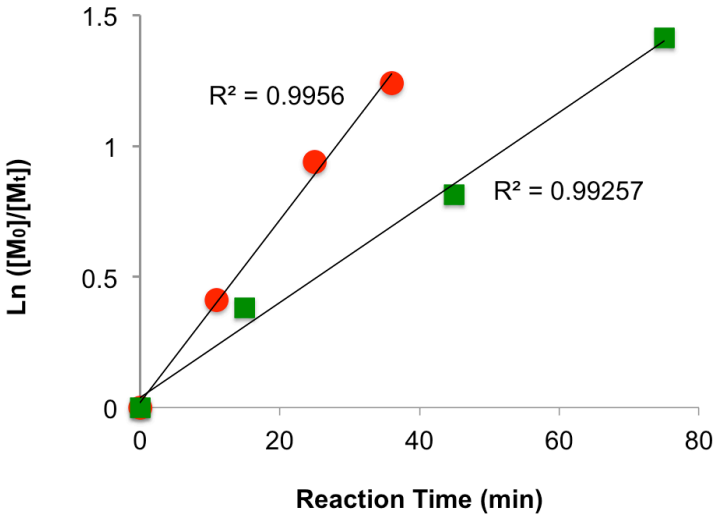


**Figure 4.2.** Ln ($[M_0]/[M_t]$) *vs* reaction time for making block copolymer **4.2** utilizing PDMS-RAFT$_{5k}$ (triangle) and PDMS-RAFT$_{10k}$ (circle) macro-RAFT agents. (M Refers to monomer **2.3**).

Molecular weigh and PDI of the purified polymers at different reaction time intervals were analyzed by gel permeation chromatography (GPC). The refractive index (RI) trace of polymer samples showed a gradual shift to shorter elution time indicating an increase in the molecular weight of the polymer (Figure 4.3). The molecular weight of the block copolymers were analyzed by comparing their RI traces to polystyrene (PS) standards indicating the production of polymers up to 31 kDa with PDIs of *ca*. 1.1.

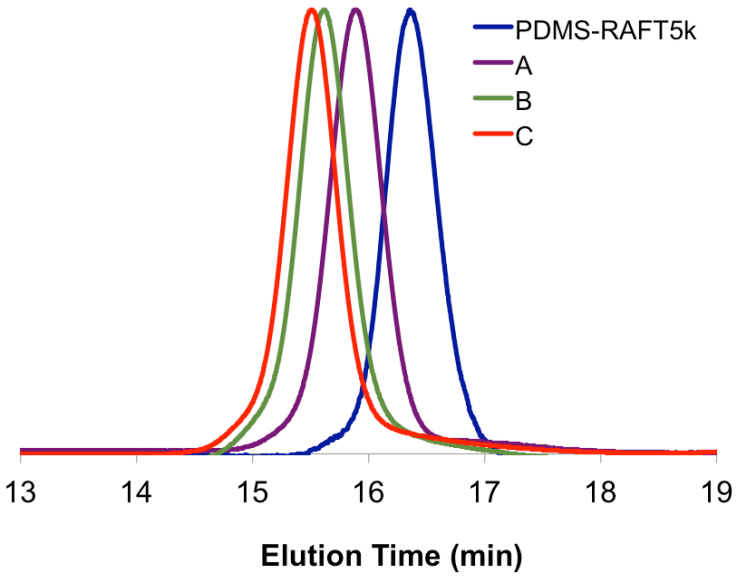


| | $M_n^*$ (kDa) | PDI |
|---|---|---|
| PDMS-RAFT$_{5k}$ | 8.1 | 1.05 |
| A | 12.5 | 1.06 |
| B | 13.9 | 1.14 |
| C | 14.2 | 1.15 |

**Figure 4.3.** RI traces, $M_n^*$, and PDI of the purified **4.2** utilizing PDMS-RAFT$_{5k}$ (10 min time intervals). $M_n^*$ is reported based on GPC analysis relative to PS standards.

PDMS-RAFT$_{10k}$ was utilized following the same reaction condition to produce block copolymers with longer PDMS block whereas the length of the metallopolymer block was held constant (PDMS$_{10k}$-*b*-(PolyCpCoCb-*r*-PMA)$_{18k}$). Similar analysis was conducted on these materials including $^1$H NMR spectroscopy (Figure A4.4) and GPC (Figure 4.4). Similar to its shorter analogue, utilizing PDMS-RAFT$_{10k}$ showed constant consumption of monomer **2.3** resulting in narrow PDI polymers with good control over the molecular weight. A small tail was observed in RI trace of the as purchased PDMS-OH$_{10k}$ and consequently in PDMS-RAFT$_{10k}$ and all of the block copolymers made from this macro-RAFT agent (Figure 4.4). Despite the tail, all polymers have very narrow PDIs (*i.e.* < 1.18). It should be noted that all block copolymers were purified only by simple precipitation to remove any unreacted monomer and no further purification such as size exclusion chromatography (SEC) column is performed.

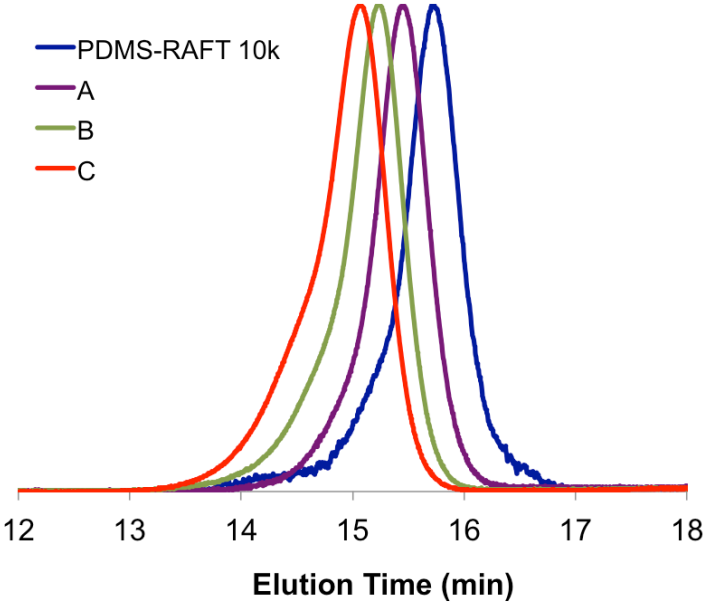


| | $M_n^*$ (kDa) | PDI |
|---|---|---|
| PDMS-RAFT$_{10k}$ | 14.5 | 1.15 |
| A | 19.9 | 1.14 |
| B | 25.8 | 1.15 |
| C | 31.1 | 1.18 |

**Figure 4.4.** RI traces, $M_n^*$, and PDI of the purified **4.2** utilizing PDMS-RAFT$_{10k}$ (20 min time intervals). $M_n^*$ is reported based on GPC analysis relative to PS standards.

The PDMS-*b*-(PolyCpCoCb-*r*-PMA) block copolymer samples (**4.2**) with two different PDMS block length were analyzed by thermal gravimetric analysis (TGA) to obtain the char yield and the decomposition temperature ($T_d$). The block copolymer samples were heated to 750 °C at a 10 °C/min ramp rate under $N_2$. Both block copolymer samples were stable up to 280 °C followed by *ca.* 70% mass loss. The PDMS$_{10k}$-*b*-(PolyCpCoCb-*r*-PMA)$_{18k}$ showed 5% less mass loss because of containing a longer PDMS block. This indicates *ca.* 30% of these block copolymers are mostly composed of inorganic materials *e.g.* silicon and cobalt.

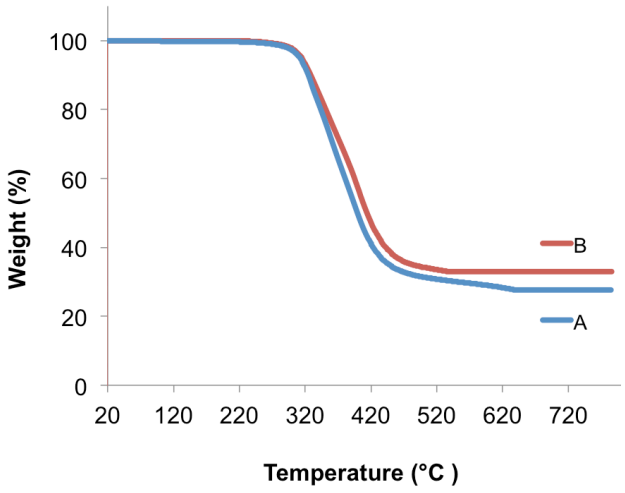


**Figure 4.5.** TGA analysis of $PDMS_{5k}$-*b*-(PolyCpCoCb-*r*-PMA)$_{18k}$ (A) and $PDMS_{10k}$-*b*-(PolyCpCoCb-*r*-PMA)$_{18k}$ (B).

Differential scanning calorimetry (DSC) analysis was performed to study the glass transition temperature ($T_g$) of the block copolymers. For both block copolymers one $T_g$ was observed at 84 °C for the PolyCpCoCb-*r*-PMA block. The $T_g$ of the PDMS block ($T_g$ ≈ -125 °C)[65] was not observed in the temperature window employed (-70 °C to +180 °C; Figure 4.6).

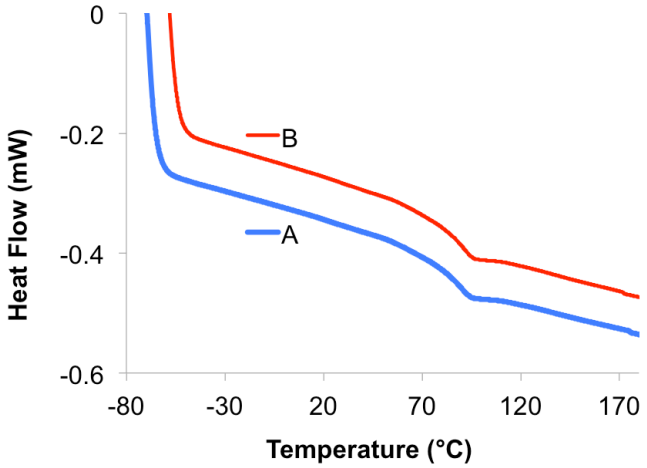


**Figure 4.6.** DSC analysis of $PDMS_{5k}$-*b*-(PolyCpCoCb-*r*-PMA)$_{18k}$ (A) and $PDMS_{10k}$-*b*-(PolyCpCoCb-*r*-PMA)$_{18k}$ (B).

### 4.2.3. Solid-State Self-Assembly

We were interested in studying phase-separation behavior of these block copolymers and for this purpose, bulk samples were prepared by drop casting a concentrated solution of the copolymer to make a *ca.* 1 mm thick sample. These were thermally annealed at 150 °C under reduced pressure for 72 hours. The sample was then quickly cooled by immersion in liquid $N_2$. The thermally annealed samples were microtomed into 50 nm thin films and visualized by transmission electron microscopy (TEM). TEM analysis revealed the presence of long-ranged order of hexagonally packed cylinder morphology. This was assigned to be the PolyCpCoCb-*r*-PMA domain as it appeared as dark circles within a PDMS matrix, the light grey background. This observation further confirmed that the PolyCpCoCb-*r*-PMA block acts as a uniform random block rather than a segmented block copolymer (Figure 4.7).

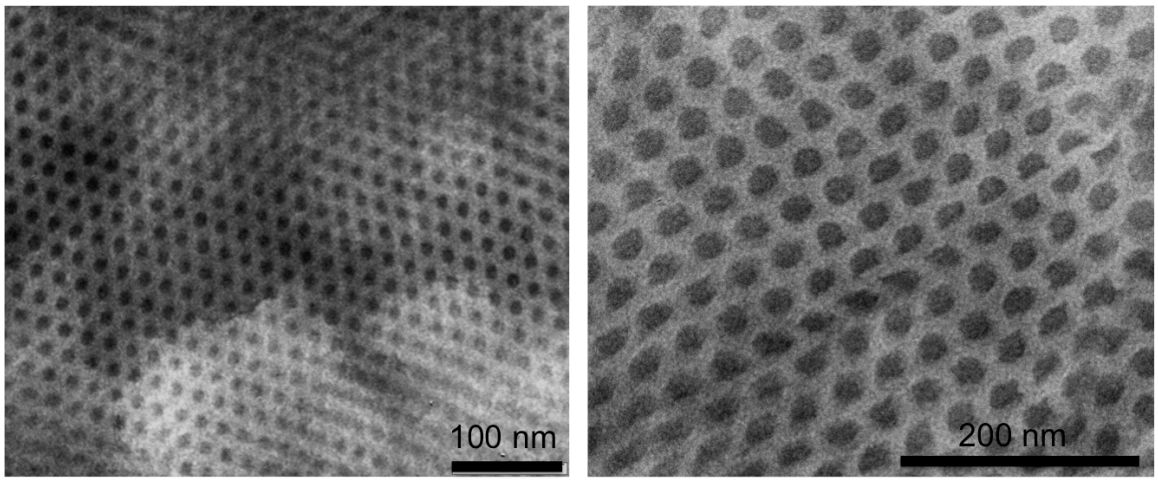


**Figure 4.7.** TEM images of phase-separated $PDMS_{5k}$-*b*-(PolyCpCoCb-*r*-PMA)$_{18k}$ (Left) and $PDMS_{10k}$-*b*-(PolyCpCoCb-*r*-PMA)$_{18k}$ (right).

Similar phase-separation behavior was observed for both block copolymers regardless of the length of the PDMS block (5 or 10 kDa). This observation indicates that the relative volume fractions of the PDMS and PolyCpCoCb-*r*-PMA block for both samples belong to the same region of the block copolymer phase diagram resulting in hexagonally packed cylinder morphology.

### 4.2.4. Pyrolysis

Thermally annealed samples were pyrolyzed under nitrogen atmosphere for 4 hours at 800 °C. The resulted pyrolyzed material was attracted to a permanent magnet indicative of cobalt containing magnetic material being present (Figure A4.1). The size and morphology of the material was analyzed by TEM imaging indicated the presence of 7±2 nm nanoparticles (Figure 4.8). Energy-dispersive X-ray spectroscopy (EDX) analysis confirmed the present of cobalt and silicon in the nanostructures (Figure 4.8).

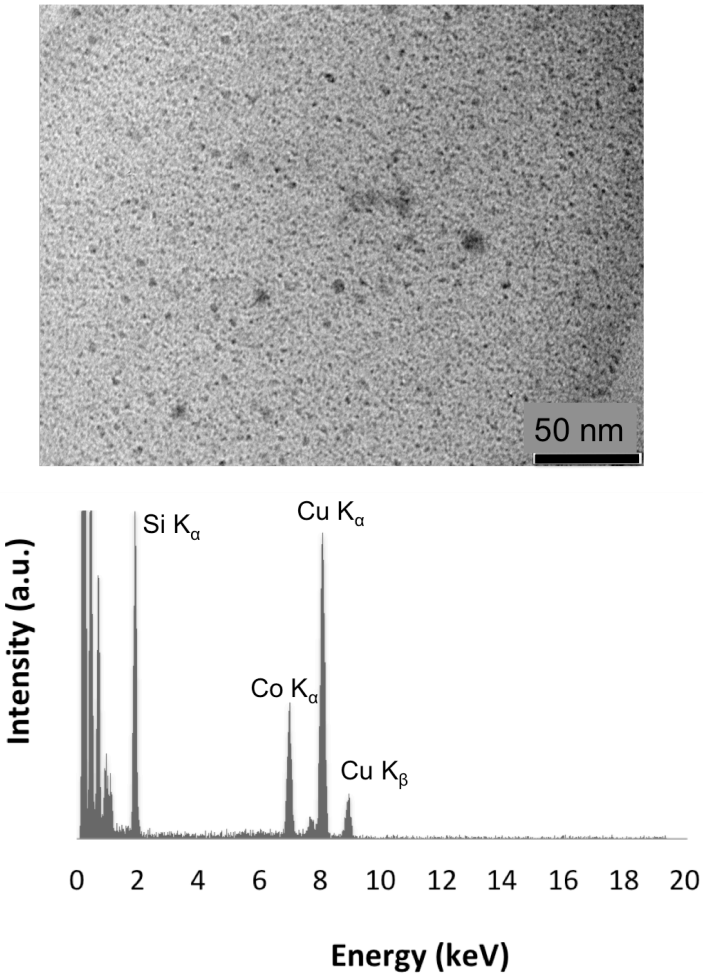


**Figure 4.8.** TEM image of the pyrolyzed $PDMS_{5k}$-*b*-(PolyCpCoCb-*r*-$PMA)_{18k}$ and its EDX analysis. (note: Copper signal is from Cu grid).

Thin film of $PDMS_{5k}$-*b*-(PolyCpCoCb-*r*-$PMA)_{18k}$ were prepared by spin coating the sample on a silicon wafer substrate. The sample was then pyrolyzed at 800 °C for 3 hours

and visualized by scanning electron microscopy (SEM) imaging. Uniformly dispersed 30-50 nm particles composed of silicon and cobalt was observed (Figure 4.9).

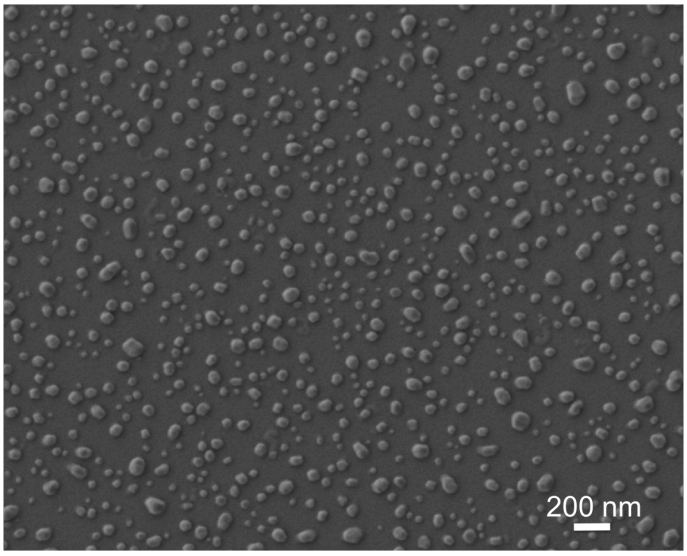


**Figure 4.9.** SEM Image of pyrolyzed $PDMS_{5k}$-*b*-(PolyCpCoCb-*r*-$PMA)_{18k}$ thin film.

### 4.2.5. Solution-State Self-Assembly

To study the solution self-assembly behavior of the block copolymers, 10 mg/mL THF samples were prepared. The solution was injected into *n*-hexane, which is a selective solvent for the PDMS block. TEM samples were prepared by drop casting samples on a TEM grid. Self-assembled structures of both block copolymer samples were studied indicating the presence of spherical micelles with *ca.* 20 nm diameter sizes regardless of the length of the PDMS block (5 or 10 kDa). The core making block (PolyCpCoCb-*r*-PMA) has the same length for both samples, whereas the corona-making block (PDMS) is different. PDMS has a low contrast under TEM (relative to the PolyCpCoCb-*r*-PMA core-making block), thus similar diameter micelles were visualized.

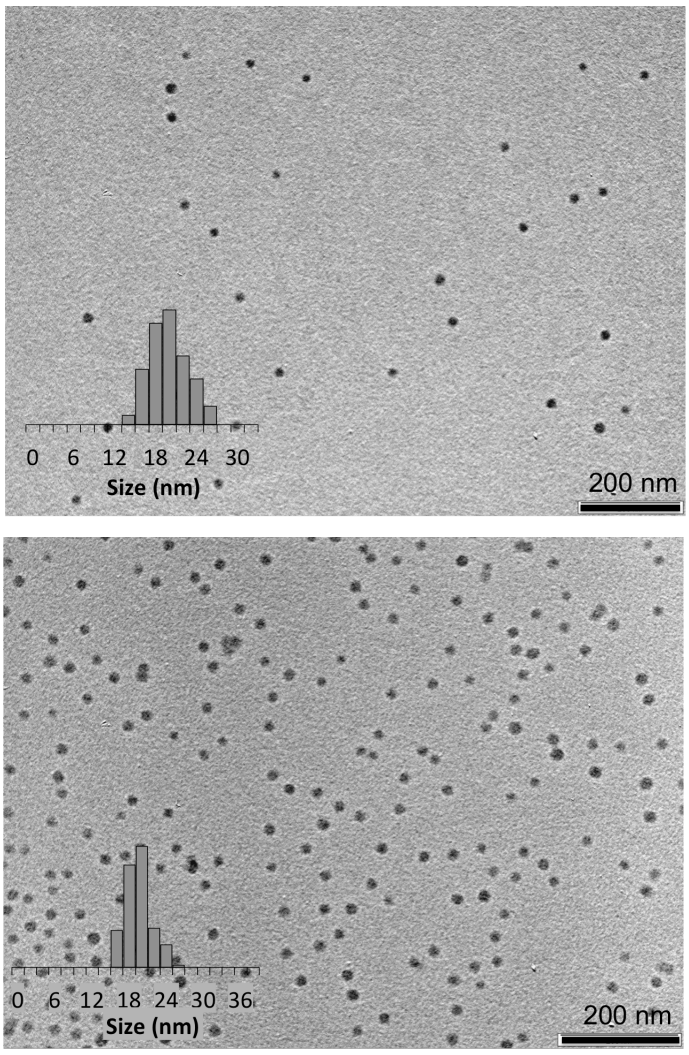


**Figure 4.10.** TEM images and size distribution (inset) of $PDMS_{5k}$-*b*-(PolyCpCoCb-*r*-PMA)$_{18k}$ (top) and $PDMS_{10k}$-*b*-(PolyCpCoCb-*r*-PMA)$_{18k}$ (bottom).

This hypothesis was further studied by analyzing the hydrodynamic radius of the resulted micelles by dynamic light scattering (DLS). The block copolymer with longer PDMS block ($PDMS_{10k}$-*b*-(PolyCpCoCb-*r*-PMA)$_{18k}$) contained particles with 28 nm hydrodynamic radius, that was 8 nm larger in diameter compared to particles made with the shorter PDMS block ($PDMS_{5k}$-*b*-(PolyCpCoCb-*r*-PMA)$_{18k}$).

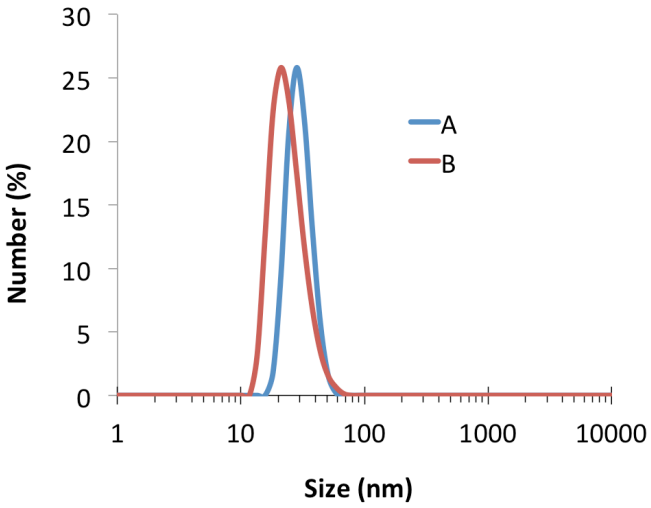


**Figure 4.11.** DLS Analysis of spherical micelles made of $PDMS_{10k}$-*b*-(PolyCpCoCb-*r*-PMA)$_{18k}$ (A) and $PDMS_{5k}$-*b*-(PolyCpCoCb-*r*-PMA)$_{18k}$ (B).

EDX analysis was used to analyze the composition of the produced spherical micelles confirming the presence of silicon and cobalt in the self-assembled structures (Figure 4.12).

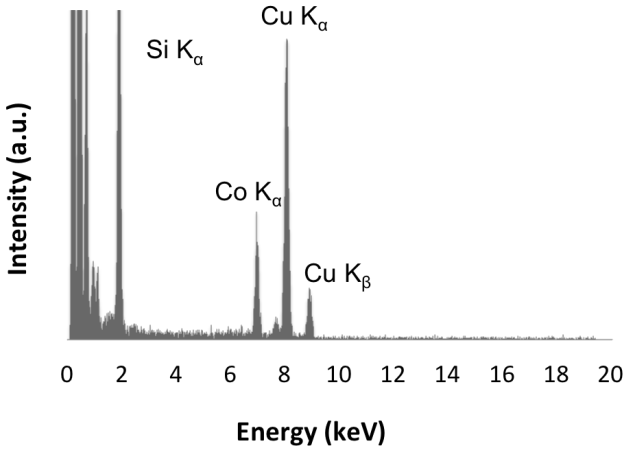


**Figure 4.12.** EDX Analysis of produced micelles. (note: Cu signals are from the copper TEM grid).

### 4.2.6. Microcontact Printing (μCP)

Preliminary studies on using $PDMS_{5k}$-*b*-(PolyCpCoCb-*r*-PMA)$_{18k}$ as ink material for soft lithographic patterning *via* microcontact printing (μCP) was performed. For patterning

the block copolymer *via* μCP, **4.2** (0.5% (w/w) in toluene) was used as ink to pattern transfer holes, lines, and pillars, to produce long-ranged patterns on a silicon wafer. Imaging the stamped silicon wafers by SEM confirmed successful pattern transfer of all three different stamps: holes, lines, and pillars (Figure 4.13).

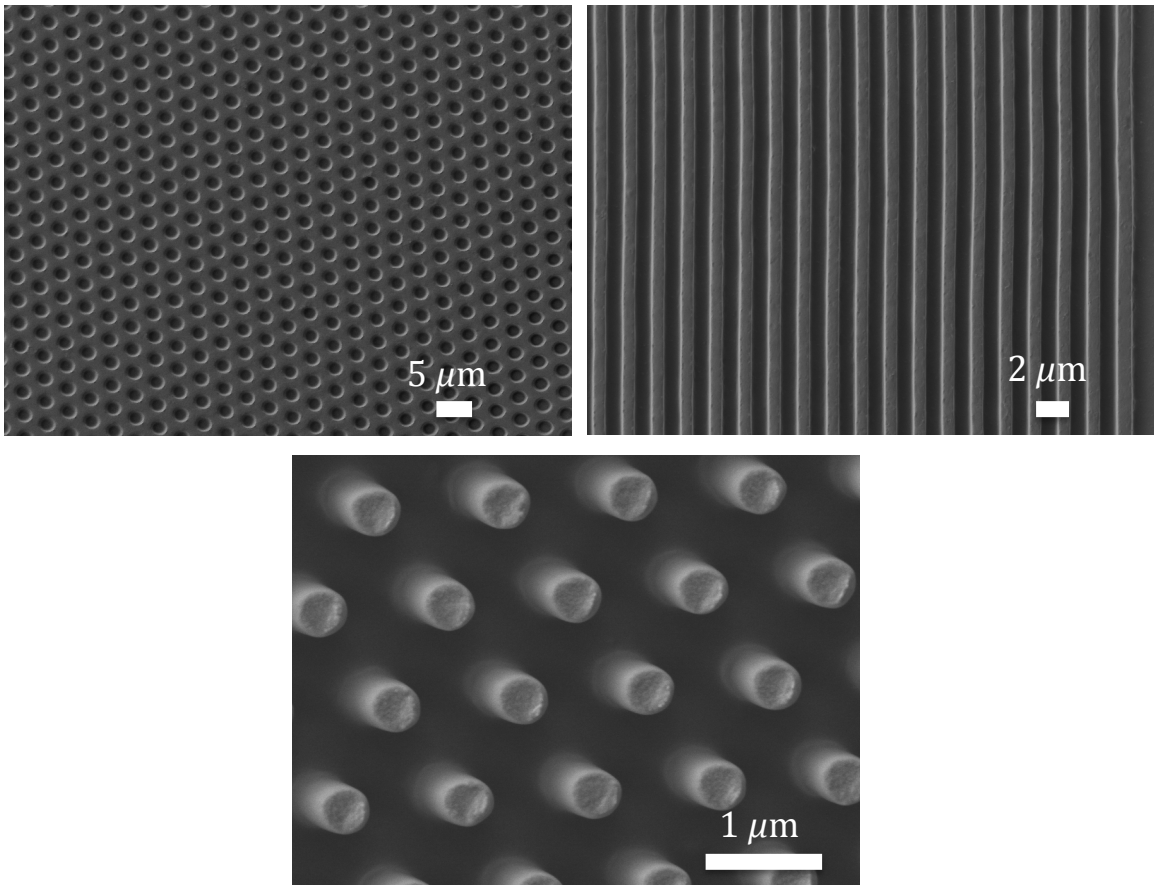


**Figure 4.13.** SEM images of holes, lines, and pillars using $PDMS_{5k}$-*b*-(PolyCpCoCb-*r*-PMA)$_{18k}$ as ink material for μCP.

### 4.3. Conclusion

A new class of block copolymers made of a polydimethylsiloxane (PDMS) block and a metallopolymer block containing $\eta^5$-cyclopentadienyl-cobalt-$\eta^4$-cyclobutadiene (CpCoCb) mixed sandwich cobaltocene (**2.3**) is introduced. Commercially available 5 and 10 kDa hydroxy terminated PDMS (PDMS-OH) with low PDI was end-capped with a reversible addition fragmentation transfer (RAFT) agent. The resulted PDMS-RAFT (**4.1**) was utilized as macro-RAFT agent to polymerize CpCoCb monomer (**2.3**). The

resulted PDMS-*b*-(PolyCpCoCb-*r*-PMA) block copolymer (**4.2**) was studied for phase-separation behavior in solution and solid-state. Long-ranged hexagonally packed cylinder of metallopolymer block in PDMS was observed in solid-state. Solution-state self-assembly of the material in *n*-hexane, a selective solvent for PDMS block, resulted in spherical micelles with metallic core stabilized with PDMS corona. Pyrolysis of block copolymer samples resulted in 30 % char yield magnetic material. The block copolymer was used as ink material in microcontact printing (μCP) to transfer hole, line, and pillar patterns of the block copolymer onto a silicon wafer. In depth studies on magnetic properties of this multifunctional block copolymer is under studies.

### 4.4. Experimental

CpCoCb monomer (**2.3**),[74] PDMS-RAFT$_{5k}$, and PDMS-RAFT$_{10k}$ (**4.1**)[75] were synthesized following previously reported literature procedure. Methyl acrylate was purchased from Sigma Aldrich, distilled and stored under nitrogen prior to use. 2,2′-Azobis(2-methylpropionitrile) (AIBN) was purchased from Sigma Aldrich and was recrystallized from methanol. Chlorobenzene was purchased form Sigma Aldrich, freeze-pump-thawed three cycles and stored under nitrogen. Tetrahydrofuran (THF), *n*-hexane, toluene, and dimethylformamide (DMF) were obtained from Caledon Laboratories and used as received. Chloroform-d (99.8 atom % D) were purchased from Cambridge Isotope Laboratories (CIL).

Nuclear magnetic resonance (NMR) spectroscopy was conducted on a Varian INOVA 400 MHz spectrometer ($^{1}$H: 399.76 MHz, $^{13}$C{$^{1}$H}: 100.52 MHz). $^{1}$H and $^{13}$C{$^{1}$H} spectra were referenced relative to chloroform residue using chloroform-d, 99.8 atom % D ($^{1}$H: $\delta$H = 7.26 ppm, $^{13}$C: $\delta$C = 77 ppm).

Fourier transform infrared (FT-IR) spectroscopy was conducted as a thin film using a Bruker Tensor 27 spectrometer, with a resolution of 4 cm$^{-1}$. The decomposition temperatures ($T_d$) were determined using a TGA/SDTA 851e Mettler Toledo instrument and Q600 SDT TA Instrument by heating samples at a rate of 10 °C/min over a temperature range of 30-600 °C. Differential scanning calorimetric (DSC) was performed on a DSC 822e Mettler Toledo instrument and Q20 DSC TA instrument at a heating rate of 10 °C/min from -70 up to 20 degrees below the $T_d$ of the compound. Glass transition temperatures ($T_g$) were obtained from the second heating cycle of DSC analysis.

Gel permeation chromatography (GPC) experiments were conducted in chromatography grade THF at concentrations of 3-5 mg/mL using a Viscotek GPCmax VE 2001 GPC instrument equipped with an Agilent PolyPore guard column (PL1113-1500) and two sequential Agilent PolyPore GPC columns packed with porous poly(styrene-*co*-divinylbenzene) particles ($M_W$ range 200 - 2000000 g/mol; PL1113-6500) regulated at a temperature of 30°C. Signal response was measured using a Viscotek VE 3580 RI detector, and molecular weights were determined by comparison of the maximum RI response with a calibration curve (10 points, 1500 - 786000 g/mol) established using monodisperse polystyrene standards supplied by Viscotek.

**Block copolymer 4.2 ($PDMS_{10k}$-*b*-(PolyCpCoCb-*r*-$PMA)_{18k}$):**

A 2 mL reaction flask was charged with a magnetic stir bar, PDMS-$RAFT_{10k}$ (**4.1**) (200 mg, 20.0 µmol, 1 *eq*.), CpCoCb monomer (370 mg, 0.600 mmol, 30 *eq*.), methyl acrylate (160 µL, 1.80 mmol, 90 *eq.*), AIBN (0.660 mg, 4.00 µmol, 0.2 *eq*.) and chlorobenzene (1.40 mL). The vessel was sealed with a rubber septa and submerged into an 80 °C oil bath. After reaction time the reaction flask was submerged into ice bath to quench the polymerization and the volatiles were removed *in vacuo*. The gummy orange residue was dissolved in minimum DCM and precipitated into stirring methanol. Yellow precipitate was collected and the above process was repeated three more times to remove any unreacted monomer. After which precipitate was collected and further purified by suspending it in DMF and precipitating it out by adding a few drops of methanol. The yellow powder was collected by centrifuge, dried *in vacuo,* and used for studies. $PDMS_{5k}$-*b*-(PolyCpCoCb-*r*-$PMA)_{18k}$ was made following the exact same procedure as above, utilizing PDMS-$RAFT_{5k}$. $^1$H NMR ($CDCl_3$; δ(ppm)): 7.39 (b), 7.21(b), 5.22 (b), 4.73 (b), 3.73 (b), 3.58 (b), 2.26 (b), 1.96 (b), 1.61 (b), 1.46 (b), 1.25 (b). 0.08 (b). $^{13}C\{^1H\}$ NMR ($CDCl_3$; δ (ppm)): 197.8, 174.4, 135.6, 134.7, 129.1, 128.3, 128.7, 127.9, 126.9, 126.1, 93.4, 87.0, 82.3, 77.8, 76.1, 63.2, 51.9, 41.1, 35.5, 34.2, 29.4, 22.6. FT-IR ($cm^{-1}$) (ranked intensity): 660 (15), 695 (6), 743 (12), 800 (1), 866 (13), 1019 (2), 1095 (14), 1165 (11), 1262 (4), 1456 (9), 1500 (8), 1598 (10), 1672 (7), 1738 (3), 2963 (5).

**Solid-state self-assembly:**

Block copolymer **4.2** (50 mg) was dissolved in THF (500 µL). The solution was drop-casted on a glass slide making a bulk film of *ca.* 1 mm thickness. The film was solvent

annealed with THF vapour in an annealing chamber for 5 hours, then air dried for 24 hours, followed by thermal annealing at 150 °C under reduced pressure for 72 hours. After which adding liquid nitrogen quenched annealing process. Annealed sample was glued on epoxy resin block and cut into ultrathin sections (50 nm thick) using a diamond knife installed on a microtome. Thin sections were transferred on a copper TEM grid and visualized by TEM.

**Pyrolysis of bulk self-assembled samples:**

Thermally annealed block copolymer **4.2** was placed in a quartz boat inside a quartz tube in the tube furnace. The tube was purged with $N_2$ for 30 min at 1 L/min flow rate. Then the flow was lowered to *ca.* 50 mL/min and the temperature of the tube furnace was increased to 800 °C at a rate of 10 °C/min. Sample was kept at 800 °C isothermal for 4 hours.

**TEM of bulk pyrolyzed sample:**

10 mg pyrolyzed sample was transferred into a vial containing 15 mL methanol. The vial was sonicated for 15 minutes, and then one drop of the solution was applied onto a carbon coated TEM grid.

**Solution-state self-assembly:**

100 μL of block copolymer **4.2** in THF (10 mg/mL) was injected into a vial containing 1 mL hexanes. Sample was left for 8 hours after which one drop was transferred on a copper TEM grid and visualized by TEM.

**DLS Analysis:**

Micelle solutions prepared as described above were filtered twice using 0.2 μL filter and analyzed by DLS.

**Thin film preparation:**

Block copolymer **4.2** in toluene (0.5% (w/w)) was prepared. Silicon wafers were cleaned by using Piranha solution (Caution!) and rinsed with deionized water and filtered propanol. Wafers were dried with air jet and were used quickly after. One drop of the solution was transferred onto substrate and it was spin coated at 1000 rpm for 60 seconds. Spin coated sample was pyrolyzed in a tube furnace at 800 °C for 4 hours. Samples were coated with 5 nm of osmium and visualized by SEM imaging.

**Microcontact printing (μCP):**

Block copolymer **4.2** in toluene (0.5% (w/w)) was prepared. Silicon wafers were cleaned by using Piranha solution (Caution!) and rinsed with deionized water and filtered propanol. Wafers were dried with air jet and used quickly after. 5 μL of the solution was transferred on the PDMS stamp and the pattern was printed on the freshly cleaned silicon wafer substrate by gentle pressure for 60 seconds. After which samples were visualized by SEM imaging.

## 4.5. References

(1) Zong, B. Y.; Goh, J. Y.; Guo, Z. B.; Luo, P.; Wang, C. C.; Qiu, J. J.; Ho, P.; Chen, Y. J.; Zhang, M. S.; Han, G. C. *Nanotechnology* **2013**, *24*, 245303.

(2) Jeong, S. J.; Xia, G.; Kim, B. H.; Shin, D. O.; Kwon, S. H.; Kang, S. W.; Kim, S. O. *Adv. Mater.* **2008**, *20*, 1898-1904.

(3) Stamm, U. *J. Phys. D: Appl. Phys.* **2004**, *37*, 3244-3253.

(4) Lu, Y.; Lal, A. *Nano Lett.* **2010**, *10*, 4651-4656.

(5) Na, S. I.; Kim, S. S.; Jo, J.; Oh, S. H.; Kim, J.; Kim, D. Y. *Adv. Funct. Mater.* **2008**, *18*, 3956-3963.

(6) Chou, S. Y.; Krauss, P. R.; Renstrom, P. J. *Science* **1996**, *272*, 85-87.

(7) Chou, S. Y.; Krauss, P. R.; Zhang, W.; Guo, L.; Zhuang, L. *J. Vac. Sci. Technol. B* **1997**, *15*, 2897-2904.

(8) Park, M.; Harrison, C.; Chaikin, P. M.; Register, R. A.; Adamson, D. H. *Science* **1997**, *276*, 1401-1404.

(9) Xia, Y.; Whitesides, G. M. *Angew. Chem., Int. Ed.* **1998**, *37*, 550-575.

(10) Stuparu, M. C.; Khan, A.; Hawker, C. J. *Polym. Chem.* **2012**, *3*, 3033-3044.

(11) Park, J.; Jang, S.; Kim, J. K. *J. Polym. Sci., Part B: Polym. Phys.* **2014**, *53*, 1-21.

(12) Yabu, H. *Polym. J.* **2013**, *45*, 261-268.

(13) Burnworth, M.; Knapton, D.; Rowan, S. J.; Weder, C. *J. Inorg. Organomet. Polym.* **2007**, *17*, 91-103.

(14) Zhou, J.; Whittell, G. R.; Manners, I. *Macromolecules* **2014**, *47*, 3529-3543.

(15) Grubbs, R. B. *J. Polym. Sci., Part A: Polym. Chem.* **2005**, *43*, 4323-4336.

(16) Schacher, F. H.; Rupar, P. A.; Manners, I. *Angew. Chem., Int. Ed.* **2012**, *51*, 7898-7921.

(17) Shunmugam, R.; Gabriel, G. J.; Aamer, K. A.; Tew, G. N. *Macromol. Rapid Commun.* **2010**, *31*, 784-793.

(18) Huo, J.; Yu, H.-J.; Deng, L.-B.; Zhou, J.-F.; Yang, Q. *J. Polym. Sci., Part B: Polym. Phys.* **2007**, *45*, 2880-2889.

(19) Ren, X.; Mandal, S. K.; Pickup, P. G. *J. Electroanal. Chem.* **1995**, *389*, 115-121.

(20) Et Taouil, A.; Husson, J.; Guyard, L. *J. Electroanal. Chem.* **2014**, *728*, 81-85.

(21) Spehar-Deleze, A. M.; Pellegrin, Y.; Keyes, T. E.; Forster, R. J. *Electrochem. Commun.* **2008**, *10*, 984-986.

(22) Zhan, H.; Wong, W. Y.; Ng, A.; Djurišić, A. B.; Chan, W. K. *J. Organomet. Chem.* **2011**, *696*, 4112-4120.

(23) Özkale, B.; Pellicer, E.; Zeeshan, M. A.; López-Barberá, J. F.; Nogués, J.; Sort, J.; Nelson, B. J.; Pané, S. *Nanoscale* **2014**, *6*, 4683-4690.

(24) MacLachlan, M. J.; Ginzburg, M.; Coombs, N.; Coyle, T. W.; Raju, N. P.; Greedan, J. E.; Ozin, G. A.; Manners, I. *Science* **2000**, *287*, 1460-1463.

(25) Thomas, K. R.; Ionescu, A.; Gwyther, J.; Manners, I.; Barnes, C. H. W.; Steiner, U.; Sivaniah, E. *J. Appl. Phys.* **2012**, *109*, 073904.

(26) Lastella, S.; Mallick, G.; Woo, R.; Karna, S. P.; Rider, D. A.; Manners, I.; Jung, Y. J.; Ryu, C. Y.; Ajayan, P. M. *J. Appl. Phys.* **2006**, *99*, 024302.

(27) Kong, J.; Kong, M.; Zhang, X.; Chen, L.; An, L. *ACS Appl. Mater. Interfaces* **2013**, *5*, 10367-10375.

(28) Ławecka, M.; Kopcewicz, M.; Ślawska-Waniewska, A.; Leonowicz, M.; Kozubowski, J.; Dzhardimalieva, G. I.; Rozenberg, A. S.; Pomogailo, A. D. *J. Nanopart. Res.* **2003**, *5*, 373-381.

(29) Rabiee Kenaree, A.; Berven, B. M.; Ragogna, P. J.; Gilroy, J. B. *Chem. Commun.* **2014**, *50*, 10714-10717.

(30) Yashtulov, N. A.; Bol'Shakova, A. N.; Revina, A. A.; Flida, V. R. *Russ. Chem. Bull.* **2011**, *60*, 1581-1585.

(31) Devadoss, A.; Spehar-Délèze, A. M.; Tanner, D. A.; Bertoncello, P.; Marthi, R.; Keyes, T. E.; Forster, R. J. *Langmuir* **2010**, *26*, 2130-2135.

(32) Lu, X.; Yavuz, M. S.; Tuan, H. Y.; Korgel, B. A.; Xia, Y. *J. Am. Chem. Soc.* **2008**, *130*, 8900-8901.

(33) Zou, W.; Wang, Y.; Wang, Z.; Zhou, A.; Li, J.; Chang, A.; Wang, Q.; Komura, M.; Ito, K.; Iyoda, T. *Nanotechnology* **2011**, *22*, 335301.

(34) Chan, W. Y.; Clendenning, S. B.; Berenbaum, A.; Lough, A. J.; Aouba, S.; Ruda, H. E.; Manners, I. *J. Am. Chem. Soc.* **2005**, *127*, 3796-3808.

(35) Cheng, J. Y.; Ross, C. A.; Chan, V. Z. H.; Thomas, E. L.; Lammertink, R. G. H.; Vancso, G. J. *Adv. Mater.* **2001**, *13*, 1174-1178.

(36) Gilroy, J. B.; Patra, S. K.; Mitchels, J. M.; Winnik, M. A.; Manners, I. *Angew. Chem., Int. Ed.* **2011**, *50*, 5851-5855.

(37) Liu, K.; Clendenning, S. B.; Riebe, L.; Chan, W. Y.; Zhu, X.; Freeman, M. R.; Yang, G. C.; Yip, C. M.; Grozea, D.; Lu, Z. H.; Manners, I. *Chem. Mater.* **2006**, *18*, 2591-2601.

(38) Zha, Y.; Maddikeri, R. R.; Gido, S. P.; Tew, G. N. *J. Inorg. Organomet. Polym.* **2013**, *23*, 89-94.

(39) Fegley, M. E. A.; Pinnock, S. S.; Malele, C. N.; Jones Jr, W. E. *Inorg. Chim. Acta* **2012**, *381*, 78-84.

(40) Hardy, C. G.; Zhang, J.; Yan, Y.; Ren, L.; Tang, C. *Prog. Polym. Sci.* **2014**, *39*, 1742-1796.

(41) Mortimer, R. J.; Dyer, A. L.; Reynolds, J. R. *Displays* **2006**, *27*, 2-18.

(42) Rider, D. A. L., Kun; Eloi, Jean-Charles; Vanderark, Lawrence; Yang, Ling; Wang, Jia-Yu; Grozea, Dan; Lu, Zheng-Hong; Russell, Thomas P.; Manners, Ian *ACS Nano* **2008**, *2*, 263-270.

(43) Clendenning, S. B.; Aouba, S.; Rayat, M. S.; Grozea, D.; Sorge, J. B.; Brodersen, P. M.; Sodhi, R. N. S.; Lu, Z. H.; Yip, C. M.; Freeman, M. R.; Ruda, H. E.; Manners, I. *Adv. Mater.* **2004**, *16*, 215-219.

(44) Zhang, J.; Chen, Y. P.; Miller, K. P.; Ganewatta, M. S.; Bam, M.; Yan, Y.; Nagarkatti, M.; Decho, A. W.; Tang, C. *J. Am. Chem. Soc.* **2014**, *136*, 4873-4876.

(45) Ren, L.; Hardy, C. G.; Tang, C. *J. Am. Chem. Soc.* **2010**, *132*, 8874-8875.

(46) Ren, L.; Zhang, J.; Hardy, C. G.; Ma, S.; Tang, C. *Macromol. Rapid Commun.* **2012**, *33*, 510-516.

(47) Yan, Y.; Zhang, J.; Qiao, Y.; Tang, C. *Macromol. Rapid Commun.* **2014**, *35*, 254-259.

(48) Zhang, J.; Yan, Y.; Chance, M. W.; Chen, J.; Hayat, J.; Ma, S.; Tang, C. *Angew. Chem., Int. Ed.* **2013**, *52*, 13387-13391.

(49) Zhang, J.; Yan, Y.; Chen, J.; Chance, W. M.; Hayat, J.; Gai, Z.; Tang, C. *Chem. Mater.* **2014**, *26*, 3185-3190.

(50) Xia, Y.; Whitesides, G. M. *Annu. Rev. Mater. Sci.* **1998**, *28*, 153-184.

(51) Bates, C. M.; Maher, M. J.; Janes, D. W.; Ellison, C. J.; Willson, C. G. *Macromolecules* **2014**, *47*, 2-12.

(52) Joshi-Imre, A.; Bauerdick, S. *J. Nanotechnol.* **2014**, *2014*, 1.

(53) Bratton, D.; Yang, D.; Dai, J.; Ober, C. K. *Polym. Adv. Technol.* **2006**, *17*, 94-103.

(54) Ito, T.; Okazaki, S. *Nature* **2000**, *406*, 1027-1031.

(55) Rogers, J. A.; Nuzzo, R. G. *Mater. Today* **2005**, *8*, 50-56.

(56) Tseng, A. A.; Notargiacomo, A.; Chen, T. P. *J. Vac. Sci. Technol. B* **2005**, *23*, 877-894.

(57) Wu, B.; Kumar, A. *J. Vac. Sci. Technol. B* **2007**, *25*, 1743-1761.

(58) Liu, K.; Fournier-Bidoz, S.; Ozin, G. A.; Manners, I. *Chem. Mater.* **2009**, *21*, 1781-1783.

(59) Vieu, C.; Carcenac, F.; Pépin, A.; Chen, Y.; Mejias, M.; Lebib, A.; Manin-Ferlazzo, L.; Couraud, L.; Launois, H. *Appl. Surf. Sci.* **2000**, *164*, 111-117.

(60) Kolodziej, C. M.; Maynard, H. D. *Chem. Mater.* **2012**, *24*, 774-780.

(61) Schnabel, W.; Sotobayashi, H. *Prog. Polym. Sci.* **1983**, *9*, 297-365.

(62) Nunns, A.; Gwyther, J.; Manners, I. *Polymer* **2013**, *54*, 1269-1284.

(63) Hadadpour, M.; Liu, Y. Q.; Chadha, P.; Ragogna, P. J. *Macromolecules* **2014**, *47*, 6207-6217.

(64) Wadley, M. L.; Cavicchi, K. A. *J. Appl. Polym. Sci.* **2010**, *115*, 635-640.

(65) Lötters, J. C.; Olthuis, W.; Veltink, P. H.; Bergveld, P. *J. Micromech. Microeng.* **1997**, *7*, 145-147.

# Chapter 5

# Synthesis and Attempts Towards Polymerization of Highly Metallized Monomers

## 5.1. Introduction

Over the past decade, metallopolymers have attracted interest as they combine the synthetic efficiency and versatility of conventional organic polymers with the interesting redox, responsive, and catalytic properties of inorganic metals.[1-3] By bringing together the chemistry of polymers with inorganic elements, metallopolymers have potential applications in electronic and magnetic materials and as precursors to ceramics and metallic nanoparticles.[4-7] Metallopolymers are good candidates to obtain well-defined nanosized metal nanoparticle *via* thermal or radiation treatment.[8-10] By utilizing highly metallized metallopolymers in electron beam lithography (EBL), UV photolithography, and soft lithography, patterned arrays of metal nanoparticles and ceramics can be produced.[4,11-14]

Following the discovery of ferrocene in the 1950s, incorporation of metallocene into polymers has expanded.[15] Metallocene containing metallopolymers attracted increased attention in material sciences because of their high thermal stability, and reversible redox property.[16,17] As ferrocene and its derivatives are readily available at relatively low cost, ferrocene-based metallopolymers have been extensively used as excellent precursors to make iron nanoparticles. Ring opening polymerization (ROP) of strained [l]silaferrocenophanes resulted in well-defined, high molecular weight poly(ferrocenylsilanes) (PFS) metallopolymer.[9,18] Upon pyrolysis at 600-1000 °C under nitrogen atmosphere, PFS yields magnetic iron nanoparticles embedded in ceramic matrix.[8,9] Pyrolysis of thin films of PFS results in the formation of nanoparticles confined in ceramic thin films.[19] Ceramics obtained as films, coatings, fibers, or bulk are attractive for practical applications.[6,20-24]

Content and composition of metal nanoparticles and ceramics directly depend on the metal content and the composition of the metallopolymer precursor. An important consideration when choosing a ceramic precursor is the char yield as it ultimately controls the utility, properties, and shape retention of the resulting material.[17] Most metallopolymers contain relatively low metal loadings and in most cases consists of only one metal type, thus are inefficient in making alloy nanoparticles.[25] The incorporation of transition metals especially ferromagnetic elements such as iron, cobalt, and nickel into metallopolymers and consequently into nanoparticles and ceramics,[25-33] is very attractive because they result in materials with interesting catalytic, magnetic, electrical, and optical properties.[10,34-38] Besides PFS containing materials, cobalt containing metallopolymers represent a major class of metallopolymers.[17,20,29-33,39-43] Incorporation of multiple metals into metallopolymers is of great interest to prepare nanoparticle alloys with potential properties in making particles with tunable magnetic properties. To enable incorporation of iron and cobalt within the same material, the Manners Group pyrolyzed PFS with pendant cobalt clusters resulting in CoFe magnetic alloy nanoparticles embedded in ceramic thin film.[39,44] This group was able to obtain superparamagnetic composites by pyrolyzing the metallopolymer at 600 °C, and ferromagnetic composites by pyrolyzing at higher temperatures.[39] The same group reported sequential ROP of [l]silaferrocenophanes and dicarba[2]cobaltococenophane followed by oxidation of the cobaltocene centers producing the only example of main-chain heterobimetallic block copolymer with ferrocene and cobaltocenium repeat units.[30,33]

The Tang Group reported sequential RAFT polymerization of cobaltocenium and ferrocene containing monomers resulting in a heterobimetallic polymer.[29,31,45] This heterobimetallic polymer was used as precursor for the preparation of CoFe hybrid nanoparticle.[29,45] By manipulating the cobalt and iron content of the metallopolymer, they were able to control the magnetic properties of the produced nanoparticles.[31]

In this study synthesis and attempts towards incorporation of variety of cobalt and iron containing monomers into macromolecules in reported. The monomer of interest is a mixed sandwich cobaltocene featuring $\eta^5$-cyclopentadienyl-cobalt-$\eta^4$-cyclobutadiene (CpCoCb) with variety of substituents incorporated onto the Cb ring. Synthesis and characterization of the CpCoCb with four thiophenes and four bithiophenes incorporated

onto the Cb ring is reported. To obtain highly metalized metallopolymer precursors with excellent control over metal contents and metal ratio, ferrocene units were incorporated onto the Cb ring. A series of metallized monomers with 1 Co, 1Co: 2Fe, and 1Co: 4Fe in each repeat unit are synthesized and attempts towards their RAFT polymerization is reported. Even though high molecular weight metallopolymers were not obtained, highly metallized oligomers with controlled number of metal atoms (up to 5 atoms) per repeat unit were produced. Use of these highly metallized materials as ink for microcontact patterning (μCP) to pattern metallized domains is discussed. Pyrolysis of patterned metallized materials to make patterned CoFe magnetic alloy nanoparticle is reported. Incorporation of these highly metallized monomers into cross-linked networks and its pyrolysis to obtain shaped magnetic ceramic is studied.

## 5.2. Results and Discussion

### 5.2.1. Monomer Synthesis

To synthesize the cobalt containing monomers with different substituents on the cyclobutadiene (Cb) ring, an established synthetic protocol was utilized. By refluxing compound **2.1**[46] with 2.2 stoichiometric equivalents of the substituted alkyne in *p*-xylene for 2 days, compound **5.1** was produced (Scheme 5.1). The functional groups on the Cb ring are the functionalities on the utilized alkyne in the cyclodimerization reaction. By using an asymmetric alkyne (R ≠ R´), mixtures of *cis* and *trans* isomers were incorporated onto the Cb ring. Following this procedure, monomer precursor with two ferrocene and two phenyl (*cis* and *trans*) incorporated onto the Cb ring was prepared (**5.1a**). Also compounds with four ferrocene (**5.1b**), four thiophene (**5.1c**), and four bithiophene (**5.1d**) units incorporated onto the Cb ring were prepared (Scheme 5.1).

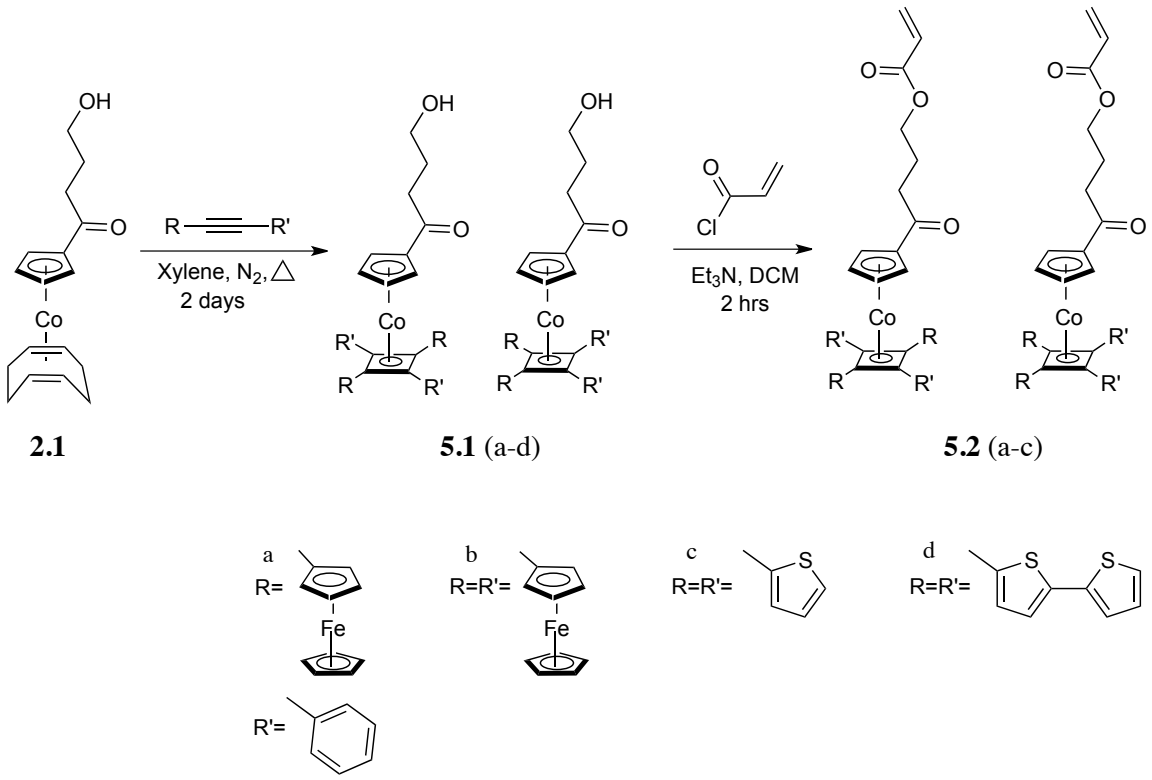


**Scheme 5.1.** Utilizing cyclodimerization chemistry to prepare derivatives of CpCoCb with different substituents onto the Cb ring.

Subsequently compound **5.1** was reacted with acryloyl chloride and triethylamine in dry dichloromethane (DCM) to install the polymerizable group and obtain the cobalt containing monomer **5.2** (Scheme 5.1). This facile and versatile method was employed to make mixed sandwich cobaltocene monomers functionalized with *cis* and *trans* isomers of phenyl/ferrocene substituents onto the Cb ring (**5.2a**) along with ferrocene (**5.2b**), and thiophene (**5.2c**) derivatives (Scheme 5.1). $^{1}$H NMR spectra of these monomers are provided in Figure 5.1. The proton signals of the vinyl moiety and the Cp ring that are common in all monomeric units are assigned.

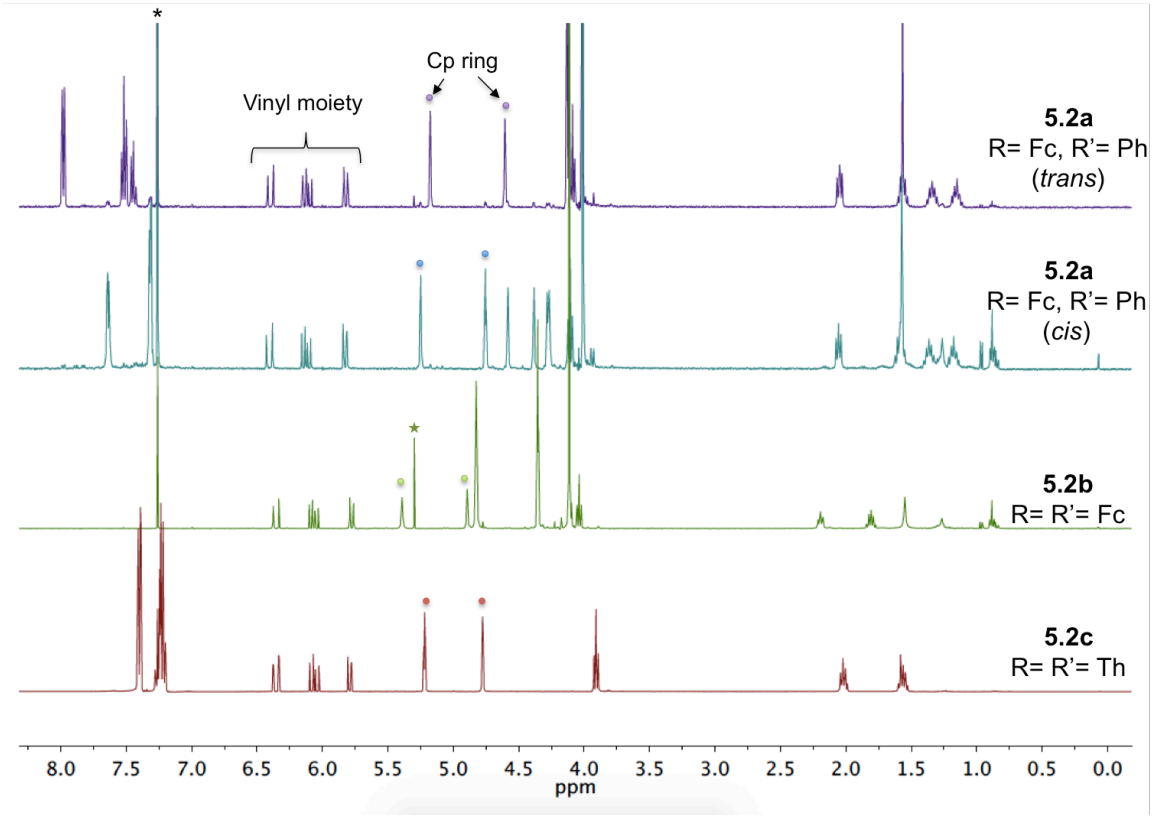


**Figure 5.1.** $^{1}$H NMR of monomer **5.2(a-c)** in $CDCl_3$ (*), [$^{\star}CH_2Cl_2$ residue].

We were able to collect solid-state structure of monomer **5.2b** and **5.2c** (Figure 5.2). Monomer **5.2b** is an interesting molecule with four ferrocene incorporated onto the Cb ring resulting in a highly metallized monomer.

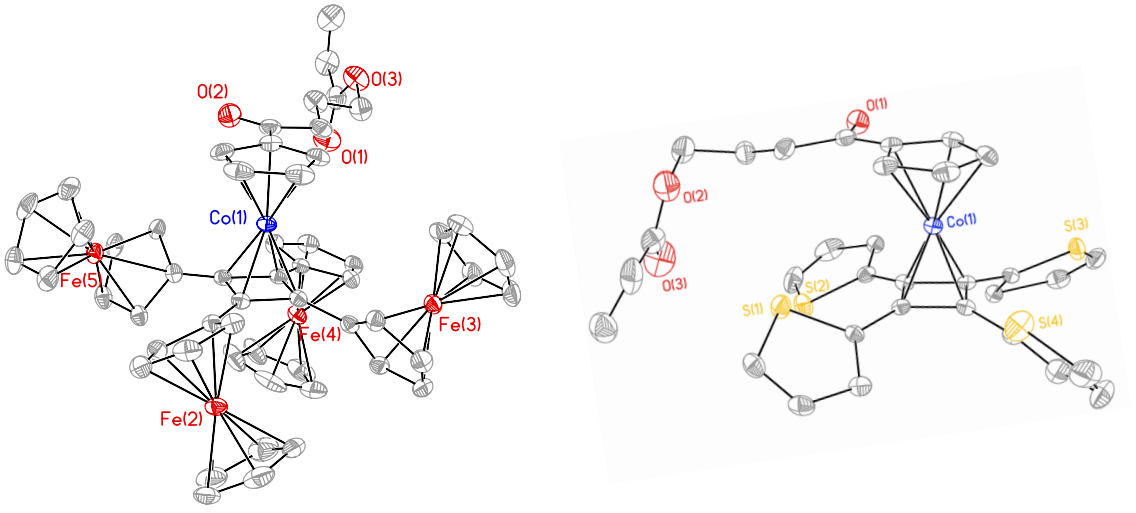


**Figure 5.2.** Solid-state structure of monomer **5.2b** (left) and **5.2c** (right).

### 5.2.2. Towards Polymerization of Highly Metalized Monomers

Synthesis and detailed polymerization of a monomeric analogue with four phenyl substituents onto the Cb ring (**2.3**) was discussed in chapter 2.[47] By replacing two or four of the phenyl groups of monomer **2.3** with ferrocene units, respectively monomer **5.2a** and **5.2b** are prepared. This enabled synthesis of monomers with one, three, and five metal centers per molecule. These highly metallized monomers with controlled number of cobalt and iron centers are good candidates to make highly metallized polymers with tunable metal content.

Following previously established RAFT polymerization conditions,[47] the RAFT agent **2.4** (1 *eq.*) was dissolved in nitrogen-saturated chlorobenzene and charged with 2,2′-azobisisobutyronitrile (AIBN) (0.2 *eq.*), monomer **5.2** (30 *eq.*), and MA (90 *eq.*) and then heated at 80 °C (Scheme 5.2).

Attempts towards RAFT polymerization of monomer **5.2c** revealed that under applied polymerization condition, polymerization does not occur. By increasing the amount of initiator over prolonged reaction time (up to 2 *eq.* over 48 hours), no sign of polymerization was observed. We hypothesized the initiation step was problematic as no sign of polymerization was observed; the monomer **5.2c** was recovered completely intact. Examining different pathways and conditions to polymerize monomer **5.2**c is being studied.

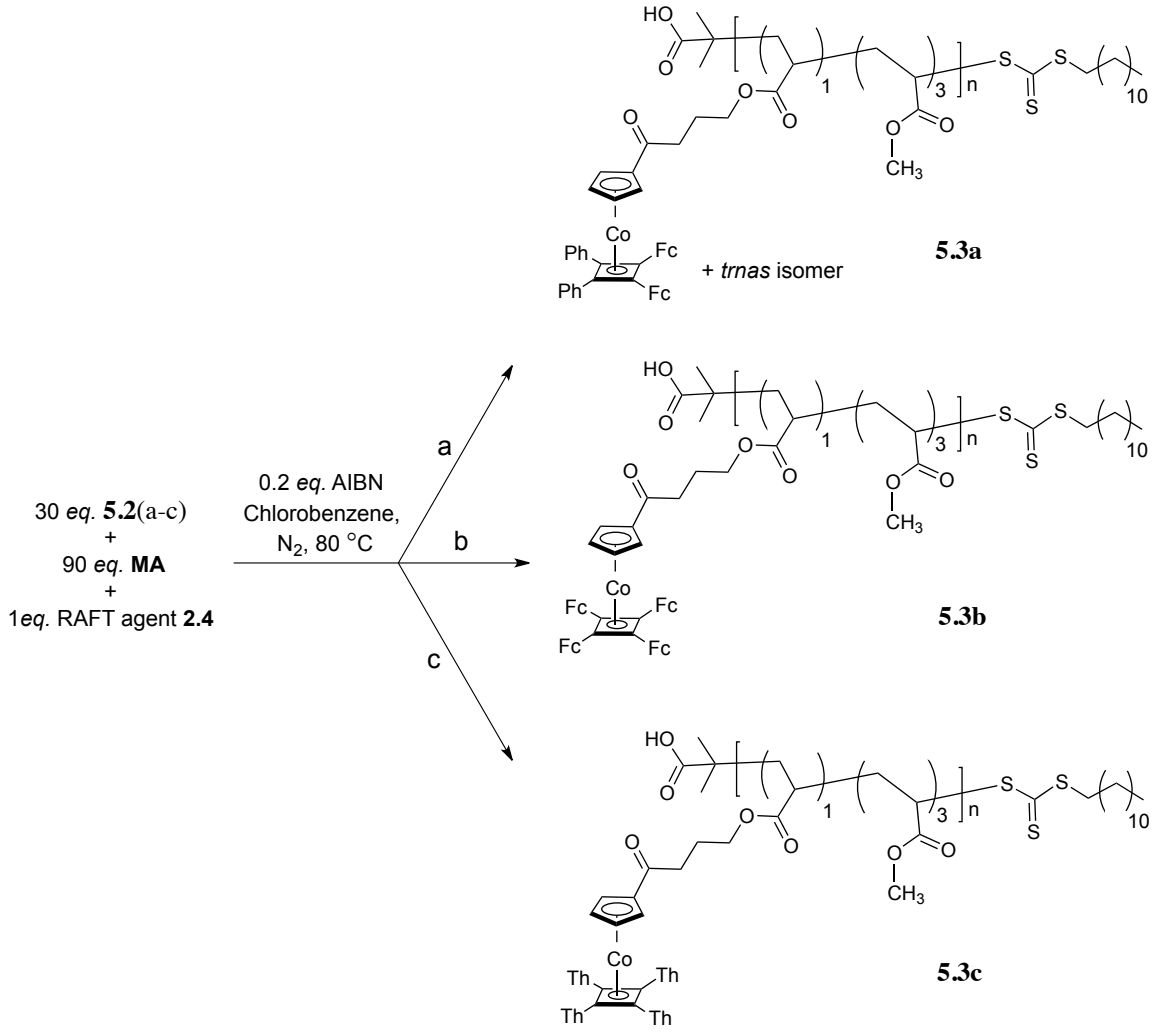


**Scheme 5.2.** Attempts towards RAFT random copolymerization of **5.2(a-c)** and MA.

Applying established RAFT polymerizations conditions on monomer **5.2a** and **5.2b** resulted in polydisperse, low molecular weight metallopolymers (**5.3a** and **5.3b**). Gel permeation chromatography (GPC) analysis of produced materials are provided in Figure 5.3. We previously showed that steric hindrance halting the polymerization of bulky monomer **2.3** was addressed by using a small monomer, *e.g.* methyl acrylate (MA) acting as a spacer. However, monomer **5.2a** and **5.2b** are drastically bulkier than monomer **2.3**. Thus, despite using three stoichiometric equivalents of MA in the random copolymerization of **5.2a** or **5.2b**, low molecular weight metallopolymers with broad PDI were obtained (Figure 5.3). The RI trace of random copolymer **2.8** is provided for comparison.

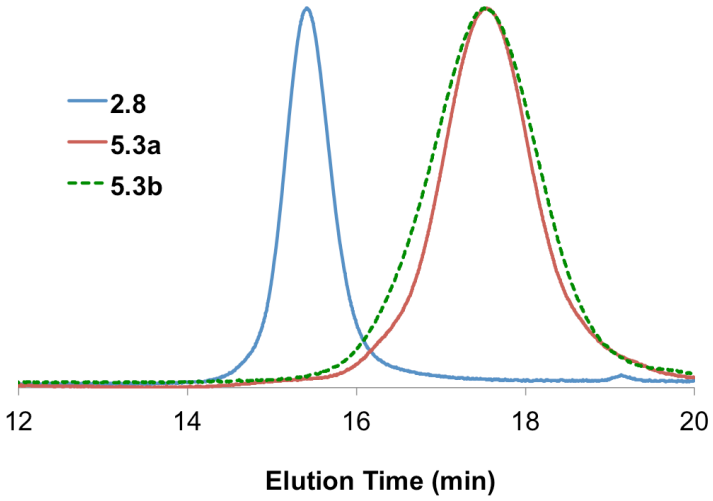


| | $M_n^*$ (kDa) | PDI |
|---|---|---|
| **2.8** | 20.7 | 1.09 |
| **5.3a** | 2.9 | 1.34 |
| **5.3b** | 2.8 | 1.34 |

**Figure 5.3.** RI traces, $M_n$, and PDI of **5.3a** and **5.3b** prepared under previously optimized RAFT polymerization condition. (**2.8** is provided for comparison).

To study the effect of longer spacer, the monomer synthesis was modified and an analogues of monomer **5.2a** with longer carbon chain spacer was prepared (**5.6**; Scheme 5.3). This was done using an analogue of the compound **2.1** with five-carbon chain spacer (**5.4**).

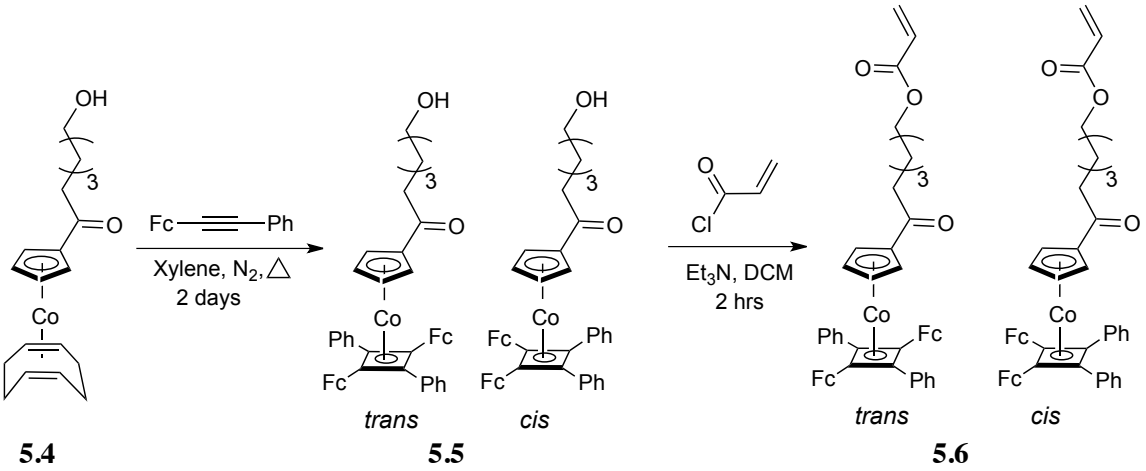


**Scheme 5.3.** Synthesis of monomers with longer carbon chain spacer.

We were able to isolate the *cis* and *trans* isomers of monomer **5.6** by selective crystallization. The solid-state structure of the *trans* isomer showed using the longer spacer (five *vs* three carbon chain) resulted in relative spatial separation of the polymerizable group and the bulky CpCoCb moiety (Figure 5.4). We were hoping this longer spacer would be helpful in overcoming the steric issue raised by the bulky monomer during polymerization.

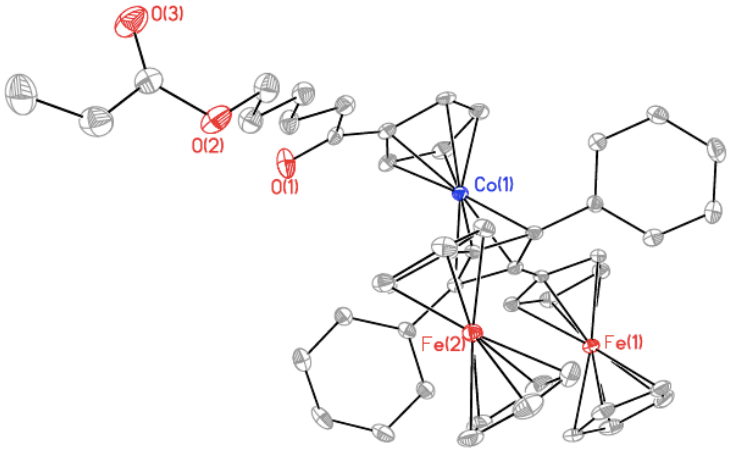


**Figure 5.4.** Solid-state structure of monomer **5.6** (*trans* isomer).

Following previously established RAFT polymerization condition, copolymerization of the monomer **5.6** with MA resulted in low molecular weight polymers. Copolymerization with higher molar ratios of MA was not effective in obtaining high molecular weight polymers with controlled PDI (Table 5.1). Utilizing a different small monomer such as styrene to act as a spacer (instead of MA), did not yield high molecular weight polymers either. Table 5.1 provides a summarized list of different conditions applied to polymerize monomer **5.6**. (see Figure A5.1-7 for $^{1}$H NMR spectra and GPC analysis of the resulting materials). Studies on alternative methods for controlled polymerization of these bulky monomers are in progress.

**Table 5.1.** Attempts towards the polymerization of monomer **5.6**.

| entry | Monomer | co-monomer | *eq.*[a] | conversion[b] (%) | $M_n$ (kDa)[c] | $M_n$ (kDa)[d] | PDI |
|---|---|---|---|---|---|---|---|
| 1 | **5.6** | MA | 4 | 50 | 12.5 | 3.4 | 1.29 |
| 2 | **5.6** | Sty | 4 | 50 | 12.5 | 6.3 | 1.28 |
| 3 | **5.6** | Sty | 8 | 60 | 15 | 8.4 | 1.35 |
| 4 | **5.6** (*cis*) | MA | 4 | 70 | 17.5 | 5.8 | 1.41 |
| 5 | **5.6** (*cis*) | MA | 6 | 70 | 17.5 | 6.9 | 1.49 |
| 6 | **5.6** (*cis*) | MA | 9 | 40 | 10 | 8.9 | 1.52 |
| 7 | **5.6** (*trans*) | MA | 9 | 50 | 12.5 | 10.9 | 1.54 |

a. stoichiometric equivalent of co-monomer, b. based on $^{1}$H NMR spectra of monomer **5.6**, c. based on monomer conversion, d. based on GPC analysis relative to PS standards.

Despite the fact that high molecular weight metallopolymers with low PDI were not obtained, highly metallized oligomers with tunable metal contents were produced. Thermal gravimetric analysis (TGA) of produced materials indicated these materials have high metal content and therefore produce high char yield residue (up to 53%).

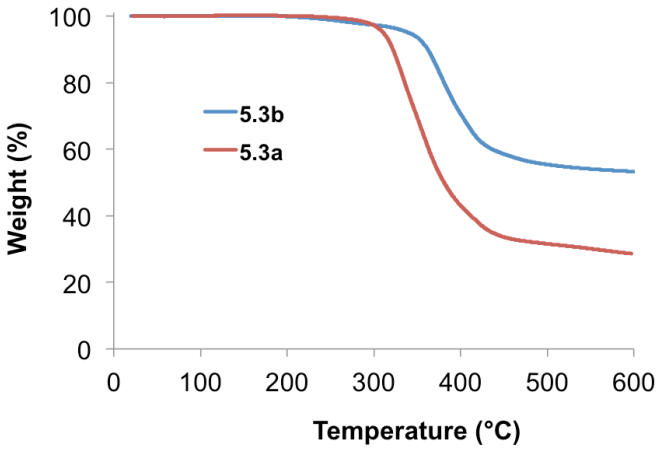


**Figure 5.5.** TGA analysis of **5.3a** and **5.3b**.

### 5.2.3. Microcontact Lithography of Highly Metalized Material

We have studied the application of these highly metallized materials as ink for microcontact patterning (μCP). PDMS stamp with pillar patterns were used to pattern transfer these highly metallized materials onto a silicon wafer substrate. A 0.5% (w/w) solution of **2.8**, **5.3a**, and **5.3b** in toluene was prepared and used as ink. PDMS stamp was loaded with 5 μL of the ink material. The stamp was brought into contact with the silicon substrate with a gentle pressure for 60 seconds. After which, the stamp was removed and the silicon wafer was visualized using SEM. Samples containing 1Co (**2.8**), 1Co: 2Fe (**5.3a**), and 1Co: 4Fe (**5.3b**) per repeat unit were used as the ink. All three samples were successfully pattern transferred confirmed by SEM imaging (A-C; Figure 5.6). To study if the material retains the shape during pyrolysis, patterned samples were pyrolyzed at 800 °C under nitrogen atmosphere for 3 hours. Pyrolyzed samples were visualized by SEM imaging. Nanometer ceramics were observed for pyrolyzed patterns where **2.8** was used as ink. This material with one cobalt per repeat unit did not keep the patterns indicated by random distribution of ceramic materials (D; Figure 5.6). By increasing the metal content in the ink material to 1Co: 2Fe (**5.3a**) and 1Co: 4Fe (**5.3b**), the pyrolyzed material formed ceramic islands while retaining the pattern (E and F respectively; Figure 5.6).

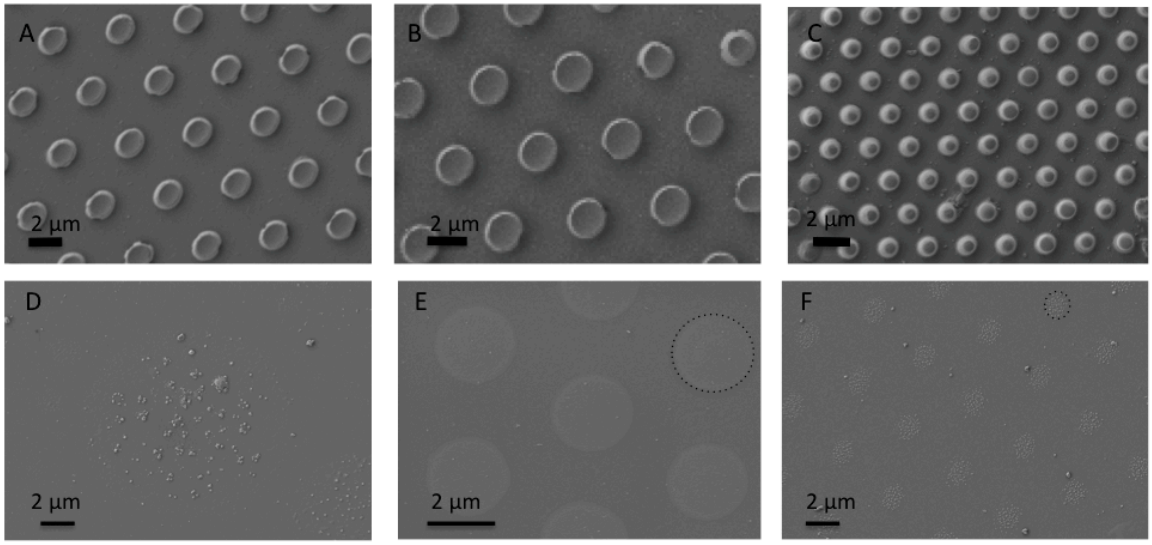


**Figure 5.6.** SEM Images of stamped material using **2.8** (A), **5.2a** (B), and **5.2b** (C) as ink. Stamped samples after pyrolysis at 800 °C using **2.8** (D), **5.2a** (E), **5.2b** (F) as ink.

### 5.2.4. Networks of Highly Metallized Material

An alternative to incorporate these highly metallized bulky monomers into macromolecules is by encasing them into cross-linked networks of polymers. A formulation using metalized monomer (**5.2a**, and **5.2b**) and tetra(ethylene glycol) diacrylate as a cross-linker with 50:50 (w/w) ratio in DMF (60% solids) was prepared. For the monomer **2.3**, because of its lower solubility, formulation with more solvent (40% solids) was prepared. Formulations were saturated with nitrogen gas, charged with AIBN (0.2 w%) and sealed in a small vial. Polymerization was carried out at 75 °C for 3 hours (Figure 5.7).

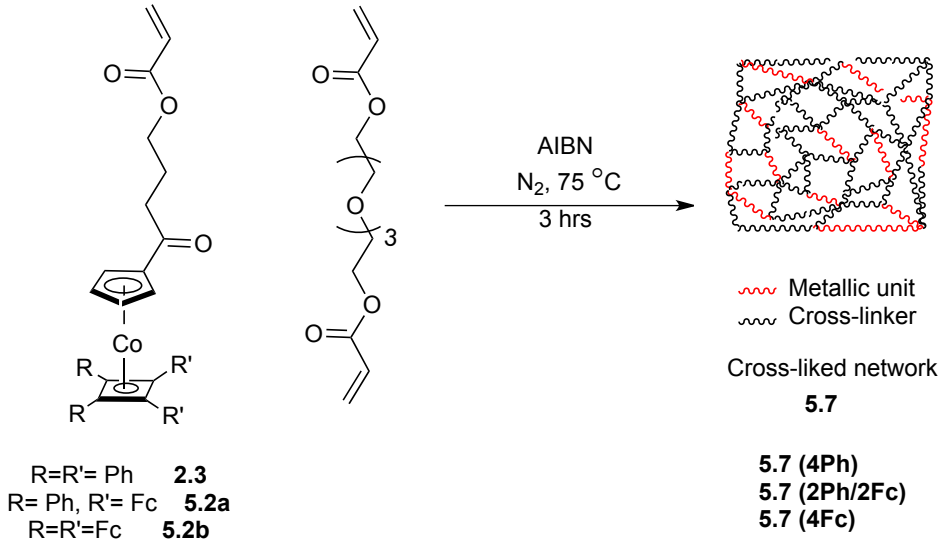


**Figure 5.7.** Cross-linked networks of metallized material using highly metallized monomers and tetraethylene glycol diacrylate as cross-linker.

After polymerization, samples were free-standing solid pucks adopting the shape of the bottom of the vial. The cross-linked networks of metallopolymers were dried in vacuum oven at 60 °C to remove any solvent residue. The pucks kept their shape during drying process and no noticeable shrinkage was observed (A; Figure 5.8).

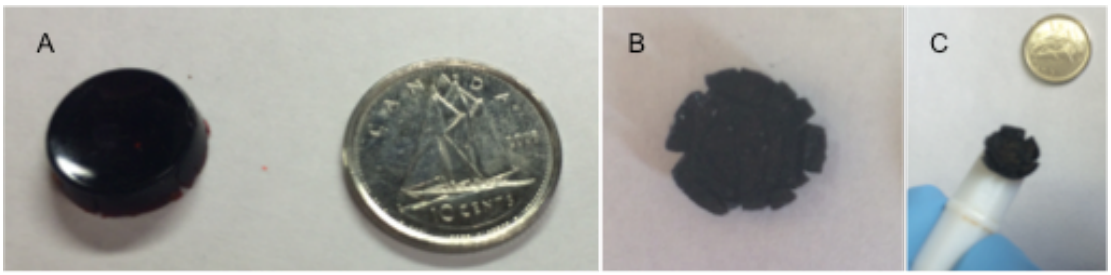


**Figure 5.8.** Free-standing puck **5.7(2Ph/2Fc)** after drying process (A), and after pyrolysis at 800 °C (B). The pyrolyzed material was attracted to permanent magnets (C).

The physical properties of the three cross-linked networks (**5.7**) with different metal contents were analyzed (Table 5.2). The cross-linked Network **5.7(2Ph/2Fc)** was the most swellable material and had a gel content of 96%, whereas network **5.7(4Ph)** and **5.7(4Fc)** produced less swellable material with respectively 88% and 70% gel content. In the case of network **5.7(4Ph)** the low solubility of the monomer resulted in its partial

aggregation in the formulation, and thus the vinyl groups were not fully accessible for polymerization. In the case of network **5.7(4Fc)**, the bulky monomer **5.2b** is postulated to limit its incorporation into the polymer network leading to a cross-linked network mostly composed of the cross-linker. The same trend was observed for the swelling ratio. The network **5.7(4Ph)** and **5.7(4Fc)** were less swellable compared to the network **5.7(2Ph/2Fc)**. Among the three monomers, **5.7(4Ph)** with one cobalt and two iron per repeat unit produced the polymer network with highest gel content (96.9 %) and highest swelling ratio (Table 5.2).

**Table 5.2.** Physical properties of cross-linked networks **5.7**.

| Network | Swelling ratio | Gel content (%) | Char yield (%) |
|---|---|---|---|
| **5.7 (4Ph)** | 1.0 ± 0.01 | 88 ± 2 | 13.5 |
| **5.7 (2Ph/2Fc)** | 1.8 ± 0.02 | 96 ± 1 | 33 |
| **5.7 (4Fc)** | 1.1 ± 0.01 | 70 ± 2 | 17 |

Thermal gravimetric analysis of the cross-linked networks was studied. The network **5.7(2Fc/2Ph)** had the highest char yield (33%) indicating higher amount of metallic monomer (**5.2a**) is incorporated into the network. This observation is in agreement with gel content and swelling ratio properties. The network **5.7(4Fc)** showed 17% char yield and the network **5.7(4Ph)** showed 13.5% char yield. As it was discussed earlier, due to the bulkiness and the low solubility of the utilized monomers, these two networks contained less metal loading and consequently had lower char yield.

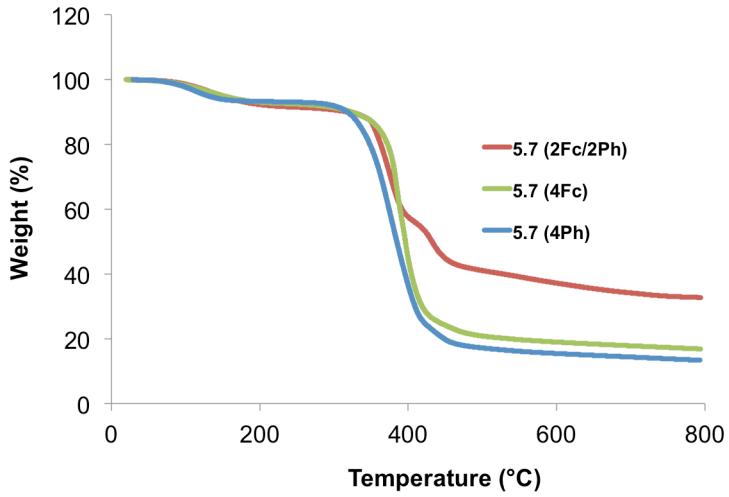


**Figure 5.9.** TGA analysis of **5.7** series.

Dried pucks were pyrolyzed at 800 °C under nitrogen flow. All three samples with different metal content kept the shape after pyrolysis and resulted in ceramic material with tunable content of cobalt and iron (B; Figure 5.8). The pyrolyzed material was magnetic as it was attracted to permanent magnet (C; Figure 5.8). Studies on magnetic properties of these materials are in process.

### 5.3. Conclusion

A series of mixed sandwich cobaltocene monomers featuring $\eta^5$-cyclopentadienyl-cobalt-$\eta^4$-cyclobutadiene (CpCoCb) with variety of substituents incorporated onto the Cb ring is introduced. We were able to install thiophene, bithiophene, and ferrocene units onto the Cb ring. Monomeric units with good control over the type and ratio of the metal content were produced. We were able to make metallized monomers with 1Co, 1Co: 2Fe, and 1Co: 4Fe incorporated in each repeat unit. Oligomers of these highly metalized materials showed up to 50% magnetic char yield. These materials were used as ink in microcontact patterning (μCP) to pattern transfer metallic domains on a silicon substrate. Patterned metallized materials were pyrolyzed resulting in patterned ceramic domains. Highly metallized monomers were incorporated into cross-linked networks. Networks showed to retain their shape during pyrolysis resulting in shaped magnetic ceramics with high char yields. Studies on the controlled polymerization of these materials are in progress. In depth studies on the correlation between metal content and their magnetic properties is

our interest. These preliminary results indicate that these highly metallized monomers are good precursors for making materials with tunable metal loading. These data show that tunable metallopolymer networks could be made providing a convenient route for the fabrication of network supported metal centers. These materials with high char yield are good candidate as resist for electron beam lithography (EBL). Incorporating them into nanosized morphologies such as block copolymers self-assembly can be used as a method to produce patterned magnetic ceramic.

### 5.4. Experimental

Compound **2.1**,[46] monomer **2.3**[47] were synthesized following previously reported literature procedure. Compound **5.4** were prepared following reported procedure by using ε-caprolactone instead of γ-butyrolactone.[46] Methyl acrylate (MA) was purchased from Sigma Aldrich and was distilled and stored under nitrogen prior to use. 2,2′-Azobis(2-methylpropionitrile) (AIBN) was purchased from Sigma Aldrich and was recrystallized in methanol prior to use. Chlorobenzene and tetra(ethylene glycol) diacrylate was purchased form Sigma Aldrich, freeze-pump-thawed three cycles and stored under nitrogen. Dimethylformamide were obtained from Caledon Laboratories and used as received. Chloroform-d (99.8 atom % D) were purchased from Cambridge Isotope Laboratories (CIL).

Nuclear magnetic resonance (NMR) spectroscopy was conducted on a Varian INOVA 400 MHz spectrometer ($^{1}$H: 399.76 MHz, $^{13}$C{$^{1}$H}: 100.52 MHz). $^{1}$H and $^{13}$C{$^{1}$H} spectra were referenced relative to chloroform residue using chloroform-d, 99.8 atom % D ($^{1}$H: $\delta$H = 7.26 ppm, $^{13}$C: $\delta$C = 77 ppm).

Fourier transform infrared (FT-IR) spectroscopy was conducted as a thin film using a Bruker Tensor 27 spectrometer, with a resolution of 4 cm$^{-1}$. The decomposition temperatures ($T_d$) were determined using a TGA/SDTA 851e Mettler Toledo instrument or Q600 SDT TA Instrument by heating samples at a rate of 10 °C/min over a temperature range of 30-600 °C. Gel permeation chromatography (GPC) experiments were conducted in chromatography grade THF at concentrations of 3-5 mg/mL using a Viscotek GPCmax VE 2001 GPC instrument equipped with an Agilent PolyPore guard column (PL1113-1500) and two sequential Agilent PolyPore GPC columns packed with porous poly(styrene-*co*-divinylbenzene) particles ($M_W$ range 200 - 2000000 g/mol;

PL1113-6500) regulated at a temperature of 30°C. Signal response was measured using a Viscotek VE 3580 RI detector, and molecular weights were determined by comparison of the maximum RI response with a calibration curve (10 points, 1500 - 786000 g/mol) established using monodisperse polystyrene standards supplied by Viscotek.

**Compound 5.1.**

Synthesis of compound **5.1a** is provided as an example. All **5.1(a-d)** series were prepared following the same procedure using the proper alkyne. In a typical reaction, a 250 mL flame dried Schlenk flask was charged with compound **2.1** (2.00 g, 6.28 mmol, 1 *eq.*), $FcC_2Ph$ alkyne (1.22 g, 13.8 mmol, 2.2 *eq.*), dry *p*-xylene (100 mL), and a stir bar. A flame-dried condenser was mounted and the solution was refluxed under $N_2$ atmosphere for 2 days. After which the reaction mixture was cooled down to room temperature and was added to *n*-hexane (400 mL) to precipitate out the crude product. Orange precipitate was collected using gravity filtration, dissolved in dichloromethane (DCM) and filtered to remove any black precipitate. The black residue collected on filter paper was discarded. DCM was concentrated to give orange oil. The crude compound was pre-adsorbed on neutral alumina and subjected to column chromatography. An orange band eluted with EtOAc: *n*-hexane (5: 95) which contained unreacted $FcC_2Ph$. Eluent was changed to EtOAc to collect compound **5.1a** in 70% yield.

**Compound 5.1; (*trans* isomer):** $^1$H NMR ($CDCl_3$; δ(ppm)): 7.98 (m, 4H), 7.44-7.56 (m, 6H), 5.18 (m, 2H), 4.61 (m, 2H), 4.12-4.13 (m, 8H), 4.02 (s, 10H), 3.48 (m, 2H), 2.23 (t, $^3J$ = 3.7 Hz, 2H), 2.05 (t, $^3J$ = 4.9, 1H), 1.58 (m, 2H). $^{13}$C NMR ($CDCl_3$; δ(ppm)): 199.4, 135.75, 130.46, 128.8, 128.2, 127.4, 93.1, 86.2, 82.4, 79.1, 69.3, 68.7, 67.5, 64.8, 28.8, 25.7, 23.4. FT-IR ($cm^{-1}$) (ranked intensity): 668 (11), 814 (8), 872 (14), 1027 (5), 1057 (4), 1260 (9), 1371 (3), 1419 (12), 1456 (1), 1559 (13), 1576 (15), 1653 (2), 2907 (6), 2936 (7), 3421 (10). HRMS (found/calculated): (782.094/ 782.098). (***cis* isomer):** $^1$H NMR ($CDCl_3$; δ(ppm)): 7.64 (m, 4H), 7.31 (m, 6H), 5.25 (*p*t, 2H), 4.75 (*p*t, 2H), 4.58 (m, 2H), 4.38 (m, 2H), 4.27 (m, 4H), 4.01 (s, 10H), 3.48 (m, 2H), 2.23 (t, $^3J$ = 3.7 Hz, 2H), 2.05 (t, $^3J$ = 4.9, 1H), 1.58 (m, 2H). $^{13}$C NMR ($CDCl_3$; δ(ppm)): 199.4, 135.8, 129.7, 128.8, 128.2, 126.9, 93.4, 86.3, 82.5, 80.18, 77.7, 77.1, 69.6, 69.4, 69.3, 68.7, 68.6, 64.8, 39.7, 28.8, 25.7, 23.4. FT-IR ($cm^{-1}$) (ranked intensity): 668 (11), 814 (8), 872 (14), 1027

(5), 1057 (4), 1260 (9), 1371 (3), 1419 (12), 1456 (1), 1559 (13), 1576 (15), 1653 (2), 2907 (6), 2936 (7), 3421 (10). HRMS (found/calculated): (782.094/ 782.098).

**Compound 5.1b:** $^{1}$H NMR ($CDCl_3$; δ(ppm)): 5.41 (m, 2H), [5.31 (s, 2H, $CH_2Cl_2$)]*, 4.91 (m, 2H), 4.84 (m, 8H), 4.37 (m, 8H), 4.13 (s, 20H), 3.54 (m, 2H), 2.28 (m, 2H), 2.24 (t, $^{3}J$ = 4.0 Hz, 1H), 1.69 (m, 2H). $^{13}$C NMR ($CDCl_3$; δ(ppm)): 200.1, 138.9, 132.1, 128.4, 127.9, 123.6, 121.8, 70.7, 69.4, 68.8, 67.2, 66.5, 29.6. FT-IR ($cm^{-1}$) (ranked intensity): 646 (14), 694 (7), 728 (2), 818 (1), 884 (13), 909 (6), 1001 (4), 1025 (9), 1105 (3), 1119 (11), 1186 (10), 1411 (12), 1436 (5), 1593 (8), 1729 (15). HRMS (found/ calculated): 998.0342/ 998.0305. Elemental analysis (found/calculated): (for $C_{53}H_{47}Fe_4CoO_2$+$CH_2Cl_2$)*: C (59.09/59.87), H (4.55/4.56). *Sample crystallized with one molecule of dichloromethane. See X-ray structure. NMR of crystals supports the observation.

**Compound 5.1c:** $^{1}$H NMR (CDCl3; δ(ppm)): 7.34 (dd, $^{4}J$ = 0.8 Hz, $^{3}J$ = 3.2 Hz, 4H), 7.29 (dd, $^{4}J$ = 0.8 Hz, $^{3}J$ = 2.4 Hz, 4H), 6.9 (dd, $^{3}J$ = 2.4 Hz, $^{3}J$ = 3.2 Hz, 4H), 5.39 (m, 2H), 4.93 (m, 2H), 3.48 (m, 2H), 2.23 (t, $^{3}J$ = 4.4 Hz, 2H), 1.90 (t, $^{3}J$ = 4.2 Hz, 1H), 1.56 (m, 2H). $^{13}$C NMR ($CDCl_3$; δ(ppm)): 199.7, 136.3, 135.2, 132.9, 130.0, 129.8, 129.7, 128.7, 128.2, 126.2, 41.8, 29.6. FT-IR ($cm^{-1}$) (ranked intensity): 550 (8), 697 (1), 822 (5), 1051 (6), 1225 (12), 1259 (9), 1374 (10), 1457 (4), 1541 (11), 1558 (13), 1669 (3), 1734 (14), 2342, (15). LRMS (EI): (found/ calculated) (590.2/ 590.3).

**Compound 5.1d:** $^{1}$H NMR ($CDCl_3$; δ(ppm)): 7.24 (m, 8H), 7.21 (m, 4H), 7.07 (m, 4H), 7.02 (m, 4H), 5.44 (m, 2H), 4.99 (m, 2H), 3.41 (m, 2H), 2.34 (t, $^{3}J$ = 4.8 Hz, 2H), 1.69 (t, $^{3}J$ = 3.6 Hz, 1H), 1.58 (m, 2H). $^{13}$C NMR ($CDCl_3$; δ(ppm)): 137.9, 137.0, 134.6, 128.6, 128.1, 124.7, 124.3, 123.9, 90.1, 89.6, 87.5, 83.7, 70.9, 36.9, 26.5. FT-IR ($cm^{-1}$) (ranked intensity): 588 (6), 730 (15), 837 (14), 907 (11), 1047 (10), 1199 (8), 1220 (5), 1253 (4), 1424 (7), 1456 (12), 1666 (13), 1373 (9), 2927 (2), 3069 (3), 3442 (1). HRMS (found/ calculated): 918.94969/ 918.942179. Elemental analysis (found/ calculated): C (58.44/ 58.80), H (3.00/ 3.40), S (26.99/ 27.91).

**Compound 5.2 (a-d):**

Synthesis of compound **5.2a** is provided as an example. All **5.2(a-c)** series were prepared following the same procedure using the proper **5.1** compound. A 250 mL flame dried round bottom flask was charged with compound **5.1a** (6.88 g, 8.80 mmol, 1 *eq.*), dry

DCM (150 mL) and triethylamine (1.85 mL, 13.0 mol, 1.5 *eq.*) followed by the addition of acryloyl chloride (1.07 mL, 13.0 mmol, 1.5 eq). The reaction mixture was stirred under $N_2$ atmosphere for 2 hours after which it was quenched with water (150 mL). Mixture was transferred to a separatory funnel and the DCM layer was collected and washed with brine (3×50 mL). Organic layers was dried over $MgSO_4$, filtered, and concentrated under reduced pressure. The red/orange solid was purified using column chromatography (neutral alumina, hexane/ ethyl acetate (12:1)) to collect compound **5.2a** in 90% yield.

**Compound 5.2a; (*trans* isomer):** $^1$H NMR ($CDCl_3$; δ(ppm)): 7.98 (m, 4H), 7.44-7.56 (m, 6H), 6.38 (dd, $^3J$ = 17.3 Hz, $^2J$ = 1.7 Hz, 1H), 6.12 (dd, $^3J$ = 17.3 Hz, $^3J$ = 10.8 Hz, 1H), 5.83 (dd, $^3J$ = 10.8 Hz, $^2J$ = 1.7 Hz, 1H), 5.18 (m, 2H), 4.61 (m, 2H), 4.12-4.13 (m, 8H), 4.11 (t, $^3J$ = 4.0 Hz, 2H), 4.02 (s, 10H), 2.05 (t, $^3J$ = 3.7 Hz, 2H), 1.58 (m, 2H), 1.36 (m, 2H). $^{13}$C NMR ($CDCl_3$; δ(ppm)): 199.4, 166.5, 135.7, 130.7, 130.4, 128.8, 128.2, 127.4, 93.1, 86.2, 82.4, 79.1, 69.3, 68.7, 67.5, 64.8, 28.8, 25.7, 23.4. FT-IR ($cm^{-1}$) (ranked intensity): 645 (12), 709 (6), 774 (15), 816 (2), 1105 (14), 1025 (11), 1194 (7), 1270 (13), 1407 (10), 1455 (5), 1662 (1), 1722 (3), 2352 (4), 2576 (8), 2948 (9). HRMS (found/calculated): (836.112/ 836.109). **(*cis* isomer):** $^1$H NMR ($CDCl_3$; δ(ppm)): 7.64 (m, 4H), 7.31 (m, 6H), 6.38 (dd, $^3J$ = 17.4 Hz, $^2J$ = 1.7 Hz, 1H), 6.12 (dd, $^3J$ = 17.4 Hz, $^3J$ = 10.7 Hz, 1H), 5.83 (dd, $^3J$ = 10.7 Hz, $^2J$ = 1.7 Hz, 1H), 5.25 (m, 2H), 4.75 (m, 2H), 4.58 (m, 2H), 4.38 (m, 2H), 4.27 (m, 4H), 4.11 (t, $^3J$ = 4.0 Hz, 2H), 4.01 (s, 10H), 2.05 (t, $^3J$ = 3.7 Hz, 2H), 1.58 (m, 2H), 1.36 (m, 2H). $^{13}$C NMR ($CDCl_3$; δ(ppm)): 199.4, 166.5, 135.8, 130.7, 129.7, 128.8, 128.2, 126.9, 93.4, 86.3, 82.5, 80.18, 77.7, 77.1, 69.6, 69.4, 69.3, 68.7, 68.6, 64.8, 39.7, 28.8, 25.7, 23.4. FT-IR ($cm^{-1}$) (ranked intensity): 645 (12), 709 (6), 774 (15), 816 (2), 1105 (14), 1025 (11), 1194 (7), 1270 (13), 1407 (10), 1455 (5), 1662 (1), 1722 (3), 2352 (4), 2576 (8), 2948 (9). HRMS (found/calculated): (836.112/ 836.109).

**Compound 5.2b:** $^1$H NMR: ($CDCl_3$; δ(ppm)) 6.38 (dd, $^2J$ = 1.6, $^3J$ = 17.6 Hz, 1H), 6.07 (dd, $^3J$ = 10.4 Hz, $^3J$ =17.6, 1H), 5.78 (dd, $^2J$ = 1.6 Hz, $^3J$ = 10.4 Hz, 1H), 5.40 (m, 2H), 4.90 (m, 2H), 4.83 (m, 8H), 4.36 (m, 8H), 4.12 (s, 20H), 4.05 (t, $^3J$ = 6.8 Hz, 2H), 2.20 (t, $^3J$ = 7.6 Hz, 2H), 1.81 (p, $^3J$ = 7.2 Hz, 2H). FT-IR ($cm^{-1}$) (ranked intensity): 646 (1), 732 (11), 909 (5), 1001 (10), 1029 (13), 1056 (7), 1106 (14), 1190 (4), 1262 (6), 1371 (3), 1408 (8), 1456 (11), 2924 (9), 1722 (15), 3094 (2). HRMS: (found/ calculated):

1052.0380/ 1052.0411. Elemental analysis (found/ calculated): C (63.68/ 63.92), H (4.63/ 4.69).

**Compound 5.2c:** $^{1}$H NMR ($CDCl_3$; δ(ppm)): 7.30 (dd, $^{4}J$ = 0.8 Hz, $^{3}J$ = 3.2 Hz, 4H), 7.28 (dd, $^{4}J$ = 0.8 Hz, $^{3}J$ = 2.4 Hz, 4H), 6.98 (dd, $^{3}J$ = 2.4 Hz, $^{3}J$ = 3.2 Hz, 4H), 6.39 (dd, $^{3}J$ = 17.4 Hz, $^{2}J$ = 1.8 Hz, 1H), 6.10 (dd, $^{3}J$ = 17.4 Hz, $^{3}J$ = 10.8 Hz, 1H), 5.81 (dd, $^{3}J$ = 10.8 Hz, $^{2}J$ = 1.8 Hz, 1H), 5.37 (m, 2H), 4.91 (m, 2H), 3.98 (t, $^{3}J$ = 8.0 Hz, 2H), 2.23 (t, $^{3}J$ = 8.0 Hz, 2H), 1.56 (m, 2H). $^{13}$C NMR ($CDCl_3$; δ(ppm)): 197.7, 166.1, 135.0, 130.6, 128.7, 128.2, 126.9, 93.5, 87.4, 82.9, 63.9, 35.9, 22.6. FT-IR ($cm^{-1}$) (ranked intensity): 550 (5), 590 (3), 698 (15), 821 (9), 985 (4), 1055 (8), 1190 (12), 1274 (7), 1372 (6), 1406 (10), 1456 (11), 1669 (13), 1719 (14), 2957 (1), 3102 (2). HRMS: (found/ calculated): 644.00236/ 644.00185. Elemental analysis (found/ calculated): C (59.34/ 59.61), H (3.95/ 3.91), S (19.22/ 19.89). M.P: 132- 135 °C.

**Compound 5.6:**

Compound **5.6** was prepared following the same procedure reported above to make the analogue with shorter carbon chain spacer (**5.2a**) and instead of compound **2.1**, compound **5.4** was employed.

**Compound 5.6; (*cis* isomer):** $^{1}$H NMR ($CDCl_3$; δ(ppm)): 7.64 (m, 4H), 7.31 (m, 6H), 6.40 (dd, $^{3}J$ = 17.4 Hz, $^{2}J$ = 1.7 Hz, 1H), 6.13 (dd, $^{3}$J = 17.4 Hz, $^{3}J$ = 10.7 Hz, 1H), 5.83 (dd, $^{3}J$ = 10.7 Hz, $^{2}J$ = 1.7 Hz, 1H), 5.25 (m, 2H), 4.75 (m, 2H), 4.58 (m, 2H), 4.38 (m, 2H), 4.27 (m, 4H), 4.11 (t, $^{3}J$ = 4.0 Hz, 2H), 4.01 (s, 10H), 2.05 (t, $^{3}J$ = 3.7 Hz, 2H), 1.58 (m, 4H), 1.36 (m, 2H). $^{13}$C NMR ($CDCl_3$; δ(ppm)): 199.4, 166.5, 135.8, 130.7, 129.7, 128.8, 128.2, 126.9, 93.4, 86.3, 82.5, 80.18, 77.7, 77.1, 69.6, 69.4, 69.3, 68.7, 68.6, 64.8, 39.7, 28.8, 25.7, 23.4. FT-IR ($cm^{-1}$) (ranked intensity): 645 (12), 709 (6), 774 (15), 816 (2), 1105 (14), 1025 (11), 1194 (7), 1270 (13), 1407 (10), 1455 (5), 1662 (1), 1722 (3), 2352 (4), 2576 (8), 2948 (9). HRMS (found/calculated): (864.140631/ 864.139946). **(*trans* isomer):** $^{1}$H NMR ($CDCl_3$; δ(ppm)): 7.98 (m, 4H), 7.52 (m, 6H), 6.38 (dd, $^{3}J$ = 17.3 Hz, $^{2}J$ = 1.7 Hz, 1H), 6.12 (dd, $^{3}J$ = 17.3 Hz, $^{3}J$ = 10.8 Hz, 1H), 5.83 (dd, $^{3}J$ = 10.8 Hz, $^{2}J$ = 1.7 Hz, 1H), 5.18 (m, 2H), 4.61 (m, 2H), 4.12 (m, 8H), 4.11 (t, $^{3}J$ = 4.0 Hz, 2H), 4.02 (s, 10H), 2.05 (t, $^{3}J$ = 3.7 Hz, 2H), 1.58 (m, 4H), 1.36 (m, 2H). $^{13}$C NMR ($CDCl_3$; δ(ppm)): 199.4, 166.5, 135.75, 130.7, 130.46, 128.8, 128.2, 127.4, 93.1, 86.2, 82.4, 79.1, 69.3, 68.7, 67.5, 64.8, 28.8, 25.7, 23.4. FT-IR ($cm^{-1}$) (ranked intensity): 645 (12), 709 (6),

774 (15), 816 (2), 1105 (14), 1025 (11), 1194 (7), 1270 (13), 1407 (10), 1455 (5), 1662 (1), 1722 (3), 2352 (4), 2576 (8), 2948 (9). HRMS (found/calculated): (864.140631/ 864.139946).

**Compound 5.3:**

In a typical polymerization reaction, a 5 mL round bottom flask was charged with methyl acrylate (44.0 µL, 0.480 mmol, 120 *eq.*), compound **2.3** (100 mg, 0.160 mmol, 60 *eq.*), **2.4** (0.980 mg, 0.270 µmol, 1 *eq.*), AIBN (0.260 mg, 0.530 µmol, 0.2 *eq.*) and chlorobenzene (300 µL) under nitrogen. The reaction flask was sealed with a rubber and submerged into 80 ºC oil bath. After desired reaction time the reaction vessel was removed from hot bath and cooled down in ice bath. The volatiles were removed *in vacuo* resulting in orange oil. The residue was dissolved in minimum dichloromethane and added to *n*-hexane. The yellow precipitate was collected and precipitated two more times to remove any unreacted monomer.

**5.3a**: $^{1}$H NMR ($CDCl_3$; δ(ppm)): 7.98-7.64 (b), 7.34-7.56 (b), 5.83 (b), 5.25 (*b*), 5.18 (*b*), 4.75 (*b*), 4.61-4.58 (*b*), 4.38 (*b*), 4.27 (b),4.11-4.13 (b), 4.02-4.01 (b), 3.65 (b), 2.05 (b), 1.58 (b), 1.36 (b).

**5.3b:** $^{1}$H NMR: ($CDCl_3$; δ(ppm)) 5.40 (*b*), 4.90 (*b*), 4.83 (*b*), 4.36 (*b*), 4.12 (b), 4.05 (b), 3.65 (b), 2.20 (b), 1.81 (b).

**Microcontact printing (µCP):**

0.5% (w/w) of **5.3a**, **5.3b**, or **2.8** in toluene was prepared. Silicon wafers were cleaned by using Piranha solution (Caution!) and rinsed with deionized water and filtered propanol. Wafers were dried with air jet and used quickly after. 5 µL of the solution was transferred on the PDMS stamp and the pattern was printed on the freshly cleaned silicon wafer substrate by gentle pressure for 60 seconds. After which samples were visualized by SEM imaging. Stamped silicon wafers were placed in a quartz boat inside a quartz tube in a tube furnace. The tube was purged by $N_2$ gas for 20 min prior to increasing the temperature to 700 °C at a rate of 10 °C per minute followed by being held isothermal for 3 hours. Sample was cooled down to room temperature a visualized by SEM imaging.

**Cross-linked Networks:**

A formulation with metalized monomer (**5.2a**, **5.2b, or 2.3**) and tetra(ethylene glycol) diacrylate in 50:50 w/w ratio in DMF (60% solids) was prepared. For monomer **2.3,**

because of its lower solubility, formulation with more solvent (40% solids) was prepared. Formulations were saturated with nitrogen gas, charged with AIBN (2 w%) and sealed in a small vial with rubber-sealed cap. Vial was transferred into a 75 °C oven and kept for 3 hours.

**Swelling Experiments:**

Weight of sample was recorded ($m_0$) and then it was immersed in dichloromethane for 4 hours. Samples were then taken out weighed quickly ($m_t$). The swelling ratio (Q) was calculated using the following equation:

$Q = (m_t - m_0)/m_0$

**Gel Content Experiment:**

Weigh of sample was recorded and then it was immersed in dichloromethane for 4 hours. Samples were then taken out and dried in vacuum oven for 2 hours before being weighed again. By comparing the original mass to the mass after extraction, gel content was obtained.

**Pyrolysis of Cross-linked Networks:**

Cross-linked sample was placed in a quartz boat inside a quartz tube in a tube furnace. The tube was purged by $N_2$ gas for 20 min prior to increasing the temperature to 800 °C at a rate of 10 °C per minute followed by being held isothermal for 3 hours.

## 5.5. References

(1) Eloi, J. C.; Chabanne, L.; Whittell, G. R.; Manners, I. *Mater. Today* **2008**, *11*, 28-36.

(2) Whittell, G. R.; Hager, M. D.; Schubert, U. S.; Manners, I. *Nat. Mater.* **2011**, *10*, 176-188.

(3) Whittell, G. R.; Manners, I. *Adv. Mater.* **2007**, *19*, 3439-3468.

(4) Nunns, A.; Gwyther, J.; Manners, I. *Polymer* **2013**, *54*, 1269-1284.

(5) Clendenning, S. B.; Fournier-Bidoz, S.; Pietrangelo, A.; Yang, G.; Han, S.; Brodersen, P. M.; Yip, C. M.; Lu, Z.-H.; Ozin, G. A.; Manners, I. *J. Mater. Chem.* **2004**, *14*, 1686-1690.

(6) Clendenning, S. B.; Han, S.; Coombs, N.; Paquet, C.; Rayat, M. S.; Grozea, D.; Brodersen, P. M.; Sodhi, R. N. S.; Yip, C. M.; Lu, Z. H.; Manners, I. *Adv. Mater.* **2004**, *16*, 291-296.

(7) Özkale, B.; Pellicer, E.; Zeeshan, M. A.; López-Barberá, J. F.; Nogués, J.; Sort, J.; Nelson, B. J.; Pané, S. *Nanoscale* **2014**, *6*, 4683-4690.

(8) Ginzburg, M.; MacLachlan, M. J.; Yang, S. M.; Coombs, N.; Coyle, T. W.; Raju, N. P.; Greedan, J. E.; Herber, R. H.; Ozin, G. A.; Manners, I. *J. Am. Chem. Soc.* **2002**, *124*, 2625-2639.

(9) MacLachlan, M. J.; Ginzburg, M.; Coombs, N.; Coyle, T. W.; Raju, N. P.; Greedan, J. E.; Ozin, G. A.; Manners, I. *Science* **2000**, *287*, 1460-1463.

(10) Corriu, R.; Gerbier, P.; Guérin, C.; Henner, B. *Angew. Chem., Int. Ed.* **1992**, *31*, 1195-1197.

(11) Clendenning, S. B.; Aouba, S.; Rayat, M. S.; Grozea, D.; Sorge, J. B.; Brodersen, P. M.; Sodhi, R. N. S.; Lu, Z. H.; Yip, C. M.; Freeman, M. R.; Ruda, H. E.; Manners, I. *Adv. Mater.* **2004**, *16*, 215-219.

(12) Clendenning, S. B.; Manners, I. *J. Vac. Sci. Technol. B* **2004**, *22*, 3493-3496.

(13) Jeong, S. J.; Xia, G.; Kim, B. H.; Shin, D. O.; Kwon, S. H.; Kang, S. W.; Kim, S. O. *Adv. Mater.* **2008**, *20*, 1898-1904.

(14) Liu, K.; Fournier-Bidoz, S.; Ozin, G. A.; Manners, I. *Chem. Mater.* **2009**, *21*, 1781-1783.

(15) Arimoto, F. S.; Haven, A. C. *J. Am. Chem. Soc.* **1955**, *77*, 6295-6297.

(16) Hardy, C. G.; Ren, L.; Zhang, J.; Tang, C. *Isr. J. Chem.* **2012**, *52*, 230-245.

(17) Hardy, C. G.; Zhang, J.; Yan, Y.; Ren, L.; Tang, C. *Prog. Polym. Sci.* **2014**, *39*, 1742-1796.

(18) Foucher, D. A.; Tang, B.; Manners, I. *J. Am. Chem. Soc.* **1992**, *114*, 6246-6248.

(19) Petersen, R.; Foucher, D. A.; Tang, B.-Z.; Lough, A.; Raju, N. P.; Greedan, J. E.; Manners, I. *Chem. Mater.* **1995**, *7*, 2045-2053.

(20) Englert, B. C.; Scholz, S.; Leech, P. J.; Srinivasarao, M.; Bunz, U. H. F. *Chem. Eur. J.* **2005**, *11*, 995-1000.

(21) Rider, D. A. L., Kun; Eloi, Jean-Charles; Vanderark, Lawrence; Yang, Ling; Wang, Jia-Yu; Grozea, Dan; Lu, Zheng-Hong; Russell, Thomas P.; Manners, Ian *ACS Nano* **2008**, *2*, 263-270.

(22) Li, L.; Li, J.; Zhong, Y.; Chen, C.; Ben, Y.; Gong, J.; Ma, Z. *J. Mater. Chem.* **2010**, *20*, 5446-5453.

(23) Ginzburg, M.; MacLachlan, M. J.; Yang, S. M.; Coombs, N.; Coyle, T. W.; Raju, N. P.; Greedan, J. E.; H., H. R.; Ozin, G. A.; Manners, I. *J. Am. Chem. Soc.* **2002**, *124*, 2625-2639.

(24) Kong, J.; Kong, M.; Zhang, X.; Chen, L.; An, L. *ACS Appl. Mater. Interfaces* **2013**, *5*, 10367-10375.

(25) Chan, W. Y.; Clendenning, S. B.; Berenbaum, A.; Lough, A. J.; Aouba, S.; Ruda, H. E.; Manners, I. *J. Am. Chem. Soc.* **2005**, *127*, 3796-3808.

(26) Friebe, L.; Liu, K.; Obermeier, B.; Petrov, S.; Dube, P.; Manners, I. *Chem. Mater.* **2007**, *19*, 2630-2640.

(27) Seidel, R.; Duesberg, G. S.; Unger, E.; Graham, A. P.; Liebau, M.; Kreupl, F. *J. Phys. Chem. B* **2004**, *108*, 1888-1893.

(28) Kulbaba, K.; Cheng, A.; Bartole, A.; Greenberg, S.; Resendes, R.; Coombs, N.; Safa-Sefat, A.; Greedan, J. E.; Stöver, H. D. H.; Ozin, G. A.; Manners, I. *J. Am. Chem. Soc.* **2002**, *124*, 12522-12534.

(29) Zhang, J.; Yan, Y.; Chance, M. W.; Chen, J.; Hayat, J.; Ma, S.; Tang, C. *Angew. Chem., Int. Ed.* **2013**, *52*, 13387-13391.

(30) Gilroy, J. B.; Patra, S. K.; Mitchels, J. M.; Winnik, M. A.; Manners, I. *Angew. Chem., Int. Ed.* **2011**, *50*, 5851-5855.

(31) Zhang, J.; Yan, Y.; Chen, J.; Chance, W. M.; Hayat, J.; Gai, Z.; Tang, C. *Chem. Mater.* **2014**, *26*, 3185-3190.

(32) Gonzalez, B.; Cuadrado, I.; Casado, C. M.; Alonso, B.; Pastor, C. J. *Organometallics* **2000**, *19*, 5518-5521.

(33) Mayer, U. F. J.; Gilroy, J. B.; O'Hare, D.; Manners, I. *J. Am. Chem. Soc.* **2009**, *131*, 10382-10383.

(34) Corriu, R. J. P. *Angew. Chem., Int. Ed.* **2000**, *39*, 1376-1398.

(35) Yajima, S.; Omori, M. *Nature* **1977**, *267*, 823-825.

(36) Ungurenasu, C.; Pinteala, M. *Macromol. Rapid Commun.* **2005**, *26*, 707-709.

(37) Lu, J.; Kopley, T.; Button, D.; Liu, J.; Qian, C.; Son, H.; Dresselhaus, M.; Kong, J. *J. Phys. Chem. B* **2006**, *110*, 10585-10589.

(38) Lastella, S.; Mallick, G.; Woo, R.; Karna, S. P.; Rider, D. A.; Manners, I.; Jung, Y. J.; Ryu, C. Y.; Ajayan, P. M. *J. Appl. Phys.* **2006**, *99*, 024302.

(39) Liu, K.; Clendenning, S. B.; Riebe, L.; Chan, W. Y.; Zhu, X.; Freeman, M. R.; Yang, G. C.; Yip, C. M.; Grozea, D.; Lu, Z. H.; Manners, I. *Chem. Mater.* **2006**, *18*, 2591-2601.

(40) Scholz, S.; Leech, P. J.; Englert, B. C.; Sommer, W.; Weck, M.; Bunz, U. H. F. *Adv. Mater.* **2005**, *17*, 1052-1056.

(41) Mîinea, L. A.; Sessions, L. B.; Ericson, K. D.; Glueck, D. S.; Grubbs, R. B. *Macromolecules* **2004**, *37*, 8967-8972.

(42) Casado, C. M.; González, B.; Cuadrado, I.; Alonso, B.; Morán, M.; Losada, J. *Angew. Chem., Int. Ed.* **2000**, *39*, 2135-2138.

(43) Yasufuku, K.; Yamazaki, H. *J. Organomet. Chem.* **1997**, *127*, 197-207.

(44) Kulbaba, K.; Resendes, R.; Cheng, A.; Bartole, A.; Safa-Sefat, A.; Coombs, N.; Greedan, J. E.; Ozin, G. A.; Manners, I. *Adv. Mater.* **2001**, *13*, 732-736.

(45) Zhang, J.; Ren, L.; Hardy, C. G.; Tang, C. *Macromolecules* **2012**, *45*, 6857-6863.

(46) Gleiter, R.; Pflaesterer, G. *Organometallics* **1993**, *12*, 1886-1889.

(47) Hadadpour, M.; Liu, Y. Q.; Chadha, P.; Ragogna, P. J. *Macromolecules* **2014**, *47*, 6207-6217.

# Chapter 6

# Conclusions and Future Directions

## 6.1. Conclusion

This dissertation embodies the controlled reversible addition fragmentation transfer (RAFT) polymerization of a mixed sandwich cobaltocene containing monomer featuring $\eta^5$-cyclopentadienyl-cobalt-$\eta^4$-cyclobutadiene (CpCoCb). Under a variety of applied RAFT polymerization conditions, the polymerization of the CpCoCb monomer resulted in only short oligomers (PolyCpCoCb) because of the steric demand associated with the bulky monomer. To overcome this problem, CpCoCb monomer was copolymerized with a smaller monomer, methyl acrylate (MA), to act as a spacer unit that provides the necessary relief for the addition of the bulky CpCoCb monomer. This resulted in a dramatic improvement in the molecular weight and the PDI of the produced random copolymer (PolyCpCoCb-*r*-PMA) by minimizing termination and chain transfer reactions. The random copolymer PolyCpCoCb-*r*-PMA was used as a macro-RAFT agent to prepare variety of high molecular weight block copolymers where one block was CpCoCb containing metallopolymer block. In this regards, block copolymers containing styrene ((PolyCpCoCb-*r*-PMA)-*b*-PS), polydimethylsiloxane (PDMS-*b*-(PolyCpCoCb-*r*-PMA)), and phosphonium salt functionalized styrene ((PolyCpCoCb-*r*-PMA)-*b*-(PS($P^+OTf^-$))) with excellent control over molecular weight and polydispersity (PDI) were prepared.

Solid-state self-assembly of (PolyCpCoCb-*r*-PMA)-*b*-PS was studied producing lamellae macro phase-separated domains.

(PolyCpCoCb-*r*-PMA)-*b*-(PS($P^+OTf^-$)) is the first example of a block copolymer consisting of a metallopolymer block and a polyelectrolyte block. Due to inherent difficulties associated with molecular weight analysis of polyelectrolytes using common techniques such as gel permeation chromatography (GPC), the polyelectrolyte block and the RAFT agent were both fluorine tagged enabling a $^{19}F$ NMR spectroscopic handle for end group analysis. Salt metathesis reaction of the polyelectrolyte block with gold salt

($HAuCl_4$) resulted in a heterobimetallic block copolymer with gold functionalized polyelectrolyte block ((PolyCpCoCb-*r*-PMA)-*b*-(PS($P^+AuCl_4^-$))). Solution-state self-assembly of this heterobimetallic block copolymer resulted in spherical micelles with a phosphonium-based polyelectrolyte core with pendant gold anions, and a cobalt containing metallopolymer corona. Reduction of these heterobimetallic micelles resulted in gold nanoparticles (AuNPs) stabilized with metallopolymers. Phase-separation behavior of (PolyCpCoCb-*r*-PMA)-*b*-(PS($P^+OTf^-$)) showed hexagonally packed cylinders of metallopolymer domains in the polyelectrolyte. To clarify the discrimination and assignment of phase-separated domains, salt metathesis with gold anion in solid-state was used to selectively stain the polyelectrolyte block. This is the first example of utilizing salt metathesis reaction to stain the phosphonium-based polyelectrolyte domains in a phase-separated block copolymer. Pyrolysis of the metallopolymer-*b*-polyelectrolyte copolymer resulted in 17% char yield of cobalt-phosphide materials that was attracted to permanent magnets, indicative of magnetic materials being present.

PDMS-*b*-(PolyCpCoCb-*r*-PMA) block copolymer was studied for phase-separation behavior in solution and solid-state. Long-ranged hexagonally packed cylinders of metallopolymer block in PDMS was observed in solid-state. Solution-state self-assembly of the material resulted in spherical micelles with metallic core stabilized with PDMS corona. Pyrolysis of the block copolymer samples resulted in 30% char yield magnetic material. The block copolymer was used as ink material in microcontact printing (μCP) to transfer hole, line, and pillar patterns onto a silicon wafer.

In addition, a series of CpCoCb containing monomers with variety of substituents such as thiophene, bithiophene, and ferrocene incorporated onto the Cb ring were prepared. Monomeric units with good control over the type and ratio of metal content with 1Co, 1Co: 2Fe, and 1Co: 4Fe were produced. Oligomers of these highly metalized materials showed up to 50% magnetic char yield. These materials were used as ink in μCP to pattern transfer metallic domains on a silicon substrate. Patterned metallized materials were pyrolyzed resulting in patterned ceramic domains. Highly metallized monomers were incorporated into cross-linked networks. The networks showed to retain their shape during pyrolysis resulting in shaped magnetic ceramics with high char yield.

## 6.2. Future Directions

The project can be expanded in many different directions. Herein a few potential extensions are provided.

### 6.2.1. CpCoCb Containing Block Copolymers; Infinite Research Area

We have established a synthetic method to make variety of block copolymers consist of a cobalt containing metallopolymer block. Expanding the scope by using CpCoCb system to make new classes of cobalt containing block copolymer provides new routs for exploration. We have shown versatility of the CpCoCb synthesis to incorporate variable substituents onto the Cb ring. For instance, ferrocene units were incorporated onto the Cb ring to produce highly metallized monomers with good control over the metal content and the metal ratio. Utilizing sequential RAFT polymerization of derivatives of CpCoCb monomer with different substituents on the Cb ring can result in an interesting class of highly metallized block copolymers.

### 6.2.2. Block Copolymer Lithography

An interesting application of metal containing block copolymers is their use in block copolymer lithography. Solid-state self-assembled morphologies with a metallic, and a non-metallic domain are good candidates for such a technique. In block copolymer lithography, the non-metallic domain of a self-assembled morphology is etched away leaving behind the metallized domains. These nanosized patterns can be used as a template to do further chemistry. Studying the applications of CpCoCb containing block copolymer in lithography techniques has potential interest.

### 6.2.3. Applications in EBL

Highly metallized metallopolymers have found applications in electron beam lithography (EBL) to directly pattern metallic domains of any desired 2D pattern by utilizing metallopolymers as resist materials. Employing highly metallized CpCoCb containing metallopolymers as a resist in EBL techniques is interesting with promising potential applications.

### 6.2.4. Magnetic Ceramic

Magnetic ceramics are an interesting research area. We have shown that all CpCoCb containing polymers (homopolymer or block copolymer) have relatively high char yield producing magnetic material. In depth studies on the composition of these ceramic precursors is interesting, since changing pyrolysis conditions such as temperature, duration, or employing reducing or inert atmosphere, properties of the end material can be tuned. Changing the metal content and metal ratio in the ceramic precursor, the magnetic properties can be altered. In depth studies on the pyrolysis conditions of CpCoCb containing metallopolymers to make tunable magnetic ceramics in our interest.

### 6.2.5. Exploring the Chemistry of Metallopolymer-*b*-Polyelectrolyte

We have reported the first example of a block copolymer consisting of a metallopolymer block and a polyelectrolyte block. Anion exchange is a facile method to incorporate functionalities into the polyelectrolyte segment of the metallopolymer-*b*-polyelectrolyte copolymer. Preliminary results incorporating a gold anion is reported. Expanding this technique using other anions could potentially introduce interesting properties. We have reported salt metathesis with a gold anion in the solid-state to selectively stain the polyelectrolyte block. Employing different metallic anions to make heterobimetallic solid-state domains is interesting. Pyrolysis of such materials to make patterned nanoparticles is a novel avenue with potential applications.

# Chapter 7

# Appendices

## Appendix 1. Permission to Reuse Copyrighted Material

### 7.1.1. American Chemical Society

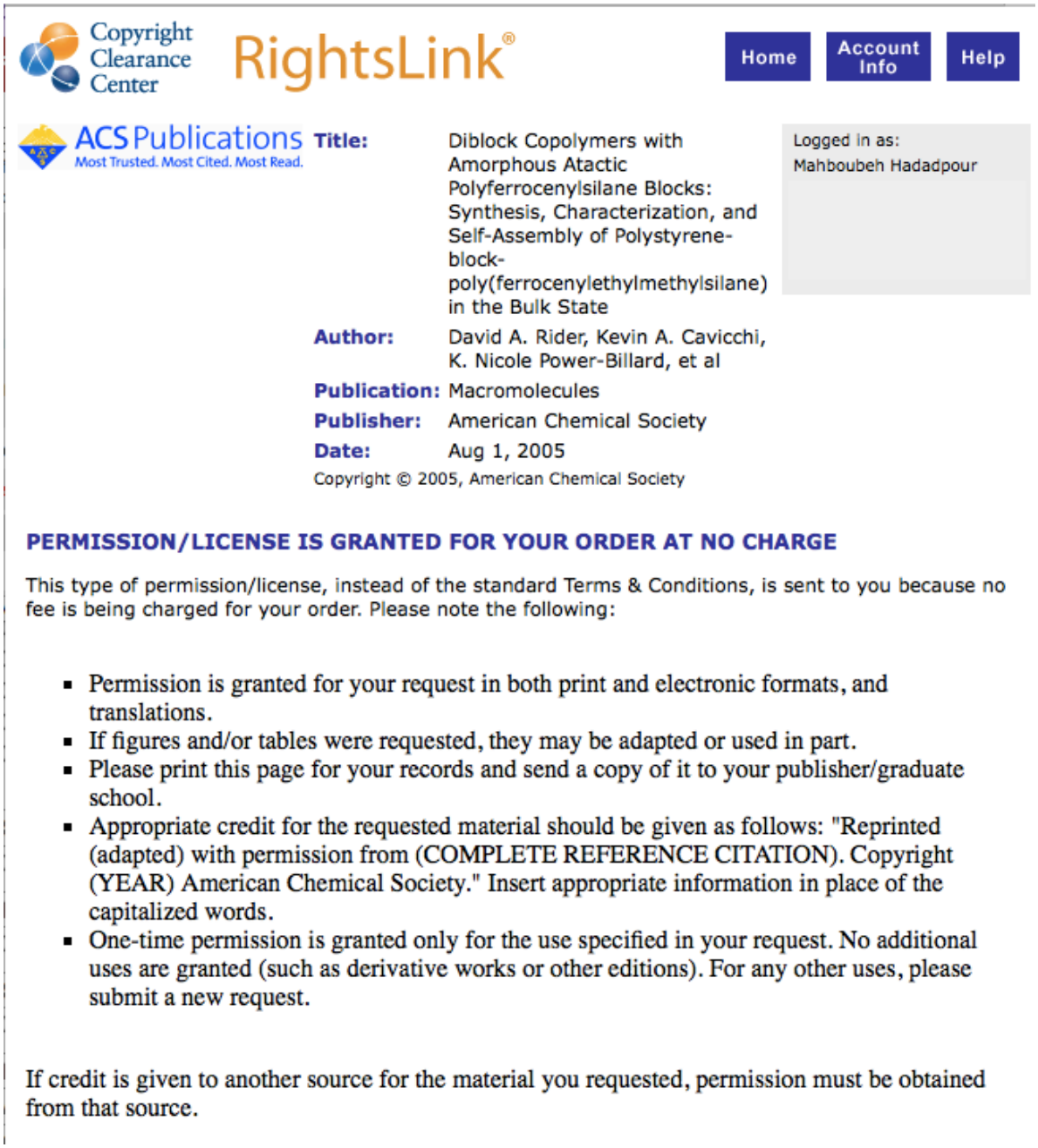

Copyright Clearance Center RightsLink®

Home | Account Info | Help

ACS Publications
Most Trusted. Most Cited. Most Read.

Logged in as:
Mahboubeh Hadadpour

**Title:** Diblock Copolymers with Amorphous Atactic Polyferrocenylsilane Blocks: Synthesis, Characterization, and Self-Assembly of Polystyrene-block-poly(ferrocenylethylmethylsilane) in the Bulk State

**Author:** David A. Rider, Kevin A. Cavicchi, K. Nicole Power-Billard, et al

**Publication:** Macromolecules

**Publisher:** American Chemical Society

**Date:** Aug 1, 2005

Copyright © 2005, American Chemical Society

**PERMISSION/LICENSE IS GRANTED FOR YOUR ORDER AT NO CHARGE**

This type of permission/license, instead of the standard Terms & Conditions, is sent to you because no fee is being charged for your order. Please note the following:

- Permission is granted for your request in both print and electronic formats, and translations.
- If figures and/or tables were requested, they may be adapted or used in part.
- Please print this page for your records and send a copy of it to your publisher/graduate school.
- Appropriate credit for the requested material should be given as follows: "Reprinted (adapted) with permission from (COMPLETE REFERENCE CITATION). Copyright (YEAR) American Chemical Society." Insert appropriate information in place of the capitalized words.
- One-time permission is granted only for the use specified in your request. No additional uses are granted (such as derivative works or other editions). For any other uses, please submit a new request.

If credit is given to another source for the material you requested, permission must be obtained from that source.

### 7.1.2. Annual Reviews

Copyright Clearance Center RightsLink®

Home | Account Info | Help

ANNUAL REVIEWS

| | |
|---|---|
| **Title:** | POLYMERSOMES |
| **Author:** | Dennis E. Discher, Fariyal Ahmed |
| **Publication:** | Annual Review of Biomedical Engineering |
| **Publisher:** | Annual Reviews |
| **Date:** | Aug 1, 2006 |

Copyright © 2006, Annual Reviews

Logged in as:
Mahboubeh Hadadpour

**Permission Not Required**

Material may be republished in a thesis / dissertation without obtaining additional permission from Annual Reviews, providing that the author and the original source of publication are fully acknowledged.

BACK | CLOSE WINDOW



### 7.1.3. Royal Society of Chemistry

| | |
|---|---|
| License Number | 3595040214195 |
| License date | Mar 23, 2015 |
| Licensed content publisher | Royal Society of Chemistry |
| Licensed content publication | Chemical Communications (Cambridge) |
| Licensed content title | Effects of nanoconfinement on the morphology and reactivity of organic materials |
| Licensed content author | Wilhelm T. S. Huck |
| Licensed content date | Jul 19, 2005 |
| Issue number | 33 |
| Type of Use | Thesis/Dissertation |
| Requestor type | academic/educational |
| Portion | figures/tables/images |
| Number of figures/tables/images | 1 |
| Distribution quantity | 3 |
| Format | print and electronic |
| Will you be translating? | no |
| Order reference number | None |
| Title of the thesis/dissertation | Exploring the Chemistry of Cyclopentadienyl-Cobalt-Cyclobutadiene Containing Polymers; Synthesis, Properties, and Self-Assembly |
| Expected completion date | May 2015 |
| Estimated size | 200 |
| Total | 0.00 USD |

### 7.1.4. John Wiley and Sons

| | |
|---|---|
| License Number | 3595040706696 |
| License date | Mar 23, 2015 |
| Licensed Content Publisher | John Wiley and Sons |
| Licensed Content Publication | Macromolecular Rapid Communications |
| Licensed Content Title | Self-Assembled Block Copolymer Aggregates: From Micelles to Vesicles and their Biological Applications |
| Licensed Content Author | Adam Blanazs,Steven P. Armes,Anthony J. Ryan |
| Licensed Content Date | Jan 22, 2009 |
| Licensed Content Pages | 11 |
| Type of use | Dissertation/Thesis |
| Requestor type | University/Academic |
| Format | Print and electronic |
| Portion | Figure/table |
| Number of figures/tables | 1 |
| Original Wiley figure/table number(s) | Figure 1 |
| Will you be translating? | No |
| Title of your thesis / dissertation | Exploring the Chemistry of Cyclopentadienyl-Cobalt-Cyclobutadiene Containing Polymers; Synthesis, Properties, and Self-Assembly |
| Expected completion date | Apr 2015 |
| Expected size (number of pages) | 200 |
| Requestor Location | Mahboubeh Hadadpour |
| Billing Type | Invoice |
| Billing address | Mahboubeh Hadadpour |
| Total | 0.00 USD |

| | |
|---|---|
| License Number | 3595041357682 |
| License date | Mar 23, 2015 |
| Licensed Content Publisher | John Wiley and Sons |
| Licensed Content Publication | Macromolecular Chemistry and Physics |
| Licensed Content Title | Double-Gyroid Morphology of a Polystyrene-block-Poly(ferrocenylethylmethylsilane) Diblock Copolymer: A Route to Ordered Bicontinuous Nanoscale Architectures |
| Licensed Content Author | Jessica Gwyther,Gudrun Lotze,Ian Hamley,Ian Manners |
| Licensed Content Date | Nov 22, 2010 |
| Licensed Content Pages | 4 |
| Type of use | Dissertation/Thesis |
| Requestor type | University/Academic |
| Format | Print and electronic |
| Portion | Figure/table |
| Number of figures/tables | 1 |
| Original Wiley figure/table number(s) | Figure 2.a |
| Will you be translating? | No |
| Title of your thesis / dissertation | Exploring the Chemistry of Cyclopentadienyl-Cobalt-Cyclobutadiene Containing Polymers; Synthesis, Properties, and Self-Assembly |
| Expected completion date | Apr 2015 |
| Expected size (number of pages) | 200 |
| Requestor Location | Mahboubeh Hadadpour |
| Billing Type | Invoice |
| Billing address | Mahboubeh Hadadpour |
| Total | 0.00 USD |

| | |
|---|---|
| License Number | 3595050082274 |
| License date | Mar 23, 2015 |
| Licensed Content Publisher | John Wiley and Sons |
| Licensed Content Publication | Advanced Materials |
| Licensed Content Title | Direct Writing of Patterned Ceramics Using Electron-Beam Lithography and Metallopolymer Resists |
| Licensed Content Author | S. B. Clendenning,S. Aouba,M. S. Rayat,D. Grozea,J. B. Sorge,P. M. Brodersen,R. N. S. Sodhi,Z.-H. Lu,C. M. Yip,M. R. Freeman,H. E. Ruda,I. Manners |
| Licensed Content Date | Feb 11, 2004 |
| Licensed Content Pages | 5 |
| Type of use | Dissertation/Thesis |
| Requestor type | University/Academic |
| Format | Print and electronic |
| Portion | Figure/table |
| Number of figures/tables | 1 |
| Original Wiley figure/table number(s) | Figure 1 |
| Will you be translating? | No |
| Title of your thesis / dissertation | Exploring the Chemistry of Cyclopentadienyl-Cobalt-Cyclobutadiene Containing Polymers; Synthesis, Properties, and Self-Assembly |
| Expected completion date | Apr 2015 |
| Expected size (number of pages) | 200 |
| Requestor Location | Mahboubeh Hadadpour |
| Billing Type | Invoice |
| Billing address | Mahboubeh Hadadpour |
| Total | 0.00 USD |

### 7.1.5. Nature Publishing Group

| | |
|---|---|
| License Number | 3595050465058 |
| License date | Mar 23, 2015 |
| Licensed content publisher | Nature Publishing Group |
| Licensed content publication | Nature Materials |
| Licensed content title | Complex and hierarchical micelle architectures from diblock copolymers using living, crystallization-driven polymerizations |
| Licensed content author | Torben Gadt, Nga Sze Ieong, Graeme Cambridge, Mitchell A. Winnik and Ian Manners |
| Licensed content date | Jan 11, 2009 |
| Type of Use | reuse in a dissertation / thesis |
| Volume number | 8 |
| Issue number | 2 |
| Requestor type | academic/educational |
| Format | print and electronic |
| Portion | figures/tables/illustrations |
| Number of figures/tables/illustrations | 1 |
| High-res required | no |
| Figures | Figure 1 |
| Author of this NPG article | no |
| Your reference number | None |
| Title of your thesis / dissertation | Exploring the Chemistry of Cyclopentadienyl-Cobalt-Cyclobutadiene Containing Polymers; Synthesis, Properties, and Self-Assembly |
| Expected completion date | Apr 2015 |
| Estimated size (number of pages) | 200 |
| Total | 0.00 USD |

## 7.1.6. American Association for the Advancement of Science

Copyright Clearance Center

**Confirmation Number: 11324001**
**Order Date: 03/23/2015**

**Customer Information**

**Customer:** Mahboubeh Hadadpour

**This is not an invoice**

**Order Details**

Science

Billing Status: **N/A**

| | |
|---|---|
| **Order detail ID:** | 66523621 |
| **ISSN:** | 0036-8075 |
| **Publication Type:** | Journal |
| **Volume:** | |
| **Issue:** | |
| **Start page:** | |
| **Publisher:** | AMERICAN ASSOCIATION FOR THE ADVANCEMENT OF SCIENCE |
| **Author/Editor:** | MOSES KING, |

**Permission Status:** Granted

**Permission type:** Republish or display content
**Type of use:** Republish in a thesis/dissertation
**Order License Id:** 3595030417127

| | |
|---|---|
| **Requestor type** | Academic institution |
| **Format** | Print, Electronic |
| **Portion** | image/photo |
| **Number of images/photos requested** | 1 |
| **Title or numeric reference of the portion(s)** | Chapter 1, Figure 1.8. Possible self-assembled structures made from diblock copolymers |
| **Title of the article or chapter the portion is from** | Chapter 1. Introduction |
| **Editor of portion(s)** | N/A |
| **Author of portion(s)** | N/A |
| **Volume of serial or monograph** | N/A |
| **Page range of portion** | 10 |
| **Publication date of portion** | May 2015 |
| **Rights for** | Main product |
| **Duration of use** | Current edition and up to 5 years |
| **Creation of copies for the disabled** | no |
| **With minor editing privileges** | no |
| **For distribution to** | Canada |
| **In the following language(s)** | Original language of publication |
| **With incidental promotional use** | no |
| **Lifetime unit quantity of new product** | Up to 499 |
| **Made available in the following markets** | Education |

| | |
|---|---|
| **The requesting person/organization** | Mahboubeh Hadadpour |
| **Order reference number** | |
| **Author/Editor** | Mahboubeh Hadadpour |
| **The standard identifier** | Thesis |
| **Title** | Exploring the Chemistry of Cyclopentadienyl-Cobalt-Cyclobutadiene Containing Polymers; Synthesis, Properties, and Self-Assembly |
| **Publisher** | University of Western Ontario |
| **Expected publication date** | Apr 2015 |
| **Estimated size (pages)** | 200 |

**Note:** This item was invoiced separately through our **RightsLink service.** More info **$ 0.00**

**Total order items: 1** **Order Total: $0.00**

## Appendix 2. Supporting Information for Chapter 2

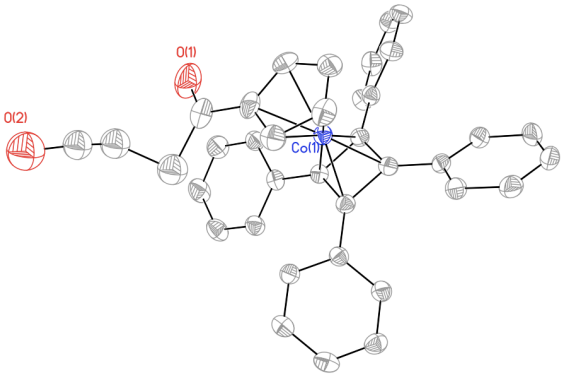


**Figure A2.1.** Solid-state structure of compound **2.2.**

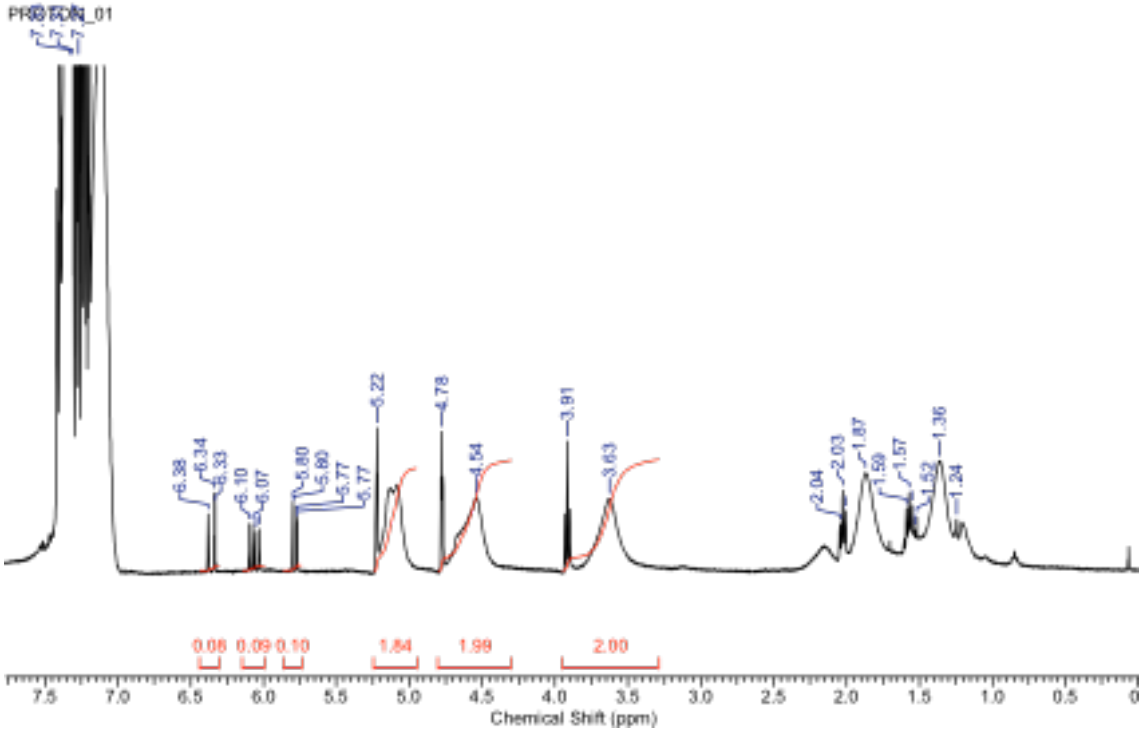


**Figure A2.2.** Crude $^{1}$H NMR spectrum of the polymer **2.5** prepared under the optimized polymerization condition (entry 15; Table 2.1).

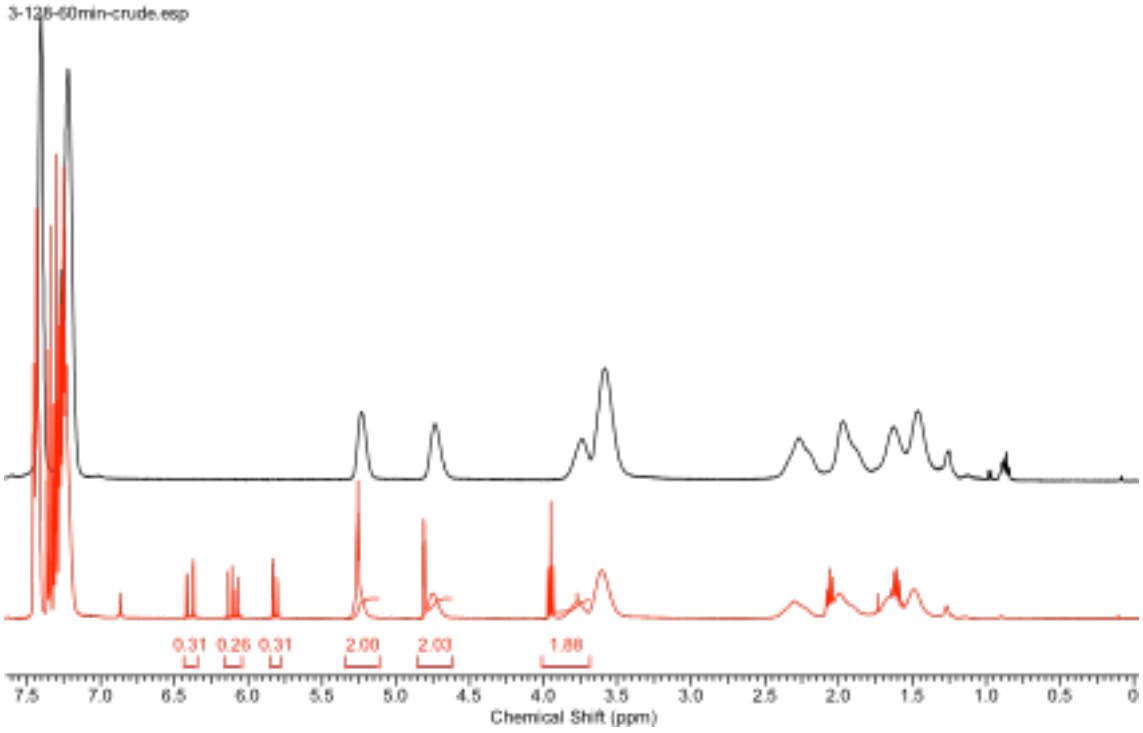


**Figure A2.3.** Crude (bottom) and purified (top) $^{1}$H NMR spectra of the polymer **2.8** (prepared under the optimized polymerization condition in presence of 3 *eq.* MA (entry 16; Table 2.1)).

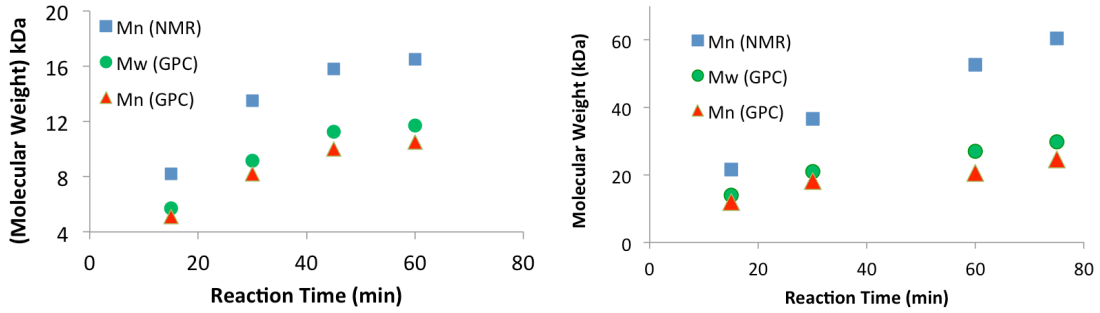


**Figure A2.4.** Expected molecular weight ($M_n$) estimated by $^{1}$H NMR spectroscopy (square) and obtained $M_n$ (triangle) and $M_w$ (circle) by GPC analysis for preparation of random copolymer **2.8** at different reaction times for target DP of 30 (top) and 120 (bottom).

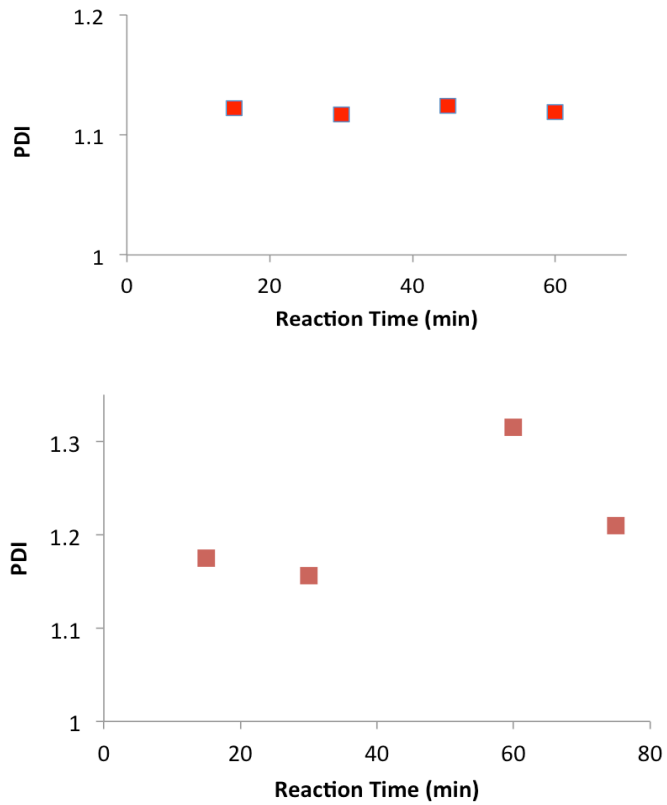


**Figure A2.5.** PDI of random copolymer **2.8** at different reaction times for target DP = 30 (top) and 120 (bottom).

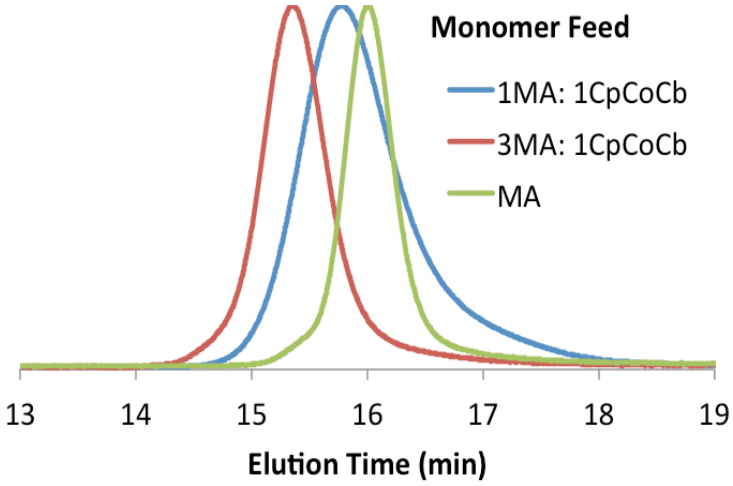


**Figure A2.6.** RI traces of random copolymer **2.8** if using 1 equivalent MA in reaction feed compared to 3 equivalent MA and RA trace of polymer in absent of monomer **2.3** (PMA only).

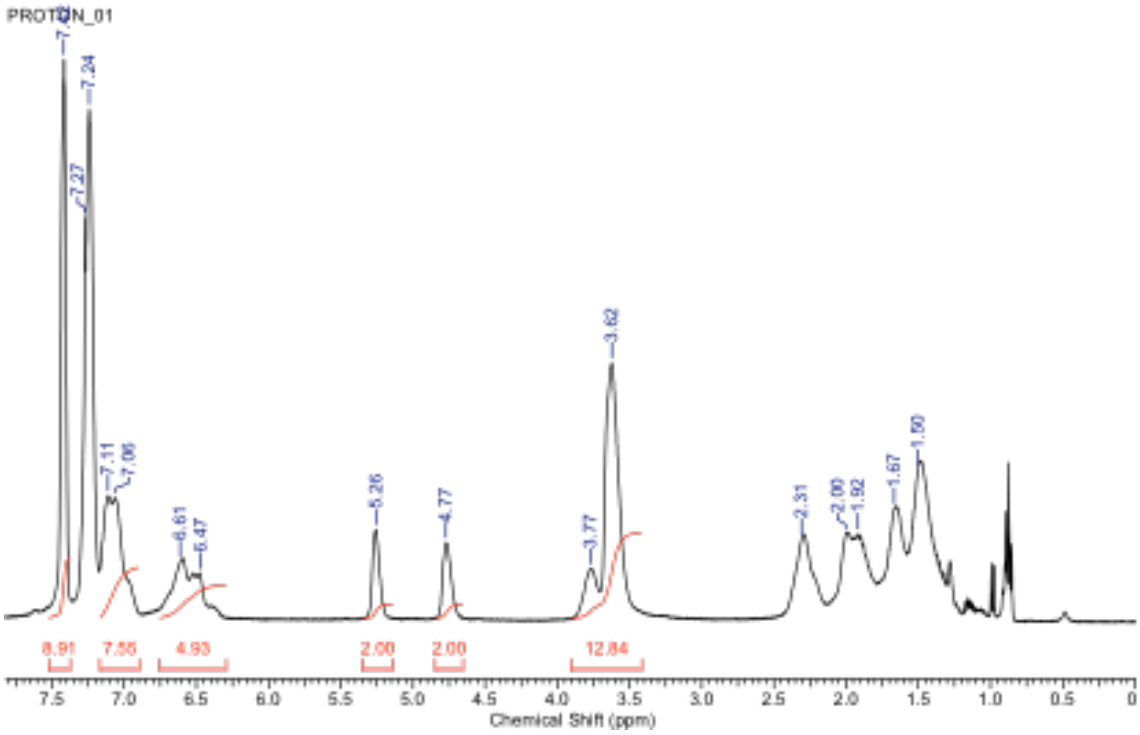


**Figure A2.7.** $^{1}$H NMR spectrum of purified block copolymer **2.9**.

## Appendix 3. Supporting Information for Chapter 3

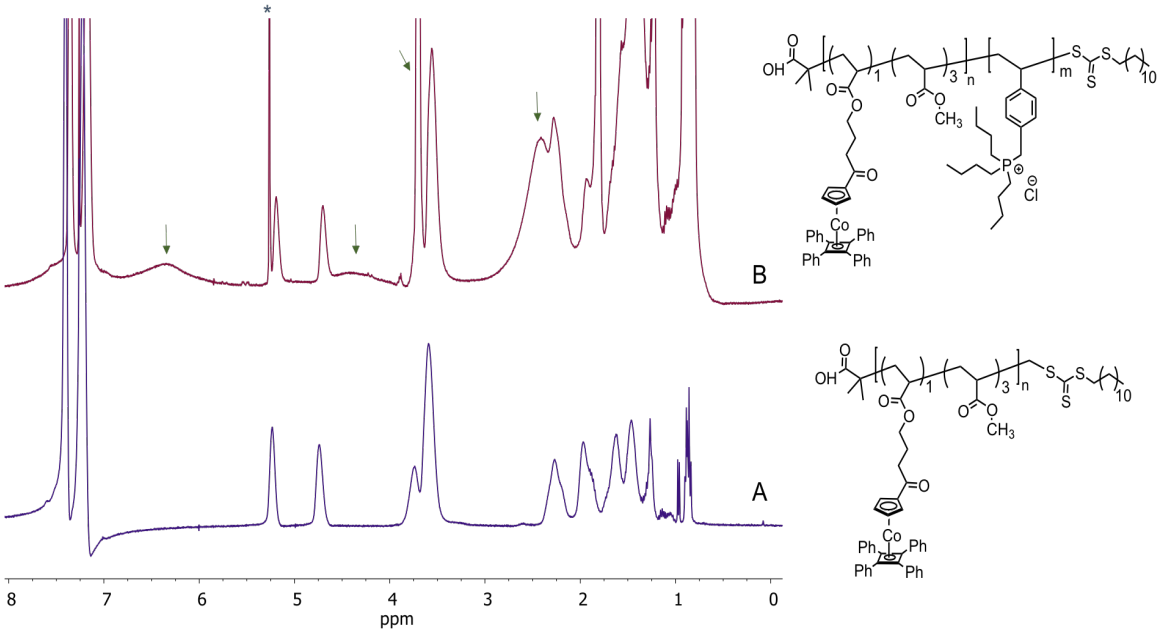


**Figure A3.1.** $^{1}$H NMR Spectrum of random copolymer **2.8** (macro-RAFT agent) (spectrum A) and block copolymer when utilizing **2.8** to polymerize monomer **3.5** (spectrum B) in deutrated chloroform. In Spectrum B, arrows point to the broad/overlapping signals of polyelectrolyte block. (*trace of dichloromethane).

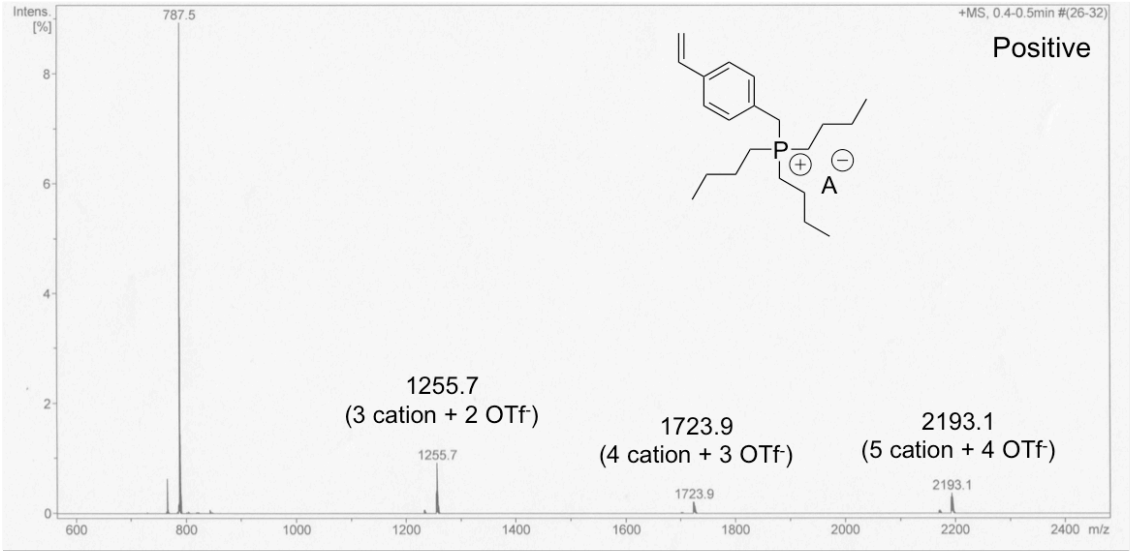


Note: Clusters with Cl such as 637 (2 cation + 1 $Cl^-$), 1027 (3 cation + 2 $Cl^-$) were not detected.

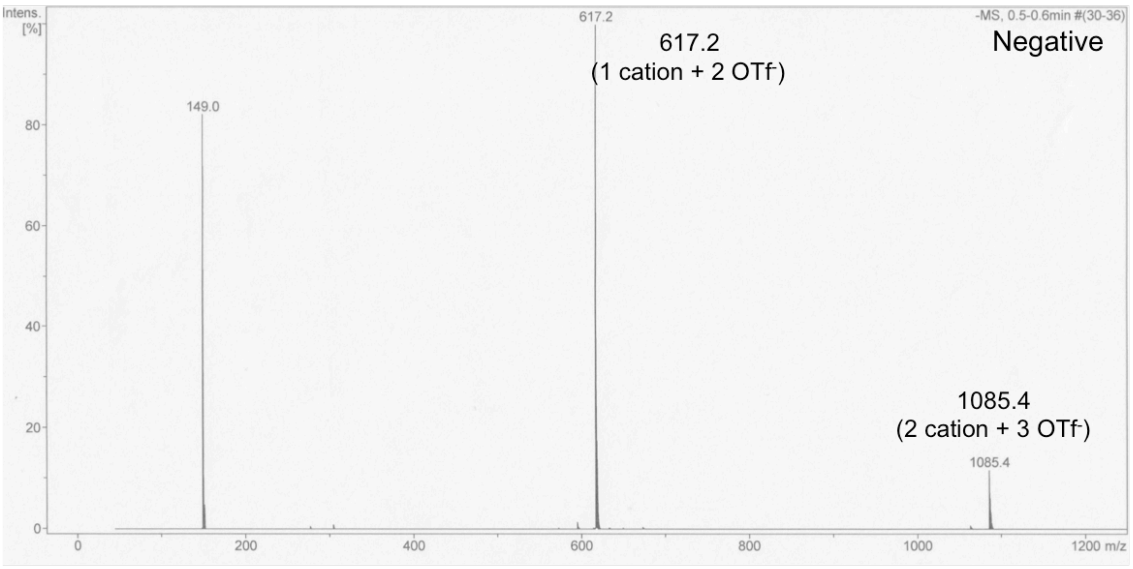


Note: Clusters with Cl such as 743 (2 cation + 3 $Cl^-$), 1099 (3 cation + 4 $Cl^-$) were not detected.

**Figure A3.2.** Positive and negative mass spectroscopy of purified **3.6**.

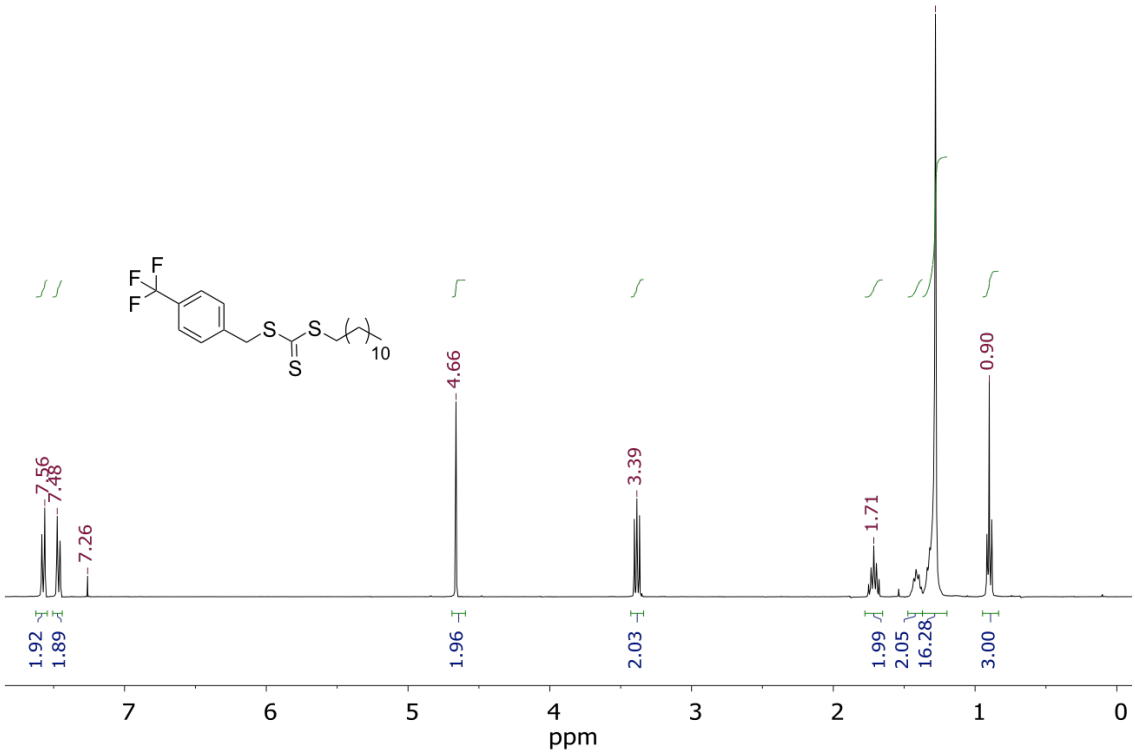


**Figure A3.3.** [1]H NMR Spectrum of purified RAFT agent **3.7** in deutrated chloroform.

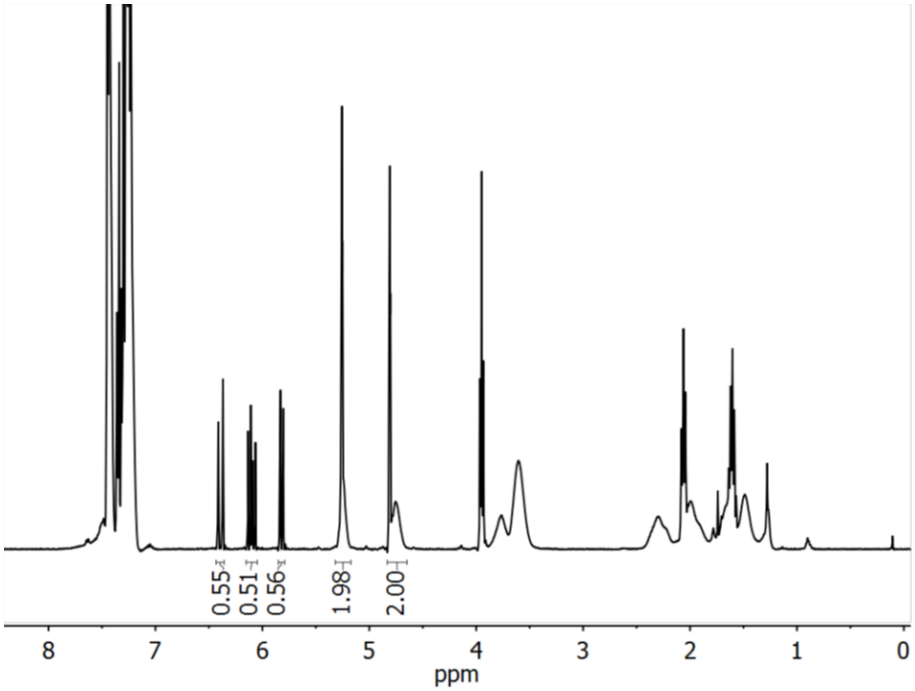


**Figure A3.4.** [1]H NMR spectrum of crude random copolymer **3.8** at 20 minutes polymerization reaction time in deutrated chloroform. (Relative integrations values indicate 47% monomer conversion).

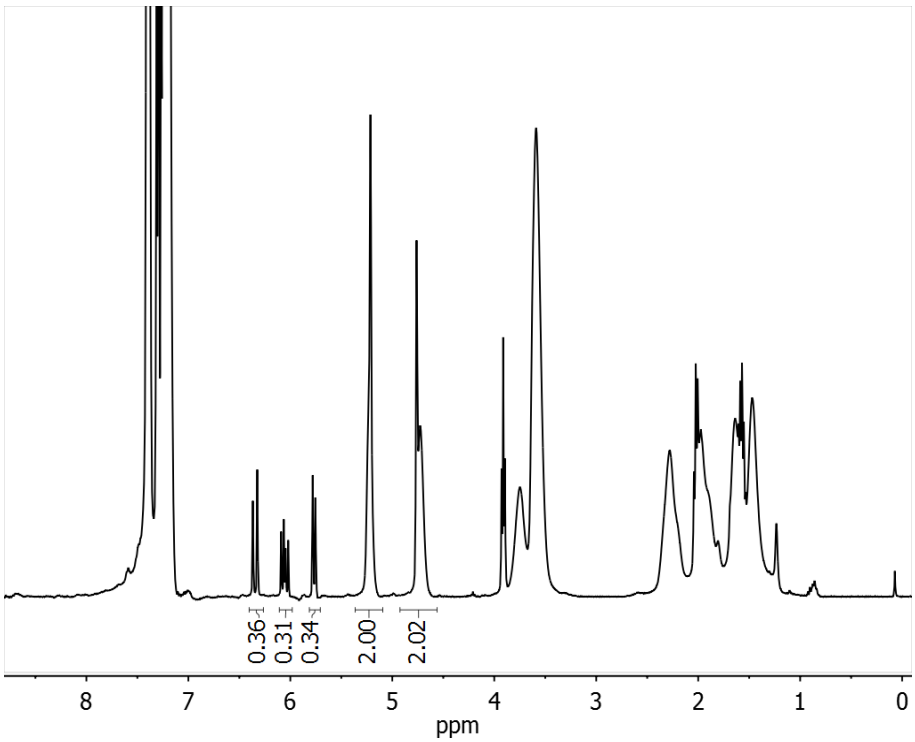


**Figure A3.5.** $^{1}$H NMR spectrum of crude random copolymer **3.8** at 40 minutes polymerization reaction time in deutrated chloroform. (Relative integrations values indicate 77% monomer conversion).

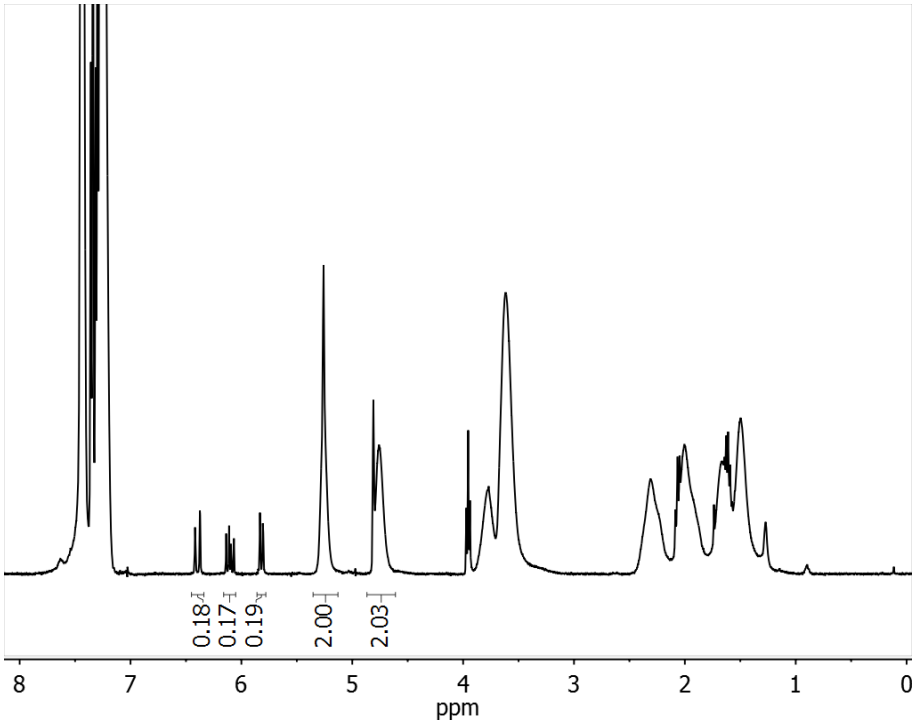


**Figure A3.6.** $^{1}$H NMR spectrum of crude random copolymer **3.8** at 60 minutes polymerization reaction time in deutrated chloroform. (Relative integrations values indicate 82% monomer conversion).

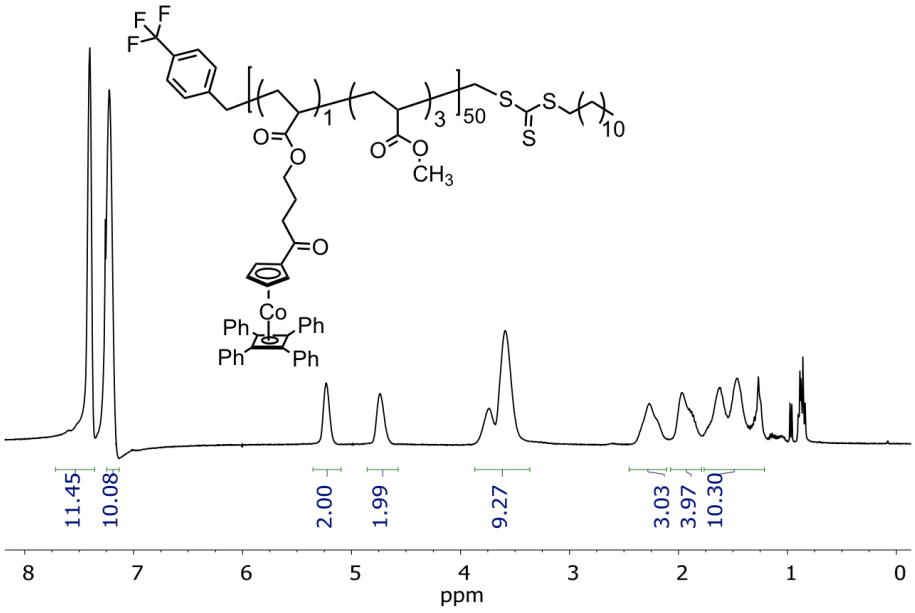


**Figure A3.7.** $^{1}$H NMR spectrum of purified random copolymer **3.8** at 60 minutes polymerization reaction time.

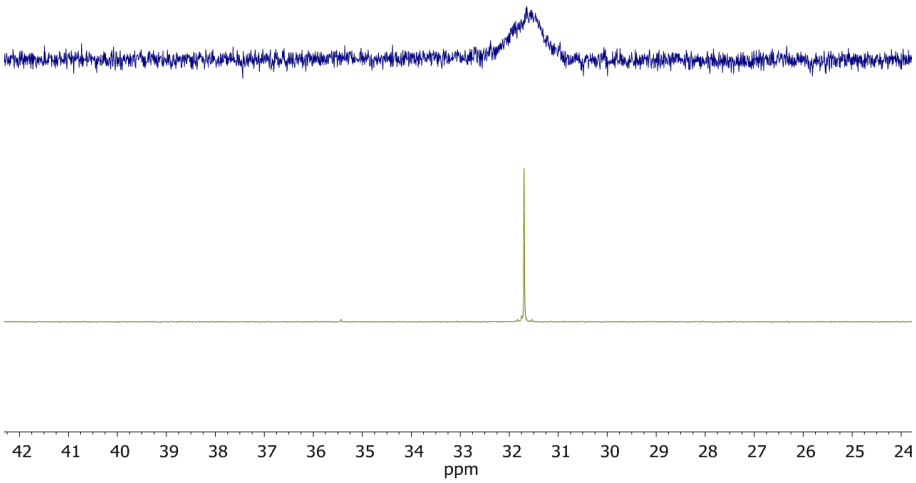


**Figure A3.8.** $^{31}$P{$^{1}$H} NMR Spectra of crude (bottom) and purified (top) **3.9**.

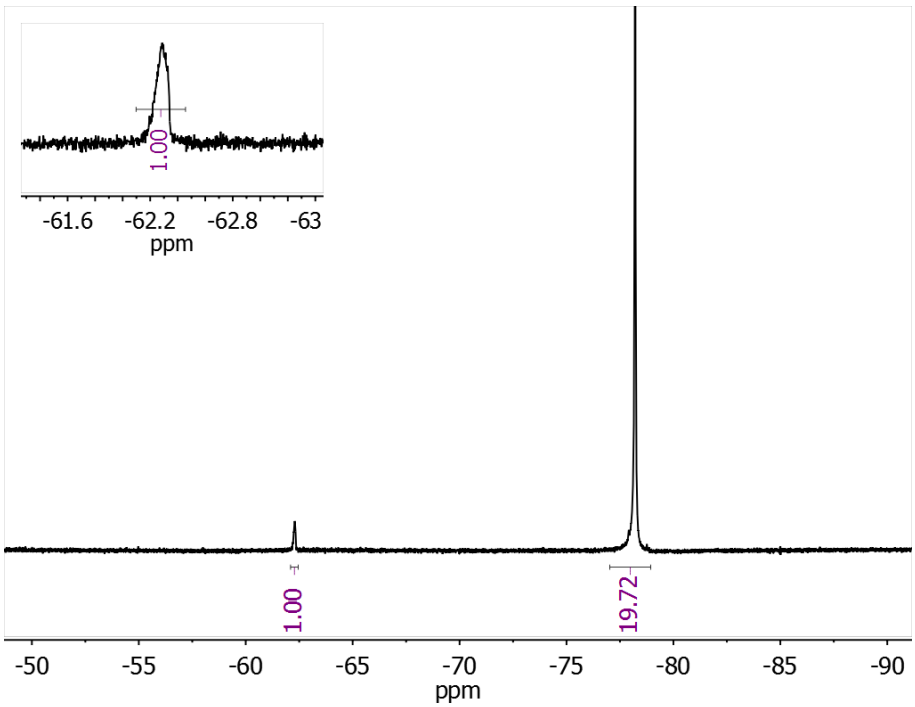


**Figure A3.9.** $^{19}F\{^{1}H\}$ NMR Spectrum of purified (PolyCpCoCb$_{50}$-*r*-PMA$_{150}$)-*b*-(PS(P$^{+}$OTf$^{-}$)$_{20}$) (**3.9**) after 15 minutes polymerization reaction time in deutrated chloroform.

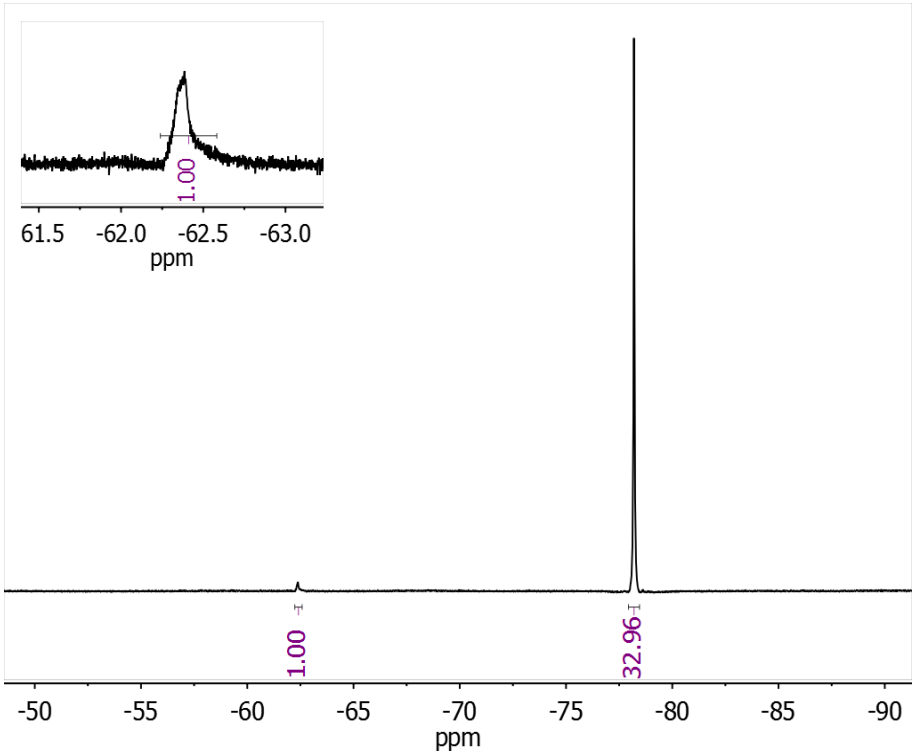


**Figure A3.10.** $^{19}F\{^{1}H\}$ NMR Spectrum of purified (PolyCpCoCb$_{50}$-*r*-PMA$_{150}$)-*b*-(PS(P$^{+}$OTf$^{-}$)$_{33}$) (**3.9**) after 30 minutes polymerization reaction time in deutrated chloroform.

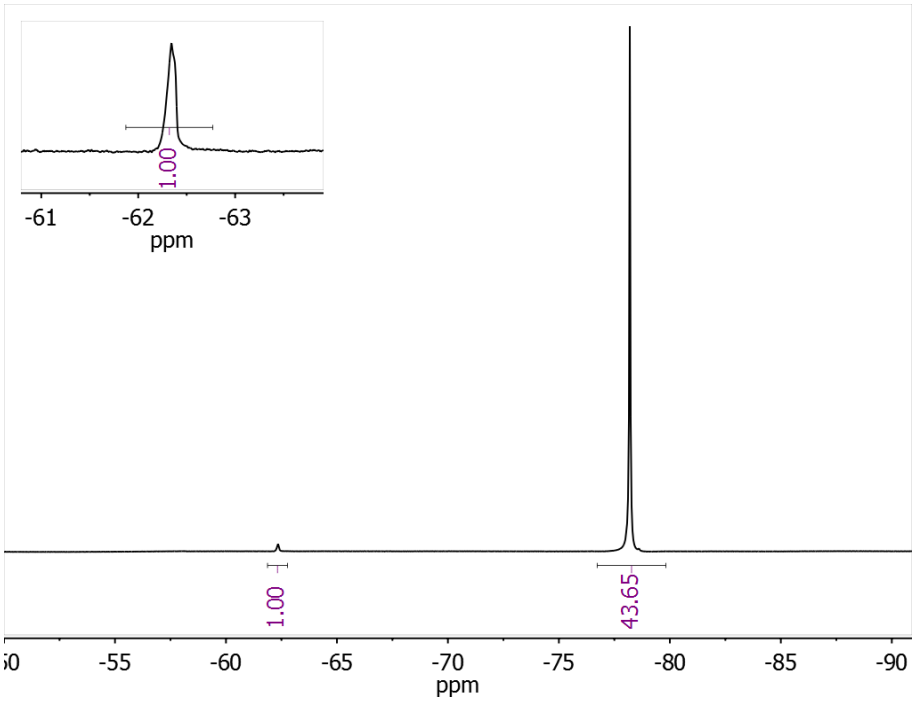


**Figure A3.11.** $^{19}F\{^{1}H\}$ NMR Spectrum of purified (PolyCpCoCb$_{50}$-*r*-PMA$_{150}$)-*b*-(PS(P$^{+}$OTf$^{-}$)$_{44}$) (**3.9**) after 45 minutes polymerization reaction time in deutrated chloroform.

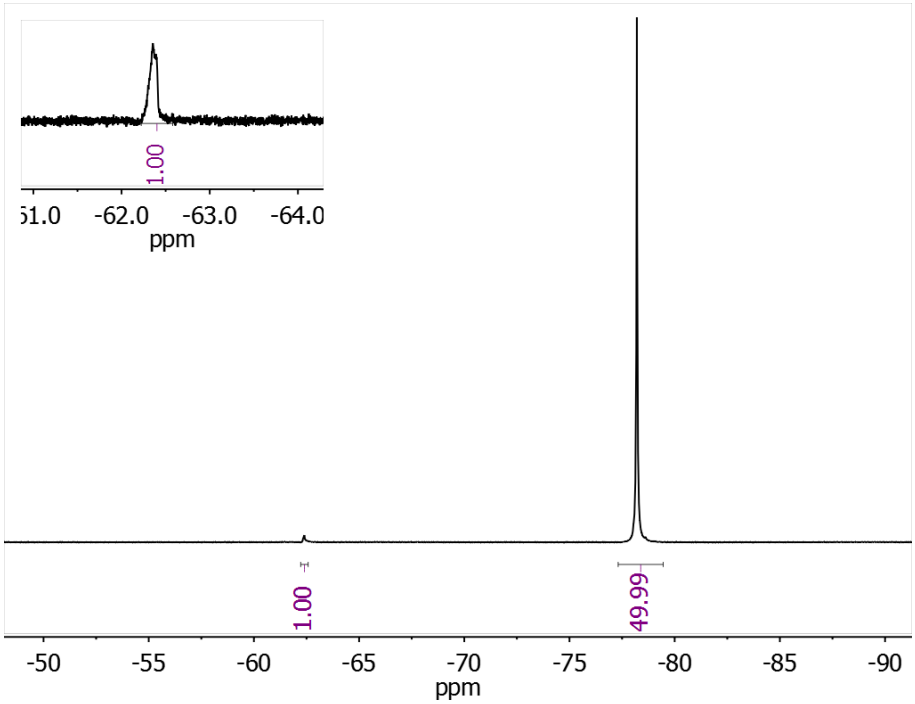


**Figure A3.12.** $^{19}F\{^{1}H\}$ NMR Spectrum of purified (PolyCpCoCb$_{50}$-*r*-PMA$_{150}$)-*b*-(PS(P$^{+}$OTf$^{-}$)$_{50}$) (**3.9**) after 60 minutes polymerization reaction time in deutrated chloroform.

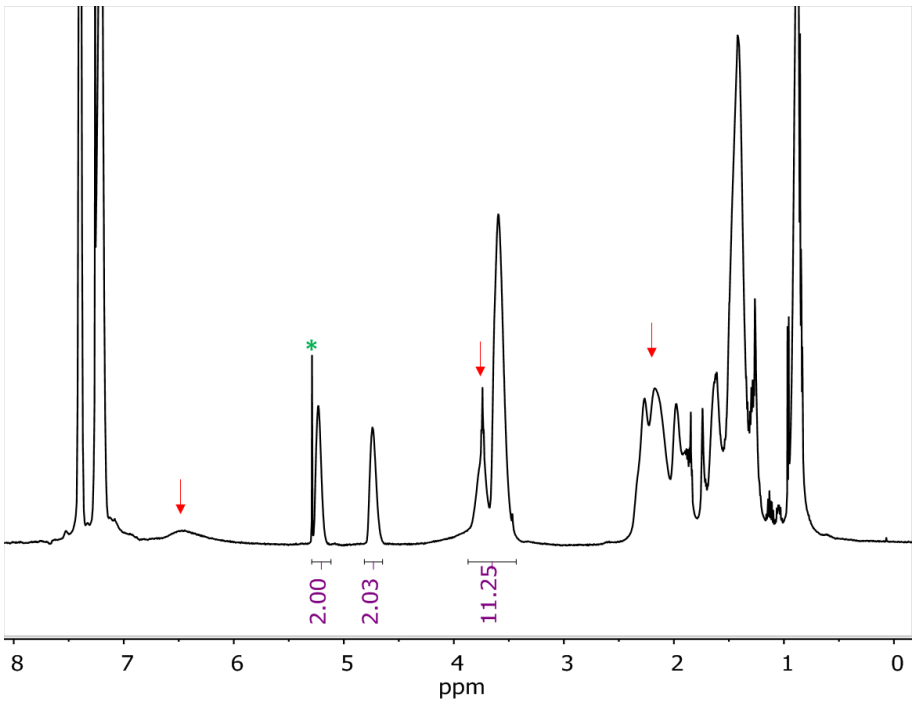


**Figure A3.13.** $^{1}$H NMR spectrum of purified block copolymer **3.9** after 60 minutes polymerization reaction time. Arrows show broad signals of polyelectrolyte block in deutrated chloroform. (*DCM residue).

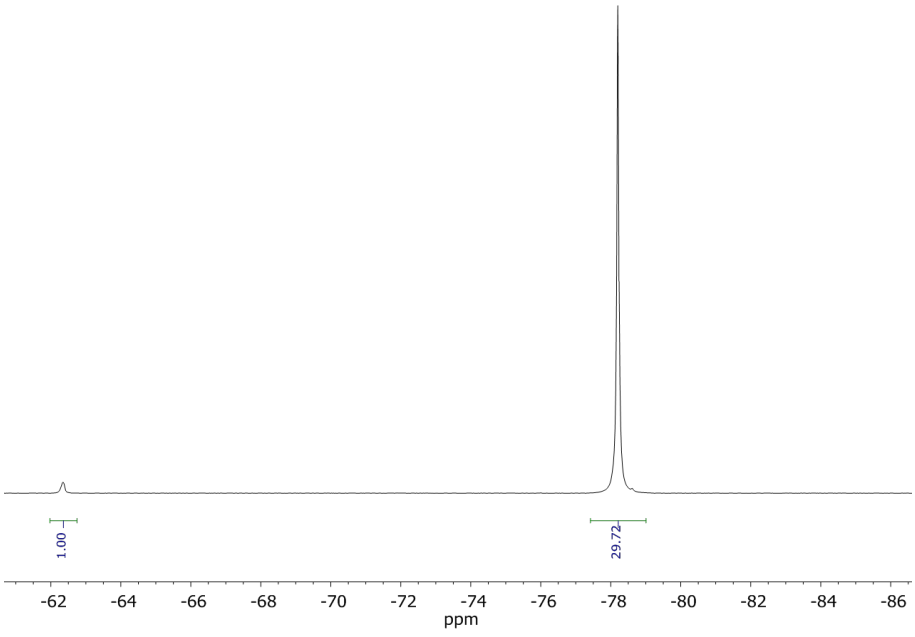


**Figure A3.14.** $^{19}$F{$^{1}$H} NMR Spectrum of purified (PolyCpCoCb$_{50}$-*r*-PMA$_{150}$)-*b*-(PS(P$^{+}$OTf$^{-}$)$_{30}$) (**3.9**).

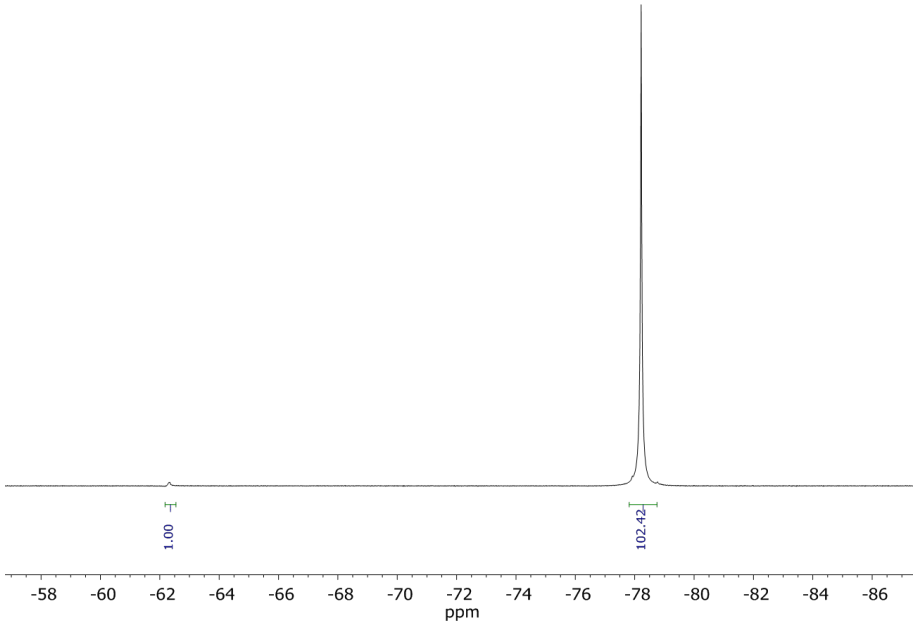


**Figure A3.15.** $^{19}F\{^{1}H\}$ NMR Spectrum of purified (PolyCpCoCb$_{50}$-*r*-PMA$_{150}$)-*b*-(PS(P$^{+}$OTf$^{-}$)$_{100}$) (**3.9**).

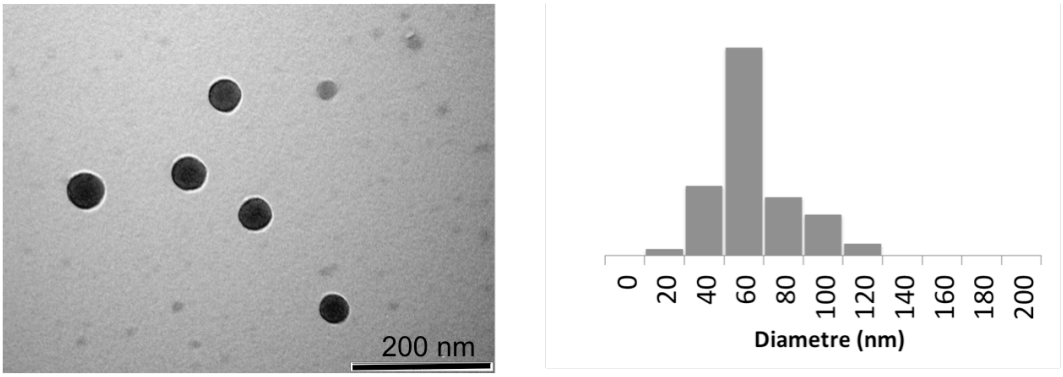


**Figure A3.16.** TEM Image of spherical micelles made by injection of THF solution of (PolyCpCoCb$_{50}$-r-PMA$_{150}$)-b-(PS(P$^{+}$OTf$^{-}$)$_{100}$) (**3.9**) into methanol and size distribution analysis based on TEM data.

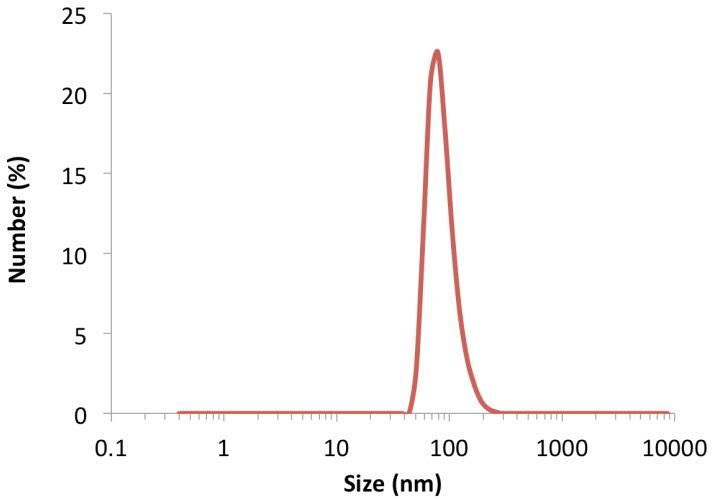


**Figure A3.17.** DLS analysis of spherical micelles made by injection of THF solution of (PolyCpCoCb$_{50}$-*r*-PMA$_{150}$)-*b*-(PS(P$^{+}$OTf$^{-}$)$_{100}$) (**3.9**) into methanol (130 nm).

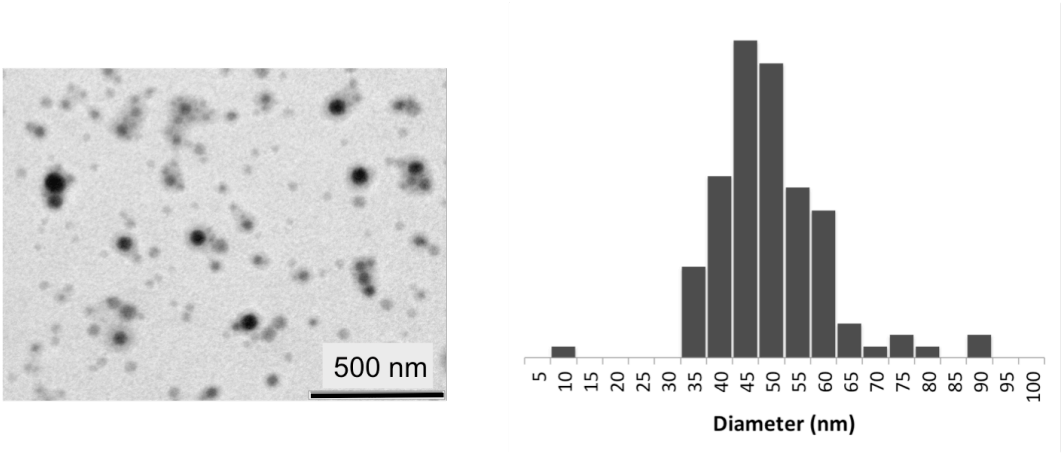


**Figure A3.18.** TEM Image of heterobimetallic micelles made by injection of DCM solution of (PolyCpCoCb$_{50}$-*r*-PMA$_{150}$)-*b*-(PS(P$^{+}$AuCl$^{-}$)$_{100}$) (**3.10**) into benzene and size distribution analysis based on TEM data.

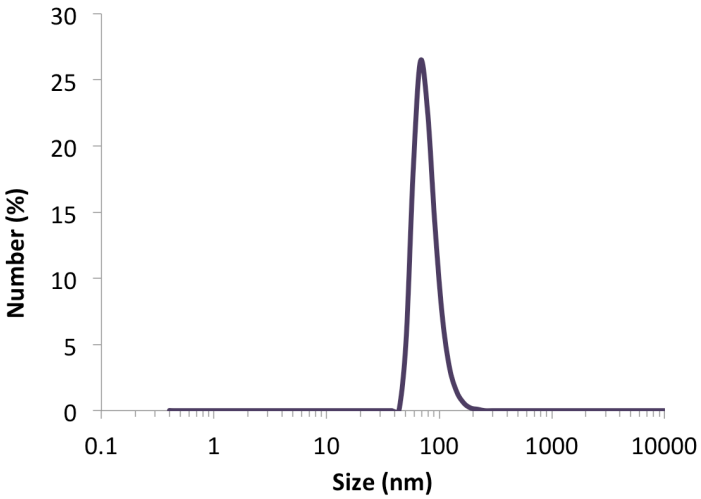


**Figure A3.19.** DLS analysis of heterobimetallic micelles made by injection of DCM solution of (PolyCpCoCb$_{50}$-*r*-PMA$_{150}$)-*b*-(PS(P$^{+}$AuCl$^{-}$)$_{100}$) (**3.10**) into benzene (65 nm).

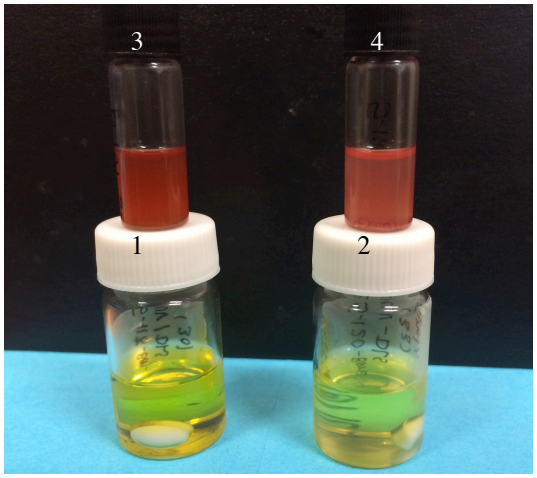


**Figure A3.20.** Heterobimetallic micelles with PS(P$^{+}$AuCl$^{-}$) core and PolyCpCoCb$_{50}$-*r*-PMA$_{150}$ corona made by injection of DCM solution of (PolyCpCoCb$_{50}$-*r*-PMA$_{150}$)-*b*-(PS(P$^{+}$AuCl$^{-}$)$_{m}$) (1; m =30, 2; m =100) into benzene. Vials on top are the same micelles samples after the core is reduced to AuNPs using NaBH$_4$ (3; m =30, 4; m =100).

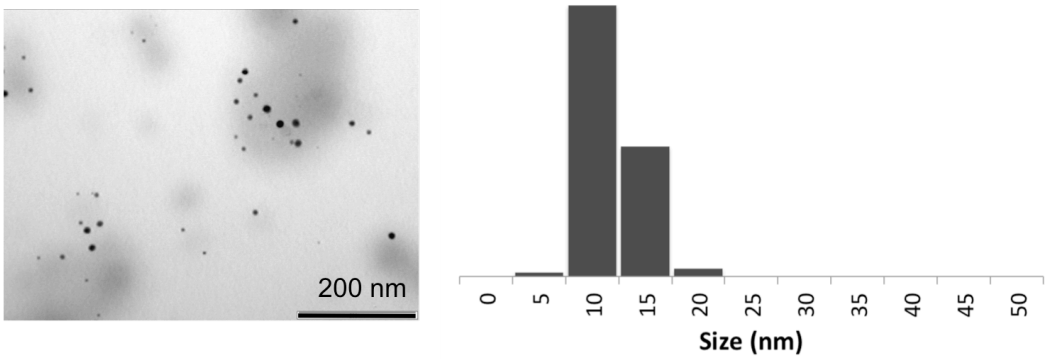


**Figure A3.21.** TEM Image of AuNPs made by reduction of heterobimetallic micelles made [(PolyCpCoCb$_{50}$-*r*-PMA$_{150}$)-*b*-( PS(P$^{+}$AuCl$^{-}$)$_{m}$)] (**3.10**) and size distribution analysis based on TEM data.

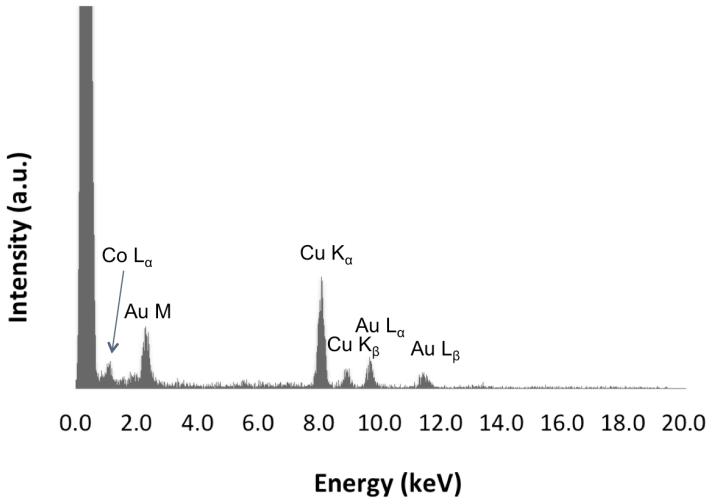


**Figure A3.22.** EDX analysis of AuNPs (copper signals are form the copper grid).

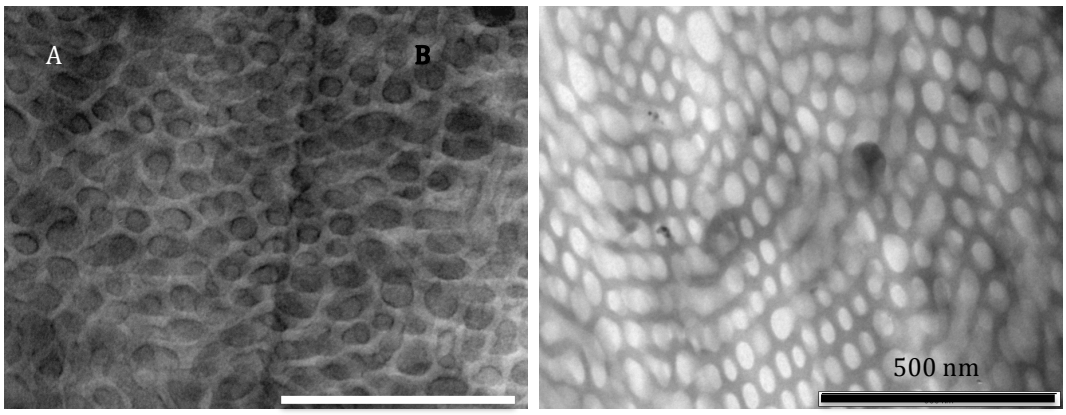


**Figure A3.23.** (A) TEM image of microtomed section of phase-separated (PolyCpCoCb$_{50}$-*r*-PMA$_{150}$)-*b*-(PS(P$^{+}$OTf$^{-}$)$_{30}$) (**3.9**) stained with $RuO_4$ (B) and stained with $HAuCl_4$.

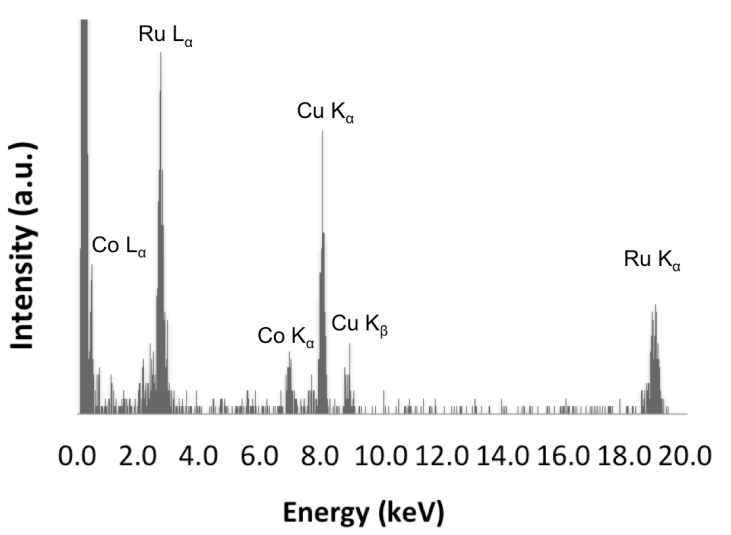


**Figure A3.24.** EDX analysis of microtomed sections of (PolyCpCoCb$_{50}$-*r*-PMA$_{150}$)-*b*-(PS(P$^{+}$OTf$^{-}$)$_{30}$) (**3.9**) stained by $RuO_4$ revealing its elemental composition.

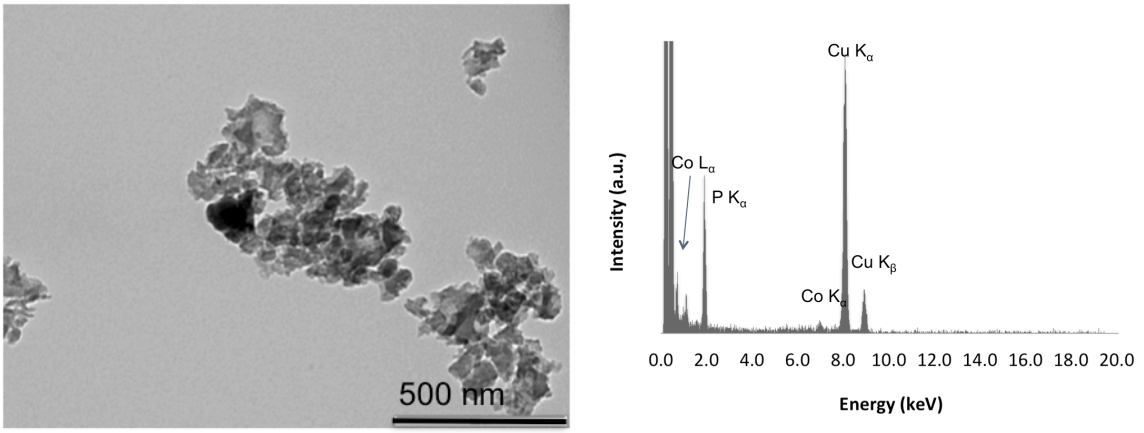


**Figure A3.25.** TEM image (left) and EDX analysis (right) of pyrolyzed (PolyCpCoCb$_{50}$-*r*-PMA$_{150}$)-*b*-(PS(P$^{+}$OTf$^{-}$)$_{30}$) (**3.9**) block copolymer.

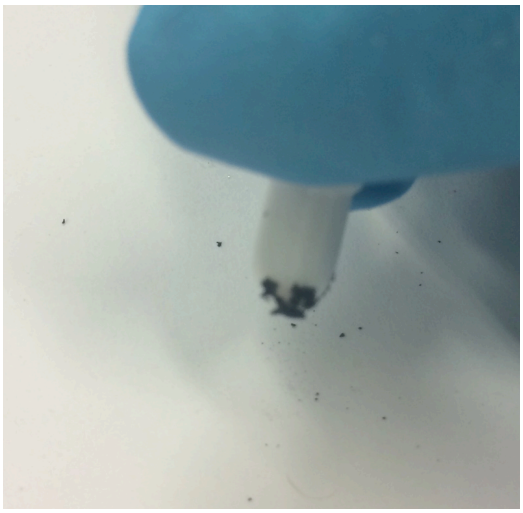

**Figure A3.26.** The pyrolyzed materials were attracted to permanent magnet, indicating the presence of magnetic particles.

## Appendix 4. Supporting Information for Chapter 4

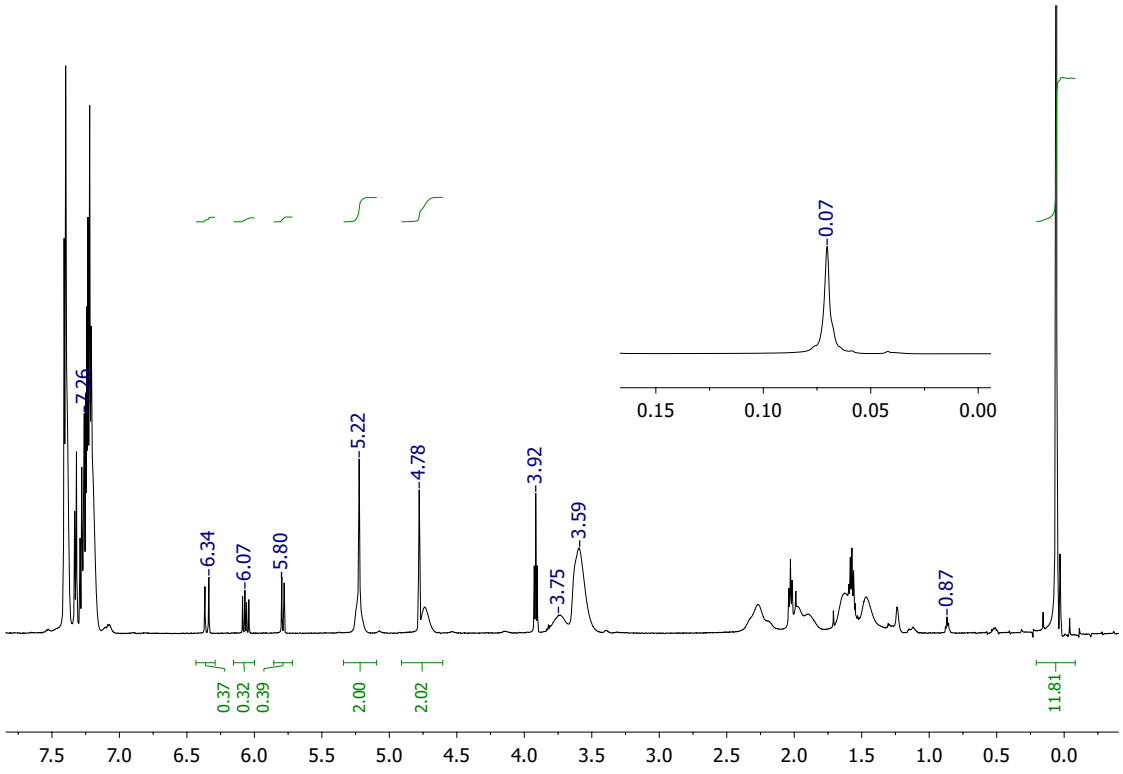


Figure A4.1. $^{1}$H NMR Spectrum of crude $PDMS_{5k}$-*b*-(PolyCpCoCb-*r*-PMA)$_{18k}$.

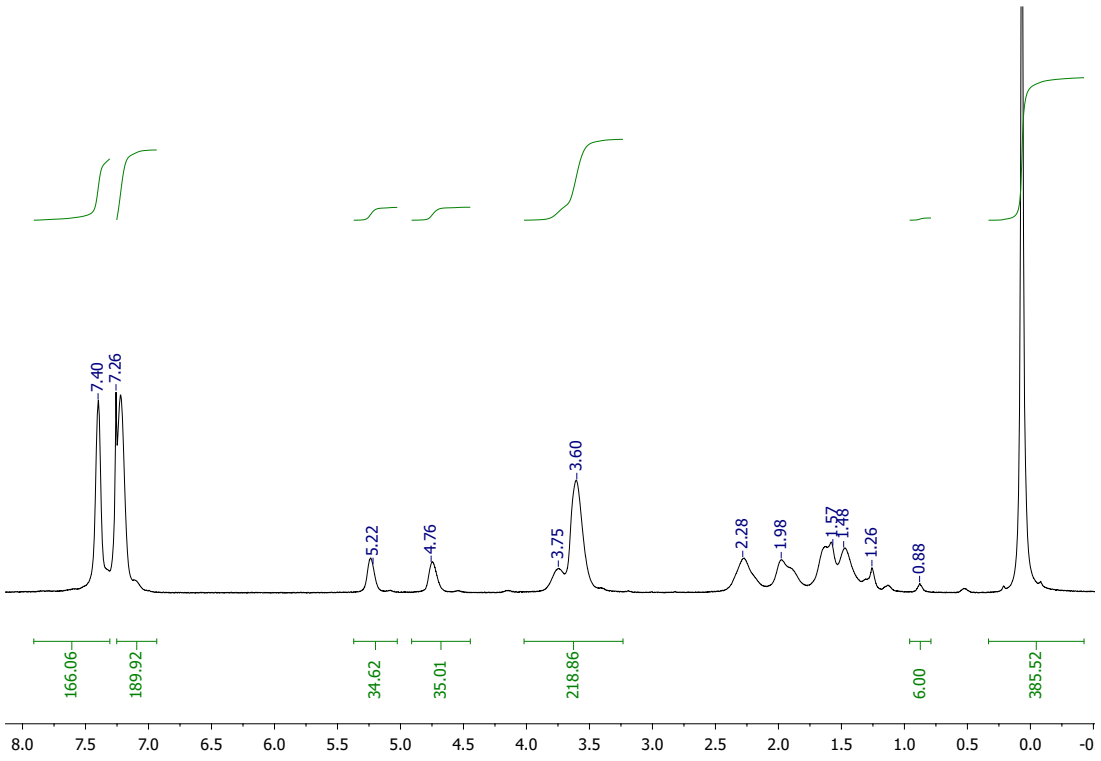


**Figure A4.2.** $^{1}$H NMR Spectrum of purified $PDMS_{5k}$-*b*-(PolyCpCoCb-*r*-PMA)$_{18k}$.

**Figure A4.3**. Pyrolyzed block copolymer gets attracted to permanent magnets.

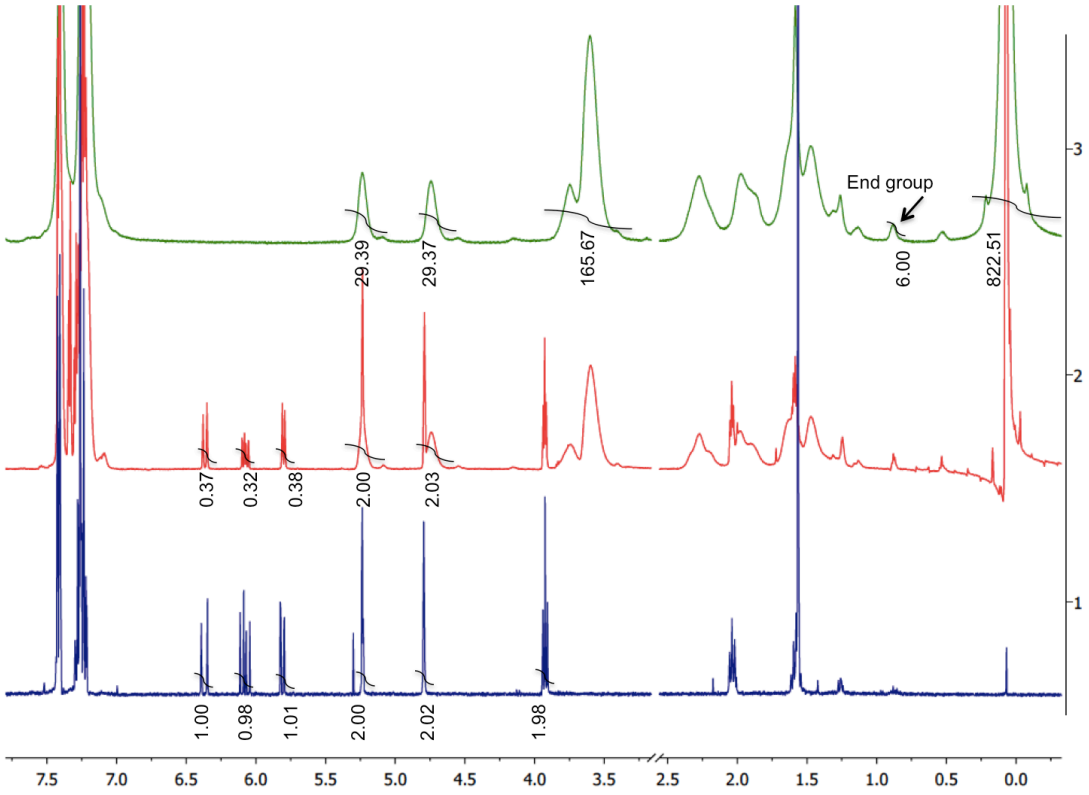


**Figure A4.4.** Stack plot of $^{1}$H NMR Spectra of 1; CpCoCb monomer (**2.3**), 2; crude $PDMS_{10k}$-*b*-$(PolyCpCoCb\text{-}r\text{-}PMA)_{18k.}$, 3; purified $PDMS_{10k}$-*b*-$(PolyCpCoCb\text{-}r\text{-}PMA)_{18k}$ (**4.2**).

## Appendix 5. Supporting Information for Chapter 5

Attempts towards polymerization of monomer **5.6**:

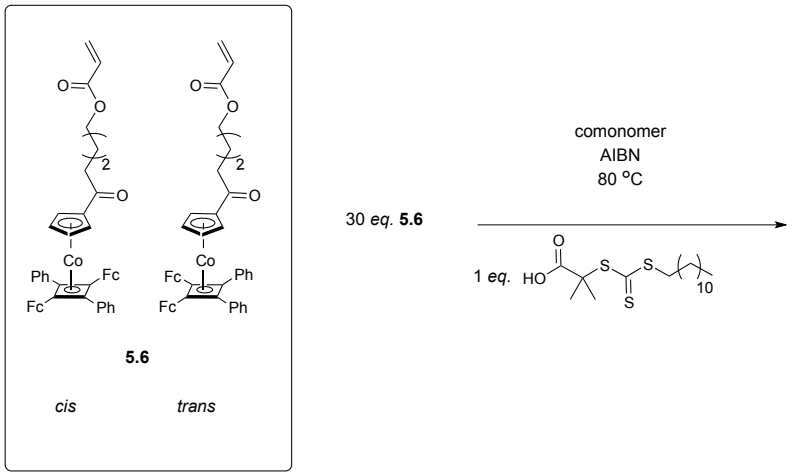


| entry | Monomer | co-monomer | *eq*.[a] | conversion[b] (%) | $M_n$ (kDa)[c] | $M_n$ (kDa)[d] | PDI |
|---|---|---|---|---|---|---|---|
| 1 | **5.6** | MA | 4 | 50 | 12.5 | 3.4 | 1.29 |
| 2 | **5.6** | Sty | 4 | 50 | 12.5 | 6.3 | 1.28 |
| 3 | **5.6** | Sty | 8 | 60 | 15 | 8.4 | 1.35 |
| 4 | **5.6** (*cis*) | MA | 4 | 70 | 17.5 | 5.8 | 1.41 |
| 5 | **5.6** (*cis*) | MA | 6 | 70 | 17.5 | 6.9 | 1.49 |
| 6 | **5.6** (*cis*) | MA | 9 | 40 | 10 | 8.9 | 1.52 |
| 7 | **5.6** (*trans*) | MA | 9 | 50 | 12.5 | 10.9 | 1.54 |

a. stoichiometric equivalent of co-monomer, b. based on $^1$H NMR spectra of monomer **5.6**, c. based on monomer conversion, d. based on GPC analysis relative to PS standards.

$^1$H NMR spectra (crude) and GPC analysis (purified) of the above attempts are as follow:

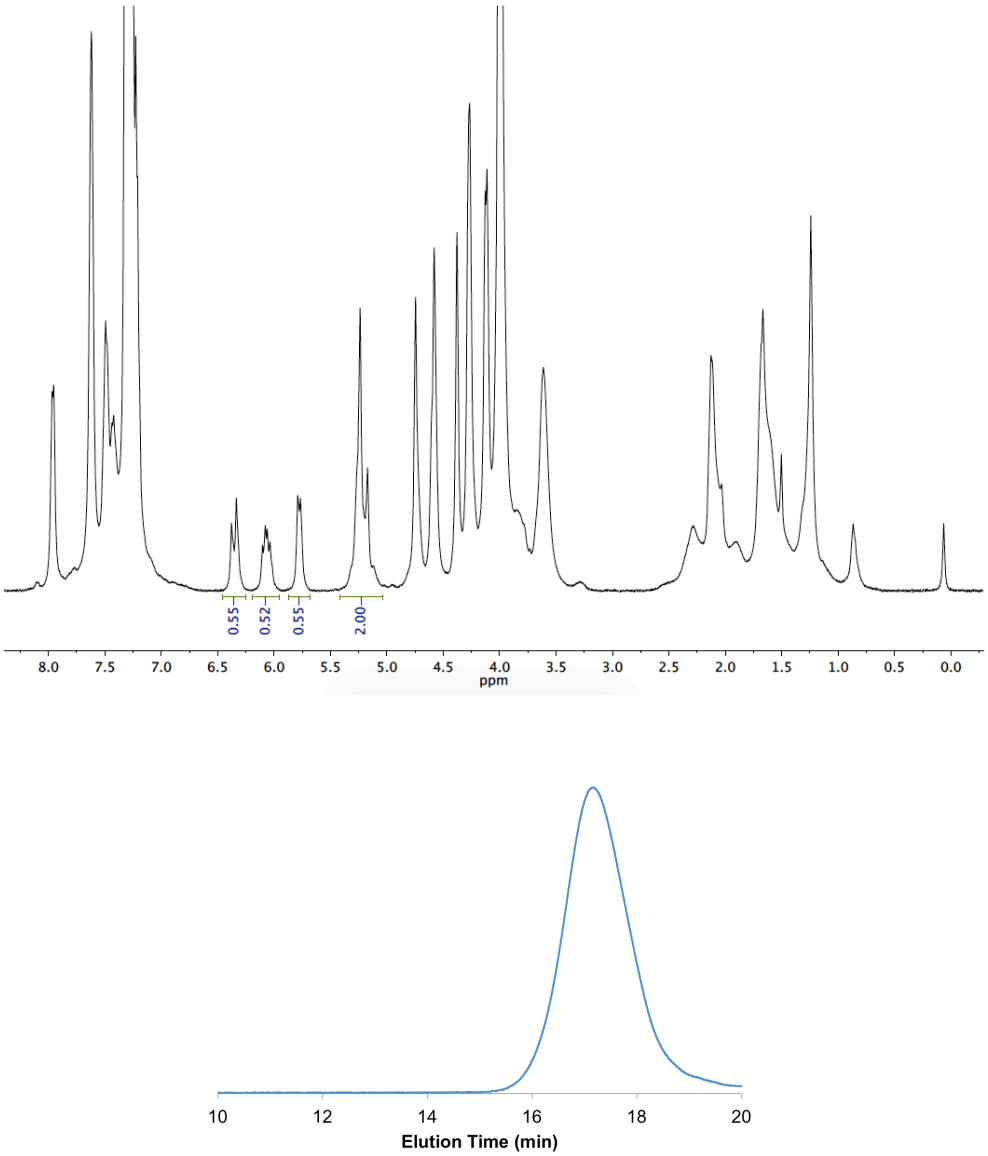


**Figure A5.1.** $^{1}$H NMR spectrum and GPC analysis of entry 1.

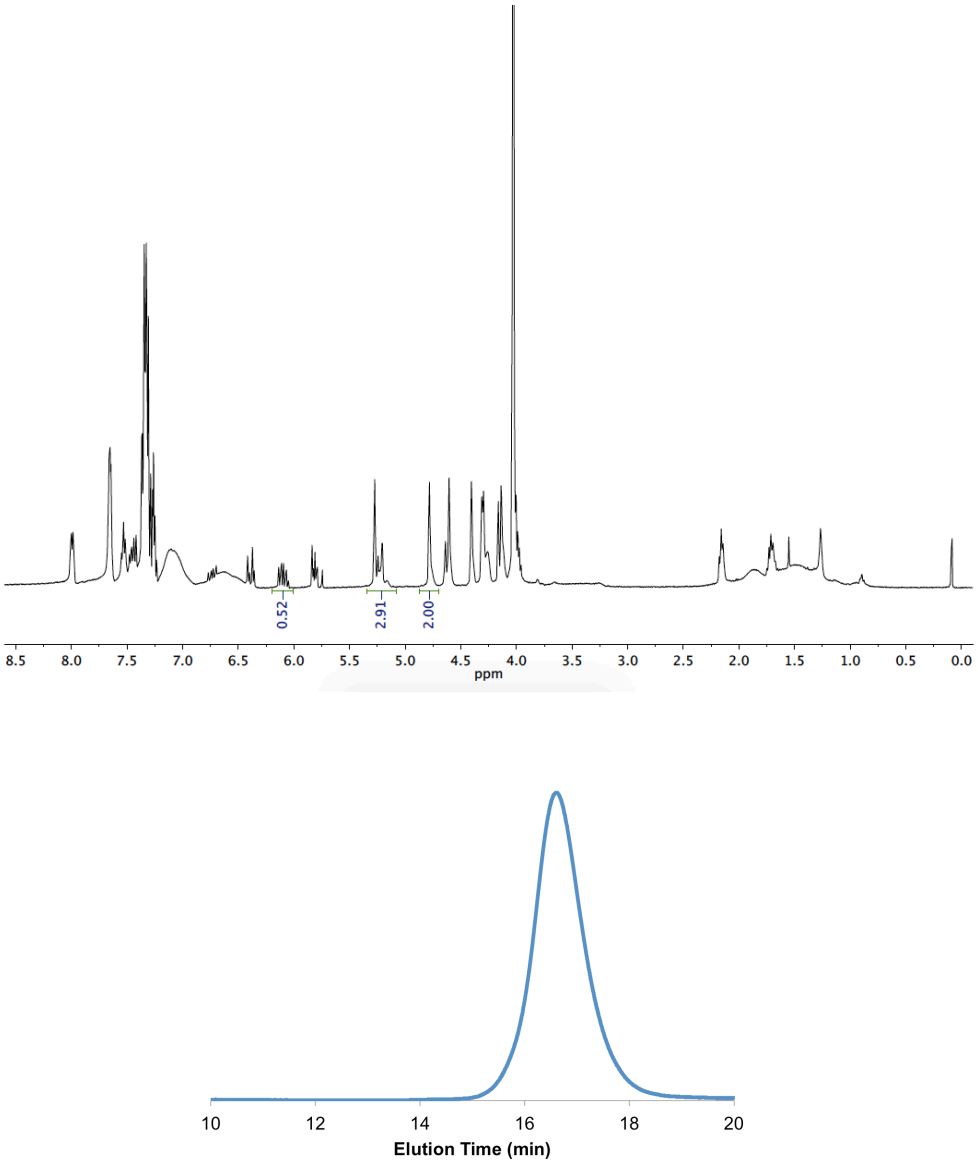


**Figure A5. 2.** $^{1}$H NMR spectrum and GPC analysis of entry 2.

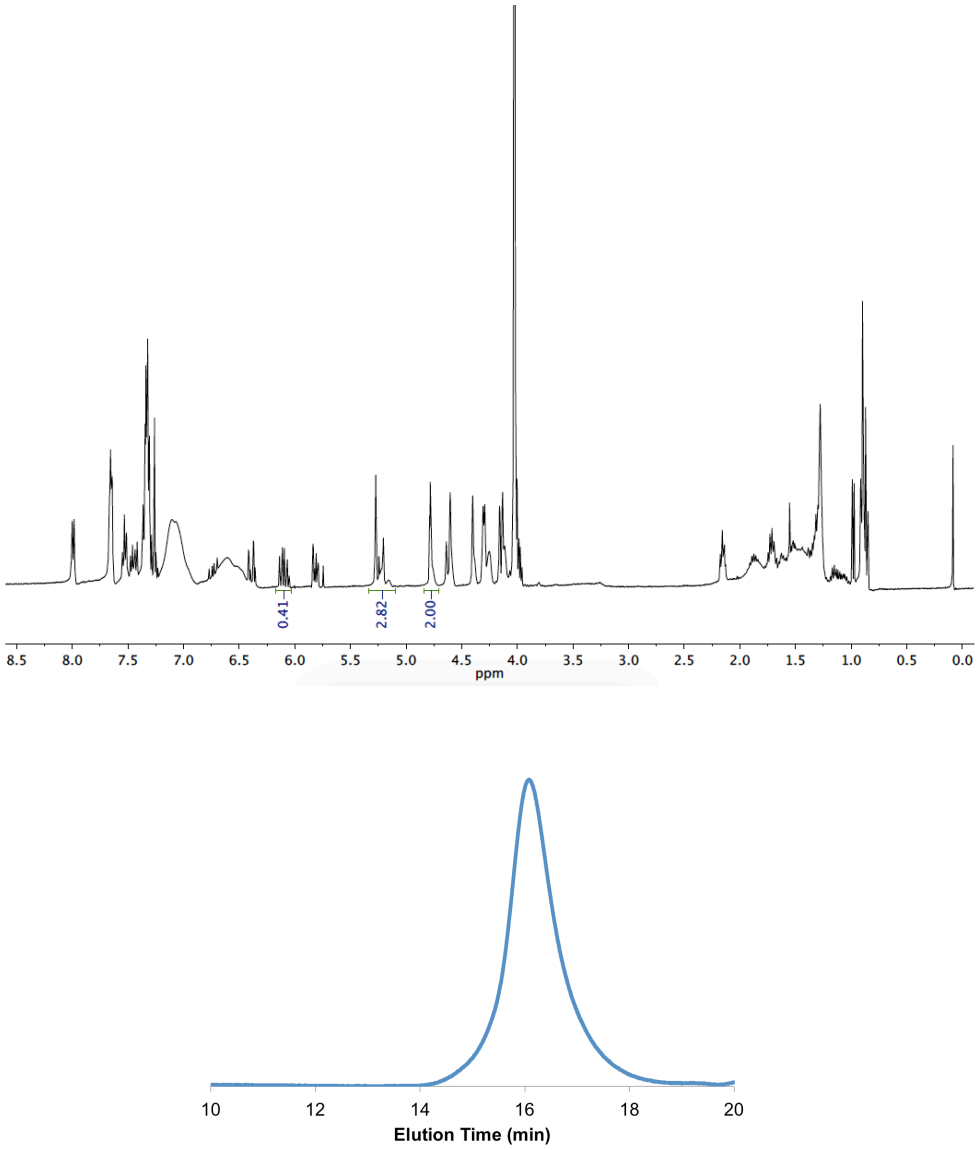


**Figure A5. 3.** $^{1}$H NMR spectrum and GPC analysis of entry 3.

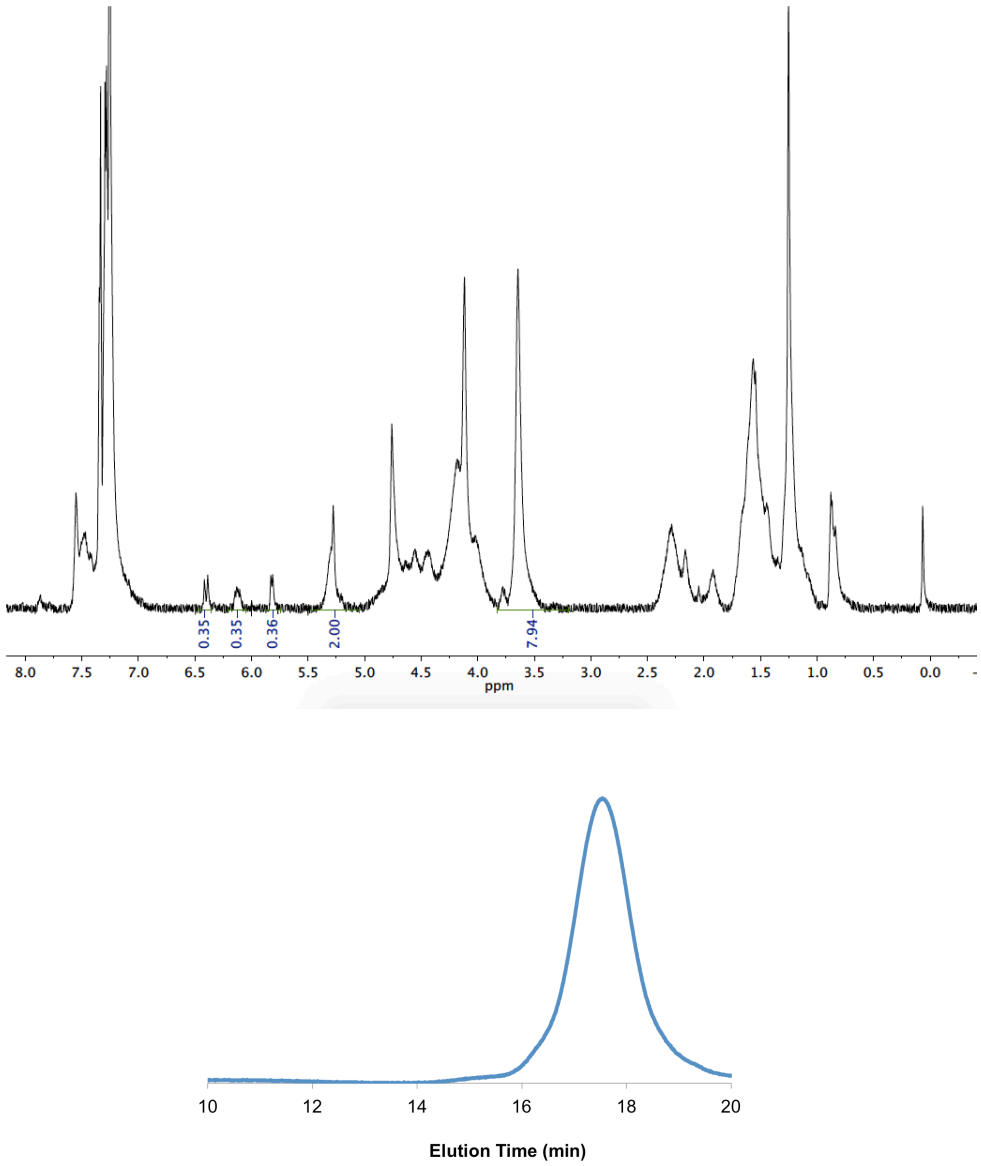


**Figure A5. 4.** $^{1}$H NMR spectrum and GPC analysis of entry 4.

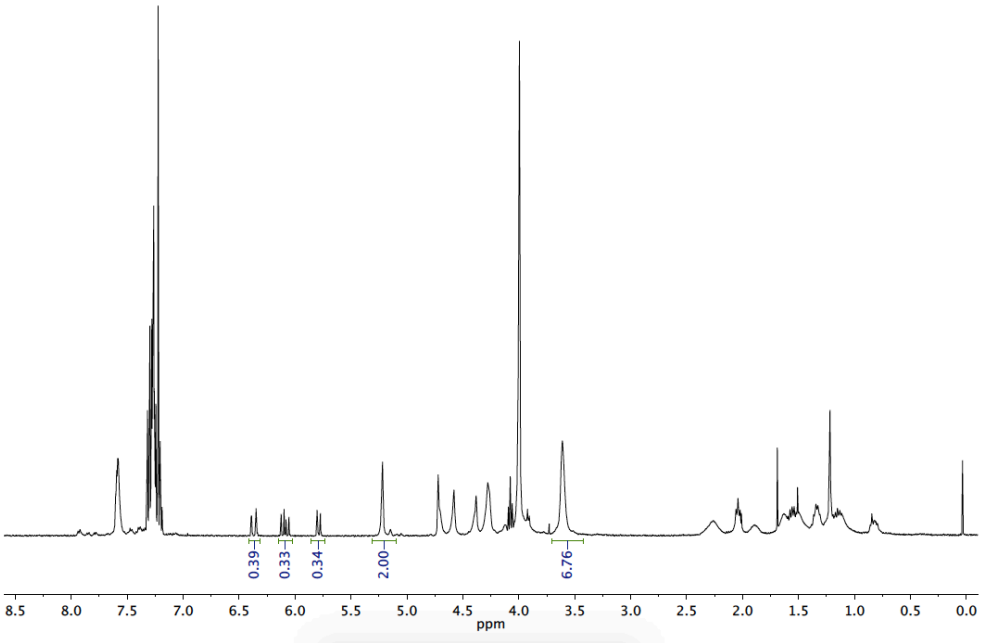


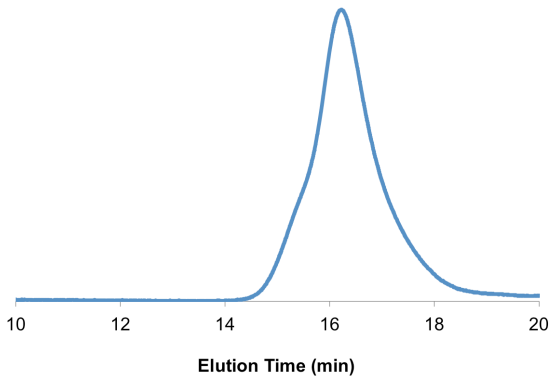


**Figure A5. 5.** $^{1}$H NMR spectrum and GPC analysis of entry 5.

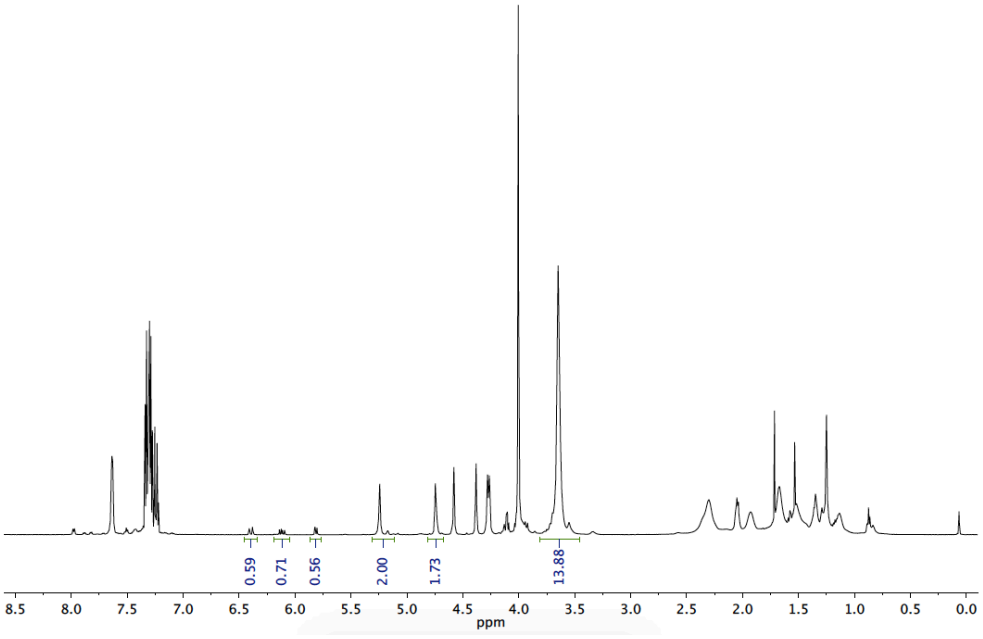


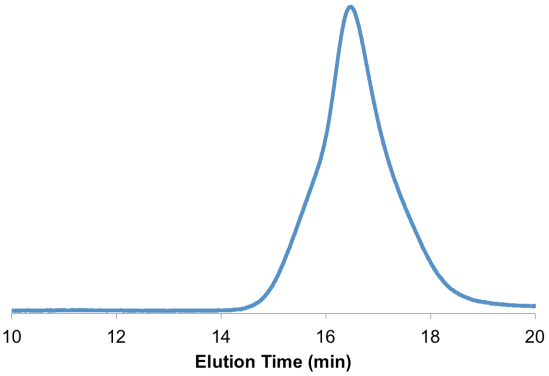


**Figure A5. 6.** $^{1}$H NMR spectrum and GPC analysis of entry 6.

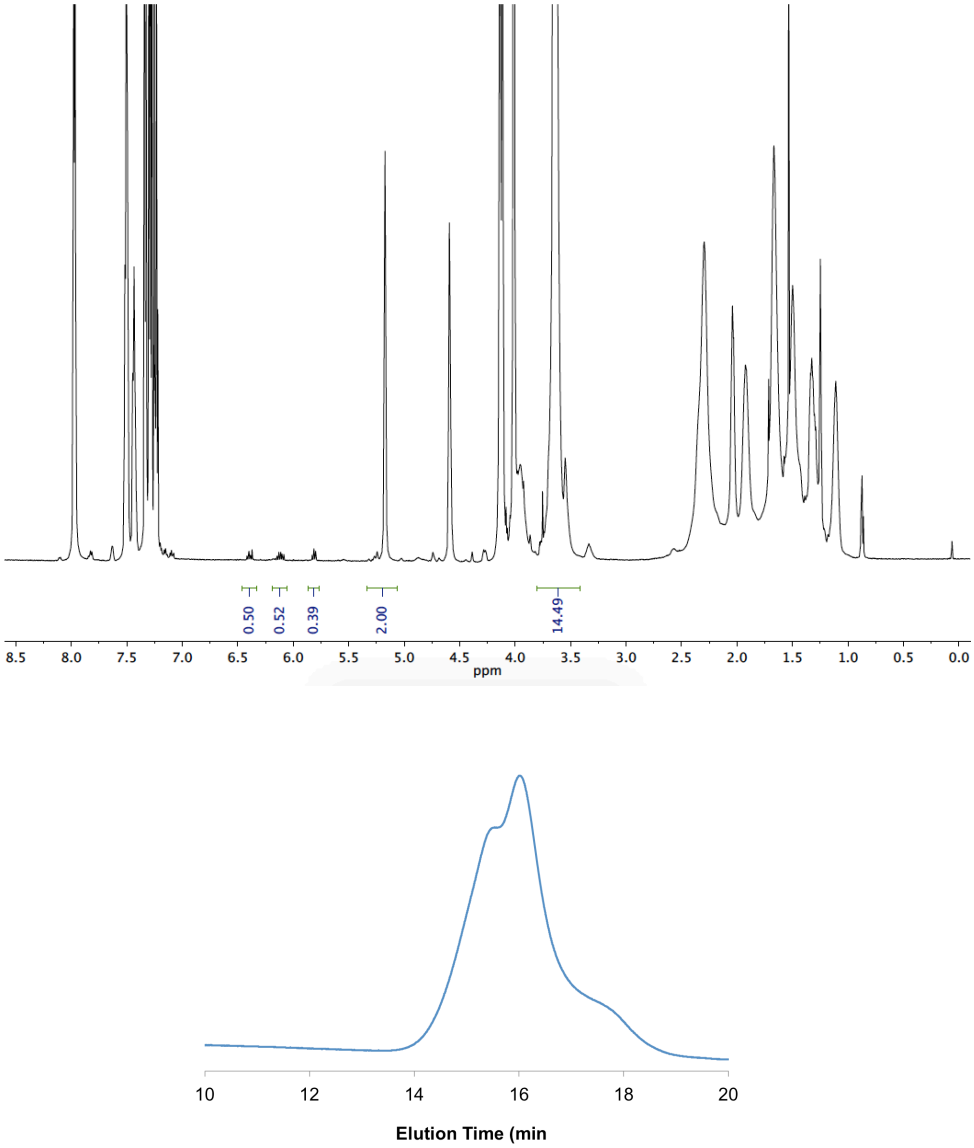


**Figure A5. 7.** $^{1}$H NMR spectrum and GPC analysis of entry 7.

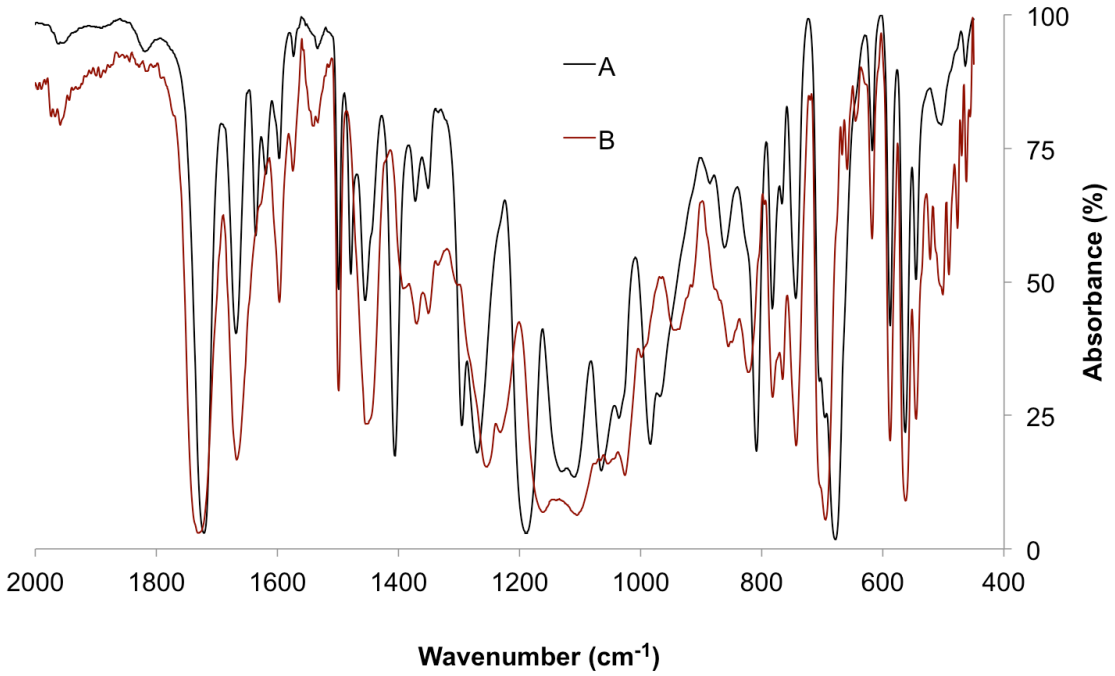


**Figure A5.8.** Normalized IR spectra of formulation mixture (A) and cross-linked network (B) of **5.7(4Ph)**.

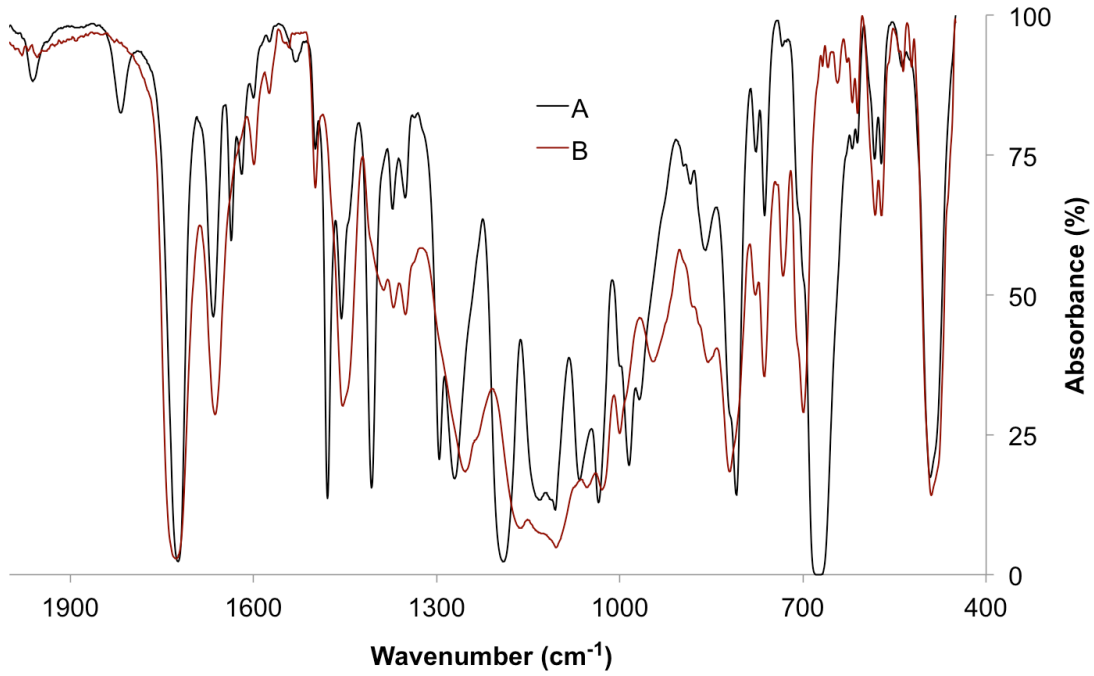


**Figure A5.9.** Normalized IR spectra of formulation mixture (A) and cross-linked network (B) of **5.7(Ph2Fc2)**.

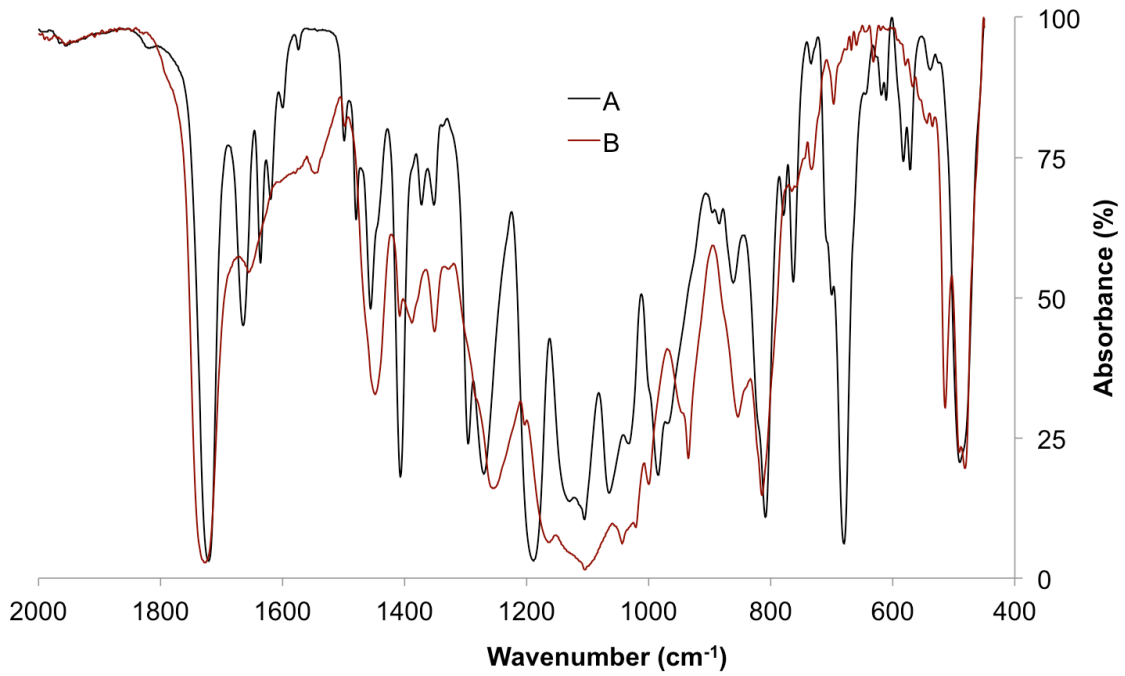


**Figure A5.10.** Normalized IR spectra of formulation mixture (A) and cross-linked network (B) of **5.7**(**Fc4**).

**Appendix 6. Curriculum Vitae**

# Mahboubeh Hadadpour

---

## PROFILE

- A skilled researcher with over 6 years of hand-on experience
- Holding international experience and willing to travel to expand her knowledge and expertise
- Experienced in communications and interacting with individuals and groups
- Effective written and verbal communication skills complemented by excellent attention to details
- Productive independent worker able to work constructively with groups of collaborators
- Excellent in analyzing and addressing problems effectively
- Ability to deal with sudden difficult situations
- Quickly adapting to a new work environment
- Punctual and skilled at time-management and meeting deadlines
- Experienced in teaching and a passionate quick learner

## EDUCATION

**Ph. D.**
Western University, London, ON — Sep 2011- May 2015
Research Supervisor: Prof. Paul J. Ragogna
Synthesis, Self-assembly, and Properties of Organometallic Polymers

**M. Sc.**
Western University, London, ON — 2009- 2011
Research Supervisor: Prof. Mark S. Workentin
Synthesis and Characterization of Functionalized Gold Nanoparticles

**B. Sc.**
K. N. T. University of Technology, Tehran, Iran — 2001- 2005
Project Supervisor: Prof. Berahman Movassagh
Methodology in the Synthesis of Thiol Esters

## PROFESSIONAL RESEARCH EXPERIENCE

**Western University**, London, ON Sep 2009 – May 2015

*Research Assistant*

. Synthesized and characterized a library of monomeric units made of organometallic compounds

. Performed reversible addition fragmentation transfer (RAFT) polymerization on organometallic monomers

. Studied the self-assembly behaviour of block copolymers in solid-state and solution-state to obtain morphologies in nanometer scale

**University of Bristol**, Bristol, UK July 2014 - Jan 2015

*Visiting Researcher*

. Purified block copolymers by performing size exclusion chromatography (SEC) column

. Prepared and analyzed nanostructures made *via* the self-assembly of block copolymers in solid-state and solution-state

. Prepared PDMS stamps to create micrometer patterns using block copolymers as ink

**University of Toronto**, Toronto, ON 2008 – 2009

*Volunteer Researcher*

. Synthesized a fluorescent anthracene-based Ligand

## INSTRUMENTS and TECHNIQUES

| | |
|---|---|
| Gel Permeation Chromatography (GPC) | Nuclear Magnetic Resonance (NMR) Spectroscopy |
| Transmission Electron Microscopy (TEM) | Size Exclusion Chromatography (SEC) |
| Scanning Electron Microscopy (SEM) | Solvent Purification System (SPS) |
| Thermal Gravimetric Analysis (TGA) | FT-IR Spectroscopy |
| Differential Scanning Calorimetry (DSC) | Dynamic Light Scattering (DLS) |
| Energy Dispersive X-ray (EDX) Spectroscopy | Schlenk-line and Glove-box (Inert Atmosphere) |
| Ultramicrotome | UV-vis Spectroscopy |

Solid-State and Solution-State Self-Assembly of Block Copolymer

# CONFERENCES, PRESENTATIONS, and PUBLICATIONS

**Presentations:**

7. **M. Hadadpour**, P. Chadha, Y. Liu and P.J. Ragogna; "Homo- and diblock copolymers derived from a mixed sandwich cobaltocene: Overcoming a tight coil to give a real "Co" polymer" Inorganic and Materials Mini Symposium, Bristol, UK, November 6th, 2014. [Oral Presentation]

6. **M. Hadadpour**, Y. Liu, P. J. Ragogna; "RAFT Conditions for the Polymerization of $\eta^5$-Cyclopentadienyl-Cobalt-$\eta^4$-Cyclobutadiene (CpCoCb) Containing Acrylate Units" *96th Canadian Society for Chemistry Conference (CSC) National Conference and Exhibition,* Quebec City, Quebec, Canada, May 26th- May 30th, 2013. [Poster Presentation]

5. **M. Hadadpour**, P. Chadha, P. J. Ragogna; "$\eta^5$-Cyclopentadienyl-Cobalt-$\eta^4$-Cyclobutadiene (CpCoCb) a Versatile Monomer to Synthesize Side-Chain Co(I) Polymers" *95th Canadian Society for Chemistry Conference (CSC) National Conference and Exhibition,* Calgary, Alberta, Canada, May 26th –May 30th, 2012. [Oral Presentation]

4. **M. Hadadpour**, Y. Liu, P. J. Ragogna; "$\eta^5$-Cyclopentadienyl-Cobalt-$\eta^4$-Cyclobutadiene (CpCoCb) Derivatives; a Versatile Monomer to Synthesize Side-Chain Co(I) Metallopolymers" Inorganic Discussion Weekend (IDW), Ottawa, Ontario, November 2nd- November 4th, 2012. [Poster Presentation]

3. **M. Hadadpour**, M. S. Workentin; "Photoinduced Coalescence of AuNP in Halogenated Solvents" *94th Canadian Society for Chemistry Conference (CSC) National Conference and Exhibition,* Montreal, Quebec, June 5th-June 9th, 2011. [Oral Presentation]

2. **M. Hadadpour**, M. S. Workentin; "Altering the Physical Properties of Gold Nanoparticles Using a Photo switchable Pyridyl-Azobenzene" *93rd Canadian Society for Chemistry Conference (CSC) National Conference and Exhibition,* Toronto, Ontario, May 29th – June 2nd 2010. [Poster Presentation]

1. **M. Hadadpour**, M. S. Workentin; "Altering the Physical Properties of Gold Nanoparticles Using a Photo Switchable Pyridyl-Azobenzene" *Ontario Nanoscience and Nanotechnology Workshop,* London, Ontario, May 16th- May 18th, 2010. [Poster Presentation]

**Publications:**

6. **Hadadpour, M**.; Chadha, P.; Ragogna, P. J. "Attempts on Polymerization of Highly Metalized Mixed Sandwich Cobaltocene Monomer" (Manuscript in preparation).

5. **Hadadpour, M**.; Ragogna, P. J. "RAFT Polymerization of Cobalt containing Monomers Using PDMS Macro-RAFT Agents to Graft block copolymers" (Submitted manuscript).

4. **Hadadpour, M**.; Gwyther, J.; Manners, I.; Ragogna, P. J. "Phosphonium-based Polyelectrolyte and Cobalt containing Metallopolymer Incorporated into a Multifunctional Block Copolymer" J. *Chem. Matter.* **2015**, *27*, 3430-3440.

3. **Hadadpour, M**.; Liu, Y.; Chadha, P.; Ragogna, P.J. "Overcoming a Tight Coil to Give a Random "Co" Polymer Derived from a Mixed Sandwich Cobaltocene" *Macromolecules* **2014**, *47*, 6207−6217.

2. Mohammadi Ziarani, G.; Badiei, A. R.; Khaniania, Y.; **Haddadpour, M.** " One Pot Synthesis of Polyhydroquinolines Catalyzed by Sulfonic Acid-functionalized SBA-15 as a New Nanoporous Acid Catalyst Under Solvent-free Conditions" *Iranian Journal of Chemistry and Chemical Engineering* **2010**, *29*, 1-10.

1. Mohammadi Ziarani, G.; Abbasi, A.; Badiei, A.; **Haddadpour, M.**; Jahangir, A. A. " 9-(2,3-Dichlorophenyl) 4a-hydroxy-3,3,6,6-tetramethyl-4,4a,5,6,9,9a-hexahydro-3H-xanthene-1,8(2H,7H)-dione" *Acta Crystallographica Section E: Structure Reports Online* **2008**, *64*.

## COURSE WORK

| | |
|---|---|
| Mechanistic Organic Chemistry | 87% |
| Advanced NMR Spectroscopy | 84% |
| Nanomaterials Architectures | 95% |
| Organic Photochemistry | 88% |
| Probing Materials with Photons | 91% |
| Polymers: Synthesis to Function | 91% |
| Catalysis | 87% |
| Public Seminar | 89% |